NAMIBIA UNIVERSITY
OF SCIENCE AND TECHNOLOGY

Faculty of Health, Natural Resources and Applied Sciences

Department of Mathematics , Statistics and Actuarial Science

Proceedings of the 1st International Conference on Mathematical and Statistical Sciences(ICMSS-1)

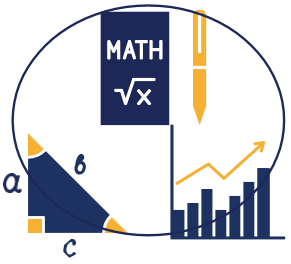

Theme: Towards Multi-disciplinary Problem-Solving Research Advancements

03 - 04 July 2023

6th Floor, High-Tech Transfer Plaza Select (HTTPS), NUST Lower Campus, Windhoek, Namibia

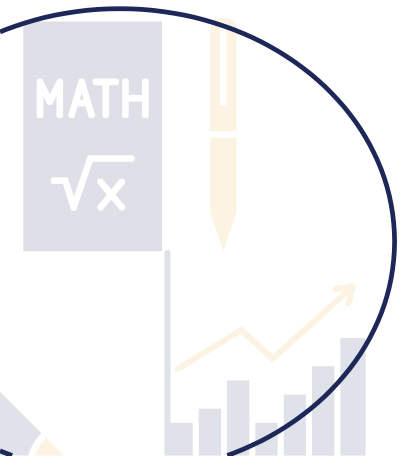

Sponsors and Partners

Bank of Namibia

KONRAD ADENAUER STIFTUNG

Namibia Scientific Society
Wissenschaftliche Gesellschaft
Science for Society

NCRST
National Commission on Research Science & Technology

ISBN:978-99916-55-80-2

ABOUT THE CONFERENCE

The 1st International Conference on Mathematical and Statistical Sciences (ICMSS-1) took place on Monday 3rd and Tuesday 4th July 2023 as a two-day Hybrid (Blended) international conference organised by the Department of Mathematics, Statistics and Actuarial Science, Namibia University of Science and Technology. It brought together physically and virtually researchers, scientists, and educators in Mathematical sciences around the world to share their research contributions and ongoing projects from diverse applications of Mathematical and Statistical Sciences. Precisely, the maiden conference provided an international forum to showcase Mathematical and Statistical Sciences capabilities for multi-disciplinary research and global problem-solving challenges and priorities. The conference package featured Plenary sessions from highly recognised academic leaders and experts and Parallel presentations of Invited Talks and Research papers spread over the following core and related thematic areas: Applied Mathematics, Applied Statistics, Reliability theory and Applications, Inventory Management and Applications, Queueing Theory and Applications, and Multi-Disciplinary research presentations. The Conference celebrated an amazing collaboration of academic institutions across the world and the support provided for the participation of their academic staff and research students. Moreover, the stakeholders collaborative support behind the provision of various conference complimentary items showcased collective interest towards advancing multi-dimensional benefits of applications of Mathematical and Statistical Sciences from their basic principles to highly advanced scientific research solutions. The maiden conference provided important foundation and feedback for more successful subsequent conference editions.

EDITORS

EDITORIAL BOARD

EDITORIAL

Editors:

Prof Sunday A. Reju
Department of Mathematics, Statistics and Actuarial Science, Namibia University of Science and Technology, Namibia.
Email: sreju@nust.na

Prof. Rakesh Kumar
Department of Mathematics, Statistics and Actuarial Science, Namibia University of Science and Technology, Namibia, and Shri Mata Vaishno Devi University, Katra, India.
Email: rkumar@nust.na, rakesh.kumar@smvdu.ac.in

It gives us immense pleasure to present to you the Proceedings of the 1st International Conference on Mathematical and Statistical Sciences (ICMSS-1), a two-day Hybrid (Blended) international conference which was organised by the Department of Mathematics, Statistics and Actuarial Science, Namibia University of Science and Technology, held on 3-4 July 2024.

The ICMSS-1 witnessed a huge participation of more than 105 delegates worldwide. The conference programme consisted of Plenary and Invited talks from highly recognised academic leaders and experts while the conference papers (or contributory talks) were spread over the following core and related thematic areas: Applied Mathematics; Applied Statistics; Reliability theory and Applications; Inventory Management and Applications; Queueing Theory and Applications, and Multi-Disciplinary research presentations. The conference led to various research collaborations and formation of research groups among the delegates.

This Conference Proceedings is the acknowledgement and brief description of extended abstracts of selected papers which were presented in the maiden International Conference.

There are five papers on mathematical modelling. First is on the latent growth mixed model of the progression of HIV using CD4 counts: a case study of NAMIBIA, the second is on penalised Markowitz portfolio model with augmented Lagrangian, the third is on Enhanced precision ecological prediction model using Adjusted Neural Networks, the fourth is on the Variational optimisation method and applications to meteorological modelling and the fifth is on Wavelet Application to Geomagnetic Disturbances Modelling and Monitoring in Power Networks. There is also a related multi-disciplinary paper on 1-D Modelling of Flood Hazards in Zambezi Kwando Linyanti Basin in Namibia.

There are four papers based on Statistics and its applications. One is on Small area estimation of household consumption expenditure in Khomas region, Namibia, using the Fay-Herriot EBLUP model, the second is on Algorithmic construction of Bayesian optimal block designs using the linear mixed effects model, the third is on Markov models for Battery Energy Storage Systems, and the fourth is based on Heavy tailed family of generalized probability distributions.

There are several research papers in Queueing theory comprising the transient as well as steady-state analyses of queueing systems. Probability generating functions, Laplace transforms and Matrix-Geometric methods have been used in the analyses of queueing systems. Queueing papers published in this Proceedings are on various concepts like customers'

impatience and catastrophes; working vacation; impatience and interruption; soft failures and N-policy; two-server tandem queueing model; optimization; phase type service; heterogeneous servers; bulk service priority queueing model; holistic approaches in queueing analysis; retrial queueing systems; retrial queueing inventory systems; phase type queueing system with startup times and vacations, and machine repair problems.

Two research papers are based on reliability analysis. One is on Cost-benefit analysis of a three non-identical unit standby system with Weibull failure and repair laws, and the other is on the Bayesian study of a two non-identical units cold standby system with preparation for repair and correlated failure and repair times.

There are two papers on inventory systems. One deals with the analysis of a perishable inventory system, and the other deals with the optimal pricing policies for perishable inventory systems.

There are three papers on Mathematics education. One is based on a Systematic analysis of digital technologies, fourth industrial revolution and mathematics education nexus in emerging economies; the second is on the Learners' perceptions of the challenges and improvement strategies in distance and online undergraduate mathematics learning in Nigeria, and the third is on Gesturing as a problem-solving strategy in Mathematics.

Finally, there is one paper on Algebra titled Gaussian and weak Gaussian $\Gamma-$Semirings.

Finally, the Editors would like to acknowledge the contributions of all authors and the editorial board members towards the publication of this proceedings.

TABLE OF CONTENTS

Algorithmic construction of Bayesian optimal block designs using the linear mixed effects model

Dibaba B. Gemechu*[1], Legesse K. Debusho[2], and Linda M. Haines[3]

[1]Department of Mathematics, Statistics and Actuarial Science, Namibia University of Science and Technology
[2] Department of Statistics, University of South Africa
[3]Department of Statistical Sciences, University of Cape Town

Abstract

One of the focuses of experimental block design is to obtain an optimal way of allocating treatments to the block and an optimal labelling of the treatments in order to obtain accurate data to estimate the parameter of interest as precisely as possible. Under the linear mixed effects model setting, where the block effects are assumed to be random, the treatment information matrix (C-matrix) is dependent on the unknown parameter θ (ratio of unknown variance components of random error and block effects). The best-guess approach has been used in literature to obtain optimal or near-optimal designs and the resultant designs can be considered as locally optimal. A locally optimal design does not account for uncertainty in the variance components. A Bayesian optimal design extends the locally optimal approach by specifying a prior distribution for the unknown parameter θ. In this study, an algorithmic approach for construction of Bayesian optimal block designs under the linear mixed effects setting was introduced and applied to the two-colour cDNA microarray experiments, where arrays are treated as a block effect. The result of the study indicates that the resultant Bayesian optimal block designs are insensitive to the shape of the prior distributions.

Keywords: Bayesian design; A- and D-optimal block designs; Linear mixed model.

1 Introduction

Consider an experimental block design with a small block size of two. If more than two treatments are to be compared, such experimental design can be considered as an incomplete block design. One of such experiments are a microarray experiments that can be used to identify genes whose expression level distributions change in response to treatment and such genes are called differentially expressed. The two-colour microarrays use two different dyes, Cyanine 3 (green) and Cyanine 5 (red), to measure gene expression. The use of two dyes allows two different nucleic acid samples, called treatments, dyed with different dyes, to be hybridized together to the same microarray slide or array. Hybridization of two target samples to the same microarray slide enables a comparison of

*Corresponding Author. Email: dgemechu@nust.na/diboobayu@gmail.com.

two treatments on a single array. Since in a two-colour microarray experiment only two treatments labelled with two different dyes are accommodated on a single array, the designs for microarray experiments constitute block designs of size two where the array is treated as the experimental block. If more than two treatments are to be compared in a microarray experiment and if it is assumed that there is no gene specific dye effect, then the microarray experiment can be considered as an incomplete block design (Dey, 2010).

Optimal or efficient designs for such experiments have been extensively studied in the design literature (for example, Kerr and Churchill, 2001a,b; Churchill, 2002; Wit et al., 2005; Landgrebe et al., 2006; Bailey et al., 2013). The design construction approaches adopted in these studies are based on fixed-effects models. Furthermore, locally optimal block designs for two colour microarray experiments under the linear mixed effects models setting, where the array effects are assumed to be random, were discussed by Sarkar et al. (2007), Gemechu et al. (2014, 2015) and Debusho et al. (2019) for a given value of $\theta \in [0, 1)$, where θ is a function of error variance and variance of random array effects. A locally optimal design depends on a given value of θ or variance components. It however does not account for uncertainty in variance components values and hence we may be tempted to identify a design as optimal or near-optimal when it is not (Bueno Filho and Gilmour, 2007). This is the known criticism against the locally optimal design (Dokoumetzidis and Aarons, 2007). One of the practical approach to obtain the variance components is to conduct a preliminary pilot experiment and use the results to get the initial estimates, then compute the optimal designs for the main experiment using them. This approach however is not always feasible due to resource constraints (Gondro and Kinghorn, 2008).

A Bayesian optimal design extends the locally optimal approach by allowing the practitioner to specify a prior distribution for θ or the variance components. Note however that different prior distributions on the variance components or different design criteria may yield different Bayesian designs (Lohr, 1995). The aim of this paper is therefore to introduce an algorithmic approach for construction of Bayesian optimal block designs under the linear mixed effects setting by introducing a prior distribution for θ and apply the method to the two-colour cDNA microarray experiments, where arrays are treated as a block effect. Attention is restricted to two criteria, Bayesian A-optimality for which the expected value of the trace of the variance-covariance matrix of all possible pairwise treatment means is minimized and Bayesian D-optimal for which the expected value of the determinant of the variance-covariance matrix of all possible pairwise treatment means is minimized.

2 Model and Information Matrix

Consider a two-colour microarray experiment comprising b arrays and v treatments replicated $r_1, \ldots, r_v$ times. The experiment can be modelled as a block design with the arrays corresponding to blocks of size 2. Specifically, suppose the treatment effects $\boldsymbol{\tau}$ are fixed and the array effects $\mathbf{b}$ are random. Then following Gemechu et al. (2014), the appropriate linear mixed effects model can be expressed in a matrix form as

$$\mathbf{y} = \mathbf{1}\,\mu + \mathbf{X}_\tau\,\boldsymbol{\tau} + \mathbf{X}_b\,\mathbf{b} + \mathbf{e} \tag{1}$$

where $\mathbf{y}$ is the $n \times 1$ response vector with $n = b\,v$, μ is the overall mean, $\mathbf{1}$ denotes the $n \times 1$ vector of ones, $\boldsymbol{\tau}$ is a $v \times 1$ vector of fixed treatment effects with attendant $n \times v$ design matrix $\mathbf{X}_\tau$, $\mathbf{b}$ is

a $b \times 1$ vector of random array effects with attendant $n \times b$ design matrix and $\mathbf{e}$ is an $n \times 1$ vector of error terms. The random effects vector $\mathbf{b}$ is taken to be distributed as $\mathcal{N}(\mathbf{0},\, \sigma_b^2\, \mathbf{I}_b)$ and the error term $\mathbf{e}$ as $\mathcal{N}(\mathbf{0},\, \sigma^2\, \mathbf{I}_n)$, where $\mathbf{I}_b$ and $\mathbf{I}_n$ denote the identity matrices of order b and n, respectively, and $\mathbf{b}$ and $\mathbf{e}$ are assumed to be independent. Under the assumption that no treatment occurs more than once in a block, the design layout is a binary block design. Furthermore, since only two treatments can be applied to a given block, the block size are equal. Ignoring the constant $1/\sigma^2$, the treatment information matrix, also called the $\mathbf{C}$-matrix, is given by

$$\mathbf{C} = \mathbf{R} - \frac{1}{k}\,\mathbf{N}\,\mathbf{N}' + \theta\,\left(\frac{1}{k}\,\mathbf{N}\,\mathbf{N}' - \frac{1}{b\,k}\,\mathbf{r}\,\mathbf{r}'\right). \tag{2}$$

where k is the block size, $\theta = \sigma^2/(\sigma^2 + k\,\sigma_b^2)$, $\mathbf{r} = (r_1, \ldots, r_v)'$ is the vector of treatment replications, $\mathbf{N}$ is treatments-blocks incidence matrix, and $\mathbf{R} = diag(r_1,\, \ldots, r_v)$. Note that that $\theta = 0$ corresponds to a fixed effects model with $\mathbf{C} = \mathbf{R} - \frac{1}{k}\,\mathbf{N}\,\mathbf{N}'$. The matrix $\mathbf{C}$ is symmetric and positive semi-definite and, since $\mathbf{C}\mathbf{1}_v = \mathbf{0}$, has $rank(\mathbf{C}) \leq v - 1$. In the present study attention is restricted to designs for which the associated information matrix has rank $v - 1$. It thus follows that the designs are connected and that all treatment contrasts, and in particular pairwise differences, are estimable (Dean et al., 2015).

3 Bayesian optimality criteria

One of the main aims of a microarray experiment is to identify differentially expressed genes. Thus it is natural to focus on design criteria which are based on the variance of the estimated pairwise treatment differences and to select designs from a set of competing designs comprising b arrays and v treatments for which the criterion of interest is in some sense optimal. Consider therefore all possible pairwise treatment differences expressed as $\mathbf{T}\boldsymbol{\tau}$ where $\mathbf{T}$ is a $\binom{v}{2} \times v$ matrix with each row comprising an element 1, an element -1 and all other elements 0, and is such that $\mathbf{T}\,\boldsymbol{\tau} = v\,\mathbf{I}_v - \mathbf{J}_v$ (Dey, 2010). Then the variance-covariance matrix of the best linear unbiased estimator of $\mathbf{T}\boldsymbol{\tau}$ is given by $\mathbf{T}\,\mathbf{C}^-\,\mathbf{T}'$, where $\mathbf{C}^-$ is an arbitrary g-inverse of $\mathbf{C}$.

Suppose that $\mathcal{D} = \mathcal{D}(v, b, k)$ represents the class of connected block designs with b blocks of size two and v treatments each member of $\mathcal{D}$ keeps $\mathbf{T}\boldsymbol{\tau}$ estimable, and assume that the model in (1) can be used for the observations generated by $\mathcal{D}$. Then a design $d_{BA}^* \in \mathcal{D}$ is said to be Bayesian A-optimal if it minimizes

$$\Psi_{BA}(d) = E_\theta\{trace(\mathbf{T}\,\mathbf{C}^-\,\mathbf{T}')\}$$

where the expectation is over θ, that is if it minimizes the average of the trace of the variance-covariance matrix of the BLUE of $\mathbf{T}\boldsymbol{\tau}$, equivalently if it minimizes

$$\Psi_{BA}(d) = \int trace(\mathbf{T}\,\mathbf{C}^-\mathbf{T}')\, f_\theta(\theta)\, d\,\theta \tag{3}$$

where $f_\theta(\theta)$ is a prior distribution of θ. In addition a design $d_{BD}^* \in \mathcal{D}$ is said to be Bayesian D-optimal if it minimizes

$$\Psi_{BD}(d) = E_\theta\{|\mathbf{T}\,\mathbf{C}^-\,\mathbf{T}'|\}$$

where the expectation is over θ (Lohr, 1995), equivalently if it minimizes

$$\Psi_{BD}(d) = \int |\mathbf{T}\,\mathbf{C}^-\,\mathbf{T}'|\, f_\theta(\theta)\, d\,\theta. \tag{4}$$

3.1 Prior distribution of θ

In this paper the inverse-Gamma (IG) distributions were used to describe the uncertainty for the variance components σ_b^2 and σ^2 (Verdinelli, 1996). Specifically,

$$\sigma^2 \sim Inverse - Gamma(a_1, b_1) \qquad \text{and} \qquad \sigma_b^2 \sim Inverse - Gamma(a_2, b_2)$$

where a_1, b_1 and a_2, b_2 are the parameters of the inverse-Gamma distributions. The assignment of univariate IG distributions for the variance components follows from the model assumption that **b** and **e** are independent. Hence, the joint probability density function of (σ^2, σ_b^2) is given by $f_{\sigma^2,\sigma_b^2} = f_{\sigma^2} \times f_{\sigma_b^2}$. Recall that $\theta = \sigma^2/(\sigma^2 + k\,\sigma_b^2)$. Now let $\alpha = \sigma^2 + k\,\sigma_b^2$, hence $\sigma^2 = \alpha\,\theta$ and $\sigma_b^2 = \alpha\,(1-\theta)/k$. The joint probability density function (pdf) of (θ, α), $f_{\theta,\alpha}(\theta, \alpha)$, can be derived using Jacobian transformation and then the marginal probability density function of θ using $f_\theta(\theta) = \int_0^\infty f_{\theta,\alpha}(\theta, \alpha) d\alpha$. Thus

$$f_\theta(\theta) = \frac{\theta^{a_2-1}\,(1-\theta)^{a_1-1}}{\overline{b}^{\,a_2}\,B(a_1, a_2)} \times \left(1 + \frac{(1-\overline{b})\,\theta}{\overline{b}}\right)^{-(a_1+a_2)} \tag{5}$$

where $\overline{b} = b_1/k\,b_2 > 0$ and $B(a_1, a_2)$ is a Beta function with parameters a_1 and a_2.

The evaluations of the integrals in (4) and (5) using the expression of $f_\theta(\theta)$ in (6) are computer intensive. However, if $f_\theta(\theta)$ is some known distribution, a Monte Carlo integral approximation could be implemented by drawing a Monte Carlo sample from $f_\theta(\theta)$. For example, consider $b_1 = k\,b_2$, i.e. $\overline{b} = 1$. Then it follows from expression (6) that

$$f_\theta(\theta) = \frac{\theta^{a_2-1}\,(1-\theta)^{a_1-1}}{B(a_1, a_2)}$$

which is a Beta distribution with parameters a_1 and a_2, denoted $Beta(a_1, a_2)$, where a_2 and a_1 are the shape and scale parameters, respectively. Different Beta distributions were used to compute the Bayesian optimal designs numerically. The following general steps (Bueno Filho and Gilmour, 2007) were used for the numerical evaluation of the Bayesian criterion values:

1. For a given connected block design $d \in \mathcal{D}(v, b, k)$, compute the information matrix as a function of θ;
2. Express the criterion conditioned on θ;
3. Assign a prior distribution of θ; and
4. Compute the Bayesian criterion value by integrating out the θ using its corresponding prior distribution.

Note that the optimal designs depend on the prior information of the variance components through the prior distribution of θ.

4 Algorithm for constructing Bayesian optimal designs

The following algorithm, adopted from the treatment exchange algorithm of Debusho et al. (2019), were used for a search of Bayesian A- and D-optimal block designs using a Beta distribution as a prior for θ. For a given parametric combination (v, b) and prior distribution of θ, the steps used in the algorithm are presented below:

Step 1: Generate an initial design at random for given (v, b, k, θ).
Step 2: Check for the connectedness of the design.
Step 3: Treatment exchange procedure: Through deletion and substitution of the treatment in a cell with the remainder of the $v - 2$ treatments at a time.
Step 4: Select the design for which the score value is optimal.
Step 5: Repeat Steps 3 & 4 until no further favourable exchanges can be effected.

The algorithm for both A- and D-optimality has been coded and implemented in the GAUSS programming language.

5 Results and Discussion

The Bayesian optimal designs were calculated for the parametric combinations $3 \leq v \leq 20$ and $b = v$ the same number of arrays as treatments, $b = v + 1$ one extra array and $b = v + 2$ two extra arrays using nine different Beta priors for θ. These values were selected for illustration purpose, however, one can also generate the optimal designs for other parametric combinations using the proposed algorithm. The prior distributions vary in shapes and includes one uniform on $[0, 1)$ $Beta(1, 1)$, two positively skewed ($Beta(0.5, 1.5)$ and $Beta(1.25, 5)$), two negatively skewed ($Beta(1.5, 0.5)$ and $Beta(5, 1.5)$), two bimodal ($Beta(0.3, 0.3)$ and $Beta(0.5, 0.75)$) and two symmetric ($Beta(5, 5)$ and $Beta(5, 10)$) which tend to normality. The Bayesian A- and D-optimal block designs results are summarized as follows:

(i) When $3 \leq v = b \leq 20$, the A- and D-optimal designs are the loop designs $C_v(v)$ for all the priors used (see Figure 1(a)), where $C_s(v)$ represents a design for v treatments in v arrays whose graphs contain a circuit of length s (Bailey, 2007).

(ii) When $b = v + 1; 3 \leq v \leq 20$, the A- and D-optimal designs are the parallel path designs $PP(x, y, z)$ of lengths x, y and z between two vertices with $x + y + z = b$ for all the priors used (see Figure 1(b)).

(iii) When $b = v + 2; 3 \leq v \leq 20$, the A- and D-optimal designs are the complete graph K_4 on four vertices with each of its six edges replace by paths (Bailey, 2007) for all the priors used (see Figure 1(c)).

The A- and D-optimal designs are robust to specification of the prior distribution, so they are insensitive to the exact shape of the prior distribution.
The numerical results in Debusho et al. (2019) show that for some set of θ in the interval $[0, 1)$, v and b values, the A-optimal designs are the loop designs, parallel path designs $PP(x, y, z)$ of lengths x, y and z between two vertices with $x + y + z = b$ and the complete graph K_4 on four vertices

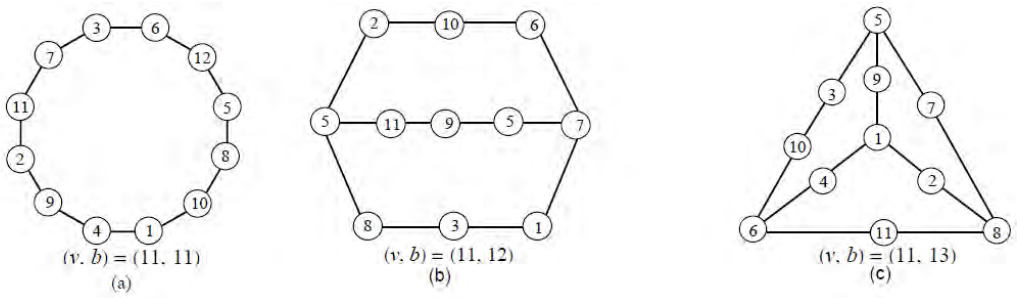

Figure 1: (a) Loop design for eleven treatments $C_{11}(11)$; (b) Parallel path design $PP(4,4,4)$ for 11 treatments in 12 blocks; and (c) Complete graph $K_4(3,2,2,2,2,2)$ for 11 treatments in 13 blocks.

with each of its six edges replace by paths for $v = b$, $b = v+1$ and $b = v+2$, respectively. However, for the parametric combinations considered in Debusho et al. (2019) the D-optimal designs are invariant of the θ values, for example for $v = b$ the D-optimal designs are the loop designs for all θ in the interval $[0, 1)$. Hence, for such v and b values the results might suggest that there is no advantage to using the Bayesian method for construction of D-optimal block designs of size two.

6 Concluding Remarks

In this paper we introduced a numerical method for construction of optimal Bayesian block designs for two-colour microarray experiments. The main focus is on implementing prior information on the error variance σ^2 and the variance of random array effects σ_b^2, through $\theta = \sigma^2/(\sigma^2 + k\sigma_b^2)$, where k is the array (block) size, by using Monte Carlo samples from appropriate prior distribution. The results presented, show that for Beta priors with different shapes, the A- and D-optimal designs are the loop designs, $PP(x, y, z)$ of lengths x, y and z between two vertices with $x + y + z = b$ and the complete graph K_4 for $v = b$, $b = v + 1$ and $b = v + 2$, respectively. In this paper it is assumed that there is no dye effect. However, if the dye effect is taken into account, then the two-colour microarray experiment can be considered as a $2 \times b$ row-column design (Bailey, 2007). The method to the construction of optimal Bayesian block designs reported here has been extended to the row-column designs and results relating to this extension will be reported elsewhere.

References

Bailey, R., Schiffl, K., and Hilgers, R.-D. (2013). A note on robustness of d-optimal block designs for two-colour microarray experiments. *Journal of Statistical Planning and Inference*, 143(7):1195–1202.

Bailey, R. A. (2007). Designs for two-colour microarray experiments. *Journal of the Royal Statistical Society Series C: Applied Statistics*, 56(4):365–394.

Bueno Filho, J. S. d. S. and Gilmour, S. G. (2007). Block designs for random treatment effects. *Journal of statistical planning and inference*, 137(4):1446–1451.

Churchill, G. A. (2002). Fundamentals of experimental design for cdna microarrays. *Nature genetics*, 32(4):490–495.

Dean, A. M., Morris, M., Stufken, J., and Bingham, D. (2015). *Handbook of design and analysis of experiments*, volume 7. CRC Press Boca Raton, FL, USA:.

Debusho, L. K., Gemechu, D. B., and Haines, L. M. (2019). Algorithmic construction of optimal block designs for two-colour cdna microarray experiments using the linear mixed effects model. *Communications in Statistics-Simulation and Computation*, 48(7):1948–1963.

Dey, A. (2010). *Incomplete block designs*, volume 57. World Scientific.

Dokoumetzidis, A. and Aarons, L. (2007). Bayesian optimal designs for pharmacokinetic models: sensitivity to uncertainty. *Journal of biopharmaceutical statistics*, 17(5):851–867.

GAUSS Programming Language. Aptech systems, inc. (2022). version 22.1.0.

Gemechu, D. B., Debusho, L. K., and Haines, L. M. (2014). A-optimal designs for two-colour cdna microarray experiments using the linear mixed effects model. In *Annual Proceedings of the South African Statistical Association Conference*, volume 2014, pages 33–40. South African Statistical Association (SASA).

Gemechu, D. B., Debusho, L. K., and Haines, L. M. (2015). A-and d-optional row-column designs for two-colour cdna microarray experiments using linear mixed effects models. *South African Statistical Journal*, 49(2):153–168.

Gondro, C. and Kinghorn, B. P. (2008). Optimization of cdna microarray experimental designs using an evolutionary algorithm. *IEEE/ACM Transactions on Computational Biology and Bioinformatics*, 5(4):630–638.

Kerr, M. K. and Churchill, G. A. (2001a). Experimental design for gene expression microarrays. *Biostatistics*, 2(2):183–201.

Kerr, M. K. and Churchill, G. A. (2001b). Statistical design and the analysis of gene expression microarray data. *Genetics Research*, 77(2):123–128.

Landgrebe, J., Bretz, F., and Brunner, E. (2006). Efficient design and analysis of two colour factorial microarray experiments. *Computational statistics & data analysis*, 50(2):499–517.

Lohr, S. L. (1995). Optimal bayesian design of experiments for the one-way random effects model. *Biometrika*, 82(1):175–186.

Sarkar, A., Parsad, R., Rathore, A., and Gupta, V. (2007). Efficient block designs for 2-colour microarray experiments.

Verdinelli, I. (1996). Bayesian design for the normal linear model with unknown error variance. Technical report, Technical Report 647, Carnegie Mellon Univ.

Wit, E., Nobile, A., and Khanin, R. (2005). Near-optimal designs for dual channel microarray studies. *Journal of the Royal Statistical Society Series C: Applied Statistics*, 54(5):817–830.

TRANSIENT SOLUTION OF A MULTI-HETEROGENEOUS SERVERS' QUEUING SYSTEM WITH IMPATIENCE AND CATASTROPHES

[1]Sapana Sharma and [2, 3]Rakesh Kumar
E-mail: sapanasharma736@gmail.com
[1]Department of Mathematics, MMEC, Maharishi Markandeshwar Deemed to be University, Mullana, Ambala, Haryana, India-133203
[2]Department of Mathematics and Statistics, Namibia University of Science and Technology, Namibia
[3]School of Mathematics, Shri Mata Vaishno Devi University, Katra, India

Abstract

In this paper, we consider a Markovian queuing system with heterogeneous servers, balking and catastrophes. The time-dependent behavior of the system is analyzed by using generating function technique. The expressions for mean and variance of the system are obtained in transient state. At last, some special cases of the model are derived and discussed.
Keywords: Transient solution, Catastrophes, Generating function, Heterogeneous servers, Balking

Queuing Model Description

In this section, we describe the queuing model. The model is based on following assumptions:

1. The arrivals to the queuing system occur in accordance with a Poisson process with parameters λ.
2. The system has multi-servers (say, c) having distinct service rates and the service times at each server are exponentially distributed. This means that the customers are always served by the fastest servers. That is, when such a server becomes available, a customer may switch to a fastest server.
3. On arrival customer either decides to enter the queue with probability p or balk with probability $1-p$.
4. Apart from this, the catastrophes may also occur at the service facility following Poisson process with rate ψ, when the system is not empty. At the moment when catastrophe occurs at the system, all the customers are destroyed, all the servers get inactivated momentarily and after the catastrophe, the servers become ready for service immediately.
5. The queue discipline is FCFS and the capacity of the system is infinite.
6. Initial condition: $P_0(0) = 1$.

Mathematical Formulation of the Model

Define $P_n(t) = P\{X(t) = n\}$, $n = 0, 1, \ldots$. The queuing model under investigation is governed by the following differential-difference equations:

$$\frac{dP_0(t)}{dt} = -(\lambda + \psi)P_0(t) + \mu_1 P_1(t) + \psi \tag{1}$$

$$\frac{dP_n(t)}{dt} = -(\lambda + \psi + \sum_{i=1}^{n}\mu_i)P_n(t) + \sum_{i=1}^{n+1}\mu_i P_{n+1}(t) + \lambda P_{n-1}(t), \quad 1 \le n < c \tag{2}$$

$$\frac{dP_c(t)}{dt} = -(\lambda p + \psi + \sum_{i=1}^{c}\mu_i)P_c(t) + \sum_{i=1}^{c}\mu_i P_{c+1}(t) + \lambda P_{c-1}(t), \; n = c \tag{3}$$

$$\frac{dP_n(t)}{dt} = -(\lambda p + \psi + \sum_{i=1}^{c}\mu_i)P_n(t) + \sum_{i=1}^{c}\mu_i P_{n+1}(t) + \lambda p P_{n-1}(t), \; n > c \tag{4}$$

Transient solution of the model

The transient state probabilities of a Markovian queuing system with multi heterogeneous servers, balking and catastrophes which is governed by the differential-difference equations (1) − (4) are obtained by using probability generation functions and Laplace Transforms, and are given by:

$$P_k(t) = b_{k,0}(t) + \psi \int_0^t b_{k,0}(u)du + \gamma \int_0^t b_{k,c-1}(u)P_c(t-u)du\,, \quad k = 0\,,1\,,\dots,c-1$$

$$P_c(t) = \sum_{n=0}^{\infty}\sum_{m=0}^{n} \frac{(-1)^m}{\gamma}\left(\frac{\alpha}{2\lambda p}\right)^{n+1}(n+1)\binom{n}{m}\left[\int_0^t A(t-u)\int_0^u B^{C(m)}(u-v)\exp\{-(\lambda p+\gamma+\psi)v\}\frac{I_{n+1}(\alpha v))}{v}dudv + \psi\int_0^t H(t-u)\int_0^u B^{C(m)}(u-v)\exp\{-(\lambda p+\gamma+\psi)v\}\frac{I_{n+1}(\alpha v))}{v}dudv\right]$$

and, for n $= 1, 2, \dots$

$$P_{n+c}(t) = n\beta^n \int_0^t \exp\{-(\lambda p+\psi+\gamma)(t-u)\}\frac{I_n(\alpha(t-u))}{(t-u)}P_c(u)du$$

where $H(t) = \int_0^t A(u)du$ and $B^{C(m)(t)}$ is m – fold convolution of B(t) with itself with $B^{C(0)} = \delta(t)$, the Dirac - delta function.

References

[1] Ammar, S.I. (2014). Transient behavior of a two-processor heterogeneous system with catastrophes, server failures and repairs. *Appl. Math. Model*., 38:2224-2234.

[2] Ancker Jr. C. J. and Gafarian, A. V. (1963a). Some queueing problems with balking and reneging I. *Oper. Res,*. 11:88-100.

[3] Ancker Jr. C. J. and Gafarian, A. V. (1963b). Some queueing problems with balking and reneging II. *Oper. Res*., 11:928-937.

[4] Barrer D.Y. (1957). Queuing with impatient customers and ordered service. *Oper. Res*., 5:650-656.

[5] Chao, X. (1995). A queuing network model with catastrophes and product form solution. *Oper. Res. Lett.*, 18:75-79.

[6] Dharmaraja, S. (2000). Transient solution of a two-processor heterogeneous system. *Math. Comput. Model.*, 32:1117-1123.

[7] Dharmaraja, S. and Kumar, Rakesh (2015). Transient solution of a Markovian queuing model with heterogeneous servers and catastrophes. *Opsearch*, 52:810-826.

[8] DiCrescenzo, A., Giorno, V. and Nobile, A.G. (2003). On the M/M/1 queue with catastrophes and its continuous approximation. *Queueing Syst.*, 43:329-347.

[9] El-Paoumy, M.S. and Nabwey, H.A. (2011). The Poissonian queue with balking function, reneging and two heterogeneous servers. *Int. J. Basic Appl. Sci*., 11:149-152.

[10] Haight, F. A. (1957). Queuing with balking I. *Biometrika,* 44:360-369.

[11] Jain, N. K. and Kumar, Rakesh (2007). Transient solution of a catastrophic-cum-restorative queuing problem with correlated arrivals and variable service capacity. *Int. J. Infor. and Manag. Sci.*, 18:461-465.

[12] Jain, N. K. and Kanethia, D. K. (2006). Transient analysis of a queue with environmental and catastrophic e_ects. *Int. J. Infor. and Manag. Sci.,* 17:35-45.

[13] Kumar R. and Sharma S.K. (2012a). An M/M/1/N queuing system with retention of reneged customers. *Pak. J. Stat. Oper. Res.,* 8:859-866.

[14] Kumar, R. and Sharma, S.K. (2012b). An M/M/1/N queuing model with retention of reneged customers and balking. *Amer. J. Oper. Res*., 2:1-5.

[15] Kumar R. and Sharma, S. (2019). Transient Solution of a Two-Heterogeneous Servers' Queuing System with Retention of Reneging Customers. *Bull. Malays. Math. Sci. Soc.,* 42:223-240.
[16] Kumar R. and Sharma S. (2018). Transient analysis of M/M/c queuing system with balking and retention of reneging customers. *Comm. Statist. Theory Methods*, 60:1318-1327.
[17] Kumar, B. K., Madheshwari, S. P. and Venkatakrishanan, K. S. (2007). Transient solution of an M/M/2 queue with heterogeneous servers subject to catastrophes. *Int. J. of Inf. Manag. Sci*., 18:63-80.
[18] Kumar, B.K. and Arivudainambi, D. (2000). Transient solution of an M/M/1 queue with catastrophes. *Comput. Math. Appl*., 10:1233-1240.
[19] Kumar, B. Krishna and Arivudainambi, D. (2001). Transient solution of an M/M/c queue with heterogeneous servers and balking, *Int. J. Inf. Manag. Sci*., 12:15-27.
[20] Morse, P. M. Queues, Inventories and Management, Wiley, New York, 1958.
[21] Raju, S. N. and Bhat, U. N. (1982). A computationally oriented analysis of the G/M/1 queue. *Opsearch*, 19:67-83.
[22] Saaty, T. L. Elements of Queuing Theory with Applications. Mc-Graw Hill, New York, 1961.
[23] Sharma, O. P. and Dass, J. (1989). Initial busy period analysis for a multichannel Markovian queue. *Optimization*, 20:317-323.
[24] Sudhesh, R. (2010). Transient analysis of a queue with system disasters and customer impatience. *Queuing Syst*., 66:95-105.
[25] Sudhesh, R, Savitha P., Dharmaraja, S. (2017). Transient analysis of a two-heterogeneous servers queue with system disaster, server repair and customers impatience. *TOP,* 25:179–205.
[26] Suranga Sampath, M. I. G. and Jicheng, L. (2018). Transient analysis of an M/M/1 queue with reneging, catastrophes, server failures and repairs. *Bull. Iran. Math. Soc.*, https://doi.org/10.1007/s41980-018-0037-6.
[27] Tarabia, A. M. K. (2011). Transient and steady-state analysis of an M/M/1 queue with balking, catastrophes, server failures and repairs. *J. Ind. Manag. Optim*., 7:811-823.
[28] Yassen, M. F. and Tarabia, A. M. K. (2017). Transient Analysis of Markovian Queueing System with Balking and Reneging Subject to Catastrophes and Server Failures. *Appl. Math. Inf. Sci.,* 11:1041-1047.
[29] Yechiali, Uri (2007). Queues with system disasters and impatient customers when system is down. *Queuing Syst.,* 56:195-202.

Modelling of Flood Hazards in Zambezi Kwando Linyanti Basin in Namibia: A 1D Flood Hazard Model

Dianah Irenge[1], Nnenesi Kgabi[2], and Sunday Reju[3]

[1]Faculty of Engineering and the Built Environment, Namibia University of Science and Technology, Windhoek, Namibia
[2]Unit for Environmental Science and Management, Faculty of Natural and Agricultural Sciences, North-West University, Potchefstroom, South Africa
[3]Department of Mathematics, Statistics and Actuarial Science, Faculty of Health, Natural Resources and Applied Sciences, Namibia University of Science and Technology, Windhoek, Namibia

29 July 2023

Abstract

Assessment, Monitoring and Predicting of flood occurrences, frequencies and intensities involve two important things, one is modelling of an observed event from historical data and second is designing a flood event. In this study, a 1- Dimensional Revitalized Rainfall-Runoff Model (1D ReFH Model) in Flood Modeller Version 6.1 used to study flood hazards and mapping in North-Eastern part of Namibia. Observed historical data from 1950 to 2018 in Zambezi Linyanti Kwando Basin were used in this study. The tool computed flood peaks based on return year flooding event. In this summary only 100years return period (Flood peaks) are presented, more flood peaks estimates and their analysis will be the major results in the full paper.

Keywords: Flood hazards; Desert flood Modelling; Flood modeller; Hydrological Modelling.

1 INTRODUCTION

Flood frequency is assessed by a common method called Index Flood (IF) or Peak discharge (Benson, 1960; Grover et al., 2002; Kjeldsen, 2007; Ravazzani et al., 2015; Machado et al., 2015; Mallebrera et al., 2011). The peak discharges (annual averages) are commonly calculated by two methods, statistical and graphical/Rainfall-Runoff Model methods (Benson, 1960; Grover et al., 2002; Villarini et al., 2011).The results are presented as a flood frequency curves made from the rating relationship (plot of stage (m) against flow (m3/s)) and hydrological models.This study uses Rainfall Runoff Model to produce rainfall hydrographs as an input to the 1D River Network (hydraulic Model) to estimate peak flows. The flood Modeler tool has a GIS interfase that makes it easier to use Digital Elevation Model (DEM) to describe the catchment, and create a 1D and 2D River networks. A 1D River Model Network for Zambezi River is created to predict flow and water levels from a designed event in 2, 5,10, 25, 50, 70, 100, 150 and 200 years return periods, along the river channel. With the DEM, a 2D model will further be created and flood maps produced.

2 METHODOLOGY

2.1 Study area

The study location is Zambezi Kwando Linyanti Basin (Figure 1) in Katima Mulilo, North Eastern part of Namibia. located at latitude 17.46666667, Longitude 24.3, elevated at 940m. This basin receives high rainfall than the rest of the basins within the country, nearly 700mm annual average. The basin receives water from rainfall and from perennial (Zambezi) and ephemeral (Kwando) rivers. The mean annual discharge for Zambezi River at Katima Mulilo hydrological station is $1130m^3/s$.

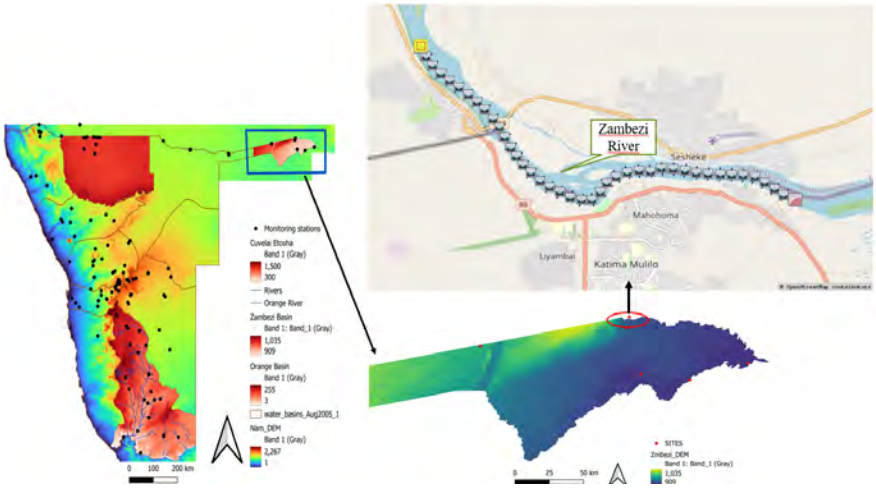

Figure 1: 1D Model Network Location for Zambezi River, Katima Mulilo

2.2 Data sources and collection

The rainfall and discharge data were collected from Meteorological Services of Namibia (NMS) and The Ministry of Agriculture Water and Forestry (MAWF) from 1950 to 2018 . Digital elevation Model (DEM) were downloaded from United states Geological Survey (USGS) website.

2.3 Flood Assessment and Analysis

Table 1, presents the summary of flood assessment and analysis criteria in this study. The study uses Flood Modeller tool (similar to HEC Hydrologic Modelling System (Ramly and Tahir, 2016) with multiple hydrological Models to assess floods (Kjeldsen, 2007). In the upstream of the River Model, the Revitalised Rainfall runoff Model(ReHF) boundary designs rainfall as an input to the Model. The ReHF, uses three components; The Loss Model, The Routing Model and Baseflow Model to estimate flood events (Peaks flows, surface runoff, baseflow and stage). The results are presented as a flood frequency curves made from the rating relationship and hydrological model methods (Benson, 1960; Grover et al., 2002; Villarini et al., 2011).

Table 1: Flood Assessment and Analysis Criteria

FLOOD			
Criteria of assessment	Index/Tool	Input	Model/Theory
Flood Occurrence	Annual Maximum (AMAX)	River flows	Statistical Model
Flood Frequency	Index flood (Flood Modeller)	Stage and River flows	Rainfall-Runoff Model and Statistical Model
Flood Frequency (Return periods)	Flood Frequency Curves (Flood Modeler)	River Peak Flows	Statistical Model

2.4 1D Model for Zambezi River Network Set up

The 1D Model for Zambezi River network was set in the Flood Modeller GIS interface. Upstream and downstream model boundary were all set utilizing flow time, ReHF and head time boundaries. The Flow-Time boundary was set upstream of the river model and simulated by flow of $100m^3/s$ to set initial conditions. Normal-depth boundary was set downstream of the river model to estimate water levels. Figure 2 shows a complete set of a simple 1D River Model network for Zambezi river.

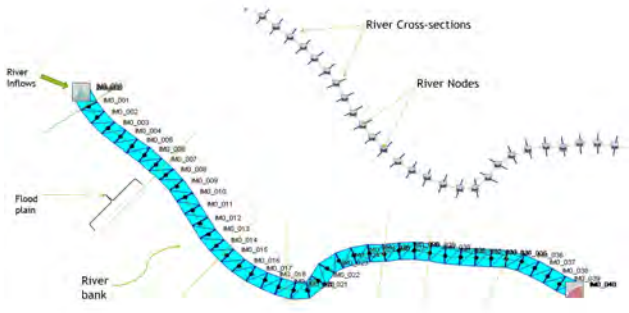

Figure 2: 1D River Model Network for Zambezi River created by Author

2.5 Rainfall Runoff model Parameters

Rainfall runoff Model (Figure 2) is made up of three components, the Loss Model, the Routing Model and Baseflow Model (representing the subsurface hydrology) all together provide Total flow as an input to the River Model (Kjeldsen, 2007).

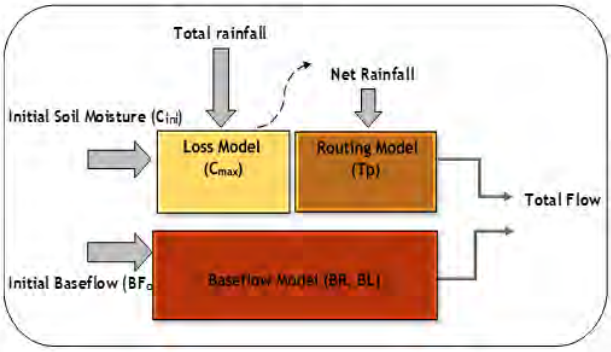

Figure 3: Schematic Representation of the Rainfall runoff Model (ReFH) as modified from (Kjeldsen, 2007).

2.6 The Loss Model Parameter

The loss model is based on the Probability Distributed Model (PDM)(Kjeldsen, 2007).

$$\frac{Q_t}{P_t} = \frac{C_{t-1}}{C_{max}} + \frac{P_t}{2C_{max}} \quad (1)$$

$$C_{ini+1} = C_{ini} + P_t \quad (2)$$

where t=1,2,3 e.t.c, (Qt/Pt) is the runoff percentage, Q(t) is Direct runoff , P(t)(mm) is Rainfall C_{ini}(mm) is initial soil moisture content, C_{max}(mm) is maximum soil moisture capacity of the catchment, (Kjeldsen and Fry, 2006; Kjeldsen, 2007).

2.7 The Routing Model Parameter

The routing model uses an instantaneous unit hydrograph (IUH) and scales it to each catchment by area and time to peak.

2.8 The Baseflow Model Parameter

The Baseflow (B) Model parameters are presented as below Kjeldsen (2007).

$$B_t = k_1 Q_{t-1} + k_2 Q_t + k_3 B_{t-1} \quad (3)$$

where t=1,2,3, B is Baseflow, Q_t is direct runoff, k_1, k_2, k_3 are Constants.

3 RESULTS

The Rainfall runoff model results (Figure 4) presents a hyetography (variation of rainfall over time), a unit hydrography $m^3/s/mm$ and hydrography (Peak Flow against time (m^3/s)). The graph indicate a Peak flow of $820m^3/s$ flood magnitude estimated from 100years return period. A 100 Year return Flood, means a flood level with a Magnitude of $820m^3/s$ has a probability of

Occurring in any given year, not necessarily after 100 years. Results for flood events of return year periods of 2, 5, 10, 15, 50,70, 100, 150 and 200 years will be presented in the full paper together with their maps. Annual Maximum (AMAX) flow peaks will be presented and will be used to validate the model results. Results of river cross-sections plots which gives information about the river (Elevation, river bed, flows, centraline, river banks, northings, eastings) and the long section plot of the entire 1D river model network will also be presented.

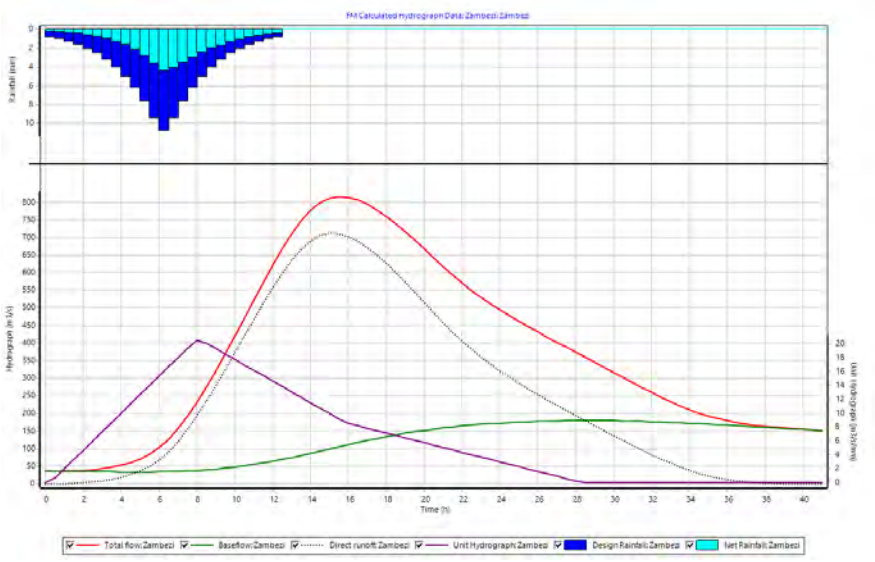

Figure 4: Peak Flow estimated at 100 years return period from a rainfall runoff model

4 CONCLUSION

Presented here are only 1D River Network Model preliminary results for Zambezi river from an on going PhD work. The full project will include a 2D Model results which will include flood Maps (1D linked to 2D). The year return periods and Annual Maximum (AMAX) flow peaks details are of significance importance especially in flood risks and Management, for example in designing Flood fences, walls, dams and bridges.

ACKNOWLEDGEMENTS

The authors acknowledge support by the UNESCO Chair on Sustainable Water Research for Climate Adaptation in Arid Environment and Namibia University of Science and Technology (2018-2021),The Namibia Meteorological Services and Hydrological Unit at Ministry of Agriculture Water and Forestry for providing the necessary ground observed data, Flood Modeller tool by Jacobs in UK and Lastly but not the least Prof Nnenesi Kgabi and Prof Sunday Reju.

References

Benson, M. (1960). Areal flood-frequency analysis in a humid region. *Hydrological Sciences Journal*, 5(3):5–15.

Grover, P. L., Burn, D. H., and Cunderlik, J. M. (2002). A comparison of index flood estimation procedures for ungauged catchments. *Canadian Journal of Civil Engineering*, 29(5):734–741.

Kjeldsen, T. and Fry, M. (2006). *Dissemination of the revitalised FSR/FEH rainfall-runoff method*. Environment Agency.

Kjeldsen, T. R. (2007). The revitalised fsr/feh rainfall-runoff method.

Machado, M. J., Botero, B. A., López, J., Francés, F., Díez-Herrero, A., and Benito, G. (2015). Flood frequency analysis of historical flood data under stationary and non-stationary modelling. *Hydrology and Earth System Sciences*, 19(6):2561–2576.

Mallebrera, M. U., Abril, A. M., and Galiano, S. G. (2011). Segura river basin: Spanish pilot river basin regarding water scarcity and droughts. In *AGRICULTURAL DROUGHT INDICES PROCEEDINGS OF AN EXPERT MEETING*, volume 1, page 2.

Ramly, S. and Tahir, W. (2016). Application of hec-geohms and hec-hms as rainfall–runoff model for flood simulation. In *ISFRAM 2015: Proceedings of the International Symposium on Flood Research and Management 2015*, pages 181–192. Springer.

Ravazzani, G., Bocchiola, D., Groppelli, B., Soncini, A., Rulli, M. C., Colombo, F., Mancini, M., and Rosso, R. (2015). Continuous streamflow simulation for index flood estimation in an alpine basin of northern italy. *Hydrological Sciences Journal*, 60(6):1013–1025.

Villarini, G., Smith, J. A., Napolitano, F., and Baeck, M. L. (2011). Analyse hydrométéorologique de la crue de décembre 2008 à rome. *Hydrological Sciences Journal*, 56(7):1150–1165.

Analysis of a Single Server Queueing Model with Working Vacation, Customer Impatience and Bernoulli Interruption

K.V.Vijayashree[1] and K.Ambika*[2]

[1]Department of Mathematics, Anna University, India
[2]Department of Applied Sciences and Humanities, Madras Institute of Technology, Anna University, Tamilnadu, India

Abstract

This paper deals with a queueing model subject to working vacation and customer impatience followed by Bernoulli scheduled vacation interruption. Customers are assumed to arrive according to a Poisson process and the single available server provides service to the arriving customers according to exponential distribution. When there are no waiting customers in the system, the server will go on a working vacation, during which the server will provide the service at a reduced rate. Customers may become impatient as a result of the slow pace of service. Depending on the demand, the server vacation may also be interrupted to enter the busy state. When the system becomes empty during the working vacation period, the server goes on a extended vacation during which no service is provided. However, customers continue to join the queue. Explicit expressions for the transient state probabilities of the model are obtained using continued fraction, generating function, and Laplace transform methods. As a special case, the theoretical results are verified with the existing results in the literature.

Keywords: Single Server Queueing Model; Customer Impatience;Bernoulli Vacation;Laplace Transforms;Generating Function.

1 Introduction

Queueing models wherein the server is unavailable to provide service for some time forms the core of vacation queueing models. Vacation queues serve as a useful tool for modelling and analyzing computer systems, communication networks, manufacturing and production systems. To cover a broad range of practical applications, it is reasonable to assume that an alternate server could replace the primary server during the vacation period. For example, in a production inventory system, the facility produces products to fulfil the customer's demands while simultaneously maintaining sufficient products in the inventory to meet the future demands. However, between any two production cycles, the idle time of the machines will be effectively used to perform maintenance action in the

*Corresponding Author. Email: ambisavi.ambika@gmail.com.

facility. This time period can be viewed as the period of vacation during which secondary task are performed at a slower rate. Another crucial aspect in the study of queueing models is customer impatience, which occurs due to the slow rate of service. The analysis of the impatience behaviour in queuing models with vacation and its variants have attracted many researchers in recent times. A study conducted by Dequan Yue and Xu (2012) examined a queueing system with the *M/M/1* model that incorporates both vacations and impatience timers, where the behavior of the timers is contingent upon the states of the server. In addition, Bouchentouf et al. (2020); Vijayashree and Ambika (2020, 2021); Selvaraju and Goswami (2013); Sampath and Liu (2020); Sudhesh et al. (2017); K.V. Vijayashree and Ambika (2021); Janani and Vijayashree (2023), and other related references have extensively investigated and conducted performance and economic analyses of various queueing models incorporating vacation/working vacation and customer impatience.

2 Motivation for the Current Model:

The motivation for developing the present model stems from the pressing need to enhance clinic management practices. In healthcare settings, challenges related to patient flow, service quality and resource utilization can lead to inefficiencies and suboptimal outcomes. By utilizing the vacation queueing approach, this study seeks to address these challenges and optimize key aspects of clinic operations. The model provides a systematic framework for analyzing patient flow dynamics, improving service quality and effectively allocating resources. Through this research, we aim to empower healthcare professionals with valuable insights that can drive improvements in patient experiences, reduce waiting times and maximize resource efficiency, ultimately leading to enhanced overall hospital management.

3 Model Description:

Consider the single available doctor providing service at the rate of μ (functional state represented by 0) for the patients who arrive in accordance with the Poisson process at rate λ. When there are no waiting customers, the doctor prefers to do online consultation (working vacation represented by state 1) at a reduced service rate of μ_v. The reduced rate of service is likely to induce a prolonged waiting time for the patients resulting in impatient behavior. We assume that customer impatience is also exponentially distributed at rate ξ. However, the vacation state of the doctor may be interrupted at times of emergency (vacation interruption) with probability $q = 1 - p$. Furthermore, when there are no customers for online consultation, the doctor can take a break for some random duration (complete vacation state represented by state 2) during which patients are allowed to join the queue and wait for service. The period of working vacation and complete vacation are both assumed to follow an exponential distribution with rate θ and θ_v respectively. Figure 1 depicts the dynamic movement between various states of the model relating to hospital management.
Let $P_{j,n}(t)$ denote the time-dependent probability for the system to be in state (j, n) where $'j'$ represents the state of the server and $'n'$ represents the number of waiting customers. Below are the presented equations that form an infinite system which governs the process:

$$P'_{1,0}(t) = -(\lambda + \theta_v)P_{1,0}(t) + (\mu_v + \xi)P_{1,1}t) + \eta P_{0,0}\,(t), \tag{1}$$

$$P'_{1,n}(t) = -(\lambda + \theta_v + \mu_v + n\xi)P_{1,n}(t) + (q\mu_v + (n+1)\xi)P_{1,n+1}(t) + \lambda P_{1,n+1}(t), \tag{2}$$

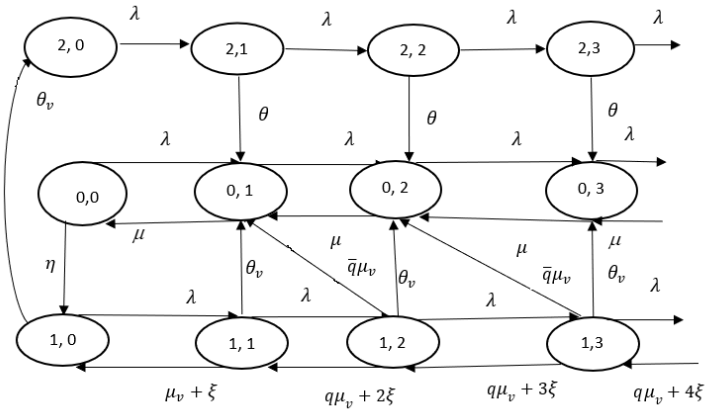

Figure 1: Visualizing State Transitions

$$P'_{2,0}(t) = -\lambda P_{2,0}(t) + \theta_v P_{1,0}(t), \tag{3}$$

$$P'_{0,0}(t) = -(\lambda + \eta) P_{0,0}(t) + \mu P_{0,1}(t), \tag{4}$$

$$P'_{2,n}(t) = -(\lambda + \theta) P_{2,n}(t) + \lambda P_{2,n-1}(t), \tag{5}$$

$$P'_{0,1}(t) = -(\lambda + \mu) P_{0,1}(t) + \theta_v P_{1,1}(t) + \mu P_{0,2}(t) + \bar{q}\mu_v P_{1,2}(t) + \theta P_{2,1}(t) + \lambda P_{0,0}(t), \tag{6}$$

and

$$P'_{0,n}(t) = -(\lambda + \mu) P_{0,n}(t) + \lambda P_{0,n-1}(t) + \mu P_{0,n+1}(t) + \theta P_{2,n}(t) + \hat{q}\mu_v P_{1,n+1}(t) + \mu_v P_{1,n}(t), \tag{7}$$

$n = 1, 2, 3, ...$

with the initial conditions $P_{1,0}(0) = 1$, and $P_{(j,n)}(t) = 0$, for all other possible values of j and n.

4 Transient Probabilities

The system of equations represented by equations (1) to (3) is transformed into a system of difference equations using Laplace transform. By applying the Laplace transform to the equations and considering the boundary conditions, explicit analytical expressions for the joint time-dependent probabilities of the system's state and the number of customers are derived. These expressions are obtained in terms of modified Bessel functions of the first kind, utilizing the generating function methodology. To describe the Laplace transform results, let is introduce $\hat{P}_{n,j}(s))$ as the Laplace transform of $P_{n,j}(t)$. By applying the Laplace transform to equations (1) to (7) and incorporating the boundary conditions, the transformed equations are as follows:

$$\hat{P}_{1,0}(s) = \left(1 + \eta \hat{P}_{0,0}(s)\right) \sum_{r=0}^{\infty} \frac{(\mu_v + \xi)^r \left[\hat{\psi}_1(s)\right]^r}{(s + \lambda + \theta_v)^{r+1}}.$$

$$\hat{P}_{1,n}(s) = \left(1 + \eta \hat{P}_{0,0}(s)\right) \hat{\psi}_n(s) \sum_{r=0}^{\infty} \frac{(\mu_v + \xi)^r \left[\hat{\psi}_1(s)\right]^r}{(s + \lambda + \theta_v)^{r+1}}, n = 1, 2, 3, \ldots$$

$$\hat{P}_{2,0}(s) = \left(1 + \eta \hat{P}_{0,0}(s)\right) \frac{\theta_v}{s + \lambda} \sum_{r=0}^{\infty} \frac{(\mu_v + \xi)^r \left[\hat{\psi}_1(s)\right]^r}{(s + \lambda + \theta_v)^{r+1}}, n = 1, 2, 3, ..$$

and

$$\hat{P}_{2,n}(s) = \left(1 + \eta \hat{P}_{0,0}(s)\right) \left(\frac{\lambda}{s + \lambda + \theta}\right)^n \frac{\theta_v}{s + \lambda} \sum_{r=0}^{\infty} \frac{(\mu_v + \xi)^r \left[\hat{\psi}_1(s)\right]^r}{(s + \lambda + \theta_v)^{r+1}}, n = 1, 2, 3, ..$$

Performing the inverse Laplace transform on the above equations yields:

$$P_{1,0}(t) = (\delta(t) + \eta P_{0,0}(t)) * \left\{ \sum_{r=0}^{\infty} e^{-(\lambda+\theta_v)t} \frac{((\mu_v + \xi)\, t)^r}{r!} * [\psi_1(t)]^{*r} \right\},$$

$$P_{1,n}(t) = (\delta(t) + \eta P_{0,0}(t)) * \psi_n(t) * \left\{ \sum_{r=0}^{\infty} e^{-(\lambda+\theta_v)t} \frac{((\mu_v + \xi)\, t)^r}{r!} * [\psi_1(t)]^{*r} \right\}, n = 1, 2, 3 \ldots$$

$$P_{2,0}(t) = (\delta(t) + \eta P_{0,0}(t)) * \theta_v e^{-\lambda t} * \left\{ \sum_{r=0}^{\infty} e^{-(\lambda+\theta_v)t} \frac{((\mu_v + \xi)\, t)^r}{r!} * [\psi_1(t)]^{*r} \right\}$$

and

$$P_{2,n}(t) = (\delta(t) + \eta P_{0,0}(t)) * \theta_v e^{-\lambda t} * \lambda^n \frac{t^{n-1} e^{-(\lambda+\theta)t}}{(n-1)!} * \left\{ \sum_{r=0}^{\infty} e^{-(\lambda+\theta_v)t} \frac{((\mu_v + \xi)\, t)^r}{r!} * [\psi_1(t)]^{*r} \right\},$$
$$n = 1, 2, 3 \ldots$$

where $\delta(t)$ denotes the Kronecker delta function and $\psi_n(t)$ denotes the inverse Laplace transform of $\bar{\psi}_n(s)$. (for details refer Vijayashree and Ambika (2021)). In these expressions, $P_{1,0}(t), P_{1,n}(t)$, $P_{2,0}(t), P_{2,n}(t)$ represent the joint time-dependent probabilities of the various system state and the number of customers. The inverse Laplace transform allows us to convert the Laplace domain representations back into the time domain, providing explicit analytical expressions in terms of the original variables.

Derivation of $P_{(0,n)}(t), n = 1, 2, 3 \ldots$

Define $Q(z,t)$ as $Q(z,t) = \sum_{n=1}^{\infty} z^n P_{0,n}(t)$

Then, $\frac{\partial Q(z,t)}{\partial t} = \sum_{n=1}^{\infty} z^n P'_{0,n}(t)$

Multiplying equation (4) by z^n and summing it over all possible values of n leads to

$$\frac{\partial Q(z,t)}{\partial t} - \left(-(\lambda + \mu) + \frac{\mu}{z} + \lambda z\right) Q(z,t)$$
$$= \theta_v \sum_{n=1}^{\infty} P_{1,n}(t) z^n + \bar{q} \mu_v \sum_{n=1}^{\infty} P_{1,n+1}(t) z^n + \theta \sum_{n=1}^{\infty} P_{2,n}(t) z^n - \mu P_{0,1}(t).$$

Integrating the above linear differential equation with respect to 't' yields—

$$Q(z,t) = \theta_v \int_0^t \sum_{n=1}^{\infty} P_{1,n}(y) z^n e^{-(\lambda+\mu)(t-y)} e^{\left(\frac{\mu}{z}+\lambda z\right)(t-y)} dy$$
$$+ \bar{q}\mu_v \int_0^t \sum_{n=1}^{\infty} P_{1,n+1}(y) z^n e^{-(\lambda+\mu)(t-y)} e^{\left(\frac{\mu}{z}+\lambda z\right)(t-y)} dy$$
$$+ \theta \int_0^t \sum_{n=1}^{\infty} P_{2,n}(t) z^n e^{-(\lambda+\mu)(t-y)} e^{\left(\frac{\mu}{z}+\lambda z\right)(t-y)} dy - \mu \int_0^t P_{0,1}(y) e^{-(\lambda+\mu)(t-y)} e^{\left(\frac{\mu}{z}+\lambda z\right)(t-y)} dy.$$

where $I_n(t)$ is the modified Bessel function of the first kind of order n. Equating the coefficient of $P_{n,1}(t)$ on either side of the above equation leads to

$$P_{0,n}(t) = \int_0^t \sum_{i=1}^{\infty} \left(\theta_v P_{1,i}(y) + \theta P_{2,i}(y) + \bar{q}\mu_v P_{1,i+1}(y)\right) \beta^{n-i} \left(I_{n-i}(\alpha(t-y)) - I_{n+i}(\alpha(t-y))\right) e^{-(\lambda+\mu)(t-y)} dy.\ n = 1, 2, 3, \ldots$$

The expression for $P_{0,0}(t)$ is explicitly obtained after rigorous computation as

$$P_{0,1}(t) = \int_0^t \sum_{i=1}^{\infty} \left(\theta_v P_{1,i}(y) + \theta P_{2,i}(y) + \bar{q}\mu_v P_{1,i+1}(y)\right) \beta^{1-i} \frac{2iI_i(\alpha(t-y))}{\alpha(t-y)} e^{-(\lambda+\mu)(t-y)} dy.$$
$$P_{0,0}(t) = C(t) * \left(\sum_{i=1}^{\infty} \left(\theta_v \psi_i(t) + \theta e^{-\lambda t} * \lambda^i \frac{t^{i-1} e^{-(\lambda+\theta)t}}{(i-1)!} + \bar{q}\mu_v \psi_{i+1}(t) \right) * e^{-(\lambda+\mu)t} \frac{iI_i(\alpha t)}{\beta^i t} \right) * \sum_{m=0}^{\infty} W^{*m}(t),$$

where $*m$ represents m-fold convolution.

$$W(t) = \eta C(t) * \sum_{i=1}^{\infty} \left(\left(\theta_v \psi_i(t) + \theta\theta_v e^{-\lambda t} * \lambda^i \frac{t^{i-1} e^{-(\lambda+\theta)t}}{(i-1)!} + \bar{q}\mu_v \psi_{i+1}(t) \right) \right)$$

and

$$C(t) = \sum_{r=0}^{\infty} e^{-\lambda t} \frac{\left((\mu_v + \xi)\, t\right)^r}{r!} * \left[\psi_1(t)\right]^{*r}.$$

5 Findings of the Numerical Study

This section emphasizes the changes in transient system size probability for various server states over time given appropriate parameters. The value of n is cut to 25 for numerical research. The other parameters are taken as $\lambda = 0.5, \mu = 0.8, \theta_v = 0.5\theta = 0.2, \mu_v = 0.8, \eta = 0.2, q = 0.8, \bar{q} = 0.2$

and $\xi = 0.1$. Figure 2 shows that as "n" increases, the probability of being in the busy state "0", decreases, suggesting a faster server operation which minimizes chances of customer overload. As "n" increases. Figure 3 shows a decreased likelihood of being in state "1", implying that extended working vacations may risk client loss. Figure 4 demonstrates a negative correlation between "n" and the probability of being in state "2", suggesting a shorter vacation duration may be necessary to mitigate client loss as "n" increases.

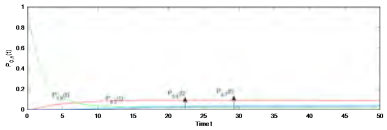

Figure 2: $P_{0,n}(t)$ Over the time 't'

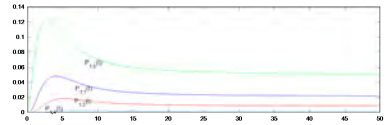

Figure 3: $P_{1,n}(t)$ Over the time 't'

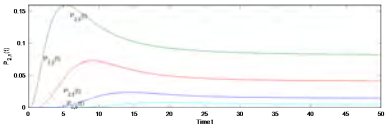

Figure 4: $P_{2,n}(t)$ Over the time 't'

6 Conclusion

This paper applies the vacation queueing model to analyze key aspects of the management of a clinic, focusing on patient flow and service quality. Through mathematical analysis, the study derives precise analytical expressions for various system states, offering insights into patient waiting times, resource utilization, and overall system performance. The models applicability and accuracy are validated through numerical figures, illustrating the impact of different parameters on the system. By utilizing the vacation queueing model, this research contributes to the valuable information for improving patient experiences, optimizing resource allocation, and enhancing overall efficiency in healthcare settings.

Acknowledgements

We would like to thank the referees for their comments, which helped improve this paper considerably

References

Bouchentouf, A. A., Guendouzi, A., and Majid, S. (2020). On impatience in M/M/1/N/DWV queue with vacation interruption. *Croatian Operational Research Review*, 11(1):21–37.

Dequan Yue, W. Y. and Xu, G. (2012). Analysis of customers' impatience in an M/M/1 queue with working vacations. *Journal of Industrial and Management Optimization*, 8(4):895–908.

Janani, B. and Vijayashree, K. (2023). Analysis of an unreliable server with soft failures and working vacations and its application in a smart healthcare system. *Results in Control and Optimization*, 10:100211.

Vijayashree.K.V, Janani,B and Ambika, K. (2021). M/M/1 queueing model with differentiated vacation and interruption. *Global and Stochastic Analysis*, 8(2):121–143.

Sampath, M. I. G. S. and Liu, J. (2020). Impact of customers' impatience on an M/M/1 queueing system subject to differentiated vacations with a waiting server. *Quality Technology and Quantitative Management*, 17(2):125–148.

Selvaraju, N. and Goswami, C. (2013). Impatient customers in an M/M/1 queue with single and multiple working vacations. *Computers and Industrial Engineering*, 65(2):207–215.

Sudhesh, R., Azhagappan, A., and Dharmaraja, S. (2017). Transient analysis of M/M/1 queue with working vacation, heterogeneous service and customers' impatience. *RAIRO - Operations Research*, 51(3):591–606.

Vijayashree, K. V. and Ambika, K. (2020). An M/M/1 queueing model subject to differentiated working vacation and customer impatience. In *Communications in Computer and Information Science*, pages 107–122. Springer Singapore.

Vijayashree, K. V. and Ambika, K. (2021). An M/M/1 queue subject to differentiated vacation with partial interruption and customer impatience. *Quality Technology and Quantitative Management*, 18(6):657–682.

M/M/1 queue with soft failures and N-Policy

B.Janani
Department of Mathematics
Rajalakshmi Institute of Technology
Chennai, Tamilnadu, India
Email: jananisrini2009@gmail.com

Abstract

The N-policy has drawn a lot of attention in the field of queue design and control. Consideration is given to a single server queueing system with soft failure and vacation. Failures are fixed right away, and as soon as they are, the system returns to its busy state. The server will wait until every customer has been served before serving any more, if any. The server will go into a dormant condition if it is idle for a prolonged period of time, and it won't be activated again until N customers have accumulated. Through the use of generating function and Laplace transform techniques, the system size probabilities in the transient state are determined in closed form.

Keywords: Soft Failure, Vacation, N policy, Dormant, Transient State

1 Introduction

The majority of the research on queuing with server failures has focused on the state of catastrophes (or disasters). In reality, catastrophes are a subset of server failures that cause system clearing; in other words, we can consider of a catastrophe as a machine failure that eliminates all system jobs simultaneously. Everyone in the line must leave right away, for instance, if a public phone or ATM breaks down. The disaster site-cleaning strategy can be used in computer systems to undertake a clearing operation on any communications that have been stored there in the event of a virus. Normal system failures, as contrast to disasters, do not shut down the entire system; instead, all customers must wait for service to restore.

2 Overview of the Model

The queueing model of a single server is considered. Arrivals join the queue at a Poisson distributed rate λ, and service occurs at an exponentially distributed rate μ. The server is subjected to random breakdowns. The breakdown can occur at any time either while providing service or even the server is idle. The random breakdowns occur at the rate β which is exponentially distributed. Once the server met with breakdown it will send to repair immediately. The repair process starts immediately which is exponentially distributed with parameter γ. During repair process arrivals are allowed to join the queue with parameter λ which is Poissonally distributed. The server will go into a dormant condition with parameter α which is exponentially distributed if it is idle for a prolonged period of time, and it won't be activated again until N customers have accumulated.

Let's use the notation $X(t)$ for the number of customers in the service line and $J(t)$ for the system's current state. The number 0,1 and 2 refers to system's state. If it is taken to be number 2, the system is thought to be in need of repair. If it is 1, the system is said to be in a functional

state. If it is in 0, the system is in dormant state. Consequently, the process $\{X(t), J(t)\}$ is a continuous time Markov chain with the transition diagram shown below

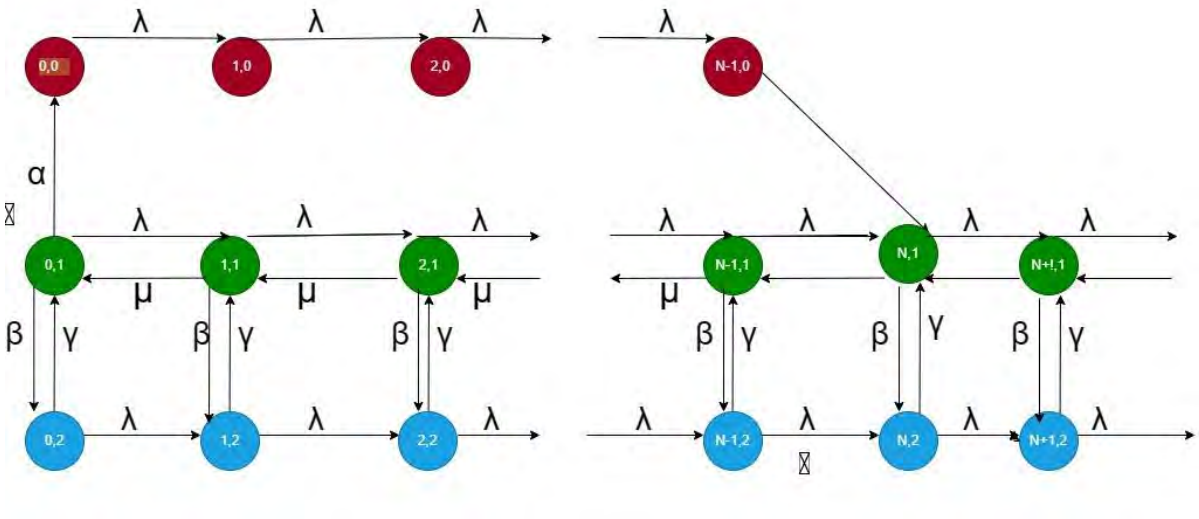

Fig. 1. Transition Diagram

Following is the model's system of governing equations.

$$P'_{0,0}(t) = -\lambda P_{0,0}(t) + \alpha P_{0,1}(t), \tag{2.1}$$

$$P'_{n,0}(t) = -\lambda P_{n,0}(t) + \lambda P_{n-1,0}(t), n = 1,2 \ldots . N-1 \tag{2.2}$$

$$P'_{0,1}(t) = -(\lambda + \alpha + \beta)P_{0,1}(t) + \mu P_{1,1}(t) + \gamma P_{0,2}(t), \tag{2.3}$$

$$P'_{n,1}(t) = -(\lambda + \mu + \beta)P_{n,1}(t) + \mu P_{n+1,1}(t) + \gamma P_{n,2}(t) + \lambda P_{n-1,1}(t), \quad n = 1,2 \ldots N-1, N+1, \ldots \tag{2.4}$$

$$P'_{N,1}(t) = -(\lambda + \mu + \beta)P_{N,1}(t) + \mu P_{N+1,1}(t) + \gamma P_{N,2}(t) + \lambda P_{N-1,1}(t) + \lambda P_{N-1,0}(t), \tag{2.5}$$

$$P'_{0,2}(t) = -(\lambda + \gamma)P_{0,2}(t) + \beta P_{0,1}(t), \tag{2.6}$$

and

$$P'_{n,2}(t) = -(\lambda + \gamma)P_{n,2}(t) + \lambda P_{n-1,2}(t) + \beta P_{n,1}(t). \quad n = 1,2,3 \ldots \tag{2.7}$$

with the initial condition $P_{0,0}(0) = 1$

3 Transient Analysis

Define

$$H(t) = \sum_{n=1}^{\infty} P_{n,2}(t), \tag{3.1}$$

Then

$$H'(t) = \sum_{n=1}^{\infty} P'_{n,2}(t). \tag{3.2}$$

Substituting the equation (2.7) in (3.2) we get

$$H'(t) + \gamma H(t) = \lambda P_{0,2}(t) + \beta \sum_{n=1}^{\infty} P_{n,1}(t), \tag{3.3}$$

Taking Laplace transform for the equation (3.3) we get

$$\widehat{H}(s) = \frac{\lambda}{s+\gamma}\hat{P}_{0,2}(s) + \frac{\beta}{s+\gamma}\sum_{n=1}^{\infty}\hat{P}_{n,1}(s), \tag{3.4}$$

Inverting the equation (3.4) yields

$$H(t) = \lambda e^{-\gamma t} * P_{0,2}(t) + \beta e^{-\gamma t} * \sum_{n=1}^{\infty} P_{n,1}(t). \tag{3.5}$$

After simplification we get,

$$\sum_{n=2}^{\infty}\hat{P}_{n,1}(s) = \sum_{j=0}^{\infty}(F(s))^j\left[\frac{-\mu}{s+\beta}\hat{P}_{1,1}(s) + \frac{\lambda}{s+\beta}\hat{P}_{0,1}(s) + \frac{\lambda\gamma}{(s+\beta)(s+\gamma)}\hat{P}_{0,2}(s) + \frac{\lambda}{s+\beta}\hat{P}_{N-1,0}(s)\right] - \hat{P}_{1,1}(s)\ . \tag{3.6}$$

where

$$F(s) = 1 - \frac{\beta\gamma}{(s+\gamma)(s+\beta)} \tag{3.7}$$

Taking Laplace transform for the equation (2.1) we get,

$$\hat{P}_{0,0}(s) = \frac{1}{s+\lambda} + \frac{\alpha}{s+\lambda}\hat{P}_{0,1}(s). \tag{3.8}$$

Taking Laplace transform for the equation (2.2) we get,

$$\hat{P}_{n,0}(s) = \left(\frac{\lambda}{s+\lambda}\right)^n \hat{P}_{0,0}(s), n = 1,2 \ldots\ldots N-1 \tag{3.9}$$

Substituting (3.8) in (3.9) gives,

$$\hat{P}_{n,0}(s) = \left(\frac{\lambda}{s+\lambda}\right)^n \frac{1}{s+\lambda} + \left(\frac{\lambda}{s+\lambda}\right)^n \frac{\alpha}{s+\lambda}\hat{P}_{0,1}(s); n = 1,2, \ldots N-1 \tag{3.10}$$

Taking Laplace transform for the equation (2.3) we get,

$$\hat{P}_{0,1}(s) = \frac{\mu}{s+\lambda+\alpha+\beta}\ \hat{P}_{1,1}(s) + \frac{\gamma}{s+\lambda+\alpha+\beta}\ \hat{P}_{0,2}(s) \tag{3.11}$$

Taking Laplace transform for the equation (2.6) we get,

$$\hat{P}_{0,2}(s) = \frac{\beta}{s+\lambda+\gamma}\ \hat{P}_{0,1}(s) \tag{3.12}$$

Substituting the equation (3.12) in (3.11) gives,

$$\hat{P}_{0,1}(s)\ = \frac{\mu}{s+\lambda+\alpha+\beta}\sum_{j=0}^{\infty}(f_1(s))^j\ \hat{P}_{1,1}(s) \tag{3.13}$$

where

$$f_1(s) = \frac{\gamma\beta}{(s+\lambda+\alpha+\beta)(s+\lambda+\gamma)} \tag{3.14}$$

Substituting the equation (3.13) into (3.8) we get,

$$\hat{P}_{0,0}(s) = \frac{1}{(s+\lambda)} + \left(\frac{\alpha}{s+\lambda}\right)\left(\frac{\mu}{s+\lambda+\alpha+\beta}\right)\sum_{j=0}^{\infty}\left(f_1(s)\right)^j \tag{3.15}$$

Inverting the equation (3.15) we get

$$P_{0,0}(t) = e^{-\lambda t} + \alpha\mu e^{-\lambda t} * e^{-(\lambda+\alpha+\beta)t} * \sum_{j=0}^{\infty}\left(f_1(t)\right)^{*j} * P_{1,1}(t) \tag{3.16}$$

where

$$f_1(t) = \gamma\beta e^{-(\lambda+\alpha+\beta)t} * e^{-(\lambda+\gamma)t} \tag{3.17}$$

Substituting the equation (3.13) into (3.10) we get,

$$\hat{P}_{n,0}(s) = \left(\frac{\lambda}{s+\lambda}\right)^n \frac{1}{s+\lambda} + \left(\frac{\lambda}{s+\lambda}\right)^n \frac{\alpha}{s+\lambda}\frac{\mu}{s+\lambda+\alpha+\beta}\sum_{j=0}^{\infty}(f_1(s))^j\ \hat{P}_{1,1}(s). \tag{3.18}$$

Inverting the equation (3.18) we get,

$$P_{n,0}(t) = \lambda^n \frac{t^n}{n!}e^{-\lambda t} + \lambda^n\alpha\frac{t^n}{n!}e^{-\lambda t} * \mu e^{-(\lambda+\alpha+\beta)t} * \sum_{j=0}^{\infty}\left(f_1(t)\right)^{*j} * P_{1,1}(t)\ . \tag{3.19}$$

Substituting the equation (3.13) into (3.12) we get,

$$\hat{P}_{0,2}(s) = \left(\frac{\beta}{s+\lambda+\gamma}\right)\left(\frac{\mu}{s+\lambda+\alpha+\beta}\right)\sum_{j=0}^{\infty}(f_1(s))^j\ \hat{P}_{1,1}(s) \tag{3.20}$$

Inverting the equation (3.20) we get,

$$P_{0,2}(t) = \mu\beta e^{-(\lambda+\gamma)t} * e^{-(\lambda+\alpha+\beta)t} * \sum_{j=0}^{\infty}\left(f_1(t)\right)^{*j} * P_{1,1}(t) \tag{3.21}$$

Substituting the equation (3.20) into (3.4) we get,

$$\hat{H}(s) = \left(\frac{\lambda}{s+\gamma}\right)\left(\frac{\beta}{s+\lambda+\gamma}\right)\left(\frac{\mu}{s+\lambda+\alpha+\beta}\right)\sum_{j=0}^{\infty}(f_1(s))^j\ \hat{P}_{1,1}(s) + \frac{\beta}{s+\gamma}\sum_{n=1}^{\infty}\hat{P}_{n,1}(s) \tag{3.22}$$

Inverting the equation (3.22) we get,

$$H(t) = \lambda e^{-\gamma t} * \beta e^{-(\lambda+\gamma)t} * \mu e^{-(\lambda+\alpha+\beta)t} * \sum_{j=0}^{\infty}\left(f_1(t)\right)^{*j} * P_{1,1}(t) + \beta e^{-\gamma t} * \sum_{n=1}^{\infty}P_{n,1}(t) \tag{3.23}$$

Substituting the equations (3.13), (3.18) and (3.20) in the equation (3.6) gives,

$$\sum_{n=2}^{\infty}\hat{P}_{n,1}(s)=\sum_{j=0}^{\infty}(F(s))^{j}\left[\frac{-\mu}{s+\beta}\hat{P}_{1,1}(s)+\frac{\lambda}{s+\beta}\frac{\mu}{s+\lambda+\alpha+\beta}\sum_{j=0}^{\infty}(f_1(s))^{j}\ \hat{P}_{1,1}(s)\right.$$
$$+\frac{\lambda\gamma}{(s+\beta)(s+\gamma)}\left(\frac{\beta}{s+\lambda+\gamma}\right)\left(\frac{\mu}{s+\lambda+\alpha+\beta}\right)\sum_{j=0}^{\infty}(f_1(s))^{j}\ \hat{P}_{1,1}(s)$$
$$\left.+\frac{\lambda}{s+\beta}\left[\left(\frac{\lambda}{s+\lambda}\right)^{N-1}\frac{1}{s+\lambda}+\left(\frac{\lambda}{s+\lambda}\right)^{nN-1}\left(\frac{\alpha}{s+\lambda}\right)\left(\frac{\mu}{s+\lambda+\alpha+\beta}\right)\sum_{j=0}^{\infty}(f_1(s))^{j}\ \hat{P}_{1,1}(s)\right]\right]$$
$$-\hat{P}_{1,1}(s)\ .$$

As all the probabilities are expressed in $\hat{P}_{1,1}(s)$, using the normalization condition we can get $P_{1,1}(t)$

4 Summary and Ideas for the future

This study takes a look at a single server queueing model with soft failures and N Policy. The server is prone to random breakdowns when delivering service or during idle periods. When the server encountered problems, the repair procedure began immediately. The server will go into a dormant condition if it is idle for a prolonged period of time, and it won't be activated again until N customers have accumulated. For the first time, explicit estimates of the transient state probabilities of an M/M/1 queue with soft failures and N policy are made. This work can be extended even further to a finite capacity and multi server system

References

1. Janani, B. (2022). Transient Analysis of Differentiated Breakdown Model. *Applied Mathematics and Computation*, *417*, 126779.
2. Janani, B., Kanagachidambaresan, G. R., & Nagarajan, D. (2022, September). Fault Tolerant Routing Design For Wireless Adhoc Sensor Network System Based On Time Dependent Probabilities of Random Vacation Model. In *2022 Second International Conference on Computer Science, Engineering and Applications (ICCSEA)* (pp. 1-6). IEEE.
3. Janani, B. (2023). Mathematical modelling of breakdowns with soft failures and explicit analytical expressions of an M/M/1 queue's transient state probabilities. *International Journal of Mathematical Modelling and Numerical Optimisation*, *13*(1), 19-33.
4. Janani, B., & Vijayashree, K. V. (2023). Analysis of an unreliable server with soft failures and working vacations and its application in a smart healthcare system. *Results in Control and Optimization*, *10*, 100211.
5. Kalidass, K., & Kasturi, R. (2012). A queue with working breakdowns. *Computers & Industrial Engineering*, *63*(4), 779-783.
6. Liu, Z., & Song, Y. (2014). The $M^X/M/1$ queue with working breakdown. *RAIRO-Operations Research*, *48*(3), 399-413.
7. Yang, D. Y., & Cho, Y. C. (2019). Analysis of the N-policy $GI/M/1/K$ queueing systems with working breakdowns and repairs. *The Computer Journal*, *62*(1), 130-143.
8. Ye, Q., & Liu, L. (2018). Analysis of $MAP/M/1$ queue with working breakdowns. *Communications in Statistics-Theory and Methods*, *47*(13), 3073-3084.

Analysis of Two Server Tandem Queueing Model having Working vacation, Re-service, Breakdown, Repair and Customer Intolerance

G. Ayyappan[1] and G. Archana @ Gurulakshmi*[2]

[1]Department of Mathematics, Puducherry Technological University, Puducherry, India
[2]Department of Mathematics, Puducherry Technological University, Puducherry, India

Abstract

A system having two heterogeneous servers with working vacation, feedback, re-service, breakdown, repair, interrupted closedown, balking and reneging is considered. The Markovian Arrival Process (MAP) is used for the customers arrival and phase type distribution are used for the service and repair time of the servers. Here we study the two heterogenous servers where one is the primary server and another one is secondary server. Customers who are gets the service from server-1 will give the positive/negative feedback of their service and if the customers are unsatisfied service from server-1 with negative feedback, they have an option to get re-service from server-2. Server-1 is considered as unreliable server, during the service time server-1 may get breakdown and immediately goes to the repair process. By using matrix analytic method, the steady state probability vector was analyzed. By using few system performance measures, we represent the numerical illustration with graphically and numerically.

Keywords: Markovian arrival process; Phase type service; Re-service; Working vacation; Customer Intolerance.

1 Introduction

The queueing problem can be seen in many real-life circumstances, including as banks, hospitals, airlines, and telecommunications. Several queueing models are developed to deliver better services to clients in a short period of time at a low cost. The concept of Markovian Arrival Process (MAP) and PH-type distribution as well as matrix analytic method was first introduced by (Neuts, 1981) and it is the generalization of exponential distribution. According to the heterogeneous queueing model, the servers offer service at varying rates. (Agarwal and Jain, 2021) initially introduced the concept of an intermittently accessible server, in which server 1 is readily available but server 2 is not; that is, server 2 does a variety of unusual and distinct jobs.

*Corresponding Author. Email: archana.g@pec.edu

2 Narration of the Model

In this model, deals a two types of tandem queue with two heterogeneous servers. Customers arrive in accordance with Markovian Arrival Process with matrix representation (D_0, D_1) of dimension m. The matrix D_0 represents for no arrival, D_1 represents the arrival of customers with infinite capacity. The fundamental arrival rates of MAP are $\lambda = \pi D_1 e_m$. The arriving customers gets service initially from server-1. After completion of service from server-1 the customers has an option to get re-service with feedback from server-2. Server-2 provides re-service only for those who are not satisfied the service from server-1. The service time of both servers which follows to phase type distribution with representation (α, T) and (β, S) of order n_1 and n_2 respectively. The feedback customers gets the re-service from server-2 with probability qf or may exit the queue with probability $(1 - qf)$. Server-1 may get breakdown during the service time then immediately goes to the repair process. The repair time is also considered as phase type distribution with parameter (β, R). After completion of the service, the server close down the system and then moves to the vacation. During the closedown time, if the customers arrives, the server starts the service to that arrived customers (Interrupted closedown). During the vacation time, if the customers arrives, the server-1 provides the service at lower rate with parameter θ. At the time of vacation, the customer may balk the system with probability b or they join the system with probability $(1 - b)$. The customer renege the system during the busy period with parameter ζ.

3 Matrix Generation under Quasi Birth and Death(QBD) Process

Let us narrate the few notation of this model which followed by generator matrix of the QBD process as follows:

Notations:

- $N_1(t)$ represents the number of customers in the system with infinite capacity at time t.
- $N_2(t)$ represents the number of customers in the buffer with finite capacity at time t.
- $C_i(t)$ stands for server-i's status at time t, where i=1,2.

$$C_1(t) = \begin{cases} 0, & \text{server-1 is in idle.} \\ 1, & \text{server-1 is busy} \\ 2, & \text{server-1 is in repair process.} \\ 3, & \text{server-1 is in closedown.} \\ 4, & \text{server-1 is idle in working vacation mode} \\ 5, & \text{server-1 is busy in working vacation mode} \end{cases}$$

$$C_2(t) = \begin{cases} 1, & \text{server-2 is busy for re-service.} \end{cases}$$

- $S_i(t)$ stands for the service phase of server-i's, where $i = 1, 2$.
- $R(t)$ stands for the repair phase of server-1.

- $A(t)$ stands for the arrival phase.

Let $\{N_1(t), N_2(t), C_1(t), C_2(t), S_1(t), S_2(t), R(t), A(t) : \quad t \geq 0\}$ is CTMC with state space as follows:

$$\Omega = l(0) \bigcup_{i=1}^{\infty} l(i)$$

where

$$\begin{aligned} l(0) =& \{(0,0,t,a) : t = 0,3,4,\ 1 \leq a \leq m\} \\ & \cup \{(0,r,t,1,c_2,a) : t = 0,3,4,\ 1 \leq r \leq K,\ 1 \leq c_2 \leq n_2,\ 1 \leq a \leq m\} \end{aligned}$$

for $i \geq 1$,

$$\begin{aligned} l(i) =& \{(i,0,t,c_1,a) : t = 0,5,\ 1 \leq c_1 \leq n_1,\ 1 \leq a \leq m\} \\ & \cup \{(i,0,2,b,a) :\ 1 \leq b \leq s,\ 1 \leq a \leq m\} \\ & \cup \{(i,r,t,1,c_1,c_2,a) : t = 1,5,\ 1 \leq r \leq K, 1 \leq c_1 \leq n_1, 1 \leq c_2 \leq n_2, \\ & \qquad\qquad 1 \leq k \leq m\} \\ & \cup \{(i,r,2,1,b,c_2,a) :\ 1 \leq r \leq K, 1 \leq b \leq s, 1 \leq c_2 \leq n_2, 1 \leq k \leq m\} \end{aligned}$$

3.1 The Infinitesimal Matrix Generation

The generating matrix Q of the CTMC is as follows:

$$Q = \begin{bmatrix} B_{00} & B_{01} & 0 & 0 & 0 & 0 & 0 & 0 & \dots \\ B_{10} & B_{11} & A_0 & 0 & 0 & 0 & 0 & 0 & \dots \\ 0 & A_2 & A_1 & A_0 & 0 & 0 & 0 & 0 & \dots \\ 0 & 0 & A_2 & A_1 & A_0 & 0 & 0 & 0 & \dots \\ 0 & 0 & 0 & A_2 & A_1 & A_0 & 0 & 0 & \dots \\ \vdots & \vdots & \vdots & \ddots & \ddots & \ddots & \ddots & \dots & \dots \end{bmatrix}.$$

The Q matrix entries B_{00}, B_{11} and A_1 represents for no arrival and no service completion, B_{01}, A_0 represents the arrival of customers and B_{10}, A_2 matrix represents the service completion with one step transition process.

4 System Analysis

We evaluate this model, beneath of the certain conditions to ensure that the system to be stable.

4.1 Analysis of System Stability condition

Let A be the matrix , where $A = A_0 + A_1 + A_2$. The invariant probability vector ς, which is referred to as a generator matrix and its satisfying

$$\varsigma A = 0, \quad \varsigma e = 1.$$

The necessary and sufficient condition of a QBD process which satisfy the condition $\varsigma A_0 e < \varsigma A_2 e$ that system to be stay in stable.

4.2 Analysis of Invariant probability vector

The invariant probability vector is denoted as X and it is divided by $X = (X_0, X_1, X_2, ...)$.
As X is a vector of Q which satisfies the relation

$$XQ = 0, \quad Xe = 1.$$

After satisfying the stability criterion, use the below equation to find the invariant probability vector X,

$$X_i = X_1 R^{i-1}, \qquad i = 2, 3, ...$$

The square matrix R created by evaluating the quadratic matrix equation, also known as the rate matrix.

$$R^2 A_2 + RA_1 + A_0 = 0.$$

By solving the following system of equations, the values of X_0 and X_1 can be determined.,

$$X_0 B_{00} + X_1 B_{10} = 0,$$
$$X_0 B_{01} + X_1 [B_{11} + RA_2] = 0,$$

with normalizing condition

$$X_0 e_{(1+Kn_2)3m} + X_1 [I - R]^{-1} e_{(2n_1+s+2Kn_1n_2+Ksn_2)m} = 1.$$

As a result, (Latouche and Ramaswami) has enhanced the calculation of the R matrix by developing a logarithmic reduction approach.

5 System Performance Measures

- When server-1 is in working vacation and server-2 is working with re-service:

$$E_{WV,BRS} = \sum_{i=1}^{\infty} \sum_{r=1}^{K} \sum_{C_1=1}^{n_1} \sum_{C_2=1}^{n_2} \sum_{a=1}^{m} i X_{ir51C_1C_2a} = X_1 (I - R)^{-1} e_{15}.$$

- Mean number of system size:

$$ES = \sum_{Z=1}^{\infty} Z X_Z e = X_1 (I - R)^{-2} e.$$

6 Numerical Results

The arrival process like $ERL - A$, $EXP - A$ and $HYP - EXP - A$ accord with renewal process and their correlation is zero. This values are taken from (Chakravarthy, 2011).
In tables , we determine the outcome of the normal service rate of server-1 (μ_1) on the expected system size (ES).
Fix $\lambda = 1$, $\mu_2 = 44$, $\theta = 0.5$, $\sigma = \eta = 2$, $\tau = 1$, $\phi = 2$, $p = 0.8$, $qf = 0.2$, $b = 0.001$, $r = 1$. We observe that from the following tables, as increasing the normal service rate of server-1 (μ_1), ES values are reduces for various combination of arrival and service times.

Table 1: Normal Service rate (μ_1) vs ES - **EXP-S**

μ_1	**EXP-A**	**ERL-A**	**HYP-A**
50	0.04581451	0.04404593	0.04697277
50.5	0.04581117	0.04404435	0.04696835
51	0.04580789	0.04404280	0.04696402
51.5	0.04580467	0.04404128	0.04695976
52	0.04580150	0.04403979	0.04695558

7 Conclusion

In this paper, a tandem queue with heterogeneous server subject to working vacation, feedback and re-service, breakdown, repair, impatient customers was studied. We considered the arrival of customers in according to Markovian arrival process and service times follows as phase type distribution. By using matrix analytic method, we found the invariant probability vector of this model. By using few performance measures, we implemented the numerical illustrations by using tables. This model can be investigate further in multi-server queue with batch arrival in according to Markovian arrival process and different service rates with working vacation under N-policy.

Acknowledgements

We would like to thank the referees for their comments, which helped improve this paper considerably

References

Agarwal, P.K., J. A. and Jain, M. (2021). $m/m/1$ queueing model with working vacation and two type of server breakdown. *Journal of Physics: Conference Series*, pages 1–15.

Chakravarthy, S. (2011). *Markovian Arrival Process*. Wiley Encyclopaedia of Operation Research and Management Science.

Latouche, G. and Ramaswami, V. *Introduction of Matrix-Analytic Methods in stochastic modeling*. Society for Industrial and Applied Mathematics, Philadelphia.

Neuts, M. (1981). *Matrix-geometric solutions in stochastic models: An algorithmic approach*. The Johns Hopkins University Press, Baltimore, London.

Optimizing inventory in business environments: Combining matrix analytical techniques with a cancellation policy, working vacation and working breakdown

G. Ayyappan[1] and N. Arulmozhi*[2]

[1]Department of Mathematics, Puducherry Technological University, Puducherry, India
[2]Department of Mathematics, Puducherry Technological University, Puducherry, India

Abstract

The inventory system of the single-server Markovian arrival process with working vacations, working breakdowns under a Bernoulli schedule, and cancellation policy are all aspects discussed in the following paper. The server begins to go on a working vacation(low service) when there is no customer in the system even if the inventory level is positive. If any customers arrive while he is end of his working vacation time, a normal busy period begins. If not, he will simply remain idle in regular mode. When a system breaks down, it either offers slow service to the current customers with probability p or immediately undergoes a repair phase with probability $q = 1 - p$. In that order, we derive the invariant vector and computation of performance measures using the matrix analytic technique.

Keywords: Working vacation, Cancellation policy, (s, Q) policy, Working breakdown, Markovian Arrival Process.

1 Introduction

An inventory is any resource that is kept to satisfy present and future needs. Spare parts, raw materials, work-in-process, and other items are examples of inventory. Inventory models are commonly utilized in hospitals, educational institutions, agriculture, industries, and banking, among other places. Queueing-inventory systems with vacations have also found broad applicability in distribution centre, manufacturing system and several other engineering systems and queueing inventory system with service facility dicussed by Berman and Sapna (2000).

1.1 Model Description

In this paper, we consider Inventory system of single server Markovian queues with working vacations, working breakdown, cancellation policy and Phase type repair. Customers arrive at the

*Corresponding Author. Email: arulmozhi.n@pec.edu

system according to a Markovian arrival process was first introduced by Neuts (1979) with a representation of (D_0, D_1) of order m. The matrix D_0 governs the transition relating to no arrival of customers. The arrival of customers is depicted in the matrix D_1 . When the inventory level is zero, arriving customers do not have permission to enter the system. The service process is divided into three stages: normal service, slow service during working vacation, and slow service during working breakdown. The normal service time of the server follows a Phase - type distribution with (γ, U) of order n. The server begins working vacation period that follows an exponential distribution η once the system gets empty and not because the inventory level has fallen to zero at a service completion moment. During the working vacation period, the server always gives slow service to customers who arrive, but the service time follows PH-distributions with depiction $(\gamma_1, \theta_1 U_1)$; $0 < \theta_1 < 1$ of order n_1. If the server examines the customer who is waiting in the system after completing this vacation, he will begin a normal busy period. Otherwise, he is dormant.

When a breakdown occurs in a regular period, we assume that the breakdowns are generated by an exponential distribution with a rate of ψ, and the system has an option: continue delivering slow service to current customers with probability p, or undergo a repair period with probability $q = 1 - p$. During the working breakdown period, the server provide slow service to current customer and service times are phase type distributed with notaion $(\gamma_2, \theta_2 U_2)$; $0 < \theta_2 < 1$ of order n_2. If no customer is present at the time of service completion during this working breakdown period, the system automatically enters a repair phase. The repair times follow Phase - type distribution with (α, T) of order l.

Due to their disappointment, customers return the purchased item. The transition rate of the product's return or cancellation is determined by $i\zeta$ whenever an item with the inventory $(S - i)$ exists. It is expected that the period of time between two successive product cancellations will be exponentially distributed. The (s, Q) strategy and lead time (β) is distributed exponentially.

2 Analysis

In the following section, we establish the queueing-inventory system's transition rate matrix. Assume that $N(t), J(t), I(t), R(t), S(t), A(t)$ described number of customers in the system, server status, inventory level, repair phases, service phases, markovian arrival phases, respectively. Consider Y=$\{Y(t) : t \geq 0\}$ where $Y(t) = \{N(t), J(t), I(t), R(t), S(t), A(t)\}$ is a $CTMC$ with state space

$$\Phi = \phi(0) \bigcup_{i=1}^{\infty} \phi(i). \tag{1}$$

where where

$\phi(0) = \{(0, 0, u_1, u_4) : u_1 \in E_S^0, u_4 \in E_m^1\} \cup \{(0, 2, u_1, u_4) : u_1 \in E_S^0, u_4 \in E_m^1\}$
$\cup \{(0, 5, u_1, u_2, u_4) : u_1 \in E_S^0, u_2 \in E_l^1, u_4 \in E_m^1\}$

and for $i \geq 1$,

$\phi(i) = \{(i, 0, 0, u_4) : u_4 \in E_m^1\} \cup \{(i, 1, u_1, u_3^{'}, u_4) : u_1 \in E_S^1, u_3^{'} \in E_{n_1}^1, u_4 \in E_m^1\}$
$\cup \{(i, 2, 0, u_4) : u_4 \in E_m^1\} \cup \{(i, 3, u_1, u_3, u_4) : u_1 \in E_S^1, u_3 \in E_n^1, u_4 \in E_m^1\}$
$\cup \{(i, 4, u_1, u_3^{''}, u_4) : u_1 \in E_S^1, u_3^{''} \in E_n^1, u_4 \in E_m^1\}$

$\cup \{(i, 5, u_1, u_2, u_4) : u_1 \in E_S^0, u_2 \in E_l^1, u_4 \in E_m^1\}$

Notations: We will need the obeying notations.

- $\otimes$ - Kronecker product of two various dimensions of matrices.
- $\oplus$ - Kronecker sum of two various dimensions of matrices reffered by Graham (1998).
- I_m- Identity matrix of $(m \times m)$ order.
- e - A column vector of the suitable size and all entries are 1.

As a result, the server is in one of the following states at any given time t:

$$J(t) = \begin{cases} 0, & \text{idle on working vacation mode,} \\ 1, & \text{busy in working vacation mode,} \\ 2, & \text{idle in normal service mode,} \\ 3, & \text{busy in normal service mode,} \\ 4, & \text{working breakdown,} \\ 5, & \text{repair} \end{cases}$$

Transition rates are:

1. Transition due to customers arrival
$(i, u_1) \to (i+1, u_1)$ with rate D_1 for $i \in N_0$, $u_1 \in E_S^0$
2. Transition due to cancellation
$(i, u_1) \to (i, u_1 + 1)$ with rate $(S-i)\zeta$ for $i \in N_0$, $u_1 \in E_S^0$
3. Transitions due to replenishment
$(i, u_1) \to (i, Q + u_1)$ with the rate β, for $i \in N_0$, $u_1 \in E_s^1$

The infinitesimal generator matrix of the Markov chain is given by:

$$Q = \begin{bmatrix} B_{00} & B_{01} & 0 & 0 & 0 & 0 & \dots \\ B_{10} & A_1 & A_0 & 0 & 0 & 0 & \dots \\ 0 & A_2 & A_1 & A_0 & 0 & 0 & \dots \\ 0 & 0 & A_2 & A_1 & A_0 & 0 & \dots \\ \vdots & \vdots & \vdots & \ddots & \ddots & \ddots & \dots \end{bmatrix} \tag{2}$$

3 Invariant Analysis

3.1 Condition for Stability

The LIQBD fashion with infinitesimal generator Q is stable if and only if

$$\boldsymbol{\chi} A_0 e < \boldsymbol{\chi} A_2 e$$

.

The stability that was found after some mathematical rearrangement is given below:

$$\begin{aligned} \chi_1[e_{n_1} \otimes D_1 e_m] + \chi_3[e_n \otimes D_1 e_m] + \chi_4[e_{n_2} \otimes D_1 e_m] + \chi_5[e_l \otimes D_1 e_m] \\ < \chi_1[(\theta_1 U_1^0 \otimes e_m)] + \chi_3[U^0 \otimes e_m] + \chi_5[\theta_2 U_2^0 \otimes e_m]. \end{aligned} \tag{3}$$

3.2 The Transition Probability Vector

Let y be the transition probability vector of the infintesimal generator Q of the process {Y(t): $t \geq 0$}. The subdivision of y by level as, $y = (y_0, y_1, y_2, ...)$, where y_0 is of dimension $(2(S+1)m + (S+1)lm)$ for $i = 0$ and $y_1, y_2, ...$ are of dimension $(2m + Sn_1m + Snm + Sn_2m + (S+1)lm)$ for $i \geq 1$. As y is a vector satisfies the relation

$$yQ = 0 \text{ and } ye = 1$$

Furthermore, while the stability criterion is satisfied, the equation gives the various levels.

$$y_j = y_1 R^{j-1},\ j \geq 2 \tag{4}$$

where R is the smallest non-negative solution of the quadratic equation

$$R^2 A_2 + RA_1 + A_0 = 0$$

and satisfies the relation $RA_2e = A_0e$ and the vector y_0, y_1 are obtained with the help of succeeding equations:

$$y_0 B_{00} + y_1 B_{10} = 0 \tag{5}$$
$$y_0 B_{01} + y_1 [A_1 + RA_2] = 0 \tag{6}$$

subject to normalizing condition

$$y_0 e_{2(S+1)m+(S+1)lm} + y_1 [I - R]^{-1} e_{2m+Sn_1m+Snm+Sn_2m+(S+1)lm} = 1 \tag{7}$$

As a result, we can compute matrix R using Logarithmic Reduction Algorithm in Latouche and Ramaswami (1993).

4 System characteristics

- Expected number of customers in the system

$$E_{system} = \sum_{i=1}^{\infty} i x_i e$$

- Expected number of items in the inventory level

$$E_{IL} = \sum_{u_1=1}^{S} u_1 [x_{00u_1} e + x_{02u_1} e + x_{05u_1} e] + \sum_{i=0}^{\infty} \sum_{u_1=1}^{S} u_1 [x_{i1u_1} e + x_{i3u_1} e + x_{i4u_1} e + x_{i5u_1} e]$$

- Expected replenishment rate

$$E_{RR} = \beta \left[\sum_{u_1=0}^{s} (x_{00u_1}e + x_{02u_1}e + x_{05u_1}e) + \sum_{i=0}^{\infty} \sum_{u_1=1}^{s} (x_{i1u_1}e + x_{i3u_1}e + x_{i4u_1}e + x_{i5u_1}e) \right]$$

- Expected reorder rate

$$E_R = x_{11s+1}(U_1^0 \otimes I_m)e + \sum_{i=2}^{\infty} x_{i1s+1}(U_1^0\gamma_1 \otimes I_m)e + x_{13s+1}(U^0 \otimes I_m)e + \sum_{i=2}^{\infty} x_{i3s+1}(U^0\gamma \otimes I_m)e + x_{14s+1}(U_2^0 \otimes I_m)e + \sum_{i=2}^{\infty} x_{i4s+1}(U_2^0\gamma_2 \otimes I_m)e$$

5 Conclusion

In this article, we discussed the queueing-inventory system's cancellation policy, working vacation and working breakdown. This study contributes to the improvement of an inventory management system's (s, Q) policy. We presented mean system size with various distributions for arrival customer. The effects of expected rates like system reorder and inventory levels are indicated.

References

Berman, O. and Sapna, K. (2000). Inventory management at service facilities for systems with arbitrarily distributed service times. *Stochastic Models*, 16:343–360.

Graham, A. (1998). *Kronecker Products and Matrix Calculus with Applications*. Ellis Harwood Ltd, Chichester.

Latouche, G. and Ramaswami, V. (1993). A logarithmic reduction algorithm for quasi-birth-death processes. *Journal of Applied Probability*, 30:650–674.

Neuts, M. F. (1979). A versatile markovian point process. *Journal of Applied Probability*, 16:764–779.

Type I Heavy-Tailed Family of Generalized Burr III Distributions with Applications

Wilbert Nkomo, Broderick Oluyede and Fastel Chipepa

June 26, 2023

Abstract

Keywords: Type I heavy-tailed, Odd Burr III, Generalized distribution, Maximum likelihood estimation, Moments, Actuarial measures.

We introduce a novel family of distributions called Type I Heavy-Tailed family of generalized Odd Burr III (TI-HT-G-OBIII) distributions. We are motivated by the desirable properties resulting in extending existing distributions, in this case, through the use of the Type-I Heavy-Tailed-G (TI-HT-G) by Zhao et al. [9] and the generalized Odd Burr III (G-OBIII) families of distributions by Alizadeh et al. [1]. Replacing the baseline cumulative distribution function (cdf) of the TI-HT-G family of distributions with the G-OBIII family of distributions yields the new family of distributions called TI-HT-G-OBIII distributions with cdf and probability density function (pdf) given by

$$F(x;c,k,\theta,\psi) = 1-\left(\frac{1-\left[1+\left(\frac{1-G(x;\psi)}{G(x;\psi)}\right)^{c}\right]^{-k}}{1-(1-\theta)\left[1+\left(\frac{1-G(x;\psi)}{G(x;\psi}\right)^{c}\right]^{-k}}\right)^{\theta} \quad (1)$$

and

$$\begin{aligned} f(x;c,k,\theta,\psi) &= \frac{\theta^2 ckg(x;\psi)\left[1+\left(\frac{1-G(x;\psi)}{G(x;\psi)}\right)^{c}\right]^{-k-1}(1-G(x;\psi))^{c-1}}{(G(x;\psi))^{c+1}} \\ &\times \left\{1-\left[1+\left(\frac{1-G(x;\psi)}{G(x;\psi)}\right)^{c}\right]^{-k}\right\}^{\theta-1} \\ &\times \left\{1-(1-\theta)\left[1+\left(\frac{1-G(x;\psi)}{G(x;\psi)}\right)^{c}\right]^{-k}\right\}^{-(\theta+1)}, \quad (2) \end{aligned}$$

respectively for $c,k,\theta>0$ and baseline parameter vector ψ.

The hazard rate function (hrf) of the TI-HT-G-OBIII family of distributions is

$$\begin{aligned} h(x;c,k,\theta,\psi) &= \frac{\theta^2 ckg(x;\psi)\left[1+\left(\frac{1-G(x;\psi)}{G(x;\psi)}\right)^c\right]^{-k-1}(1-G(x;\psi))^{c-1}}{(G(x;\psi))^{c+1}} \\ &\times \left\{1-\left[1+\left(\frac{1-G(x;\psi)}{G(x;\psi)}\right)^c\right]^{-k}\right\}^{-1} \\ &\times \left\{1-(1-\theta)\left[1+\left(\frac{1-G(x;\psi)}{G(x;\psi)}\right)^c\right]^{-k}\right\}^{-1}, \end{aligned} \tag{3}$$

for $c,k,\theta>0$, and baseline parameter vector ψ.
The linear representation of TI-HT-G-OBIII family of distributions is given by

$$\begin{aligned} f(x;c,k,\theta,\psi) &= \sum_{r,s,t,v,w=0}^{\infty}(-1)^{r+s+v+w}(1-\theta)^r ck\theta^2\binom{-(\theta+1)}{r}\binom{\theta-1}{s} \\ &\times \binom{-[k(r+s+1)+1]}{t}\binom{-c(t+1)-1}{v}\binom{v+c(t+1)-1)}{w} \\ &\times \left(\frac{(w+1)}{(w+1)}\right)G^w(x;\psi))g(x;\psi) \\ &= \sum_{w=0}^{\infty}\eta_{w+1}g_{w+1}(x;\psi), \end{aligned} \tag{4}$$

where $g_{w+1}(x;\psi) = (w+1)G^w(x;\psi))g(x;\psi)$ is the exponentiated-G (Exp-G) distribution with power parameter $(w+1)$ and

$$\begin{aligned} \eta_{w+1} &= \sum_{r,s,t,v=0}^{\infty}(-1)^{r+s+v+w}(1-\theta)^r ck\theta^2\binom{-(\theta+1)}{r}\binom{\theta-1}{s}\left(\frac{1}{w+1}\right) \\ &\times \binom{-[k(r+s+1)+1]}{t}\binom{-c(t+1)-1}{v}\binom{v+c(t+1)-1)}{w}. \end{aligned} \tag{5}$$

Therefore, the TI-HT-G-OBIII family of distributions can be written as an infinite linear combination of the Exp-G densities from which structural properties of the TI-HT-G-OBIII family of distributions including moments, order statistics, probability weighted moments, and Rényi entropy were deduced.

Sub-families of the new distribution were deduced and some special cases were presented for the Weibull, Kumaraswamy and Pareto (type I) baseline distributions to demonstrate flexibility and adaptability of the developed distribution in handling both monotonic and non-monotonic hazard rate shapes.

Risk measures such as value at risk (VAR), tail value at risk (TVaR), tail variance (TV) and tail variance premium (TVP) were also derived. Numerical simulations for the risk measures of the TI-HT-OBIII-W, a member of the TI-HT-G-OBIII were obtained, studied and compared to the type I heavy-tail Weibull (TI-HT-W) and a sub-model of the TI-HT-OBIII-W. The results were based on random samples of size n=100 for 1000 repetitions generated from each one of the used distributions. Numerical simulations results showed that the Type I Heavy-Tailed Odd Burr III-Weibull (TI-HT-OBIII-W) had higher values of VaR, TVaR, TV and TVP proving that it has a heavier tail compared to the selected models.

Model parameters were estimated using the maximum likelihood method. We conducted a Monte Carlo simulation study to evaluate the consistency of the estimates using mean square errors and average bias. We observed that the mean values approximated the true parameter values and the root mean square error and average bias decayed towards zero for all parameters as the sample size gets large.

Two real data examples were fitted to the TI-HT-OBIII-W distribution and compared to several non-nested models including some known Heavy-Tailed distributions. The following goodness-of-fit (GoF) statistics were used: -2 log likelihood ($-2\log(L)$), Akaike Information Criterion ($AIC = 2p - 2\log(L)$), Consistent Akaike Information Criterion ($CAIC = AIC + 2\frac{p(p+1)}{n-p-1}$), Bayesian Information Criterion ($BIC = p\log n - 2\log(L)$ (where n is the number of observed parameters, while the number of calculated parameters is p), Cramér-von Mises (W^*) and Andersen-Darling (AD). These statistics were used to verify the model that fits best for a given data set. Preference is given to the model with the highest K-S statistic p-value and the lowest value for other statistics criteria. The TI-HT-OBIII-W distribution was compared to the transmuted exponentiated generalized Weibull distribution (TExGW) proposed by Yousof et al. [8], the type I heavy-tailed Weibull distribution (TI-HT-W) introduced by Zhao et al. [9], the heavy-tailed beta power transformed Weibull distribution (HTBPTW) introduced by Zhao et al. [10], the Weibull Lomax distribution (WL) by Tahir et al. [6], Kumaraswamy Weibull distribution (KW) introduced by Cordeiro et al. [4] and the exponential Lindley odd log-logistic Weibull (ELOLLW) proposed by Korkmaz et al. [5].

The first dataset represents stress-rupture life data, a real life example also presented by Cooray and Ananda [3], also reported by Cordeiro et al. [2] was fitted to the TI-HT-OBIII-W distribution and other non-nested models, including some known heavy-tailed distributions. The TI-HT-OBIII-W model performed better than the non-nested models.

Moreso, the TI-HT-OBIII-W model closely followed both the empirical cumulative distribution function (ECDF) and the Kaplan-Meier (K-M) curves on the stress-rupture life. The total time on test (TTT) plots and hazard rate function (hrf) plots suggested a non-monotonic hazard rate.

The second data set applied was taken from Xu et al [7]. (2003, Applied Soft Computing), describing a reliability study on turbochargers in diesel engines. The TI-HT-OBIII-W model out-competed the contending models evidenced by the probability plots and superimposed densities as well as goodness-of -fit statistics. The TI-HT-OBIII-W closely followed ECDF and K-M survival curves proving that the model truly describes the data very well.

The newly suggested model is exceptionally adaptable and outperforms several well-known statistical models including those that are heavy-tailed.

References

[1] Alizadeh, M., Cordeiro, G., Nascimento, A., Lima, and M. Ortega, E.M.M., (2017). Odd Burr Generalized Family of Distributions with some Applications, *Journal of Statistical Computation and Simulation* 87, pp. 367 389.

[2] Cordeiro, G. M., Alizadeh, M., and Ortega, E. M., (2014). The Exponentiated Half-logistic Family of Distributions: Properties and Applications. *Journal of Probability and Statistics*.

[3] Cooray, K. and Ananda, M. M., (2008). A Generalization of the Half-normal Distribution with Applications to Lifetime Data. *Communications in Statistics Theory and Methods*, 37(9), pp. 1323–1337.

[4] Cordeiro, G. M., Ortega, E. M. and Nadarajah, S., (2010). The Kumaraswamy Weibull Distribution with Application to Failure Data. *Journal of the Franklin Institute*, 347(8), pp. 1399–1429.

[5] Korkmaz, M. C., Yousof, H. M. and Hamedani, G. G., (2018). The Exponential Lindley odd Log-Logistic-G Family: Properties, Characterizations and Applications. *Journal of Statistical Theory and Applications*, 17(3),pp. 554-571.

[6] Tahir, M., Cordeiro, G. M., Zubair, M., (2014). The Weibull-Lomax distribution: Properties and Applications. *Hacettepe University Bulletin of*

Natural Sciences and Engineering Series B: Mathematics and Statistics. 10.15672/HJMS.2014147465.

[7] Xu, K., Xie, M., Tang, L. Ching., and Ho, S. L., (2003). Application of Neural Networks in Forecasting Engine Systems Reliability. *Applied Soft Computing.* 2, pp 255-268.

[8] Yousof, H. M., Afify, A. Z., Alizadeh, M., Butt, N. S., Hamedani, G., Ali, M. M., (2015). The Transmuted Exponentiated Generalized-G Family of Distributions. *Pakistan Journal of Statistics and Operation Research*, 11(4), pp. 441-464.

[9] Zhao, W., Khosa, S.K., Ahmad, Z., Aslam M., Afify, A.Z., (2020). Type-I Heavy-Tailed Family with Applications in Medicine, Engineering and Insurance. *PLoS ONE* 15(8): e0237462.

[10] Zhao, J., Ahmad, Z., Mahmoudi, E., Hafez, E. H., and Mohie El-Din, M. M., (2021). A New Class of Heavy-Tailed Distributions: Modeling and Simulating Actuarial Measures. *Dynamic Analysis, Learning, and Robust Control of Complex Systems*, Article ID 5580228, pp. 1-18

Gesturing as a problem solving strategy in Mathematics: The case of nonverbal reasoning

Beata Dongwi

St Paul's College Namibia; bdongwi@spcnam.org

Introduction

Although verbal utterances often come to mind first when considering communication, no discussion of communication is complete without the inclusion of nonverbal communication (Matsumoto, Frank, & Hwang, 2017). Nonverbal representations of ideas are common in mathematics instruction (Alibali et al., 2014) and serve many functions. However, in this paper, the focus is on nonverbal reasoning while solving mathematical problems. Bodily movements that mediate gestures are essential to mathematics problem solving, as they constitute mental processes such as thinking, reasoning and sense making. Alibali and Nathan (2012) assert that "gestures are often taken as evidence that the body is involved in thinking and speaking about the ideas expressed in those gestures" (p. 248).

Case study

In this paper, the focus is on the students' solutions to the "Dice task":

The dice task

On a dice, the number on opposite faces add up to 7. The dice in the diagram is rolled edge over edge along the path until it rests on the square labelled X. What is the number on top in that position?

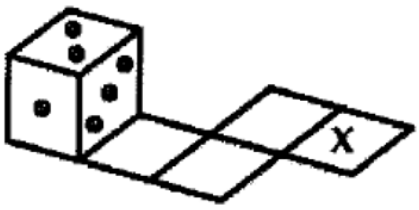

Figure 1: The dice task

This was one of the problems that the students were asked to solve during individual task-based interviews. The tasks were designed to evoke the use of visual methods as opposed to linear algebra hence the argument is on the efficacy of nonverbal thinking and reasoning in mathematical problem solving. Some were purely word problems and others were word problems accompanied by a diagram (Figure 1). The students solved the tasks in the presence of the author and the interviews were video-recorded. Video recordings provided access to the data that would not otherwise be available in other forms of data collection. It enables the researcher to ascribe meaning to the participants' bodily movements, facial expressions and other forms nonverbal utterances, which I refer to as gestures in this paper.

Students' solutions: three gestural categories

From the data, I have noticed that students first form a mental image of the problem irrespective whether it has an accompanying diagram or not. These mental images were observed via gestures and accessed through probing. The use of gestures in this study, and specifically in this "Dice task", are be grouped into three categories: perceptual aspects drive theoretical aspects (or not), blending perceptual and theoretical aspects, and theoretical aspects drive perceptual aspects (or not). It is however noteworthy to state that the students did not need to get the answers right in order to affirm their use of gestures in problem solving strategies. The data analysis classified a variety of visual aspects but I do not have space to report on them here.

A) Perceptual aspects drive theoretical aspects (or not)

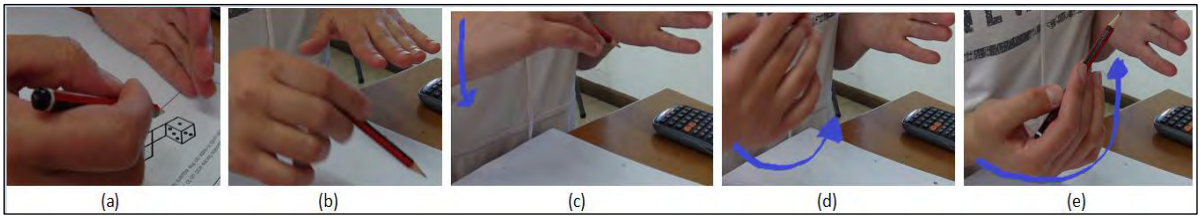

Figure 2: Ellena's gestures during the cube task

Ellena's left hand represents the position (orientation) of the dice while her right hand shows the direction of the next move. She uttered, "*This one goes here*" (b) before she became silent and used gestures in (c) through (e). The sequence of her movement through these gestures was top-side-bottom. After a few cycles of hand gestures and whispers, she requested for a model of a cube that she used to find the solution. She calibrated the model with numbers from 1 to 6, depicting the numbers on the faces of a dice that she literally rolled next to the given diagram. She pronounced three as the answer to the question. Unlike other participants, there was little to no confusion in Ellena's problem solving strategy for this task. She constantly reminded herself of what the main question was and she often repeated it "*what is the number on top in that position?*" Hence, as she rolled the dice both in her mind and on paper, she kept her goal in check.

For this task, Ellena did not make any calculations or any drawings. She only used mind pictures combined with hand gestures for her problem-solving strategy.

B) Blending between perceptual and theoretical aspects

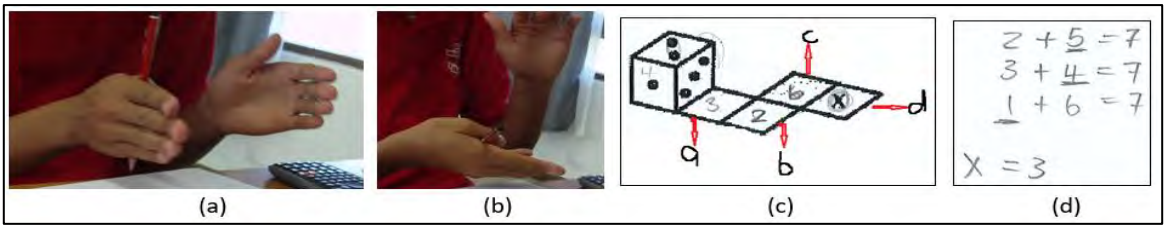

Figure 3: Jordan's gestures during the cube task

Jordan related the dice in the given diagram to a cube when he visualised the opposite sides of the dice. "*So if it is a cube, this side and this side will add up to 7, each one of the opposite faces*" (Figure 3a). He silently used hand gestures as he proceeds through problem solving. Asked to reveal what was in his mind he explained as follows:

> *See now this one is two* [circles the top of a dice with a pencil and writes 2 as he speaks (Figure 3a)] *and the opposite will be 4…no… sorry 5 is equal to 7…we are looking for what will be the number when it fell on x* [circles the *x*]. *So it's gonna be 3 plus 4 is equal to 7, 1 plus 6 equals... When it's lying like that* [uses his hands to demonstrate the movement (KI) (Figure 3b)], *it will lie on 3* [writes 3, 2 and 6 on the square path to indicate the number that will land on each square as the dice is rolled (Figure 3c)]. *…the opposite number will be 4, so when it move to the side, 3, 2* [uses a pencil to visualise a rolling dice], *6 and 1 then it will be… Okay* [holds his arms and rolling his head as if though moving a dice from one square to the next] *here we have 3; x equals to 3*.

Thus, Jordan visually demonstrated the actual rolling of the given dice by blending the perceptual with the theoretical. Although he initially thought $x = 3$ was the solution to question, he later rectified it as he concluded that 3 was the number on top when 4 landed on square X.

C) Theoretical aspects drive perceptual aspects (or not)

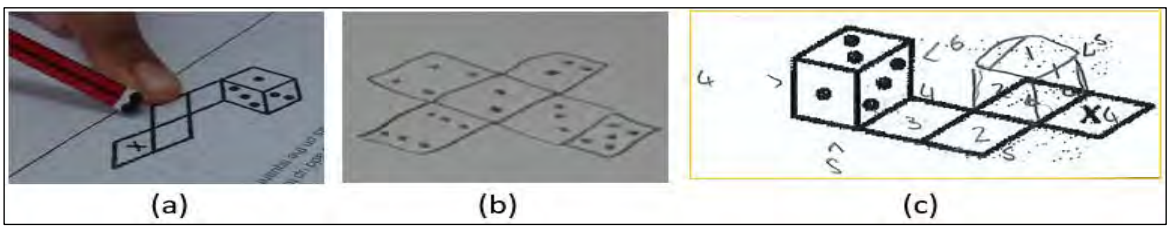

Figure 4: Millie's gestures during the cube task

Millie paused a few times whenever she reached the third square with her imaginary rolling dice (Figure 4a). She would then repeat the whole rolling process all over again. She admitted at one point to have gotten a little confused by the dynamic pictures in her mind. She sketched

a net of the dice (Figure 4b), turned the whole worksheet around to ensure a true representation of the given diagram. She worked from the net to sketch a dice on the third square (Figure 4c). Using the two sketches, she gestured with her fingers as she again imaginatively moved her dice this time through the third square.

Just because we have only seen Millie's theoretical aspect of the "Dice task", this does not imply that the whole process was only theoretical. It also could mean that much of her gestural utterances occurred as mental images that could not be visually observed. However, if we look at another task that she solved, we can see how the blending of her nonverbal utterances with her verbal utterances. With Millie, it depends on the type of the task. As we illustrated in Figure 5, she added her own theoretical aspects to the given diagram but in other cases were the tasks did not have any accompanying diagrams, her gestures took a different format. Figure 5 below illustrate Millie's gestures coupled with verbal utterances of the clock task:

> *...now imagine a clock is behind you and you can see it in the mirror. There are dots instead of numbers. The hands look as if though they are saying twenty-five to three. What time is it really?*

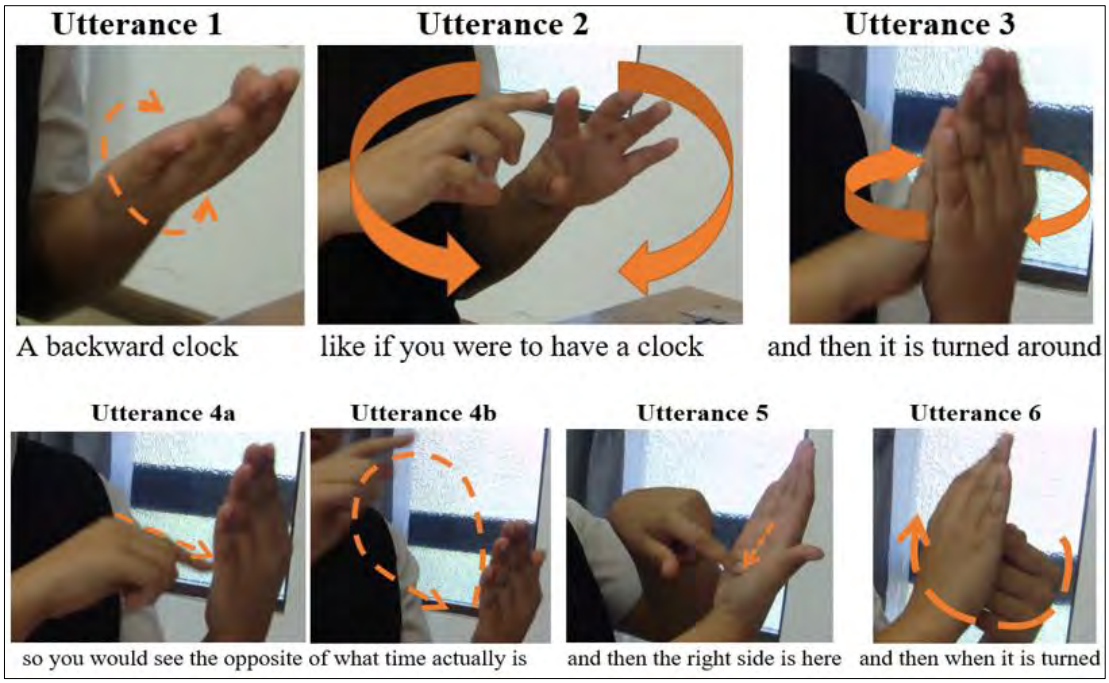

Figure 5: Millie's gestures during the clock task

This shows that the types of gestures that a student uses in problem solving depend inter alia on the nature of the task and not necessarily on the student's preference of visual imagery as opposed to algebraic methods.

Conclusion

The findings demonstrate how gestures and gesturing played an important role in mathematical (word) problem solving, which was prevalent in all selected students' responses. Further, students engaged different types of gestures to construct mathematical meaning, which was strongly embedded in their bodily actions. That is, no amount of technological advancement shall be able to replace the human effect of gesturing as a thinking and reasoning process as a gestures are embodied.

References

Alibali, M. W., & Nathan, M. J. (2012). Embodiment in mathematics teaching and learning: Evidence from learners' and teachers' gestures. *Journal of the Learning Sciences*, *21*(2), 247–286.

Alibali, M. W., Nathan, M. J., Wolfgram, M. S., Church, R. B., Jacobs, S. A., Johnson Martinez, C., & Knuth, E. J. (2014). How Teachers Link Ideas in Mathematics Instruction Using Speech and Gesture: A Corpus Analysis. *Cognition and Instruction*, *32*(1), 65–100. https://doi.org/10.1080/07370008.2013.858161

Matsumoto, D., Frank, M. G., & Hwang, H. S. (2017). *Nonverbal communication science and applications*. *Sage Publications Inc.* Los Angeles. https://doi.org/10.4324/9781351308724

An Investigation on M/PH/1 Queueing Model with Single Working Vacation, Breakdown, Repair and Standby Server

BABY SAROJA K[1] and SUVITHA V*[2]

[1,*2]Department of Mathematics, Faculty of Engineering and Technology, SRM Institute of Science and Technology, Kattankulathur 603 203, India

Abstract

We consider a single server queueing model with three service types, each with three phases. In which the customers arrive according to a Poisson process and the service time of each customer follows Hyper-Erlang distribution. We analysed the model with interruptions, such as breakdown, repair and single working vacation. The standby server works whenever the main server under breakdown. Using the matrix geometric method, the steady-state probability vector of the model is examined and finally, some numerical examples are presented.

Keywords: Hyper-Erlang distribution; Breakdown; Repair; Single working vacation; Standby server.

1 Introduction

In queuing theory, specific algorithms have been developed by Neuts (5) and Latouche & Ramaswami (4) for queues in which service times are Phase type distributed. Later Chakrvarthy (2) developed the Matrix Geometric Method. Xu et al. (6) analyzed the performance of a Hyper-Erlang queueing model for wireless nertwrok nodes. Deepa and Kalidass (3) studied an $M/M/1/N$ queue with working breakdowns and vacations. Chakravarthy and Kulshrestha (1) considered the queueing model with server breakdown, repair, vacations, backup server and analyzed the system using matrix geometric method. The integration of literature review and the development of a mathematical model establishes a strong foundation for our research.

2 Description of the Mathematical Model

1. We assume that the customers arrive into the system according to Poisson process.

*Corresponding Author. Email:suvithav@srmist.edu.in

2. The system has a single server with three types of service. When the customers enter the system, they can select any type of service with probabilities $\delta_1, \delta_2, \delta_3$ with service rate $\gamma_1, \gamma_2, \gamma_3$. Each type of service follows Erlang phase-type (PH) distribution. Hence, the service distribution follows Hyper-Erlang distribution.

3. The main server goes on a working vacation when the system is empty and provides service at a reduced rate whenever the customers arrive into the system at that time. The duration of working vacation is modeled with an exponential distribution with rate α. The main server may get breakdown during the busy or working vacation period with rate ψ and is sent for repair immediately, and at that moment the standby server instantaneously takes over the service. When a repair is completed, the very next moment the main server takes over the service from the standby server. Also, make a note that the standby server does not breakdown. The repair times are exponentially distributed with rate ϵ.

4. The duration of service offered by the main server in busy peiod, working vacation period and also the standby server are considered to be PH distribution denoted by (β, V), $(\beta, \tau V)$ and $(\beta, \zeta V)$, of order n respectively. Note that the service rate of the main server in busy period, working vacation period and the standby server are given by μ, $\tau\mu$ and $\zeta\mu$ respectively, where $\mu = [\beta(-V)^{-1}e]^{-1}$. Moreover, we denote V^0 as the column vector satisfying $Ve + V^0 = 0$.

$$V = \begin{bmatrix} -\mu_1 & 0 & 0 \\ 0 & -\mu_2 & 0 \\ 0 & 0 & -\mu_3 \end{bmatrix}, \quad V^0 = \begin{bmatrix} \mu_1 \\ \mu_2 \\ \mu_3 \end{bmatrix}$$

where $\mu_1 = \mu_2 = \mu_3 = 3\mu$, since the service time of each type follows Erlang distribution.

3 The Quasi Birth-Death Process

Now, we define the variables needed to describe the model under study.

- $N(t)$ indicates the number of customers in the system at time t.
- $S(t)$ indicates the state of the server at time t.

$$S(t) = \begin{cases} 1, & \text{main server is busy} \\ 2, & \text{main server under repair and} \\ & \text{standby server on progress} \\ 3, & \text{main server under working vacation} \end{cases}$$

- $B(t)$ indicates the phase of service process at time t.
- $J(t)$ indicates the type of service at time t.

Then $\{(N(t), S(t), B(t), J(t)), t \geq 0\}$, is a continuous-time Markov chain with state space as

$$\Omega = S(0) \cup S(i)$$

where,
$S(0) = \{(0, s) : 1 \leq s \leq 3\}$ and $S(i) = \{(i, s, b, j) : 1 \leq s \leq 3;\ 1 \leq b \leq 3;\ 1 \leq j \leq 3\}$, for $i \geq 1$.
The generator matrix is as below,

$$Q = \begin{bmatrix} B_{00} & B_{01} & \dots & & \\ B_{10} & A_1 & A_0 & \dots & \\ \vdots & A_2 & A_1 & A_0 & \dots \\ & \vdots & A_2 & A_1 & A_0 & \dots \\ & & \vdots & \vdots & \vdots & \end{bmatrix}$$

4 Main Results

We compute the steady-state probabilities of the system by using the matrix-geometric method.

4.1 The Stability Condition

Let the stationary probability vector π be partitioned as

$$\pi_l = \{(\pi_{l1}, \pi_{l2}, \pi_{l3}), 1 \leq l \leq 9\}$$

of the irreducible generator $A = A_0 + A_1 + A_2$.

$$A = \begin{bmatrix} T_1 & \delta_2\gamma_1V^0\beta & \delta_3\gamma_1V^0\beta & \psi I_3 & 0 & 0 & 0 & 0 & 0 \\ \delta_1\gamma_2V^0\beta & T_2 & \delta_3\gamma_2V^0\beta & 0 & \psi I_3 & 0 & 0 & 0 & 0 \\ \delta_1\gamma_3V^0\beta & \delta_2\gamma_3V^0\beta & T_3 & 0 & 0 & \psi I_3 & 0 & 0 & 0 \\ \epsilon I_3 & 0 & 0 & T_4 & \delta_2\zeta\gamma_1V^0\beta & \delta_3\zeta\gamma_1V^0\beta & \epsilon I_3 & 0 & 0 \\ 0 & \epsilon I_3 & 0 & \delta_1\zeta\gamma_2V^0\beta & T_5 & \delta_3\zeta\gamma_2V^0\beta & 0 & \epsilon I_3 & 0 \\ 0 & 0 & \epsilon I_3 & \delta_1\zeta\gamma_3V^0\beta & \delta_2\zeta\gamma_3V^0\beta & T_6 & 0 & 0 & \epsilon I_3 \\ \alpha I_3 & 0 & 0 & \psi I_3 & 0 & 0 & T_7 & \delta_2\tau\gamma_1V^0\beta & \delta_3\tau\gamma_1V^0\beta \\ 0 & \alpha I_3 & 0 & 0 & \psi I_3 & 0 & \delta_1\tau\gamma_2V^0\beta & T_8 & \delta_3\tau\gamma_2V^0\beta \\ 0 & 0 & \alpha I_3 & 0 & 0 & \psi I_3 & \delta_1\tau\gamma_3V^0\beta & \delta_2\tau\gamma_3V^0\beta & T_9 \end{bmatrix}$$

where,

$$T_g = \begin{cases} \gamma_k(V + \delta_k V^0\beta) - \psi I_3, & k = g,\ 1 \leq g \leq 3; \\ \gamma_k(\zeta V + \delta_k\zeta V^0\beta) - 2\epsilon I_3, & k = g-3, 4 \leq g \leq 6; \\ \gamma_k(\tau V + \delta_k\tau V^0\beta) - (\alpha + \psi)I_3, & k = g-6, 7 \leq g \leq 9; \end{cases}$$

The steady-state equations should satisfy $\pi A = 0$, $\pi e = 1$ and using the condition $\pi A_0 e < \pi A_2 e$ from (5), we obtain the stability condition of the proposed model.

4.2 Analysis of the steady-state probability vector

Let $P = (p_0, p_1, p_2, ...)$ be the steady-state probability vector associated with Q. Let

$$p_0 = (p_{01}, p_{02}, p_{03}), \tag{1}$$

$$p_i = (p_{i11}, p_{i12}, p_{i13}, p_{i21}, p_{i22}, p_{i23}, p_{i31}, p_{i32}, p_{i33})\ for\ i \geq 1. \tag{2}$$

such that

$$PQ = 0, Pe = 1 \tag{3}$$

The steady-state probability vector P could be calculated using the following equations:

$$p_i = p_1 R^{(i-1)} \text{ for } i \geq 2 \tag{4}$$

$$R^2A_2 + RA_1 + A_0 = 0 \quad (5)$$
$$p_0B_{01} + p_1(A_1 + RA_2) = 0 \quad (6)$$
$$p_0e + p_1(I - R)^{-1}e = 1 \quad (7)$$

where, R is the minimal non-negative solution of the matrix quadratic equation (5). Using the normalization equation (7) we get the probabilities p_0 and p_1 and obtained the steady-state probability vector.

5 Numerical Illustrations

To understand the qualitative aspects of the working vacation, breakdown-repair, standby queueing model under study, we illustrate a few numerical examples. We analyze different scenarios by varying the parameters of the model.

5.1 Illustration: 1

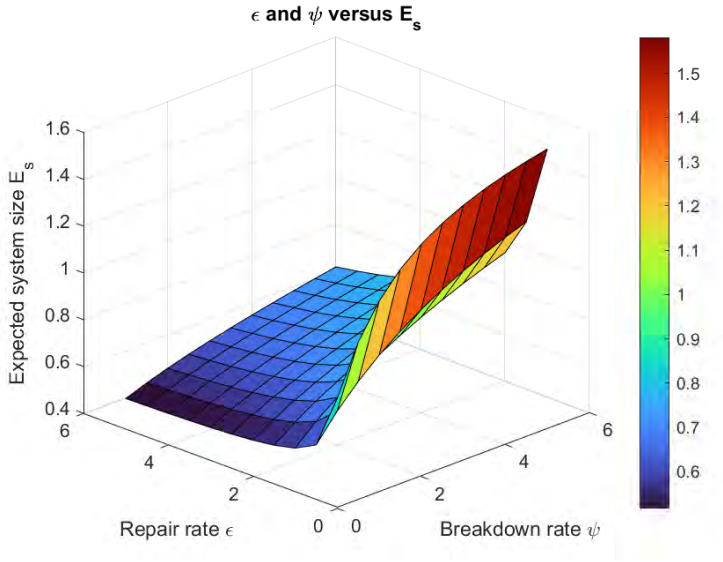

Figure 1: Varying ϵ and ψ on E_s

In Figure 1, we picturise the influence of the breakdown rate(ψ) and repair rate(ϵ) of the server on the expected system size E_s. We fix $\lambda = 1$, $\mu = 4$, $l = 3$, $\zeta = 0.5$, $\tau = 0.7$, $\delta = (0.5, 0.3, 0.2)$, $\gamma = (0.9, 0.7, 0.5)$ and $\alpha = 2$ for which the stability condition holds. As the repair rate increases, the server will be back to the service faster. It reduces the expected system size. Increase in the breakdown rate causes the expected system size higher. An increase in breakdown rate causes frequent breakdowns. As the repair rate decreases, the server gets unavailable often. This causes an increase in the system size.

5.2 Illustration: 2

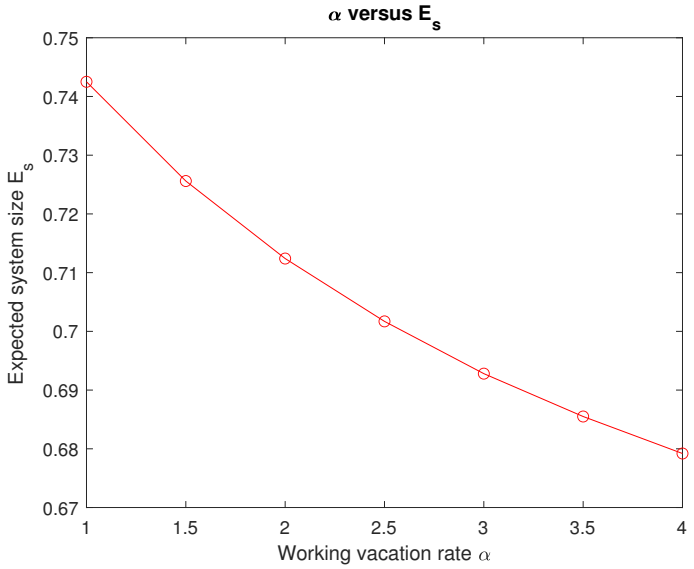

Figure 2: Varying α on E_s

In Figure 2, we investigate the influence of the working vacation rate α on the expected size of the system. For satisfying the stability condition, we take $\lambda = 1$, $\mu = 4$, $\psi = 2.8$, $\epsilon = 2.5$, $\zeta = 0.5$, $\tau = 0.7$ and $l = 3$. As the vacation rate α increases, the expected system size decreases. This is due to an increase in the vacation rate which implies a decrease in the duration of vacation time. As a result, the duration of the server availability in busy period increases, which results in a drop in the expected system size.

6 Conclusion

In this paper, an investigation on the steady state solution of our single server Markovian queueing model with three types of service in which each types provides serivces in three phases includes breakdown, repair and standby server is obtained using matrix-geometric method. Some important performance measures are obtained. In future, the work can be extended this work to generalized multiphase queueing system.

References

[1] Chakravarthy, S. R., Kulshrestha, A. A queueing model with server breakdowns, repairs, vacations, and backup server, Operations Research Perspectives, 7 (2020), 100-131

[2] Chakravarthy, S. R. Introduction to Matrix Analytic Methods in Queues 1: Analytical and Simulation Approach-Basics, John Wiley and Sons (2022).

[3] Deepa, B., Kalidass, K. An M/M/1/N Queue with Working Breakdowns and Vacations. International Journal of Pure and Applied Mathematics, 119(10) (2018), 859-873.

[4] Latouche, G., Ramaswami, V. Introduction to matrix analytic methods in stochastic modeling. Society for Industrial and Applied Mathematics (1999).

[5] Neuts, M. F. Matrix Geometric Solutions in Stochastic Models: An Algorithmic Approach, Johns Hopkins University Press. Baltimore, MD, USA (1981).

[6] Xu, X., Wang, W., and Xu, S. Performance of a queuing model with Hyper-Erlang distribution service for wireless network nodes. Fourth International Conference on Wireless Communications, Networking and Mobile Computing, IEEE (2008).

1st International Conference on Mathematical and Statistical Sciences - ICMSS-1
July 03-04, 2023. Namibia University of Science and Technology, Windhoek, Namibia

Variational Optimisation Method and Applications to Meteorological Modelling

Gabriel S. Mbokoma[1], Sunday A. Reju[1], Nnenesi Kgabi[2] & Benson E. Obabueki[1]
[1]Department of Mathematics, Statistics and Actuarial Sciences, Namibia University of Science and Technology, Windhoek, Namibia
gmbokoma@nust.na, sreju@nust.na, bobabueki@nust.na

[2]Unit for Environmental Sciences and Management, North-West University, Potchefstroom, South Africa
Nnenesi.Kgabi@nwu.ac.za

ABSTRACT

Data assimilation techniques, for example, provide the best estimate of the state of a system by incorporating observational data into a numerical model and uses observational data to generate an analysis that best estimates the present state of the atmosphere. This paper in particular aims to employ an appropriate variational data assimilation technique to develop a mathematical optimal representation model of the key meteorological parameters associated with the Namibian atmosphere. Due to the complexity of the Namibian atmosphere, an appropriate variational data assimilation technique was employed to develop the mathematical models as it enables the assimilation (or acclimatisation or accommodation) of non-linear observations of the analysis variables. Among the two alternative variational data assimilation methods of 3-dimensional variational data assimilation (3D-Var) and 4-dimensional variational data assimilation (4D-Var), the latter was employed in the development of the optimal model as it is time dependent. Particular optimal models for each parameter were developed from the general optimal representation model and were solved by using a numerical Limited-Memory Broyden-Fletcher-Goldfarb- Shanno (L-BFGS) iterative method to obtain the optimal solutions. Overall best optimal estimates for temperature, humidity, and wind speed at most weather stations were observed.

Keywords: *Variational data assimilation, 0ptimal model; 0ptimal estimates; 4D-Var; L-BFGS*

INTRODUCTION

According to Watkinson (2006), data assimilation is a method that provides the best estimate of the state of a system by incorporating observational data into a numerical model. Johnson (2003) points out that data assimilation uses observational data to generate an analysis that best estimates, for example, the present state of the atmosphere. Several different data assimilation techniques have been developed to solve problems, varying in computational functional cost, optimality and speed.

The National Center for Atmospheric Research Staff (Eds.), defined data assimilation as a process of combining observations from a wide variety of sources and forecast output from the weather prediction model as shown by figure 1 below.

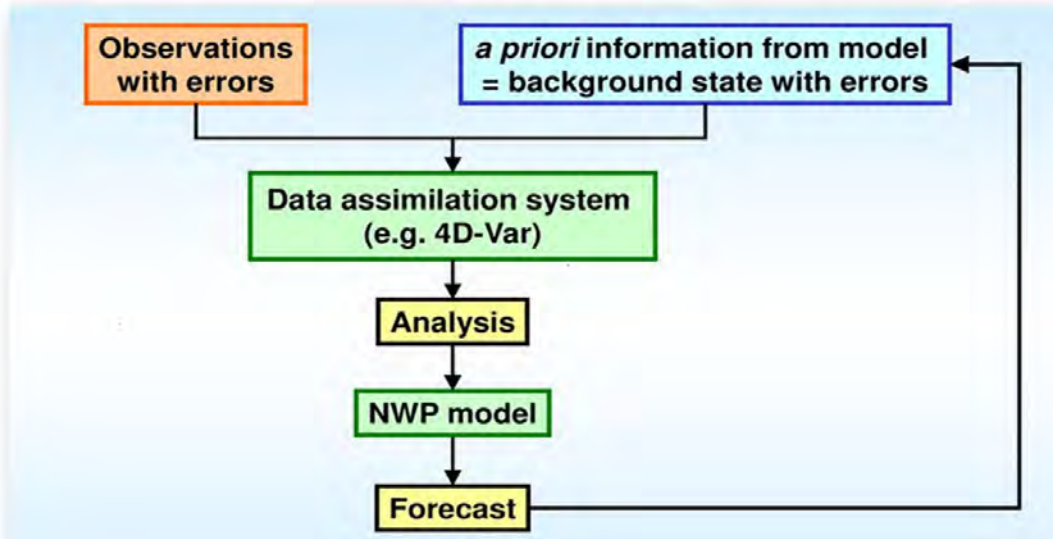

Figure 1: Demonstration of the evolve of data assimilation.

Describtion of variational data assimilation modelling

Let $\mathbf{X} = \mathbb{R}^n$ be the *model space* and let $\mathbf{x} \in \mathbf{X}$ be the model's state vector. By using $\mathbf{x}^t \in \mathbf{X}$ the *truth* or the *true state* of the system can be determined. As explained earlier, the outcome of a previous forecast can serve as the background information in the new analysis, denoted by $\mathbf{x}^b$, where b refers to *background*.

The evolution of an atmospheric or oceanic system from t_{i-1} to time t_i is governed by an equation of the form

$$\mathbf{x}^b(t_i) = M_{i-1}[\mathbf{x}^a(t_{i-1})], \tag{1}$$

where $M : \mathbf{X} \longrightarrow \mathbf{X}$ is the (non-linear) *model operator* that represents the dynamical model and is a function from the model space into itself.

Let $Y = \mathbb{R}^p$ be the *observation space*. Observations $\mathbf{y}^o \in \mathbf{Y}$ become available through the *observational model*

$$\mathbf{y}^o = H(\mathbf{x}^t) + \varepsilon_0, \tag{2}$$

where $H : \mathbf{X} \longrightarrow \mathbf{Y}$ is the (non-linear) *observation operator*, a function from the model space to the observation space, with ε_o being the observation error.

One of the approach used to model such problem is the Three-Dimensional Variational method (3D-Var), in which one intends to find the optimal analysis $\mathbf{x}^a$ that minimises the

functional

$$J(x) = \frac{1}{2}(\mathbf{x} - \mathbf{x}^b)^T \mathbf{B}^{-1}(\mathbf{x} - \mathbf{x}^b) + \frac{1}{2}[\mathbf{y}^o - H(\mathbf{x})]^T \mathbf{R}^{-1}[\mathbf{y}^o - H(\mathbf{x})] \tag{3}$$

The above functional is defined as the distance between the model state $\mathbf{x}$ and the background $\mathbf{x}^b$, weighted by the inverse of the background error covariance plus the distance to the observations $\mathbf{y}^o$ weighted by the inverse of the observation error covariance.

If the observations are distributed not only in space but also in time, then the 3D-Var is advanced to the Four-Dimensional Variational assimilation method (4D-Var), in which the minimisation of the corresponding functional is defined over four dimensions (meaning 3 dimensions for space and 1 dimension for time).

The 4D-Var cost function includes a term measuring the distance to the background at the beginning of the time interval, together with a sum accounting for the observations collected over a k-hour time window. This is given as:

$$J[\mathbf{x}(t_0)] = \frac{1}{2}[\mathbf{x}(t_0) - \mathbf{x}^b(t_0)]^T \mathbf{B}_o^{-1}[\mathbf{x}(t_0) - \mathbf{x}^b(t_0)] + \frac{1}{2}\sum_{i=0}^{N}[H(\mathbf{x}_i) - \mathbf{y}_i^o]^T \mathbf{R}_i^{-1}[H(\mathbf{x}_i) - \mathbf{y}_i^o] \tag{4}$$

The cost function is minimized with respect to the *initial* state of the model with the time interval $\mathbf{x}(t_o)$ and the analysis at the time of the interval is given by the *model integration* from the solution:

$$\mathbf{x}(t_n) = M_o[\mathbf{x}_{(t_0)}] \tag{5}$$

which is the approached used for this study.

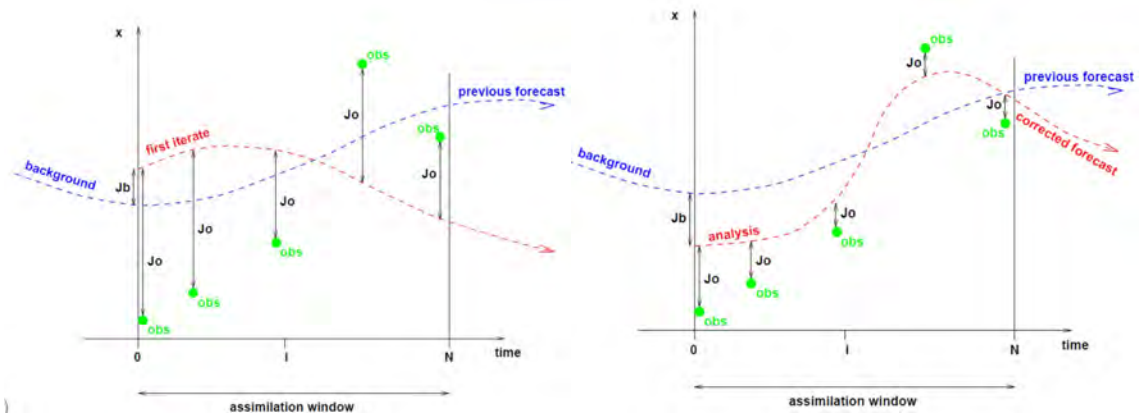

Trajectory given by the first guess. Trajectory given by the analysis.

Figure 2: Representation of 4D-Var approach, illustrating the trajectory of the initial guess and analysis (Vrugt et al., 2005).

4D-Var minimisation using L-BFGS iterative method

L-BFGS shares many features with other quasi-Newton algorithms, but is very different in how the matrix-vector multiplication $d_k = -\mathbf{H}_k g_k$ is carried out, where d_k is the approximate Newton's direction, g_k is the current gradient, and $\mathbf{H}_k$ is the inverse of a Hessian matrix (Nocedal, 1980).

If one considers a given $\mathbf{x}_k$, the position at the k-iteration and $g_k \equiv \nabla f(\mathbf{x})$ where f is the function being minimised with all column vectors. The assumption is that one has stored the last m updates of the form

$$s_k = x_{k+1} - x_k \tag{6}$$

$$y_k = g_{k+1} - g_k. \tag{7}$$

If $\rho_k = \frac{1}{y_k s_k}$ then $\mathbf{H}_k^0$ will be the initial approximate of the inverse Hessian that the estimate at iteration k begins with.

This means that the algorithm is based on the L-BFGS recursion for the inverse Hessian as given below:

$$\mathbf{H}_{k+1} = (I - \rho_k s_k y_k^T)\mathbf{H}_k(I - \rho_k y_k s_k^T) + \rho_k s_k s_k^T. \tag{8}$$

Optimal representation model for the key meteorological parameters

The key meteorological parameters represented in optimal representation model were temperature (T), humidity (Q) and wind speed (P). These were the state variables considered in the model.

Below is the map showing the selected 14 SASSCAL weather stations.

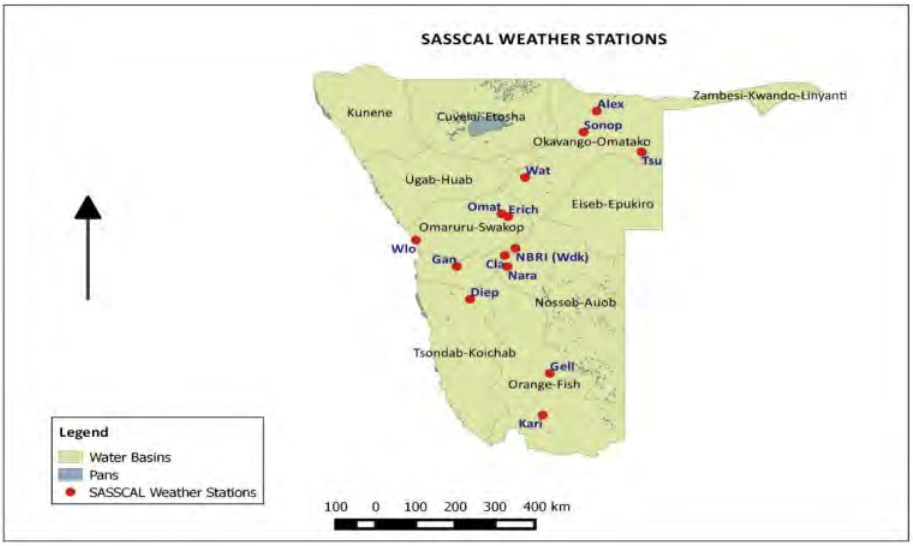

Figure 3: Weather Stations Map

Specific optimal temperature (T) representation model

The particular model of temperature (T) is given by

$$\text{Mininise} \quad J(\mathbf{T}) = \frac{1}{2}(\mathbf{T}-\mathbf{T}^b)^T\mathbf{B}^{-1}(\mathbf{T}-\mathbf{T}^b) + \frac{1}{2}\sum_{i=1}^{N}(H(\mathbf{T}_i)-\mathbf{y}_i^o)^T\mathbf{R}^{-1}(H(\mathbf{T}_i)-\mathbf{y}_i^o) \quad (9)$$

subject to

$$\mathbf{T}_i = M_i(\mathbf{T}_{i-1}) \quad (10)$$

with the background estimate

$$\mathbf{T}_0^b = \mathbf{T}_0 + \epsilon_T^b \quad (11)$$

and the observations vector is given by

$$\mathbf{y}_i^o = H(\mathbf{T}_i) + \epsilon_T^o. \quad (12)$$

While M_i is the time-evolution operator (forward integral) that propagates change in $\mathbf{T}_i$ from t_0 to t_i, H is the observation linear operator that maps $\mathbf{T}_i$ to the observation vector $\mathbf{y}_i^o$.

T is given by:

$$\mathbf{T} = (\mathbf{T}_{Alex};\mathbf{T}_{Tsu}\mathbf{T}_{Wat};\mathbf{T}_{Omat};\mathbf{T}_{Wdk};\mathbf{T}_{Wlo};\mathbf{T}_{Nara};\mathbf{T}_{Diep};\mathbf{T}_{Kari};\mathbf{T}_{Sonop};\mathbf{T}_{Enrich};\mathbf{T}_{Cla};\mathbf{T}_{Gan};\mathbf{T}_{Gell})$$

where **T** is the information from the grid-points and observation-points.

Grid-points:
$\{1-Alex;2-Tsu;3-Wat;4-Omat;5-Wdk;6-Wlo;7-Nara;8-Diep;9-Kari\}$ denoted by letters from $(1-9)$.

Observation-points: $\{A-Sonop;B-Enrich;C-Cla;D-Gan;E-Gell\}$ denoted by numbers from $(A-E)$.The incremental approach to find an initial model state $\mathbf{T}_0$ at time t_0 that minimises the temperature (T) particular model in terms of increments,

$$\delta\mathbf{T}_i = \frac{dM_i(T)}{dT}, \quad \delta\mathbf{T}_{i-1} = M_i\delta\mathbf{T}_{i-1} \quad (13)$$

where $\mathbf{M}_i$ is a matrix and given as follows:

$$\mathbf{M} = \begin{bmatrix} \frac{d(\mathbf{T}_1)}{d\mathbf{T}_1} & 0 & \cdots & 0 \\ 0 & \frac{d(\mathbf{T}_2)}{d\mathbf{T}_2} & \cdots & 0 \\ \vdots & \vdots & \ddots & \vdots \\ 0 & 0 & \cdots & \frac{d(\mathbf{T}_9)}{d\mathbf{T}_9} \end{bmatrix} = \begin{bmatrix} 1 & 0 & 0 & 0 & 0 & 0 & 0 & 0 & 0 \\ 0 & 1 & 0 & 0 & 0 & 0 & 0 & 0 & 0 \\ 0 & 0 & 1 & 0 & 0 & 0 & 0 & 0 & 0 \\ 0 & 0 & 0 & 1 & 0 & 0 & 0 & 0 & 0 \\ 0 & 0 & 0 & 0 & 1 & 0 & 0 & 0 & 0 \\ 0 & 0 & 0 & 0 & 0 & 1 & 0 & 0 & 0 \\ 0 & 0 & 0 & 0 & 0 & 0 & 1 & 0 & 0 \\ 0 & 0 & 0 & 0 & 0 & 0 & 0 & 1 & 0 \\ 0 & 0 & 0 & 0 & 0 & 0 & 0 & 0 & 1 \end{bmatrix}$$

which is an identity matrix (Trémolet, 2007).

The model is similar to both humidity(**Q**) and wind speed (**P**) specific optimal representation models.

Results and Simulation

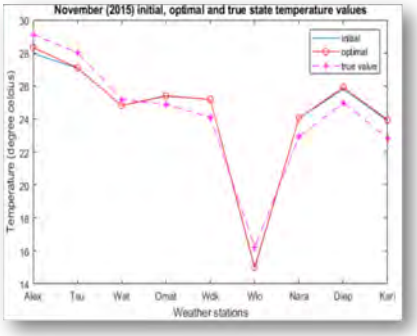

Initial, optimal and true state temperature.

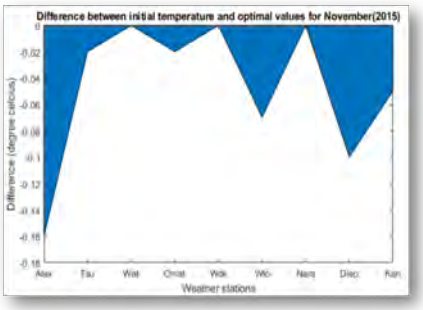

Difference between initial and optimal temperature.

Figure 4: Temperature optimal solution for November 2015.

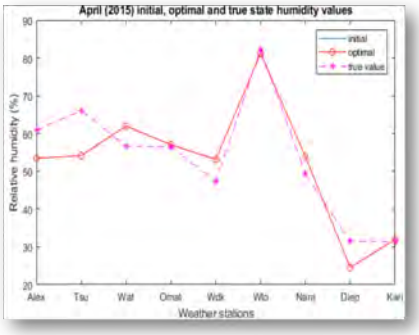

Initial, optimal and true state humidity.

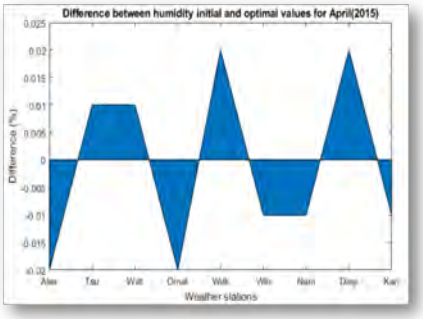

Difference between initial and optimal humidity.

Figure 5: Humidity optimal solution for April 2015.

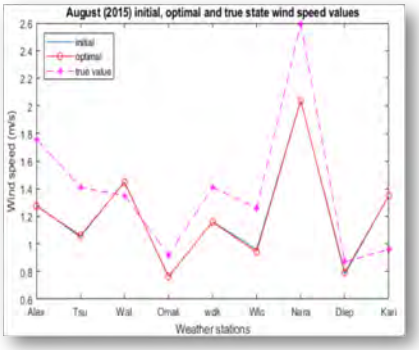

Initial, optimal and true state wind speed.

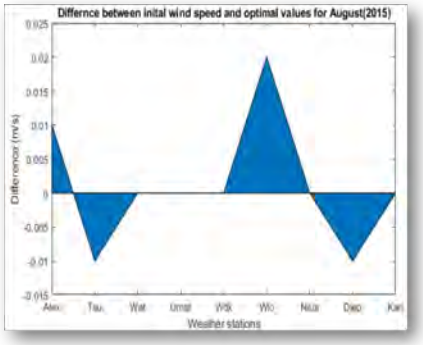

Difference between initial and optimal wind speed.

Figure 6: Wind speed optimal solution for August 2015.

Conclusion

The main objective of the developed model was to minimise the errors in the variation between the model states and the background information for the key meteorological parameters representation models to obtain optimal estimates of the temperature, humidity and wind speed true state values. This study demonstrated how optimal estimates of the key meteorological parameters could be obtained by using the L-BFGS iterative method and how the variational approach (data assimilation) could be used to develop optimisation models.

More importantly, this demonstrate how one could use partial noisy observations from observation point weather stations to estimate the optimal temperature, humidity and wind speed for grid point weather stations and it worked. It was observed that the closeness of observations points to grid-points had some measurable impact, in obtaining reasonable optimal estimates. By using the 2015 monthly average data for meteorological parameters the results were good as expected.

References

Johnson, C. (2003). *Information Content of Observation in Variation Data Assimilation*. PhD thesis, University of Reading, Berkshire, England.

Nocedal, J. (1980). Updating quasi-newton matrices with limited storage. *Mathematics of computation*, 35(151):773–782.

Trémolet, Y. (2007). Model-error estimation in 4d-var. *Quarterly Journal of the Royal Meteorological Society: A journal of the atmospheric sciences, applied meteorology and physical oceanography*, 133(626):1267–1280.

Vrugt, J. A., Diks, C. G., Gupta, H. V., Bouten, W., and Verstraten, J. M. (2005). Improved treatment of uncertainty in hydrologic modeling: Combining the strengths of global optimization and data assimilation. *Water resources research*, 41(1).

Watkinson, L. (2006). *Four dimensional variational data assimilation for Hamiltonian problems*. PhD thesis, University of Reading, Berkshire, England.

A QUEUEING SYSTEM WITH $M/M/c$ HETEROGENEOUS ARRIVALS, TWO KINDS OF WORKING VACATIONS AND IMPATIENT CUSTOMERS

YOHAPRIYADHARSINI R S[1] and SUVITHA V*[2]

[1,2*]Department of Mathematics, Faculty of Engineering and Technology, SRM Institute of Science and Technology, Kattankulathur - 603 203, Tamil Nadu, INDIA

July 15, 2023

Abstract

In this paper, we analyse $M/M/c$ queue with two kinds of Working Vacations (WVs) and impatient customers. Whenever a customer arrives at the system, an impatient timer will start. If the service is not finished before the impatience timer perishes then the customer may leave the system. Each time after serving all the customers, the system becomes empty and then the server starts 1st kind of vacation. After that the server begins 2nd kind of WV whenever a system has no customers. When the server returns from either 1st kind or 2nd kind of WV, if there is at least one customer in the system, the server changes to busy period. Here, we using Probability Generating Functions (PGFs) to derive the steady state probabilities. Performance measures are presented and numerical illustrations are also provided in this paper.

Keywords: Steady state; Impatient customer; c- server.

1 Introduction

Queueing systems with two kinds of vacations and impatient customers occur in our daily life. Several authors have treated the impatience phenomenon under various assumptions. Kumar and Shinde Kumar and Shinde (2020) deal with bulk arrival and bulk service under vacation and interruption they also analyse the steady-state behavior as well as determine the different performance size distributions obtained by using supplementary variable technique. Gupta and Kumar Gupta and Kumar (2021) consider an $M/M/1$ retrial queueing model with a waiting server subject to working vacation, vacation interruption, breakdown and repair. Bounkhel et al. Bounkhel et al. (2019) analyse flexible single-server queueing system considered in this paper. Vyshna and Julia Unni and Mary (2020) describe $M/M/1$ queueing system with two kinds of vacations with distinct durations. Kumar and Sharma Kumar and Sharma (2019) analyse the transient solution of

*Corresponding Author. Email: suvithav@srmist.edu.in

a Markovian queuing system with two heterogeneous servers and retention of reneging customers. Majid et al. Majid et al. (2019) study an infinite capacity of $M/M/1$ queuing model under working vacation policy with the customer impatience.

2 The Model Description

We consider a $M/M/c$ queuing system with two kinds of WVs and impatience customers.

- The arrival of customers according to a Poisson process with heterogeneous arrival rate $\lambda_i, (i = 0, 1, 2)$ for busy, 1st and 2nd kind of WV.
- Two kind of WVs are considered.
  (i) 1st kind of WV: The server can only go on WV each time the system becomes empty.
  (ii) 2nd kind of WV: If no customer is waiting in the system for service when he returns from a 1st kind of WV.
- Each server has an independently and identically distributed exponential service time distribution with rate μ_b for busy period. During a 1st and 2nd kind of WV, the arriving customers are served at the rates of μ_{v_1} and μ_{v_2}. The lower service rates are provided on both kinds of WVs.
- We assume that the durations of both kinds of WVs are exponentially distributed with parameters ϕ_1 and ϕ_2.
- A customer who arrives and finds at least one customer (i.e c customers) in the system, when all the servers are on busy period, 1st and 2nd kind of WV then the customer decides to enter the queue with probabilities β_0, β_1 and β_2. (balk with probabilities β_0', β_1' and β_2')
- The servers activate an impatience timer, which is exponentially distributed with parameters ϵ_0, ϵ_1 and ϵ_2.
  Let $\mathcal{N}(t)$ be the number of customers in the system at time t, and $\mathcal{J}(t)$ represents the servers state at time t. The process $\{\mathcal{N}(t), \mathcal{J}(t); t \geq 0\}$ is defined as a continuous-time Markov process with a state space,
  $\Omega = \{(0, j), j = 1, 2\} \bigcup \{(n, j), j = 0, 1, 2; n \geq 1\}$.
  Let us define the steady state probabilities as,
  $P_{n,j} = \lim_{t\to\infty} P[\mathcal{N}(t) = n, \mathcal{J}(t) = j], n \geq 0, j = 1, 2$
  $P_{n,j} = \lim_{t\to\infty} P[\mathcal{N}(t) = n, \mathcal{J}(t) = j], n \geq 1, j = 0$

The steady state balance equations are presented as follows:

$$(\lambda_0 + \mu_b + \epsilon_0)P_{1,0} = \phi_1 P_{1,1} + \phi_2 P_{1,2} + 2(\mu_b + \epsilon_0)P_{2,0}, n = 1 \quad (1)$$

$$(\lambda_0 + n(\mu_b + \epsilon_0))P_{n,0} = \phi_1 P_{n,1} + \phi_2 P_{n,2} + \lambda_0 P_{n-1,0} + (n+1)(\mu_b + \epsilon_0)P_{n+1,0}, \quad 2 \le n \le c-1 \quad (2)$$

$$(\lambda_0\beta_0 + n(\mu_b + \epsilon_0))P_{n,0} = \phi_1 P_{n,1} + \phi_2 P_{n,2} + \lambda_0 P_{n-1,0} + (c\mu_b + (n+1)\epsilon_0)P_{n+1,0}, \quad n = c \quad (3)$$

$$(\lambda_0\beta_0 + c\mu_b + n\epsilon_0)P_{n,0} = \phi_1 P_{n,1} + \phi_2 P_{n,2} + \lambda_0\beta_0 P_{n-1,0} + (c\mu_b + (n+1)\epsilon_0)P_{n+1,0}, \quad n \ge c+1 \quad (4)$$

$$(\lambda_1 + \phi_1)P_{0,1} = (\mu_b + \epsilon_0)P_{1,0} + (\mu_{v_1} + \epsilon_1)P_{1,1}, n = 0 \quad (5)$$

$$(\lambda_1 + \mu_{v_1} + \epsilon_1 + \phi_1)P_{1,1} = \lambda_1 P_{0,1} + 2(\mu_{v_1} + \epsilon_1)P_{2,1}, n = 1 \quad (6)$$

$$(\lambda_1 + n(\mu_{v_1} + \epsilon_1) + \phi_1)P_{n,1} = \lambda_1 P_{n-1,1} + (n+1)(\mu_{v_1} + \epsilon_1)P_{n+1,1}, \quad 2 \le n \le c-1 \quad (7)$$

$$(\lambda_1\beta_1 + n(\mu_{v_1} + \epsilon_1) + \phi_1)P_{n,1} = \lambda_1 P_{n-1,1} + ((n+1)\epsilon_1 + c\mu_{v_1})P_{n+1,1}, n = c \quad (8)$$

$$(\lambda_1\beta_1 + (c\mu_{v_1} + n\epsilon_1) + \phi_1)P_{n,1} = \lambda_1\beta_1 P_{n-1,1} + ((n+1)\epsilon_1 + c\mu_{v_1})P_{n+1,1}, n \ge c+1 \quad (9)$$

$$\lambda_2 P_{0,2} = (\mu_{v_2} + \epsilon_2)P_{1,2} + \phi_1 P_{0,1}, n = 0 \quad (10)$$

$$(\lambda_2 + (\mu_{v_2} + \epsilon_2) + \phi_2)P_{1,2} = \lambda_2 P_{0,2} + 2(\mu_{v_2} + \epsilon_2)P_{2,2}, n = 1 \quad (11)$$

$$(\lambda_2 + n(\mu_{v_2} + \epsilon_2) + \phi_2)P_{n,2} = \lambda_2 P_{n-1,2} + (n+1)\mu_{v_2} + \epsilon_2)P_{n+1,2}, 2 \le n \le c-1 \quad (12)$$

$$(\lambda_2\beta_2 + n(\mu_{v_2} + \epsilon_2) + \phi_2)P_{n,2} = \lambda_2 P_{n-1,2} + ((n+1)\epsilon_2 + c\mu_{v_2})P_{n+1,2}, n = c \quad (13)$$

$$(\lambda_2\beta_2 + c\mu_{v_2} + n\epsilon_2 + \phi_2)P_{n,2} = \lambda_2\beta_2 P_{n-1,2} + ((n+1)\epsilon_2 + c\mu_{v_2})P_{n+1,2}, n \ge c+1 \quad (14)$$

The normalizing condition is as follows,

$$\sum_{n=1}^{\infty} P_{n,0} + \sum_{n=0}^{\infty} P_{n,1} + \sum_{n=0}^{\infty} P_{n,2} = 1$$

Using normalization condition and steady-state equations, we can obtained the steady-state probabilities and mean size of system.

3 Application

Here, we consider that the scenario in railway station and assume that more than one ticket counters (c-counters) are available. The passengers are waiting in the ticket counters to take tickets. Here we consider that the Booking Clerk (ticket issuer) are not busy for all the time. On that time the Booking Clerk (BC) may take a WV. When the BC gives a ticket to passengers, other passengers wait for service. An impatient passengers may either join a line or balk and return at a later time. The BC begins a 1st kind of WV, after giving tickets to all the passengers. On returning from this vacation, if no one is waiting for service, then the BC will take a 2nd kind of WV. When the BC comes back from either 1st or 2nd kind of WV, if any passengers comes to the line for service continuously, the BC switches to a busy period.

4 Numerical Analysis

In this section we find performance measures numerically by using MATLAB software. We fix the parameters as $\lambda_0 = 12, \lambda_1 = 6, \lambda_2 = 5.5, \beta_0 = 0.9, \beta_1 = 0.2, \beta_2 = 0.1, \epsilon_0 = 25, \epsilon_1 = 9, \epsilon_2 = 3, \phi_1 = 0.8, \phi_2 = 0.5, \mu_b = 8.5, \mu_{v_1} = 7, \mu_{v_2} = 6.5$. In table 1, we increase the λ_0, λ_1 and λ_2 values. Then, the mean system size L_s also increase. In table 2, we increase the μ_b, μ_{v_1} and μ_{v_2} values. Then, the the mean system size L_s decrease.

Table 1: Effect of $\lambda_0, \lambda_1, \lambda_2$ on mean system size

λ_0	L_s	λ_1	L_s	λ_2	L_s
11.1	0.0052687	5.1	0.0101353	5.6	0.0234454
11.2	0.0069058	5.2	0.0112086	5.7	0.0268522
11.3	0.0085430	5.3	0.0122877	5.8	0.0302274
11.4	0.0101804	5.4	0.0133728	5.9	0.0335716
11.5	0.0118178	5.5	0.0144637	6.0	0.0368854
11.6	0.0134553	5.6	0.0155605	6.1	0.0401693
11.7	0.0150929	5.7	0.0166631	6.2	0.0434239
11.8	0.0167306	5.8	0.0177716	6.3	0.0466498
11.9	0.0183684	5.9	0.0188860	6.4	0.0498474
12.0	0.0200063	6.0	0.0200063	6.5	0.0530172

Table 2: Effect of $\mu_b, \mu_{v_1}, \mu_{v_2}$ on mean system size

μ_b	L_s	μ_{v_1}	L_s	μ_{v_2}	L_s
7.6	0.0687955	7.1	0.0196466	5.6	0.0399694
7.7	0.0633709	7.2	0.0192897	5.7	0.0376143
7.8	0.0579473	7.3	0.0189355	5.8	0.0352956
7.9	0.0525245	7.4	0.0185839	5.9	0.0330123
8.0	0.0471027	7.5	0.0182350	6.0	0.0307635
8.1	0.0416817	7.6	0.0175445	6.1	0.0285483
8.2	0.0362616	7.7	0.0166631	6.2	0.0263658
8.3	0.0308423	7.8	0.0172029	6.3	0.0242152
8.4	0.0254239	7.9	0.0168637	6.4	0.0220956
8.5	0.0200063	8.0	0.0165268	6.5	0.0200063

5 Conclusion

Our queueing model approach is examined using PGFs. The steady state probabilities, various performance measure, and some numerical analysis are presented in this paper. In future, this model can be develop by C-server with various kinds of vacations, customer feedback, breakdown and impatience customers.

References

Bounkhel, M., Tadj, L., and Hedjar, R. (2019). Steady-state analysis of a flexible markovian queue with server breakdowns. *Entropy*, 21:259.

Gupta, P. and Kumar, N. (2021). Performance analysis of retrial queueing model with working vacation, interruption, waiting server, breakdown and repair. *Journal of Scientific Research*, 13:833–844.

Kumar, J. and Shinde, V. (2020). Performance of bulk queue under vacation and interruption. *Advances and Applications in Mathematical Sciences*, 19:969–986.

Kumar, R. and Sharma, S. (2019). Transient solution of a two-heterogeneous servers queuing system with retention of reneging customers. *Bulletin of the Malaysian Mathematical Sciences Society*, 42:223–240.

Majid, S., Manoharan, P., and Ashok, A. (2019). Analysis of an M/M/1 queueing system with working vacation and impatient customers. *American International Journal of Research in Science, Technology, Engineering and Mathematics*, 2019:314–322.

Unni, V. and Mary, K. J. R. (2020). M/M/1 multiple vacations queueing systems with differentiated vacations under mixed strategy of customers. *AIP Conference Proceedings*, 2020:1–8.

Gaussian and Weak Gaussian Γ−Semirings

Tilak Raj Sharma and Anuj Sharma

Department of Mathematics
Himachal Pradesh University Regional Centre Khaniyara,
Dharamshala, Himachal Pradesh (India)-176218
Gmail: trpangotra@gmail.com

Abstract

In this paper we introduce a Γ− semiring R which is a weak Gaussian Γ− semiring for which the content formula $c(f)\alpha c(g) \subseteq r(c(f\alpha g)$ holds for all $f, g \in R[x]$ and prove that R is weak Gaussian if and only if each prime ideal of R is $k-$ prime ideal.

Keywords: Gaussian Γ−semiring, weak Gaussian Γ−semiring, bounded distributive lattice, local Γ− semiring.

---

1 Introduction

Semirings provide the most natural common generalization of the theory of rings, also it provides an important tool in the development of different branches of science. But the set of all non positive integers and set of all m x n matrices do not form semirings because multiplication is not a binary operation for above sets. So another mathematical operation came in to existance, which is known as Γ− semiring. The notion of Γ in algebra was introduced by N. Nobusawa [8] in 1964. In 1995, the concept of Γ−semiring was introduced by Rao [4] as a generalization of Γ−ring, ternary semiring, semigroups and semirings.

One of the interesting concept for studying polynomial rings is the concept of the content of a polynomial. Let R be a commutative ring with identity, x an indeterminate over the ring R and the content of a polynomial $f \in R[x]$ denoted by $c(f)$ to be the $R-$ ideal generated by the coefficients of f. A Dedekind-Mertens content formula that is a generalization of Gauss lemma on primitive polynomials, which states that for all $f, g \in R[x]$ there exists a non negative integer $m \leq \deg(g)$ such that $c(f)^m c(fg) = c(f)^{m+1}c(g)$.([1]).

This paper is devoted to weak Gaussian Γ−semirings. Here we construct a Γ−semiring which is a weak Gaussian Γ− semiring, but not a $k-\Gamma-$ semiring. The motive of this paper is to generalize the results of weak Gaussian semirings for Γ−semirings.

2 Preliminaries and Examples

The following definitions are from [4, 7, 8] which are felt to be inseparable part of this paper.

Definition 2.1. *Let R and Γ be two additive commutative semi group. Then R is called a $\Gamma-$ semiring if there exists a mapping $R \times \Gamma \times R \to R$ denoted by $x\alpha y$ for all $x, y \in R$ and $\alpha \in \Gamma$ satisfying the following conditions:*

(i) $(x + y)\alpha z = x\alpha z + y\alpha z$.

(ii) $x\alpha(y + z) = x\alpha y + x\alpha z$.

(iii) $x(\alpha + \beta)z = x\alpha z + x\beta z$.

(iv) $(x\alpha y)\beta z = x\alpha(y\beta z)$ *for all* $x, y, z \in R$ *and* $\alpha, \beta \in \Gamma$.

Example 2.2. *Obviously, every semiring R is a $\Gamma-$ semiring. Let R be a semiring and Γ be a commutative semigroup. Define a mapping $R \times \Gamma \times R \to R$ denoted by $x\alpha y = xy$ for all $x, y \in R$ and $\alpha \in \Gamma$. Then R is a $\Gamma-$ semiring.*

Example 2.3. *Let M be a $\Gamma-$ ring and let R be the set of ideals of M. Define addition in the natural way and if $A, B \in R$, $\gamma \in \Gamma$, let $A\gamma B$ denote the ideal generated by $\{x\gamma y | x, y \in M\}$. Then R is a $\Gamma-$ semiring*

Definition 2.4. *A $\Gamma-$ semiring R is said to have a zero element if $0\gamma x = 0 = x\gamma 0$ and $x + 0 = x = 0 + x$ for all $x \in R$ and $\gamma \in \Gamma$.*

Definition 2.5. *A $\Gamma-$ semiring R is said to have a identity element e, if for all $x \in R$ there exists $\alpha \in \Gamma$ such that $e\alpha x = x = x\alpha e$.*

Definition 2.6. *A $\Gamma-$ semiring R is said to have a strong identity element e, if for all $x \in R$, $e\alpha x = x = x\alpha e$, for all $\alpha \in \Gamma$.*

Definition 2.7. *A $\Gamma-$ semiring R is said to be commutative if $x\gamma y = y\gamma x$ for all $x, y \in R$ and for all $\gamma \in \Gamma$.*

Definition 2.8. *An element x of a $\Gamma-$ semiring R is said to be additive idempotent if and only if $x + x = x$. If every element of R is additive idempotent then R is called additive idempotent $\Gamma-$ semiring. It is denoted by $I^+(\Gamma R)$.*

Definition 2.9. *A non empty subset I of a $\Gamma-$ semiring R is said to be left (right) ideal of R if I is sub semi group of $(R, +)$ and $x\alpha y \in I (y\alpha x \in I)$ for all $y \in I, x \in R$ and $\alpha \in \Gamma$.*

Definition 2.10. *An ideal in a $\Gamma-$ semiring R is called finitely generated if and only if it can be generated by a finite set.*

Definition 2.11. *If I is both left and right ideal of R, then I is known to be an ideal of R.*

Definition 2.12. *An ideal I of a $\Gamma-$ semiring R is called k-ideal if for $x, y \in R, x + y \in I$ and $y \in I$ implies that $x \in I$.*

Definition 2.13. *A $\Gamma-$ semiring R is a $k-\Gamma-$ semiring if every ideal of R is $k-$ ideal.*

Definition 2.14. *An ideal P of R is prime if for any two ideals A and B of R, $A\Gamma B \subseteq P$ we have, either $A \subseteq P$ or $B \subseteq P$.*

Definition 2.15. *A proper ideal M of a $\Gamma-$ semiring R is said to be maximal ideal if there does not exist any other proper ideal of R containing M properly.*

Definition 2.16. *A $\Gamma-$ semiring R is lattice ordered if and only if it has the structure of a lattice such that for all $x, y \in R$*

(i) $x + y = x \vee y$

(ii) $x\alpha y \leq x \wedge y$.

Definition 2.17. *[6] If $p(x) = a_0 + a_1x + \ldots + a_nx^n$ and $q(x) = b_0 + b_1x + \ldots + b_mx^m$ are both in $R[x]$, then $p(x) = q(x)$ if and only if $n = m$ and $a_i = b_i$ for every integer $i \geq 0$.*

Definition 2.18. *[6] If $p(x) = a_0 + a_1x + \ldots + a_nx^n$ and $q(x) = b_0 + b_1x + \ldots + b_mx^m$ are both in $R[x]$, if $n = m$ then $p(x) + q(x) = c_0 + c_1x + \ldots c_nx^n$, where $c_i = a_i + b_i$ for every integer $i \geq 0$.*
Further in case $n \neq m$. Let $n < m$ then put all $a_i = 0$ for $n \leq i \leq m$. Similarly if $n > m$ put all $b_i = 0$.

Definition 2.19. *[6] If $p(x) = a_0 + a_1x + \ldots + a_nx^n$ and $q(x) = b_0 + b_1x + \ldots + b_mx^m$ are both in $R[x]$, then for all $\alpha \in \Gamma$, we have $p(x)\alpha q(x) = c_0 + c_1x + \ldots c_{n+m}x^{n+m}$, where $c_t = \Sigma_{i=0}^{t} a_i\alpha b_{t-i}$ with $a_i = 0$ for $i > n$ and $b_i = 0$ for $i > m$ and for all $\alpha \in \Gamma$.*

M. M. K. Rao [6] found that with above operations of addition and multiplication $R[x]$ is a $\Gamma-$semiring. Nasehpour in [7] has defined content of a arbitrary polynomial in semirings. Analogously, we define content of any polynomial in $\Gamma-$semirings.

Definition 2.20. *Let $f \in R[x]$, then the content of a polynomial f is denoted by $c(f)$ to be an ideal of R generated by the coefficients of f.*

Remark 2.21. *Throughout this paper, R will denote a commutative $\Gamma-$ semiring with zero element $'0'$ and identity element $'1'$ unless otherwise stated.*

3 Main Results

The following results are proved in [9].

Theorem 3.1. *[9] If R be a commutative $\Gamma-$semiring with identity and M is its $R_\Gamma-$semimoudle and $r \in R, m \in M$, $f, f' \in R[x]$ and $g, g' \in M[x]$ following formulas hold:*

(i) $c(f + f') \subseteq c(f) + c(f')$ *and* $c(g + g') \subseteq c(g) + c(g')$

(ii) $c(f\alpha f') \subseteq c(f)\alpha c(f')$ *and* $c(f\alpha g) \subseteq c(f)\alpha c(g)$, *for all* $\alpha \in \Gamma$

(iii) If one of f and g is monomial (i.e. $f = rx^n$ or $g = mx^n$) then $c(f\alpha g) = c(f)\alpha c(g)$. In particular, $c(r\alpha f) = r\alpha c(f)$ and $c(f\alpha m) = c(f)\alpha m$.

Theorem 3.2. *[9] Let R be a commutative $\Gamma-$semiring with strong identity and M be an $R_\Gamma-$semimodule. Then M is a $k-$ $R_\Gamma-$semimodule if and only if $[(c(f)\alpha)^m c(f)]\alpha c(g) = [(c(f)\alpha)^{m-1}c(f)]\alpha c(f\alpha g)$, for all $f \in R[x]$, $g \in M[x]$, $\alpha \in \Gamma$ and $deg(g) = m$.*

If we take $M = R$ in theorem 3.2 then we get **Dedekind- Mertens lemma for $k - \Gamma-$ semirings** as follows:

Theorem 3.3. *[9] Let R be a commutative $\Gamma-$semiring with identity then R is a $k-$ $\Gamma-$semiring, if and only if $[(c(f)\alpha)^m c(f)]\alpha c(g) = [(c(f)\alpha)^{m-1}c(f)]\alpha c(f\alpha g)$, for all $f, g \in R[x], \alpha \in \Gamma$ and $deg(g) = m$.*

Theorem 3.4. *[9] Let R be a $\Gamma-$ semiring and P be an ideal of R. If x is an indeterminate over R, then $P[x]$ is a prime ideal of $R[x]$ if and only if P is a prime $k-$ideal of R.*

Definition 3.5. *A commutative $\Gamma-$semiring R is said to be Gaussian if $c(f\alpha g) = c(f)\alpha c(g)$, for all $f, g \in R[x]$ and $\alpha \in \Gamma$.*

Theorem 3.6. *[9] Every bounded distributive lattices is a Gaussian $\Gamma-$ semiring.*

The following results are proved in [2]

Theorem 3.7. *[2] Let R be a $\Gamma-$ semiring and P be a proper ideal of R. If $x \in r(P)$ then $(x\gamma)^{n-1}x \in I$ for some positive integer n and for all $\gamma \in \Gamma$.*

Theorem 3.8. *[2] Let R be a commutative $\Gamma-$ semiring then $r(I) = \{x \in R \mid (x\gamma)^{n-1}x \in I$, for some positive integer n and for all $\gamma \in \Gamma\}$ where I is a proper ideal of R*

There are some non $k-\Gamma-$semirings, for which the content formula $c(f)\alpha c(g) \subseteq r(c(f\alpha g)$ does not hold for all $f, g \in R[x]$. In following we give an example of such $\Gamma-$semirings.

Example 3.9. *Let $R = \{0, 1, a\}$ be a multiplicative $\Gamma-$idempotent $\Gamma-$semiring in which $1 + a = a + 1 = a$ and there exist $\alpha \in \Gamma$ such that $a\alpha a = a$. Let $f = 1 + ax$ and $g = a + x$. Now $f\alpha g = (1 + ax)\alpha(a + x) = a + x + a^2x + ax^2 = a + (1 + a^2)x + ax^2 = a + (1 + a)x + ax^2 = (a + ax + ax^2)$, This implies that $c(f\alpha g) = \{0, t\}$ and $c(f)\alpha c(g) = R$ while $r(c(f\alpha g)) = r(0, a) = (0, a)$ Thus, $c(f)\alpha c(g) \nsubseteq r(c(f\alpha g))$.*

Definition 3.10. *Let R be a $\Gamma-$semiring, then R is called a weak Gaussian $\Gamma-$semiring, if $c(f)\alpha c(g) \subseteq r(c(f\alpha g))$ for all $f, g \in R[x]$ and $\alpha \in \Gamma$.*

Theorem 3.11. *Let R be a weak Gaussian $\Gamma-$ semiring then $r(I)$ is a $k-$ideal for each ideal I of R.*

The following theorem is proved in [3].

Theorem 3.12. *[3] Let R be a $\Gamma-$ semiring and $r(I)$ is a $k-$ideal for each ideal I of R then each prime ideal of R is $k-$ideal.*

Theorem 3.13. *Let R be a $\Gamma-$ semiring. Then each prime ideal of R is $k-$ideal if and only if R is a weak Gaussian $\Gamma-$ semiring.*

Let P be a commutative monoid then a subset Q of P is said to be submonoid of P if $0 \in Q$ and $p+q \in Q$ for all $p, q \in Q$. A submonoid is said to be $k-$ submonoid if $p+q, q \in Q$ then $q \in Q$ for all $p, q \in Q$. A monoid P is $k-$ monoid if all its submonoids are $k-$ submonoids. Finally, the monoid P is said to be additive idempotent if $x+x=x$ for all $x \in P$.

Theorem 3.14. *Let P be an additive idempotent commutative monoid and Γ additive commutative semigroup . Let $R = P \cup \{1\}$ and $a+1 = 1+a = 1$ for all $a \in R$. Define multiplication over R as $a\alpha b = 0$ for all $a, b \in P, \alpha \in \Gamma$ and $b\alpha 1 = 1\alpha b = b$ for all $b \in R$ and $\alpha \in \Gamma$. Then*

(i) R is a $\Gamma-$semiring and P is the only maximal ideal of R with $P\Gamma P = (0)$

(ii) R is a weak Gaussian $\Gamma-$ semiring

(iii) $I \neq R$ is a $k-$ideal of R if and only if I is a $k-$ submonoid of P for all $I \subseteq P$

(iv) R is a $k-\Gamma-$semiring if and only if P is a $k-$ monoid

(v) R is a Gaussian $\Gamma-$semiring if and only if P is a $k-$ monoid.

Finally, we give an example of a $\Gamma-$ semiring which is not a weak Gaussian $\Gamma-$ semiring.

Example 3.15. *Let R be a $\Gamma-$ semiring with strong identity. Let $a+b=1$ be such that either $a=1$ or $b=1$ and $a\alpha b = 1$ implies $a = b = 1$, for all $a, b \in R$ and $\alpha \in \Gamma$. Let $P = R[x] - \{1\}$. Then P is a prime ideal of $R[x]$. Since $x, x+1 \in P$ and $1 \notin P$, so P is not a $k-$ ideal of $R[x]$. Thus $R[x]$ is not a weak Gaussian $\Gamma-$ semiring. We obtain another example by taking $R = \mathbb{B} = \{0, 1\}$.*

References

[1] J.T. Arnold and R. Glimer, *On the content of polynomials,* Proc. Amer. Math. Soc. 40(1970), 556-562.

[2] T.K. Dutta and S.K. Sardar, *Semiprime ideals and irreducible ideals of a $\Gamma-$semiring*, Novi Sad J. Math., 30, no. 1(2000), 97-108.

[3] Shweta Gupta, Ph.D. Thesis entitled, *On Some Problems In a $\Gamma-$ semirings*, completed on April 2018.

[4] M.M. Krishana Rao,$\Gamma-$ *semirings-I* , Southeast Asian Bull. of Math., Vol.19(1995), 49-54.

[5] M.M. Krishana Rao, $\Gamma-$ *semirings-II* , Southeast Asian, Bull. of Math., Vol.21(1997), 281-287.

[6] M.M. Krishana Rao, $\Gamma-$ *semirings* , Ph.D. Thesis submitted to Andhra University in 1994.

[7] Peyman Nasehpour, *On the Content of polynomials over Semirings and its applications*, J. Algebra Appl. 15 (5) (2013), 1-28.

[8] N.Nobusawa,*On a generalization of the ring theory*, Osaka J. Math. 1 (1964), 81-89.

[9] Tilak Raj Sharma and Anuj Sharma, *Content of polynomials over* $\Gamma-$ *semirings and applications*, communicated to J.P. Journal of Algebra, Number theory and Applications.

Enhanced Precision Ecological Prediction Model using Adjusted Neural Networks

Nikodemus S. Amon, Sunday A. Reju, Benson E. Obabueki

Department of Mathematics, Statistics and Actuarial Science
Namibia University of Science and Technology, Windhoek, Namibia

Abstract

Ecological modelling is among the widely researched areas in applied mathematics and one that always inspires new ideas. In this study, we extend the concept of ecological modelling using neural networks beyond conventional methods of modelling ecological data by employing high-precision prediction using adjusted neural networks.

The study employed the Levenberg-Marquardt algorithm to train, validate and test the neural networks, in which the performance of each neural network was assessed by the mean square error between targeted output data and the predicted values of the neural network which, specifically was the overall aim of this study. In this study, the daily data were used to predict selected meteorological parameters, namely, Surface temperature, and wind speed, at Sachinga and Bagani weather stations in Namibia for over one year from 01 July 2021 to 31 June 2022.

The results of the high-precision prediction of wind speed and surface temperature at Sachinga and Bagani weather stations presented in this study strongly suggest that a choice of an appropriate neural network structure should be made by the researcher based on the size of the dataset to avoid model overfitting or model underfitting and in turn, increasing the model performance.

Keywords: Artificial Neural Networks, Back Propagation, Ecological modelling, Ecological Proximity Prediction, Ecological Zones, Inter/cross-ecological Prediction, Long Short Term Memory

1. Introduction

In recent years neural networks have received considerable attention and have often been mentioned along with terms such as artificial intelligence, deep learning, and machine learning. Neural Networks, also referred to as artificial neural networks (ANN), are data processing systems that are designed to learn from observations, through studies inspired by the ability of the human brain.

Present capabilities for rapid and accurate computations with electronic computers make it possible to build very complex neural network ecological models that include the analyses of many relationships between eco-variables. The high computational ability of neural networks makes them a suitable substitute for traditional ecological modelling.

The ability of neural networks to adjust their inner structure leads to the classification of neural networks into two major categories, namely, supervised learning and unsupervised learning. Various scholars and researchers have made a number of attempts, using both categorical classes of neural networks to develop efficient neural network models for weather forecasting and ecological modelling. Examples include using unsupervised learning neural network such as self-organising map (SOM) and supervised learning neural network such as multilayer perceptron using Levenberg-Marquardt algorithm as a learning algorithm. Khun, (2010) reflected on two general approaches that are used in weather forecasting which are empirical and dynamical approaches.

According to Webster, (1976), the development of a model that contains ecological dimensions are somewhat more difficult than the development of a mathematical model with numbers that are dimensionless and nonrepresentative of real relationships. In addition, ecological processes are often nonlinear and influenced by many factors. In this work, we will endeavour to contribute to the widespread use of ANNs in various research fields of ecological modelling consequent to the development of the Long Short Term Memory (LSTM) in parallel distributed computing networks.

1.1. Neural network

A Neural network can trivially be defined as a network of neurons, which is a nonlinear model constructed by linking multiple neurons together in such a way that the output of one neuron becomes an input of another neuron to arbitrarily represent a complex nonlinear processes that relate the input and output of any given system.

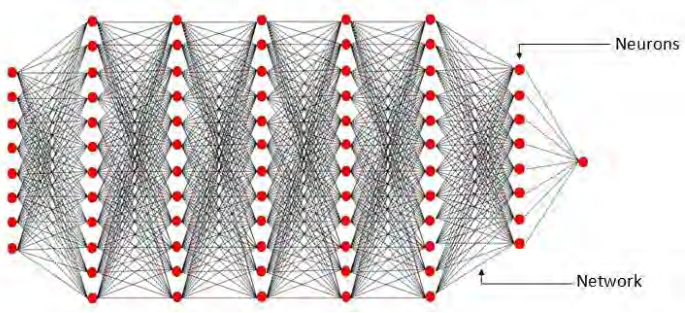

Figure 1: Illustration of a neural network with 7 layers

1.2. Universal approximation theorem

The universal approximation theorem states that any continuous function defined on a compact set can be arbitrarily well approximated by a neural network with at least one hidden layer with a finite number of weights.

2. Recurrent Neural Network

RNNs have a feedback loop, unlike the feedforward neural network. This loop allows the neural network to do sequential processing of sequential inputs. An RNN can then be understood as a multiple repetition of a similar network, where the information passes through in each time step.

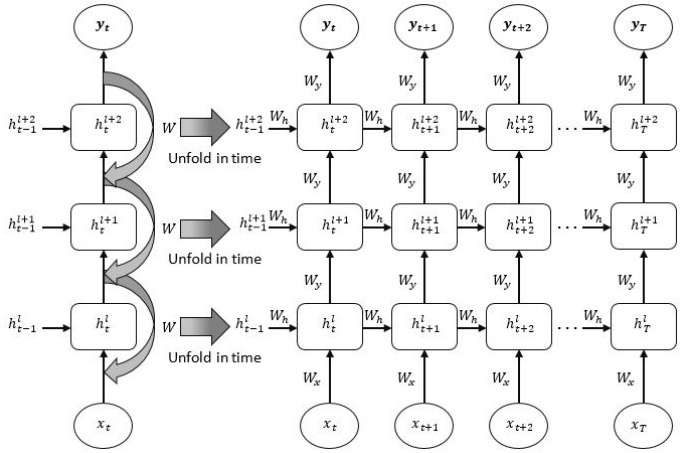

Figure 2: Three-layer RNN structure.

2.1. Long Short Term Memory (LSTM) Neural Network

Long Short-Term Memory (LSTM) neural network is an advanced type of Recurrent Neural Network (RNN) that is capable of avoiding the problem of vanishing gradient problem, which arises from the unfolding of an RNN when training the network with a gradient-based learning method.

The LSTM block operates almost in a similar way to the simple RNN block. That is, they both receive an input every time step from the memory block of the last time-step through recurrent connections. This current information is then succeeded to the next block.

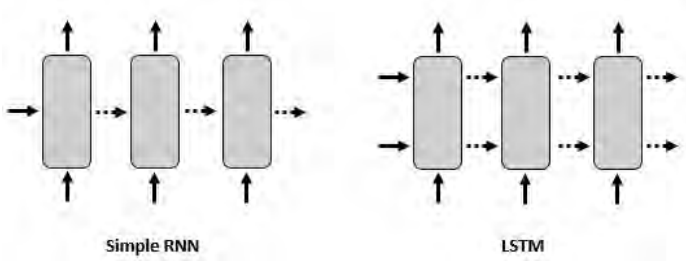

Figure 3: Simplified architecture of a Simple RNN and LSTM

The fundamental difference in the structure of the simple RNN and LSTM is that the LSTM has two streams of information. One stream goes through all the gates and the other goes through the cell connections of the LSTM block. The LSTM memory block contains one or more memory cells and three gating units that are shared by all the cells in the block. The gate units are the input gate, forget gate, and output gate. The input gate specifies what information is added to the cell state. The forget gate defines what information is removed from the cell state, while the output gate specifies what information from the cell state is used in the next cell state.

Input gate:

$$i^{(t)} = \sigma\left(W_i x^{(t)} + R_i y^{(t-1)} + b_i\right), \tag{1}$$

Forget gate:

$$f^{(t)} = \sigma\left(W_f x^{(t)} + R_f y^{(t-1)} + b_f\right), \tag{2}$$

Output gate:

$$o^{(t)} = \sigma\left(W_o x^{(t)} + R_o y^{(t-1)} + b_o\right), \tag{3}$$

Block input/Input node:

$$z^{(t)} = \tanh\left(W_z x^{(t)} + R_z y^{(t-1)} + b_z\right), \tag{4}$$

where the subscripts i, f, o, z denote the input, forget, output, and block input entries respectively, and $i, f, o, z = 0, 1, ..., n$.

Therefore the cell state is given as:

$$c^{(t)} = z^{(t)} \odot i^{(t)} + c^{(t-1)} \odot f^{(t)}, \tag{5}$$

where $x^{(t)}$ is the input vector for the time step t and $\odot$ is a Hadamard product operator otherwise known as the element-wise product, or entry wise product or Schur product operator. This operator is a binary operation that operates on matrices of the same dimension and produces a matrix of the same dimension as the operands.

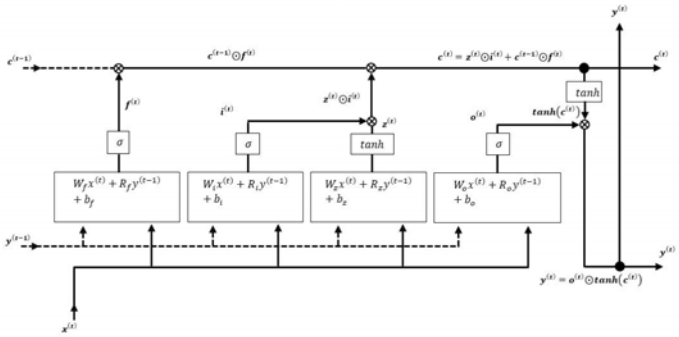

Figure 4: LSTM Memory block without peephole

Thus the output of the LSTM block is then given by,

$$y^{(t)} = o^{(t)} \odot \tanh\left(c^{(t)}\right), \tag{6}$$

where σ in figure 4 is the sigmoidal activation function. The Ws are the neural network weights, Rs represent the weights for the outputs of the previous LSTM block, the bs are the bias parameters, z is the input node of the memory block, and c is called the cell state of the memory cell and y is the block output.

3. Nonlinear Sensitivity Based Learning Algorithm

The update rule for the Levenberg-Marquard algorithm is given as

$$w^{(k+1)} = w^{(k)} - \left[J_{(k)}^T J_{(k)} + \mu I\right]^{-1} J_k e_k. \tag{7}$$

Using the chain rule, let us look at the partial derivative of the output of the memory block with respect to the inputs of the memory block. The figure below shows an LSTM model with three memory blocks.

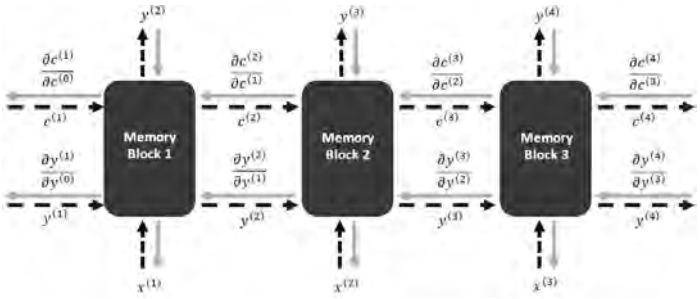

Figure 5: LSTM Back Propagation

These partial derivatives are referred to as sensitivity, given as

$$S_i^{(t)}|_{x_n} = \frac{\partial y_i^{(t)}}{\partial x_i^{(t)}}(x_n), \tag{8}$$

The output of the LSTM with three memory blocks given in figure 5 is as follows:

$$y_i^{(t)} = \sigma\left(\sum_{i=0}^{n} W_{io} x_i^{(t)} + \sum_{i=0}^{n} R_{io} y_i^{(t-1)}\right) \odot \tanh\left(\sum_{i=0}^{n} z_i^{(t)} \odot i_i^{(t)} + \sum_{i=0}^{n} c_i^{(t-1)} \odot \right. \tag{9}$$

Therefore the Nonlinear Sensitivity Based Learning Algorithm is given as

$$\frac{\partial y_{\iota+1}^{(t)}}{\partial y_\iota^{(t)}} \approx \left[W_{(k-1)}^{(t)} - \left[J_{(k-1)}^T J_{(k-1)} + \mu I\right]^{-1} J_{(k-1)} e_{k-1}\right] \sigma_\iota'\left(y_\iota^{(t)}\right), \tag{10}$$

and

$$\frac{\partial y_i^{(\tau+1)}}{\partial y_i^{(\tau)}} \approx \left[W_{(k-1)}^{(t)} - \left[J_{(k-1)}^T J_{(k-1)} + \mu I\right]^{-1} J_{(k-1)} e_{k-1}\right] \sigma_\iota'\left(y_i^{(\tau)}\right). \tag{11}$$

Therefore we obtain the measures of the index of Adjoint sensitivities given as

$$s_i^{(k)} = \frac{\partial \xi\left(y_{\iota+1}^{(t)}\right)}{\partial y_\iota^{(t)}} = W_{\iota j}^{(t)} \sigma_\iota'\left(y_\iota^{(t)}\right) \tag{12}$$

and

$$s_i^{(k)} = \frac{\partial \xi\left(y_i^{(\tau+1)}\right)}{\partial y_i^{(\tau)}} = W_{ij}^{(\tau)} \sigma_i'\left(y_i^{(\tau)}\right). \tag{13}$$

4. Analysis of High Precision Prediction using Adjusted Neural Network (Sachinga and Bagani Station)

It is important for the modeller to explore neural network model adjustment by making changes in the number of hidden neurons and the number of delays to obtain high precision during prediction.

Figure 6: North-Eastern Namibia

Given that Bagani weather station is a remote station and most of the key weather characteristics such as air temperature and humidity are not recorded we will use wind speed and surface temperature data to make such predictions.

4.1. High Precision Prediction of Wind Speed at Sachinga and Bagani using Adjusted Neural Network

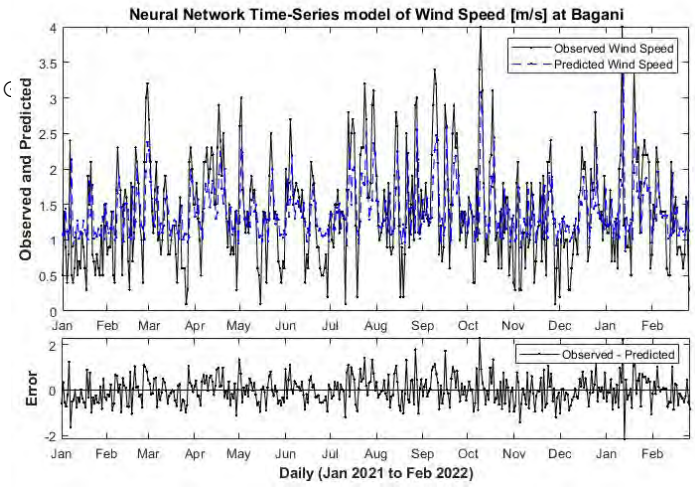

Figure 7: Adjusted Neural Network Prediction of Wind speed and Bagani weather station

The time series shown in the figure above reveals the high-precision predictions of wind speed at secunda and bagani weather stations in the north east of Namibia. The high precision was obtained by making adjustments to the neural network structure by reducing the number of hidden neurons from 10 to 4 hidden neurons and reducing the number of hidden delays from 2 to 1. The reason why these adjustments lead to a high precision prediction is because the adjustments make up for the

model overfitting which has a tendency to produce the model precision.

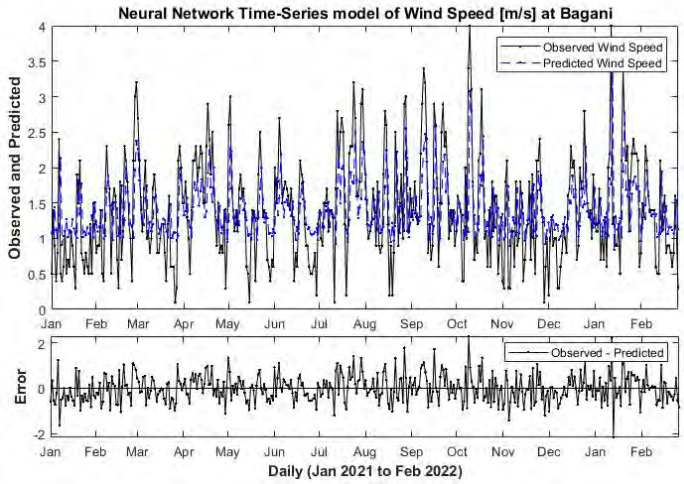

Figure 8: Adjusted Neural Network Prediction of Wind speed at Sachinga weather station

The plot below indicates that the model performed best with only four hidden neurons and a one-time delay. The change in model structure does not have a monotonic increase or decrease in the performance however the modeller can select the best performance depending on how much the change In the model structure improves the performance of the prediction.

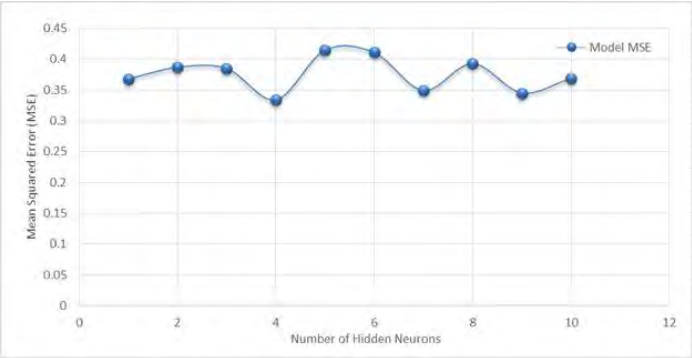

Figure 9: Neural Network Model Performance after the adjustment to the number of hidden neurons

4.2. High Precision Prediction of Surface temperature at Sachinga and Bagani using adjusted Neural Network

Achieving high precision predictions through adjusting the structure of a neural network model shows that the change in time delay of the recurrent Neural Network model improves the model even when the data set is characterized by high fluctuations and unpredictability. The results show that making changes to the neural network structure by adjusting the number of hidden layers outperforms the prediction that was done using ecological proximity prediction and sensitivity analysis that is limited to making changes in the input data sets only.

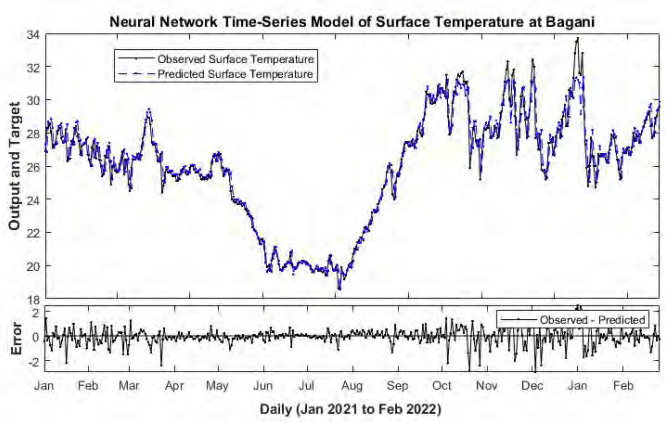

Figure 10: Adjusted Neural Network Prediction of Surface Temperature at Bagani weather station

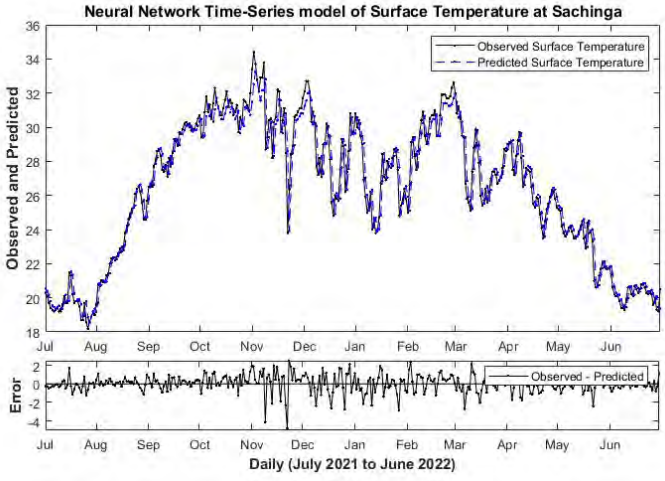

Figure 11: Adjusted Neural Network Prediction of Surface Temperature at Sachinga weather station

A careful examination of various network structures and how they perform during the prediction of different variables makes a significant difference when the modeller is trying to obtain a minimum error in the prediction. The model adjustment considered in this study was only applied to wind speed and surface temperature, however, it can be extended to the evaluation of the datasets of precipitation, humidity, solar irradiance, etc. using other methods such as Bayesian regularization, amongst others.

5. Discussion

Due to the difficulties of data availability for some weather variables in some of the ecological regions, high precision prediction of selected weather variables was only done at Sachinga and Bagani weather stations. The high precision prediction output of the neural network that was obtained during the prediction of wind speed in surface temperature at Sachinga and Bagani weather stations affirmed that the neural network has

potential, under the right circumstances, to obtain high degree of precision during the prediction of such weather variables irrespective of the type of ecological zone in which the weather station is located.

6. Summary and conclusions

The choice of an appropriate neural network structure should be made by the researcher based on the size of the dataset to avoid model overfitting or model underfitting and in turn increasing the model performance. In this study, the proposed approaches are tested with data of 8 selected SASSCAL weather stations across Namibia. Evaluation of these methods using more stations data can be considered. In addition, other LSTM neural networks designs can be further explored in the future.

7. References

Castillo, E., Gonejo, A. J., Pedregal, P., Garcia, R., & Alguacil, N. (2001). Building and Solving Mathematical Programming Models in Engineering and Science (M. B. Allen, D. A. Cox, & P. Lax (eds.)). JOHN WILEY & SONS, INC. http://www.gams.com/

Khun, Y. W. (2010). A Study on Soft Computing Approach in Weather Forecasting (Issue April). Universiti Teknologi Malaysia.

Kullback, S. (1968). Information theory and statistics. John Wiley Sons, 2, 35-400 Inc. https://doc.lagout.org/Others/Information Theory/ Information Theory/Information theory and statistics - Solomon Kullback.pdf

Loehle, C. (1987). Applying artificial intelligence techniques to ecological modeling. Ecological Modelling, 4, 191–212. https://doi.org/10.1016/0304-3800(87)90097-4

Wang, Y. J., Feng, Q. Y., Wang, H., & Chai, L. H. (2010). New simulation method of ecosystem evolution based on neural network. Sixth International Conference on Natural Computation, 4, 749–753. https://doi.org/10.1109/ICNC.2010.5584381

Webster, D. A. (1976). Mathematical Models. In Ecological Modeling and Simulation 2, 32–40.

Wenger, S. J., & Olden, J. D. (2012). Assessing transferability of ecological models: an underappreciated aspect of statistical validation. Methods in Ecology and Evolution, 3, 260–267. https://doi.org/10.1111/j.2041-210X.2011.00170.x

Yeung, D. S., Cloete, I., Shi, D., & Ng, W. W. Y. (2009). Sensitivity Analysis for Neural Networks. In G. Rozenberg (Ed.), Angewandte Chemie International Edition, 3, 951–952. Springer. https://doi.org/10.1007/978- 3-642-02532-7

Markov Models for Dimensioning and Provisioning of Battery Energy Storage Systems (BESS) for Off-Grid Green Mobile Network Base Station Sites

Godlove Suila Kuaban *[1], Tadeusz Czachórski[1], and Piotr Czekalski[2]

[1]Institute of Theoretical and Applied Informatics, Polish Academy of Sciences, Bałtycka 5, 44-100 Gliwice, Poland
[2]Faculty of Automatic Control, Electronics and Computer Science , The Silesian University of Technology , Akademicka 16, 44-100 Gliwice, Poland

Abstract

There is a growing desire by mobile network operators and other stakeholders to reduce carbon emissions from the operation of mobile networks. The widespread adoption of ultra-dense 5G and Internet of Things (IoT) networks will likely increase the energy demand from these networks significantly. In this paper, we model the density of the time required to charge BESS to its full capacity when the renewable energy sources can generate enough energy to meet the needs of the base station site and the density of the time required to completely deplete the energy stored in BESS when the renewable energy sources cannot generate a sufficient amount of energy to meet the demand of the site. We also investigate the influence of the design parameters, such as the energy supply-demand ratio, on the distribution of the time required to charge BESS to its full capacity (for a supply-demand ratio greater than one) and the time required to completely deplete the energy stored in BESS (for supply-demand ratio less than one).

Keywords: Markov Models; dimensioning of green networks; battery energy storage systems (BESS); green mobile networks.

1 Introduction

Mobile communication technologies are playing significant role in the socio-economic development of every society worldwideGelenbe and Abdelrahman (2018). Their widespread adoption has led to the deployment of massive numbers of base station sites to handle the growing number of users, increasing the carbon footprint, especially in off-grid areas where base station sites are powered using diesel generators. Stochastic models such as Markovian models have been applied to size Battery Energy Storage Systems (BESS) for Green base station sites in mobile networks. These models are based on the discretisation or quantisation of energy delivered to BESS into energy packets and then analysed using well-known Markovian modelling methods used to analyse

*Corresponding Author. Email: gskuaban@iitis.pl.

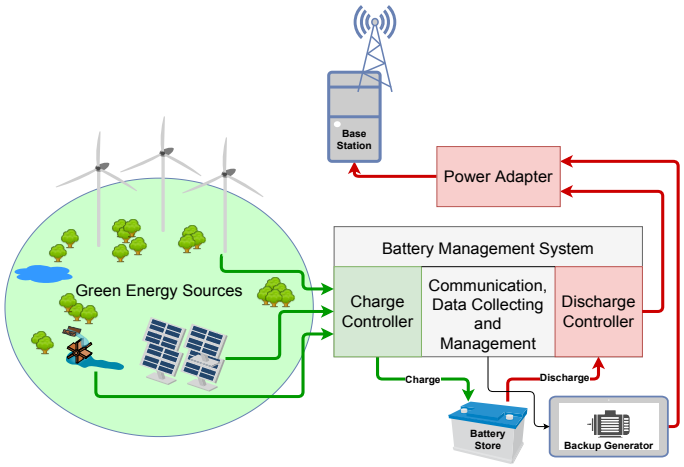

Figure 1: The architecture of a green base station site.

computer networks. An alternative approach is to use a diffusion process to represent the energy content of BESS and its dynamic evolution over time as inCzachórski et al. (2022b); Kuaban et al. (ress); Czachórski et al. (2022a).
The energy packet-based Markov model for battery energy storage systems for green base station sites supplied by renewable energy sources was discussed in Gelenbe and Abdelrahman (2018). In this paper, we model the density of the time required to charge BESS to its full capacity when the renewable energy sources can generate enough energy to meet the needs of the base station site and the density of the time required to completely deplete the energy stored in BESS when the renewable energy sources cannot generate a sufficient amount of energy to meet the demand of the site.

2 Markov models for battery energy storage system

Consider a base station site that is powered using energy generated from renewable energy sources such as solar or wind energy systems. If this energy is greater than the energy demand of the base station site, the Battery energy storage (BESS) system is charged. When the renewable energy system cannot generate sufficient energy to supply the site, the battery energy storage system is discharged to supply the site. If the battery energy storage system is completely discharged, the backup generator picks up (although the cost of running the generator is high, it prevents the site from shutting down).
Suppose that initially, we have i energy packets (for $i \in [1,\ B]$) in BESS at time $t = 0$. Also, let the random variable T represent the time after which the battery becomes empty, which is the first passage time of the process from $N(0) = i$ to $N(t) = 0$ (when all the energy stored in the battery is completely depleted), that is $T =\in f\{t > 0 : N(t) = 0 \mid N(0) = i\}$. The density of the time required to deplete the energy stored in BESS completely is modelled by the density of the time required for the Markov process that starts at a point i to reach 0 (see, e.g. Takagi and Tarabia (2009)). Hence, the Laplace transform of density of the distribution of the time required to deplete

the energy stored in BESS completely is:

$$\bar{h}_{i,0}(s) = \varrho^{-i} \frac{[\eta(s)]^{B-i}[\eta(s)-1] + [\xi(s)]^{B-i}[\xi(s)-1]}{[\eta(s)]^{B}[\eta(s)-1] + [\xi(s)]^{B}[\xi(s)-1]} \tag{1}$$

where,

$$\xi(s) = \frac{s+\lambda+\mu-\sqrt{(s+\lambda+\mu)^2-4\lambda\mu}}{2\lambda},$$

$$\eta(s) = \frac{s+\lambda+\mu+\sqrt{(s+\lambda+\mu)^2-4\lambda\mu}}{2\lambda},$$

and $\varrho = \lambda/\mu$ is the energy supply-demand ratio. Also, assuming that initially, the BESS is fully charged ($i = B$), then the first passage time from $N(0) = B$ to $N(t) = 0$ is

$$\bar{h}_{B,0}(s) = \varrho^{-B} \frac{[\eta(s)-1] + [\xi(s)-1]}{[\eta(s)]^{B}[\eta(s)-1] + [\xi(s)]^{B}[\xi(s)-1]} \tag{2}$$

and for oversized or large battery capacity,

$$\lim_{B\to\infty} \bar{h}_{i,0}(s) = [\xi(s)]^{i} \tag{3}$$

It is essential to know the time required to charge BESS to its full capacity when the renewable energy sources can generate enough energy to meet the energy demand of the site and store extra energy in BESS to be used later when the renewable energy sources are not able to generate sufficient energy to meet the demand of the site. The time required to charge BESS for an initial amount of energy i to its full capacity is given in the Laplace domain and can be adapted from equation (1) as (we cite the result with a minor correction to the original Takagi and Tarabia (2009) p.223: ϱ is replaced by ϱ^{B-i}):

$$\bar{h}_{i,B}(s) = \varrho^{-(B-i)} \frac{\{[\eta(s)]^{i+1} - [\xi(s)]^{i+1}\} - \{[\eta(s)]^{i} - [\xi(s)]^{i}\}}{\{[\eta(s)]^{B+1} - [\xi(s)]^{B+1}\} - \{[\eta(s)]^{B} - [\xi(s)]^{B}\}} \tag{4}$$

Assuming that BESS was initially empty (i = 0), then the first passage time of the process from $N(0) = 0$ to $N(t) = B$ is

$$\bar{h}_{0,B}(s) = \varrho^{-B} \frac{[\eta(s)-\xi(s)] - [\eta(s)-\xi(s)]}{\{[\eta(s)]^{B+1} - [\xi(s)]^{B+1}\} - \{[\eta(s)]^{B} - [\xi(s)]^{B}\}} \tag{5}$$

For very large battery capacity,

$$\lim_{B\to\infty} \bar{h}_{i,B}(s) = [\xi(s)]^{B-i} \tag{6}$$

3 Results

In the numerical results presented, we consider that the capacity of BESS is $B = 100$ KWh. Typically, an average energy demand of a based station site required to power all the equipment in the site is between 1 KW and 3 KW Mohamad Aris and Shabani (2015). In this paper, we consider the site's energy demand of $\mu = 1$ KW. The energy supply-demand ratio, ϱ, is varied by varying the mean energy supply rate λ leaving the energy demand rate, μ constant.

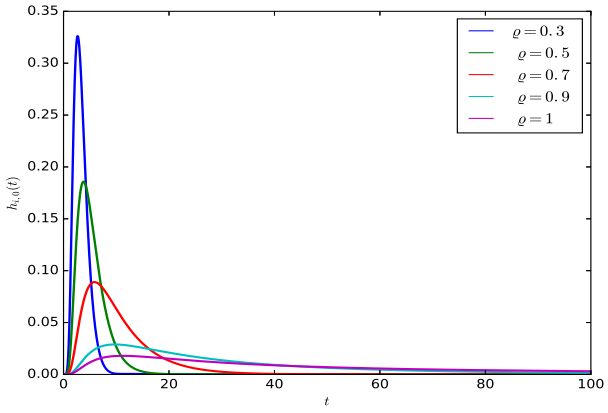

Figure 2: The influence of ϱ on the probability density of the time after which the energy stored in the BESS is completely depleted, $h_{i,0}(t)$, for $\lambda = \{0.3, 0.5, 0.7, 0.9, 1\}$, $\mu = 1$, $i = 10$, $\bar{h}_{i,0}(s)$ given by eq(1) numerically inverted.

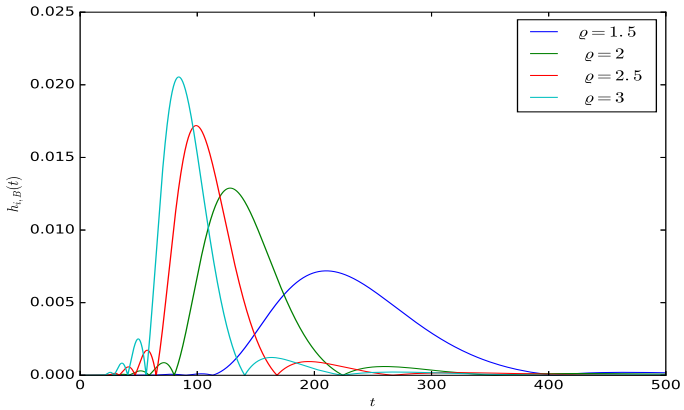

Figure 3: The influence of ϱ on the probability density of the time after which the BESS is fully charged, $h_{i,B}(t)$, for $i = 10$, $\lambda = \{1.5, 2, 2.5, 3\}$, $\mu = 1$, $B = 100$, $\bar{h}_{i,B}(s)$ given by eq(4) numerically inverted.

Figure 3 shows the influence of ϱ on the probability density of the time, after which the energy stored in the BESS is completely depleted. It can be seen that the probability of the time after which the energy stored in the BESS is completely depleted decreases with increasing ratio of the energy supplied to the BESS to the energy drawn, ϱ. Similarly, the influence of the energy supply-demand ratio, ϱ on the density of the distribution of the time required to charg BESS to its full capacity is shown in Figure 3.

4 Conclusion

The results presented in this study shows that by increasing the energy supply-demand ratio ϱ, the probability of completely depleting the energy stored in BESS is decreased, increasing the reliability and the energy self-sustainability of the site. Also, It can be observed that as ϱ increases, the time required to charge BESS to its full capacity increases. We intend to extend this study by investigating the influence of other design parameters.

References

Czachórski, T., Erol Gelenbe, G. S. K., and Marek, D. (2022a). Optimizing energy usage for an electric drone. In Gelenbe., E., Jankovic, M., Kehagias, D., Marton, A., and Vilmos, A., editors, *Security in Computer and Information Sciences. EuroCybersec 2021. Communications in Computer and Information Science*, pages 61–75. Springer, Cham.

Czachórski, T., Gelenbe, E., and Kuaban, G. S. (2022b). Modelling energy changes in the energy harvesting battery of an iot device. In *Proceedings of the 2022 30th International Symposium on Modeling, Analysis, and Simulation of Computer and Telecommunication Systems (MASCOTS)*, pages 81–88, Nice, France. IEEE.

Gelenbe, E. and Abdelrahman, O. H. (2018). An energy packet network model for mobile networks with energy harvesting. *Nonlinear Theory and Its Applications*, 9(3):322–322.

Kuaban, G. S., Gelenbe, E., Czachórski, T., Czekalsk, P., and Tangka, J. K. (2023 (in press)). Modelling of the energy depletion process and battery depletion attacks for battery-powered internet of things (IoT) devices. *Sensors*.

Mohamad Aris, A. and Shabani, B. (2015). Sustainable power supply solutions for off-grid base stations. *Energies*, 8(10):10904–10941.

Takagi, H. and Tarabia, A. M. (2009). *Explicit Probability Density Function for the Length of a Busy Period in an M/M/1/K Queue*. Springer, Spring Street, New York, NY 10013, USA.

Single Server Bulk Service Priority Queue With Differentiate Breakdown, Repair, Close Down, Set Up And Multiple Vacation (ICMSS-1)

Ayyappan G[1] and Nithya S*[2]

[1]Department of Mathematics, Puducherry Technological University, Puducherry-605014, India

[2]Department of Mathematics, Puducherry Technological University, Puducherry-605014, India

Abstract

This study deals with the steady state analysis of single server non preemptive priority queueing system with differentiate breakdown, repair, close down, setup and multiple vacation. For this purpose, customers were grouped into two various categories priority and ordinary customers. These customers arrived according to poisson arrival processes. The server consistently afforded single service for priority customers and the general bulk service for ordinary customers, and the service were based on general distribution. Ordinary customers were served only if the batch size was greater than 'a' or less than or equal to 'b', else the server would not start service until the accumulation of 'a' customers. In this study, Supplementary variable technique and probability generating function are generally used to solve the Laplace transforms of time-dependent probabilities of system states. Finally, performance measures are evaluated and expressed in numerical values.

Keywords: Batch arrivals; Bulk service; Priority queues; Differentiate Breakdown; Closedown; Setup; Multiple Vacation.

1 Description of the Model

Let $\lambda_1, \lambda_2 > 0$ be the arrival rate for priority and ordinary customers respectively. Priority and ordinary customers ordinate in batches with distinct queues (Ayyappan G. (2018)). Server renders single service for priority customers and general bulk service for ordinary customers with service rate $\mu_i(\nu)$, $i = 1, 2$ respectively. Hard and soft failure rates are exponentially distributed, with rates of α_1 and α_2, respectively (Rajadurai P. (2018)). The repair time for soft failure follows exponential distribution with rate η_1 and the repair time for hard failure follows general distribution with rate $\eta_2(\nu)$. The random variable for vacation time, V, has a $\gamma(\nu)$ general distribution. On vacation completion, if the queue length is less than 'a', then the server goes for another vacation and so on. The close down and setup time's random variable C and S follows an arbitrary distribution with rate $\alpha(\nu)$ and $\beta(\nu)$respectively.

*Corresponding Author. Email: nithyamouttouraman@gmail.com

2 Equation Governing the System

$$\begin{aligned}\frac{\partial}{\partial t}P_{m,n}(\nu,t)+\frac{\partial}{\partial \nu}P_{m,n}(\nu,t) =& -(\lambda_1+\lambda_2+\alpha_1+\alpha_2+\mu_1(\nu))P_{m,n}(\nu,t)\\ &+\lambda_1(1-\delta_{0m})\sum_{i=1}^{m}c_iP_{m-i,n}(\nu,t)\\ &+\lambda_2(1-\delta_{0n})\sum_{j=1}^{n}c_jP_{m,n-j}(\nu,t) \quad \text{for } m,n\geq 1.\end{aligned} \tag{1}$$

$$\begin{aligned}\frac{\partial}{\partial t}Q_{m,n}(\nu,t)+\frac{\partial}{\partial \nu}Q_{m,n}(\nu,t) =& -(\lambda_1+\lambda_2+\alpha_1+\alpha_2+\mu_2(\nu))Q_{m,n}(\nu,t)\\ &+\lambda_1(1-\delta_{0m})\sum_{i=1}^{m}c_iQ_{m-i,n}(\nu,t)\\ &+\lambda_2(1-\delta_{0n})\sum_{j=1}^{n}c_jQ_{m,n-i}(\nu,t) \quad \text{for } m,n\geq 1.\end{aligned} \tag{2}$$

$$\begin{aligned}\frac{\partial}{\partial t}C_{m,n}(\nu,t)+\frac{\partial}{\partial \nu}C_{m,n}(\nu,t) =& -(\lambda_1+\lambda_2+\beta(\nu))C_{m,n}(\nu,t)\\ &+\lambda_1(1-\delta_{0m})\sum_{i=1}^{m}c_iC_{m-i,n}(\nu,t)\\ &+\lambda_2(1-\delta_{0n})\sum_{j=1}^{n}c_jC_{m,n-i}(\nu,t) \quad \text{for } m,n\geq 1.\end{aligned} \tag{3}$$

$$\begin{aligned}\frac{\partial}{\partial t}V_{m,n}(\nu,t)+\frac{\partial}{\partial \nu}V_{m,n}(\nu,t) =& -(\lambda_1+\lambda_2+\gamma(\nu))V_{m,n}(\nu,t)\\ &+\lambda_1(1-\delta_{0m})\sum_{i=1}^{m}c_iV_{m-i,n}(\nu,t)\\ &+\lambda_2(1-\delta_{0n})\sum_{j=1}^{n}c_jV_{m,n-i}(\nu,t) \quad \text{for } m,n\geq 1.\end{aligned} \tag{4}$$

$$\begin{aligned}\frac{\partial}{\partial t}S_{m,0}(\nu,t)+\frac{\partial}{\partial \nu}S_{m,0}(\nu,t) =& -(\lambda_1+\lambda_2+\phi(\nu))S_{m,0}(\nu,t)\\ &+\lambda_1c_i\sum_{i=1}^{m}S_{m-i,0}(\nu,t) \quad \text{for } m\geq 1.\end{aligned} \tag{5}$$

$$\begin{aligned}\frac{\partial}{\partial t}S_{0,n}(\nu,t)+\frac{\partial}{\partial \nu}S_{0,n}(\nu,t) =& -(\lambda_1+\lambda_2+\phi(\nu))P_{0,n}(\nu,t)\\ &+\lambda_2c_j\sum_{j=1}^{n}P_{0,n-j}(\nu,t) \quad \text{for } n\geq a.\end{aligned} \tag{6}$$

$$\frac{\partial}{\partial t}S_{m,n}(\nu,t)+\frac{\partial}{\partial \nu}S_{m,n}(\nu,t)=-(\lambda_1+\lambda_2+\phi(\nu))S_{m,n}(\nu,t)$$
$$+\lambda_1 c_i\sum_{i=1}^{m}S_{m-i,n}(\nu,t)+\lambda_2 c_j\sum_{j=1}^{n}S_{m,n-j}(\nu,t) \tag{7}$$
$$\text{for } m\geq 1,\quad n\geq a.$$

$$\frac{d}{dt}R^{(1)}_{m,n}(\nu,t)+\frac{d}{d\nu}R^{(1)}_{m,n}(\nu,t)=-(\lambda_1+\lambda_2+\eta_1)R^{(1)}_{m,n}(\nu,t)$$
$$\alpha_1\int_0^\infty(P_{m,n}(\nu,t)+Q_{m,n}(\nu,t))d\nu \tag{8}$$
$$\text{for } m,n\geq 1.$$

$$\frac{\partial}{\partial t}R^{(2)}_{m,n}(\nu,t)+\frac{\partial}{\partial \nu}R^{(2)}_{m,n}(\nu,t)=-(\lambda_1+\lambda_2+\eta_2(\nu))R^{(2)}_{m,n}(\nu,t)$$
$$+\lambda_1(1-\delta_{0m})\sum_{i=1}^{m}c_i R^{(2)}_{m-i,n}(\nu,t)$$
$$+\lambda_2(1-\delta_{0n})\sum_{j=1}^{n}c_j R^{(2)}_{m,n-i}(\nu,t) \tag{9}$$
$$\text{for }\ m,n\geq 1.$$

The boundary condition is defined at $\nu=0$

$$P_{m,n}(0,t)=\int_0^\infty P_{m+1,n}(\nu,t)\mu_1(\nu)d\nu+\int_0^\infty Q_{m+1,n}(\nu,t)\mu_2(\nu)d\nu$$
$$+\int_0^\infty S_{m+1,n}(\nu,t)\gamma(\nu)d\nu+\int_0^\infty R^(2)_{m+1,n}(\nu,t)\eta_2(\nu)d\nu \tag{10}$$
$$+R^{(1)}_{m+1,n}(t)\eta_1,$$

$$Q_{0,0}(0,t)=\sum_{n=a}^{b}\int_0^\infty P_{0,n}(\nu,t)\mu_1(\nu)d\nu+\sum_{n=a}^{b}\int_0^\infty Q_{0,n}(\nu,t)\mu_2(\nu)d\nu$$
$$+\sum_{n=a}^{b}\int_0^\infty S_{0,n}(\nu,t)\phi(\nu)d\nu+\sum_{n=a}^{b}\int_0^\infty R^(2)_{0,n}(\nu,t)\eta_2(\nu)d\nu \tag{11}$$
$$+\sum_{n=a}^{b}R^(1)_{0,n}(t)\eta_1,$$

$$Q_{0,n}(0,t)=\int_0^\infty P_{0,b+n}(\nu,t)\mu_1(\nu)d\nu+\int_0^\infty Q_{0,b+n}(\nu,t)\mu_2(\nu)d\nu$$
$$+\int_0^\infty S_{0,b+n}(\nu,t)\phi(\nu)d\nu+\int_0^\infty R^(2)_{0,b+n}(\nu,t)\eta_2(\nu)d\nu \tag{12}$$
$$+R^{(1)}_{0,b+n}(t)\eta_1,\qquad \text{for }\ n\geq 1.$$

$$C_{0,0}(0,t) = \int_0^\infty P_{0,0}(\nu,t)\mu_1(\nu)d\nu + \int_0^\infty Q_{0,0}(\nu,t)\mu_2(\nu)d\nu + \int_0^\infty R^(2)_{0,0}(\nu,t)\phi(\nu)d\nu + R^(1)_{0,0}(t)\eta_1, \tag{13}$$

$$C_{0,n}(0,t) = \int_0^\infty P_{0,n}(\nu,t)\mu_1(\nu)d\nu + \int_0^\infty Q_{0,n}(\nu,t)\mu_2(\nu)d\nu + \int_0^\infty R^(2)_{0,n}(\nu,t)\phi(\nu)d\nu + R^(1)_{0,n}(t)\eta_1, \quad \text{for} \quad n < a. \tag{14}$$

$$C_{m,n}(0,t) = 0, \quad \text{for} \quad m \geq 1, \quad n \geq a. \tag{15}$$

$$V_{0,n}(0,t) = \int_0^\infty C_{0,n}(\nu,t)\beta(\nu)d\nu + \int_0^\infty V_{0,n}(\nu,t)\gamma(\nu)d\nu, \quad \text{for} \quad n < a. \tag{16}$$

$$V_{m,n}(0,t) = \int_0^\infty C_{m,n}(\nu,t)\beta(\nu)d\nu, \quad \text{for} \quad m,n \geq 0. \tag{17}$$

$$S_{0,0}(0,t) = 0, \tag{18}$$

$$S_{0,n}(0,t) = 0, \quad \text{for} \quad m = 0 \quad n < a. \tag{19}$$

$$S_{0,n}(0,t) = \int_0^\infty V_{0,n}(\nu,t)\gamma(\nu)d\nu, \quad \text{for} \quad m = 0 \quad n \geq a \tag{20}$$

$$S_{m,n}(0,t) = \int_0^\infty V_{m,n}(\nu,t)\gamma(\nu)d\nu, \quad \text{for} \quad m \geq 1 \quad n \geq 0 \tag{21}$$

$$R^{(2)}_{m,n}(0,t) = \alpha_2 \int_0^\infty P_{m-1,n}(\nu,t)\mu_1(\nu)d\nu + \alpha_2 \int_0^\infty Q_{m,n}(\nu,t)\mu_2(\nu)d\nu, \quad \text{for} \quad m,n \geq 0 \tag{22}$$

$$P_{m,n}(0) = R^{(1)}_{m,n}(0) = Q_{m,n}(0) = R^{(2)}_{m,n}(0) = V_{m,n}(0) = 0 = C_{m,n}(0) = S_{m,n}(0), \quad \text{for} \quad m,n \geq 0, \tag{23}$$

are the initial conditions.

3 Steady State Analysis

Using Tauberian property,

$$\lim_{s\to 0} s\overline{f}(s) = \lim_{t\to\infty} f(t).$$

Despite of the state of the system the probability generating function (PGF) of the queue size

$$W_q(z_h, z_l) = \frac{Nr(z_h, z_l)}{Dr(z_h, z_l)}, \tag{24}$$

4 Stability condition

The probability generating function has to satisfy $W_q(1,1) = 1$ (Jeyakumar S. (2012)). Further, We have to find the unknown probabilities,$W_{0,k}$, $k = 0, 1, 2....b-1$. This expressions have been used to relate the idle probabilities, $I_{(0,k)}$ $k = 0, 1, 2....a-1$, then the LHS of the above expression should be greater than zero. Thus $W_q(1,1) = 1$ the appropriate condition should be satisfied if $2D_1^{'}(z)D_2{'}(z)\psi_1(z)\psi_2^{'}(z) > 0$. If $\rho < 1$.

5 The Expected Queue Lengths

The expected queue length for priority $L_{q_1} = \dfrac{d}{dz_1} W_q(z_1, 1)|_{z_1=1}$ (25)

The expected queue length for ordinary queue $L_{q_2} = \dfrac{d}{dz_2} W_q(1, z_2)|_{z_2=1}$ (26)

The expected waiting time for priority queue is $W_{q_1} = \dfrac{L_{q_1}}{\lambda_1}$ (27)

The expected waiting time for ordinary queue is $W_{q_2} = \dfrac{L_{q_2}}{\lambda_2}$ (28)

6 Numerical Results

This segment shows the numerical and graphical behaviour of this model. We examined the usual service time, breakdown, repair and vacation time are distributed exponentially. Table 1 exhibits that when an arrival rate (λ_1) for priority queue escalates, then the expected queue length (L_{q_1}, L_{q_2}) and the expected waiting time (W_{q_1}, W_{q_2}) also rise at $\lambda_2 = 1.5$, $\alpha_1 = 0.5$, $\alpha_2 = 0.7$, $\mu = 5$, $\eta_1 = 4$, $\eta_2 = 6$, $\gamma = 10$, $\theta = 0.8$, $\phi = 0.9$, $\beta = 15$ and $\lambda_1 = 1.0$ to 1.6.

Table 1: Effect of priority arrival rate (λ_1).

λ_1	L_{q_1}	W_{q_1}	L_{q_2}	W_{q_2}
1.0	0.5436	2.3094	0.5436	1.5396%
1.1	0.6207	2.3689	0.5642	1.5793%
1.2	0.6936	2.4316	0.5780	1.6211%
1.3	0.7625	2.4977	0.5865	1.6651%
1.4	0.8272	2.5675	0.5908	1.7117%

References

Ayyappan G., U. J. (2018). Analysis of mixed priority retrial queueing system with two way communication and working breakdown. *Journal of Mathematical Modeling*, 3:570–580.

Jeyakumar S., S. B. (2012). A study on the behaviour of the server breakdown without interruption in a $M^{[X]}/G(a,b)/1$ queueing system with multiple vacations and closedown time. *Applied Mathematics and Computation*, 219:2618–2633.

Rajadurai P., Saravanarajan M.C., Chandrasekaran V.M. (2018). A study on $M/G/1$ feedback retrial queue with subject to server breakdown and repair under multiple working vacation policy. *Applied Mathematics and Computation*, 57: 947-962.

Learners' Perceptions of the Challenges and Improvement Strategies in Distance and Online Undergraduate Mathematics Learning in Nigeria

Comfort O. Reju*[1] and Loyiso C. Jita[2]

[1]Distance Learning Institute, University of Lagos, Nigeria
[2]Dean, Faculty of Education, Universit y of the Free State, Bloemfontein, South Africa
[3]...

Abstract

In order to address the diverse needs of the present-day distance and online mathematics learners, it is necessary to obtain the opinions of the learners on the improvement strategies of the programme. In distance and online learning (DOL) education in Nigeria, different strategies to improve mathematics learning have been incorporated. The aim of this paper is to provide students' standpoint on the challenges and improvement strategies of learning mathematics through the distance and online method of education. The study explores how internet connectivity issues, institutional strategies and facilitation skill development impacted upon mathematics students' engagement in distance and online mode of learning. In this study, distance and online mathematics learners from two Open and Distance Learning (ODL) universities who were in the third-year of their study was interviewed. A thematic analysis and a word-for-word narrative inquiry approach that encourages students to tell their story was adopted in analysis. The findings indicated among others a need for provision of efficient, viable and affordable internet connectivity in their schools, inclusion of several online mathematics activities for students learning in this mode and provision of relevant mathematical resources for effective learning. It was recommended that the school in collaboration with the government should provide costless personal computers equipped with mathematical functions for effective mathematics learning. The students' opinion presented in this paper can be used as informed improvement strategies designed to enhance distance and online mathematics learning in ODL universities in Nigeria.

Keywords: Improvement strategies, students' perception, distance and online mathematics education

1 Introduction

Recently, universities and colleges have engaged in exploring the potentials of distance and online technology education with a bid of enhancing teaching and learning (Strategic Review of Online Education, 2015). The immediate outcome of technological abilities has brought about learning

*Corresponding Author. Email: okwyrej@gmail.com

mathematics through the distance and online mode, thereby increasing the student needs for high-tech prospects. One of the reasons why distance and online mathematics education has remained popular in the recent times is that several studies have proved its practices and revealed there is no significant differences in the learning outcome between traditional face-to-face and online distance learners (Ashby, Sadera, and McNary, 2011; Jones, and Long, 2013; Kalelioglu, 2017). Consequently, learning mathematics through any mode has no significant differences on its effectiveness (Burns, Duncan, Sweeney, North and Ellegood, 2013). A logical question that arises from this study is how learners perceive the improvement strategies of learning mathematics through distance and online education in Nigeria.

Distance Learning Institute (DLI), University of Lagos as a dual mode institute and National Open University of Nigeria (NOUN) (a single mode) are among the higher learning institutions approved to practice distance and online education in Nigeria. Mathematics has been one of the programmes of these institutions, though little has been known about how the learners perceive learning mathematics through this mode. One of the improvement strategies incorporated in the guideline for best practices of Open and Distance Learning in Nigeria, the National University Commission (NUC) (2009: 5) stated that: the 'students should have access to ICT to assist their learning. For specific programmes (mathematics inclusive), functional internet access would be required for all study centres. In order to realise this guideline, it means that the processes and procedures of administering the programme has to be met and there is a need for the learners input concerning the progress of the programme. It was on this basis that the authors felt it is essential to explore the perception of mathematics learners as stakeholders in distance and online learning (use henceforth as DOL) education. This will help to provide accurate view of the mathematics students learning in this mode while adding to the existing literatures on perception.

In distance and online education, learners are expected to be engaged and participate in the learning processes. Study has shown that online distance learners as autonomous students are influenced by positive perception they have toward technologies (Drennan, Kennedy, and Pisarski 2006; Jarjat and Ajlouni 2021). Also, as the opportunities call for these learners to relate with their facilitators and tutors, remarks are gathered on the issues in connection with challenges and improvement strategies. Such remarks are concerned with access to viable internet connectivity, interactive online facilitation, computer with mathematical functions and symbols. The view of the authors is that little research has been carried out based on the combined study involving DLI and NOUN to establish the learners' position of these issues. The purpose of this study is to uncover the perception of the mathematics learners on the issue that concerns their mathematics education advancement. This paper tends to answer the following questions: How do the learners appraise learning mathematics through this mode? What are the major challenges the learners experience while learning mathematics through the distance and online mode?

2 Literature Review

The review of literatures is based on three concepts pertinent to this paper – the learners' perceptions of DOL, learners perceived challenges of DOL, learners perceived improvement of DOL.

The Learners' Perceptions of DOL

Understanding learners' views in DOL is very vital in learning mathematics through this mode. Despite the notable roles, demand and general acceptance of DOL in most of the higher institutions of learning, many still hold diverse opinions about this mode of learning. The views have affected the administration of DOL in these institutions in many ways. Experience has shown that not all online education is effective due to hindrances associated with learning through this mode. However, institutions are to make deliberate efforts in controlling the hindrances for the benefit of the learners (Aziz, Musa, Aziz, Malik, and Khalid, 2020).

Perception is the view and experience the learners have in learning mathematics through DOL. The opinion of learners matters so much in online mathematics learning because, learning through this mode cannot be effective without the learners' acceptance. Studies have shown that learners liked the convenience experienced in online learning, especially when there is no alternative, though the learners show preference for face-to-face if available and affordable (Lowe, Mestel and Williams 2016). In the study 'online learning experiences of the learners', researcher indicated that the mentally preparedness and willingness to embark on self-development in learners was because of the positive attitude and interest they have with respect to DOL (Kalelioglu, 2017).

Learners Perceived Challenges of DOL

Most institutions of higher learning in the recent time have actively been into utilizing the potentials DOL technology has in improving the modern-day learning practices. This has brought sharp advancement in education across the globe. In Nigeria, the development in technology has brought about the adoption of online tools necessary in DOL delivery across the tertiary institutions as seen in National Open University of Nigeria (NOUN), Distance Learning Institute (DLI) of University of Lagos among others (Adu, Eze, Salako, and Nyangechi, 2013).

Challenges to effective DOL in most of institutions as perceived by the learners include internet connectivity, mental health of the learners, learning platform services, quality of learning materials, technophobia among the tutors and learners, assessment and feedback (Jaradat and Ajlouni, 2021). Aziz et al. (2020) maintain that attitudes and technology skills are the major challenges DOL faces. Their study argue that most learners have negative belief regarding online learning, there is minimal tutor-learner interactions, lack confidence and fear of self-study especially when complicated calculations (as in the case of mathematics) are involved. They suggest that these problems should not be ignored by the institution administering DOL in order to avoid the lasting negative impact it will create on the learners.

The study of Umoh and Akpan (2014) suggest there are lack of virtual learning environment and ICT centres with internet facilities to assist the online mathematics learners. Some researchers have identified irregular power supply, internet facilities, access to computer and technological proficiency as some of challenges perceived by the learners in DOL in Nigeria (Oyeleke and Adebisi, 2015). Furthermore, the learners noted how problematic it could be writing mathematical equations using computer technology. These challenges are similar with the experience of mathematics learners at Philippine (Bringula, Reguyal, Tan and Ulfa 2021). In addition, the learners lack personal learning space that guarantee freedom from all forms of distractions and studying the mathematics content on their own is very challenging, hence, they prefer interacting with their tutors on face-to-face

setting.

Learners Perceived Improvement of DOL
The expectation of the learners in DOL from experience are usually high and they believe that the basic need of learning through this mode should be met, but in some cases, their satisfaction is kept at either low or moderate level (Kalelioglu, 2017). Kalelioglu (2017) listed some conditions that guarantee the learners improvement level to include conducive virtual classroom, availability of relevant study materials that can be accessed from different devices, defined course duration, flexible assessment structure with prompt feedback and active learner-tutor interaction.

3 Methods

3.1 Research Design

This research explored students' opinion on the challenges and improvement strategies of learning mathematics through the distance and online method of education at two ODL higher education universities in Nigeria. Qualitative research approach which is exploratory by nature was used in this study (Maguire and Delahunt 2017). This research design in general allows deep studying of fewer population with the aim of generating the individual learners' interaction, reflection, interpretation and perception within the context of the study (Creswell 2014).

3.2 Participants

Two ODL institutions DLI and NOUN third year learners participated in this study. This is because the institutions present DOL standards, practices and traditions helpful in this study. Purposive sampling approach was adopted because the researchers want to take control and make sure only DOL mathematics education learners are involved in the study. This is different from the study of (Irfan, Kusumaningrum, Yulia and Widodo 2020) whose participants are mathematics teachers from various institutions. The learners from the two institutions that took part in the study have opportunity to attend voluntary weekly and, in some cases, biweekly meetings organised by their department.

3.3 Research Instrument

The instrument which aimed at collecting data from DOL mathematics education learners was self-designed by the researchers and validated by experts in curriculum.

3.4 Data Collection and Analysis

Data was collected using semi-structured interview. This is because semi-structured interviews have the quality that allowed the researchers to organise the questions in a structured(closed) and unstructured (open-ended) to allow unanticipated responses from the learners. This creates flexibility of the interviewer and interviewees to interact with the aim of generating appropriate and suitable data to find an answer to the research questions in this study. The identity of the interviewees was not disclosed in the study to ensure confidentiality. Thematic analysis was used to analyse the participants narrations.

Figure 1: The key themes, sub-themes and refine sub-themes of learners perceived challenges

4 Results

The study examined the opinion of distance and online mathematics learners on the challenges and improvement strategies that necessitate the effective mathematics learning in this mode. The result presented focused on the data collected from the semi-structured interviews that was conducted. The views of the learners were captured to answer the questions raised in this study. The challenges the mathematics education learners identified after organising the data methodically, are seen on the mode of instructional delivery, facilitation/support services, assessment procedures and technology for learning.

The mathematics learners from DLI and NOUN indicated the challenges they face in online mathematics education to include: limited and difficulty in accessing learning materials, study materials were not designed to support self-learning, mode of assignment not well defined, lack of feedback, poor online facilitation, lack of adequate support, non-availability of Internet connectivity and limited access to newer technology.

5 Improvement Strategies

The learners' perception on the improvement strategy to the challenges identified were as follow: availability of course materials, simplifying the course material to accommodate all categories of learners, providing prompt feedback to the learners, employ trained mathematics tutors, provide study centres equipped with modern technology and effective and affordable Internet. The perception the participants as stated are supported by Kalelioglu 2017) and Hudal, Wahyuni, Fauziyah (2021).

Figure 2: The themes and sub-themes of the learners' perceived improvement strategies.

References

Adu, E. O., Eze, I. R., Salako, E. T., and Nyangechi, J. M. (2013). E-learning and distance education in Nigeria. International Journal of Science and Technology, 2(2), 203-210.

Ashby, J., Sadera, W. A., and McNary, S. W. (2011). Comparing student success between developmental math courses offered online, blended, and face-to-face. Journal of Interactive Online Learning, 10(3), 128-140.

Aziz, N. A. A., Musa, M. H., Aziz, N. N. A., Malik, S.A. and Khalid, R. M. (2020). A Study on Barriers Contributing to an Effective Online Learning among Undergraduates' Students. Open Journal of Science and Technology, 3(Issue 1), 17-23.

Bringula, R., Reguyal, J. J., Tan, D. D and Ulfa, S. (2021). Mathematics self-concept and challenges of learners in an online learning environment during COVID-19 pandemic. Smart Learning Environments, 8(22). 1-23. https://doi.org/10.1186/s40561-021-00168-5

Burns, K., Duncan, M. Sweeney II, D. C., North, J. W., and Ellegood, W. A. (2013). A longitudinal comparison of course delivery modes of an introductory Information Systems Course and their impact on a subsequent Information Systems course. MERLOT Journal of Online Learning and Teaching, 9(4), 453-467.

Creswell, J. W. 2014. Research Design: Qualitative, Quantitative and Mixed Methods Approach (4th ed.). Los Angeles: Sage Publications.

Drennan, J. A., Kennedy, J., and Pisarski, A. (2006). Factors affecting student attitudes toward flexible online learning in management education. Journal of Educational Research, 98(6), 331-338.

Hudal, N., Wahyuni, T. S. and Fauziyah, F. D. (2021). Students' Perceptions of Online Mathematics Learning and Its Relationship Towards Their Achievement. Advances in Social Science, Education and Humanities Research, 529, 522-529.

Irfan, M., Kusumaningrum, B., Yulia, Y., and Widodo, S. A. (2020). Challenges during the pandemic: Use of e-learning in mathematics learning in higher education. Infinity, 9(2), 147-158.

Jaradat, S. and Ajlouni, A. (2021). Undergraduates' Perspectives and Challenges of Online Learning during the COVID-19 Pandemic: A Case from the University of Jordan. Journal of Social Studies Education Research, 12(1), 149-173.

Jones, S.J. and Long, V.M. (2013). Learning equity between online and on-site mathematics courses. MERLOT Journal of Online Learning and Teaching, 9(1), 1–12.

Kalelioglu, F. (2017). Online Learning Experience of the Learners: Their Readiness, Expectations and Level of Satisfaction. International Journal of Management and Applied Science, 3(3). 12-16.

Lowe,T., Mestel, B. and Willams, G. (2016). Perceptions of online tutorials for distance learning in mathematics and computing. Research in Learning Technology, 24, 1-14.

Maguire, M. and Delahunt, B. (2017). Doing a Thematic Analysis: A Practical, Step-by-Step Guide for Learning and Teaching Scholars. AISHE-J, 8(3), 3351-33514.

National Universities Commission (NUC). 2009. Guidelines for Open and Distance Learning in Nigerian Universities. http://nuc.edu.ng/wp-content/uploads/2015/01/GUIDELINES-FOR-OPEN-AND-DISTANCE-LEARNING-IN-NIGERIAN-UNIVERSITIES.pdf

Oyeleke, O. and Adebisi, T. A. (2015). Distance Education Modes in Nigeria: Students' Perceptions and Preference. Ife Journal of the Humanities and Social Studies (IJOHUSS), 2(2), 81-99. Strategic Review of Online Education (2015). Report of the Faculty Council on Teaching and Learning, Princeton University

Holistic Approaches in Queueing Analysis: Incorporating a Multi-Feature Queue with Failover Server, Multiple Vacations, Timely Feedback, Flexible Offering, Disruptions, and Restoration

G. Ayyappan[1] and S.Sankeetha*[2]

[1]Department of Mathematics, Puducherry Technological Institution, Puducherry, India
[2]Department of Mathematics, Saradha Gangadharan College, Puducherry, India

Abstract

Two types of services are explored in this paper: classic server and main server, both of which provide both regular and optional services. The Markovian Arrival Process (MAP) governs how customers come, and phase type determines how service time is distributed. The backup server covers the work of classic server at slow rate when he is subjected to breakdown due to technical issue or on vacation. Also immediate feedback will be provided under dissatisfaction of the customer. This system has been represented as a QBD Process that investigates steady state with the use of matrix analytic techniques, employing finite-dimensional block matrices. Our model's waiting time distribution has been examined in more detail during the busy times. Performance measures of the system are evaluated and also established few numerical and graphical representations.

Keywords:Markovian Arrival Process; Phase type service; Vacation; Optional service; Interruptions.

1 Introduction

Markovian Arrival Process (MAPs) (Neuts (1979)) which are characterized by their inter arrival time distribution, are a key concept used to describe the arrival of customers in a queueing system. The mathematical function known as the Laplace transform, which characterizes the probability distribution of the inter arrival periods, is what distinguishes MAP. the mean number of customers in the system, the mean waiting time, or the change of having a specific number of customers in the system can all be calculated using the Laplace transform and other queueing system performance measures. By using an m-dimensional parameter matrix (D_0, D_1), where D_1 and D_0 reign over the transition associated with arrival and no arrivals, respectively, Chakravarthy (2010) has written extensively about MAP. Several real-world queueing systems, including computer systems, manufacturing systems, communication networks, and transportation systems,can be modeled using MAPs.

*Corresponding Author. Email: somename@university.edu.

2 Model Description

Consider a system with two servers, the main server and the classic server, where customers arrive in a single queue using the Markovian arrival process (MAP). This arrival is represented by two matrices of order m, D_0 denoting no arrival and D_1 denoting arrival. When there is no one ahead, the arriving customer receives immediate service. The server provides standard service to all, but optional services are provided only based on the needs of the customer. After receiving standard service, the customer is given the opportunity to demand re-service immediately if they are dissatisfied with the service received. The main server is inactive while there are no users using the system, whereas the classic server goes on multiple vacations. The classical server's service will be subjected to interpretation due to technical breakdowns, which will be covered by the backup server by providing fresh service in a dilatory rate for the customer. The backup server provides normal service or remains idle when there are no customers in the system. Due to monetary constraints, two points must be stated. For beginning, the backup server will not provide fast feedback or optional servers. Second, despite the fact that both the backup and main servers are free, customers are only permitted to receive service from the main server after the repair or vacation is completed. The classic server either serves the customer by taking over the backup server or leaves the system when it is empty.

For regular and optional services, the server period of the main and classic servers pursues a phase type distribution given by (α_1, T_1) and (α_2, T_2) of order n_1 and n_2. Similarly, the backup server's regular service time is distributed according to the phase type distribution given by $(\alpha_1, \theta T_1)$, where $0 < \theta < 1$. Then the vector T_1^0, T_2^0 is given by $T_1^0 + eT_1 = 0$ and $T_2^0 + eT_2 = 0$. The classic server goes on vacation at an exponential rate of ξ. At the rate of ψ, breakdown follows exponentially. While repairing, the phase type distribution is followed (β, R) of order r. In addition, R_0 denotes the column vector meeting $R^0 + eR = 0$.

Let $\{(N(t), G(t), L_1(t), L_2(t), R(t), M(t)); t \geq 0\}$ represent the model by the Markov Process with the state space $\Omega = l(0) \cup l(1) \cup l(i)$ where

$$l(0) = \{(0,0,l) : 1 \leq l \leq m\} \cup \{(0,4,l_3,l) : 1 \leq l_3 \leq r, 1 \leq l \leq m\}$$

$$\begin{aligned} l(1) = {} & \{(1,g,l_2,l) : g = 1,2,10; 1 \leq l_2 \leq n_2, 1 \leq l \leq m\} \\ & \cup \{(1,3,l_3,l) : 1 \leq l_3 \leq r, 1 \leq l \leq m\} \\ & \cup \{(1,5,l_1,l) : 1 \leq l_1 \leq n_1, 1 \leq l \leq m\} \\ & \cup \{(1,9,l_1,l_3,l) : 1 \leq l_1 \leq n_1, 1 \leq l_3 \leq r, 1 \leq l \leq m\} \\ & \cup \{(1,14,l_2,l_3,l) : 1 \leq l_2 \leq n_2, 1 \leq l_3 \leq r, 1 \leq l \leq m\} \end{aligned}$$

$$\begin{aligned} for \quad i \geq 2, \quad l(i) = {} & \{(i,5,l_1,l) : 1 \leq l_1 \leq n_1, 1 \leq l \leq m\} \\ & \cup \{(i,g,l_1,l_2,l) : g = 6,7,11,12; 1 \leq l_1 \leq n_1, 1 \leq l_2 \leq n_2, 1 \leq l \leq m\} \\ & \cup \{(i,g,l_1,l_3,l) : g = 8,13; 1 \leq l_1 \leq n_1, 1 \leq l_3 \leq r, 1 \leq l \leq m\} \\ & \cup \{(i,10,l_2,l) : 1 \leq l_2 \leq n_2, 1 \leq l \leq m\} \end{aligned}$$

The generator matrix of our Markov chain is $Q = \begin{bmatrix} B_{00} & B_{01} & 0 & 0 & 0 & 0 & 0\cdots \\ B_{10} & B_{11} & B_{12} & 0 & 0 & 0 & 0\cdots \\ 0 & B_{21} & A_1 & A_0 & 0 & 0 & 0\cdots \\ 0 & 0 & A_2 & A_1 & A_0 & 0 & 0\cdots \\ 0 & 0 & 0 & A_2 & A_1 & A_0 & 0\cdots \\ \cdots & \cdots & \cdots & \cdots & \ddots & \ddots & \cdots \end{bmatrix}$

where each of elements are block matrix and

- $J(t)$ be the position of the regular server.
- $L_1(t)$ is it the service phase for regular service.
- $L_2(t)$ is it the service phase for optional service.
- $R(t)$ is it the repair phase.
- $M(t)$ is the phase of the Markovian Arrival Process.

$$J(t) = \begin{cases} 0, & \text{if main server is idle and classic server is on vacation} \\ 1, & \text{if main server is idle and classic server is busy with regular service} \\ 2, & \text{if the classic server is engaged in optional service and the main server is not} \\ 3, & \text{if main server is idle and backup server is engaged regular service} \\ 4, & \text{if the classic server and the backup server are both not in use} \\ 5, & \text{if main server is engaged in regular service and classic server is on vacation} \\ 6, & \text{if main server is engaged in regular service and classic server is engaged in regular service} \\ 7, & \text{if main server is engaged in regular service and classic server is engaged in optional service} \\ 8, & \text{if both the main server and the backup server are engaged in regular service} \\ 9, & \text{if main server is engaged in regular service and backup server is idle} \\ 10, & \text{if main server is engaged in optional service and classic server is on vacation} \\ 11, & \text{if main server is engaged in optional service and classic server is engaged in regular service} \\ 12, & \text{if both the main server and the classic server is engaged in optional service} \\ 13, & \text{if main server is engaged in optional service and backup server is engaged in regular service} \\ 14, & \text{if main server is engaged in optional service and backup server is idle} \end{cases}$$

3 Analysis of System Stability Condition

Let A be an irreducible infinitesimal generator matrix defined as the sum of the square matrix A_0, A_1 and A_2 , that is, $A = A_0 + A_1 + A_2$ of order $m(n_1 + n_2 + 2n_1(2n_2 + r))$ and let the row vector ρ be represented by $\rho = (\rho_0, \rho_1, \rho_2, \rho_3, \rho_4, \rho_5, \rho_6, \rho_7)$ is the steady state probability vector of A satisfies the set of equations $\rho A = 0$ along with the normalizing condition $\rho e = 1$. The dimension of $\rho_0 = n_1 m$, $\rho_1 = \rho_2 = \rho_5 = \rho_6 = n_1 n_2 m$, $\rho_3 = \rho_7 = n_1 r m$ and $\rho_4 = n_2 m$. The necessary and sufficient condition for the QBD process to obtain stability is by satisfying the condition $\rho A_0 e < \rho A_2 e$

4 The Invariant Probability Vector

Here, X represents solution for the infinitesimal generator Q and the normal condition, that is, $Xe = 1$. This X is slpitted up depending on status of the server $(X_0, X_1, X_2, ...)$ where all X_i are row vector each of various dimensions. X_0 is $m(1 + r)$, X_1 is $m(3n_2 + n_1 + r(1 + n_1 + n_2))$and the remaining probability vectors $X_2, X_3, ...$ are of equal dimension $m(n_1 + n_2 + 2n_1(2n_2 + r))$ The probability vector X follows a matrix geometric structure under the steady state is as underlying,

$$X_i = X_1 R^{i-1}, i = 2, 3, 4, ...,$$

where R , is the solution of the matrix quadratic equation and this matrix R is called the rate matrix.

$$R^2 A_2 + R A_1 + A_0 = 0$$

and the boundary states X_0 and X_1 is obtained by solving the equations

$$\begin{gathered} X_0 B_{00} + X_1 B_{10} = 0 \\ X_0 B_{01} + X_1 B_{11} + X_2 B_{21} = 0 \\ X_1 B_{12} + X_2 (A_1 + R A_2) = 0 \end{gathered}$$

subject to a condition of normalization

$$X_0 e_{m(1+r)} + X_1 e_{m(3n_2+n_1+r(1+n_1+n_2))} + X_2 (I - R)^{-1} e_{m(n_1+n_2+2n_1(2n_2+r))} = 1$$

Finding the rate matrix R is necessary before attempting to solve the set of equations mentioned above. However, Latouche and Ramaswami (1999) created the Logarithmic Reduction Approach, an algorithm that makes it simple to produce R.

Theorem 4.1 *The structure of the rate matrix R is* $R = \begin{bmatrix} s_{11} & s_{12} & s_{13} & s_{14} & s_{15} & s_{16} & s_{17} & s_{18} \\ 0 & s_{22} & s_{23} & s_{24} & 0 & s_{26} & s_{27} & s_{28} \\ 0 & s_{32} & s_{33} & s_{34} & 0 & s_{36} & s_{37} & s_{38} \\ 0 & s_{42} & s_{43} & s_{44} & 0 & s_{46} & s_{47} & s_{48} \\ s_{51} & s_{52} & s_{53} & s_{54} & s_{55} & s_{56} & s_{57} & s_{58} \\ 0 & s_{62} & s_{63} & s_{64} & 0 & s_{66} & s_{67} & s_{68} \\ 0 & s_{72} & s_{73} & s_{74} & 0 & s_{76} & s_{77} & s_{78} \\ 0 & s_{82} & s_{83} & s_{84} & 0 & s_{86} & s_{87} & s_{88} \end{bmatrix}$

5 Investigation of Waiting Time Distribution

The likelihood that the customer won't have to wait for service increases depending on whether there are no customers in the system or at least one customer. In a Markov chain, $\omega = (*) \cup \bar{2}, \bar{3}, \bar{4}, ...$ provides the absorption time where

$$\begin{aligned}(*) = (0,0) &\cup \{(0,4,l_3) : 1 \le l_3 \le r\} \\ &\cup \{(1,g,l_2) : g = 1,2,10; 1 \le l_2 \le n_2\} \\ &\cup \{(1,3,l_3) : 1 \le l_3 \le r\} \\ &\cup \{(1,5,l_1) : 1 \le l_1 \le n_1\} \\ &\cup \{(1,9,l_1,l_3) : 1 \le l_1 \le n_1, 1 \le l_3 \le r\} \\ &\cup \{(1,14,l_2,l_3) : 1 \le l_2 \le n_2, 1 \le l_3 \le r\}\end{aligned}$$

$$\begin{aligned}for \quad i \ge 2, \quad \bar{(i)} = &\{(i,5,l_1) : 1 \le l_1 \le n_1\} \\ &\cup \{(i,g,l_1,l_2) : g = 6,7,11,12; 1 \le l_1 \le n_1, 1 \le l_2 \le n_2\} \\ &\cup \{(i,g,l_1,l_3) : g = 8,13; 1 \le l_1 \le n_1, 1 \le l_3 \le r\} \\ &\cup \{(i,10,l_2) : 1 \le l_2 \le n_2\}\end{aligned}$$

The generator matrix of our Markov chain is $\bar{Q} = \begin{bmatrix} 0 & 0 & 0 & 0 & 0\cdots \\ C_0 & C & 0 & 0 & 0\cdots \\ 0 & C_1 & C & 0 & 0\cdots \\ 0 & 0 & C_1 & C & 0\cdots \\ \cdots & \cdots & \ddots & \ddots & \cdots \end{bmatrix}$

where each element are block matrix.

6 Cost Analysis

For our model under consideration, lets now impose a cost linked to various system executive measures. Then construct a cost function TC defined as $TC = CH * E_{system} + P_{IV} * CIV + P_{IBR} * CIBR + P_{IBO} * CIBO + P_{IBSR} * CIBSR + P_{IBSI} * CIBSI + P_{BRV} * CBRV + P_{BRBR} * CBRBR + P_{BRBO} * CBRBO + P_{BRBSR} * C + P_{BRBSR} * C + P_{BRBSI} * CBRBSI + P_{BOV} * CBOV + P_{BOBR} * CBOBR + P_{BOBO} * CBOBO + P_{BOBSR} * CBOBSR + P_{BOBSI} * CBOBSI + \psi * C11 + \gamma * C12 + \mu_1 * C13 + \mu_2 * C14 + \mu_3 * C15$

References

Chakravarthy, S. (2010). *Markovian Arrival Processes.* Wiley Encyclopedia of Operations Research and Management Science.

Latouche, G. and Ramaswami, V. (1999). *Introduction to Matrix Analytic Methods in Stochastic Modeling.* American Statistical Association,Virginia and the Society for Industrial and Applied Mathematics, Pennsylvania, 2nd edition.

Neuts, M. F. (1979). A versatile markovian point process. *Journal of Applied Probability*, 16:764–779.

Economic Analysis of a Retrial Queueing System with Balking, Orbit Search, Multiple Vacation, and Unreliable Server

Suman Kaswan, Mahendra Devanda, Chandra Shekhar*,
Department of Mathematics, Birla Institute of Technology and Science Pilani, Pilani Campus, Pilani, Rajasthan, 333 031 (India).
sumanchaudharymh@gmail.com; mahendradevandamaths@gmail.com; chandrashekhar@pilani.bits-pilani.ac.in

Abstract

This study aims to examine the orbital search concept within Markovian retrial queueing systems, considering the opportunity of multiple vacation policies and challenge of server breakdowns. The system dynamics are characterized by an infinite number of inflow-outflow balanced equations, encompassing distinguished stochastic processes such as arrival, service, search, repair, and vacation. To establish a theoretical foundation, we employ the probability generating function (PGF) technique to derive system characteristics. Firstly, we compute the stationary probabilities of the proposed model. Secondly, we derive key system metrics, including the mean orbit size. Finally, we formulate a total cost function. Subsequently, we conduct a comprehensive analysis of the numerical results for these system characteristics, taking into account various system parameters. The experimental findings reveal noteworthy similarities in trends between the graphical and analytical perspectives.

Keywords: Retrial queue; Orbital search; Multiple working vacations; Server breakdown; Social group optimization.

1 Introduction

In retrial queueing systems, customers wait remotely, as there is no physical queue available within the system. When a customer initially enters the system as a primary customer and finds an idle server, immediate service is provided. However, if the server is busy, the customer joins the orbit and reattempt for service again as a retrial customer. For a comprehensive understanding of the development of retrial queues, relevant sources such as [1], [2], [3], [4], and [5] provide detailed insights.

In retrial queueing systems, customers enter the orbit when the server is occupied, and they reattempt to get service. Consequently, impatience among customers intensifies due to long server's busy period, leading them to decide whether to balk from the system with a certain probability. Noteworthy studies on balking phenomena in retrial queuing systems include [6], [7], and [8].

In previous studies on retrial queues, it has been commonly observed that after completing service, the server remains idle until the arrival of the next customer either from orbit or new. However, in this model, we have introduced an orbital search mechanism, wherein the server actively searches for customers within the orbit instead of remaining idle. The incorporation of orbital search is a notable aspect of this study. Relevant works pertaining to orbital search include [9], [10], and [11]. In situations where the server finds no customers during the orbit search and there are no arrivals of primary customers, the server takes a vacation until at least one customer arrives in the system. The notion of multiple vacation has been investigated in studies such as [12] and [13]. Furthermore, in our model, an unreliable server undergoes immediate repair following a breakdown, resulting in a pause in service provision. During this time, customers within the system patiently wait for the completion of service. The dynamics of an unreliable server have been explored in research works such as [14] and [15].

2 Model description

For the mathematical modeling of the proposed model, we consider the following notations and assumptions:

*Corresponding author

- There are two types of customers: primary customers and retrial customers.
- The arrival process follows a Poisson process, and the inter-arrival times for primary and retrial customers are exponentially distributed with parameters λ and α, respectively.
- Customers are served on a First-Come, First-Served basis.
- The server is susceptible to breakdown and immediately undergoes repair. The inter-breakdown and repair time follow exponential distribution with rates ν and ξ, respectively.
- After completing customer' service, the server decides whether to remain idle or go for an orbit search for customers. The probabilities of remaining idle and conducting an orbital search are denoted as q and p, respectively, which are complimentary to each other. The inter-orbital search times follow an exponential distribution with parameter θ.
- When the server finds no customers either through arrival or orbital search, it takes a vacation following Poisson process with rate δ. The duration of the server's vacation follows an exponential distribution with rate γ.
- Customers, except when the server is idle, exhibit impatience when customer unable to find service in reattempting. They may balk with probabilities q_0, q_1, and q_2 when the server is busy, on vacation, or in a breakdown state, respectively.
- All stochastic processes are assumed to be independent of each other.

3 Steady-state analysis

The service system described above can be addressed using queueing theoretic approach which can be effectively modeled as a quasi-birth-and-death (QBD) process, wherein system states is denoted as $\{(N, J); N \geq 0, J = 1, 3, 4 \cup (N,j); N \geq 1, J = 0, 2\}$. In this context, N represents the number of customers present within the system and J signifies the state of the server. The joint probability distribution function $P_{n,j}$ represents the long-run steady-state proportion that the system remains in state $(N = n, J = j)$. Let $\{P_{n,0}, n \geq 1; P_{n,1}, n \geq 0; P_{n,2}, n \geq 1; P_{n,3}, n \geq 0; P_{n,4}, n \geq 0; \}$ be the stationary distribution of the Markov chain $\{N(t), J(t), t \geq 0\}$. This distribution provides insights into the probabilistic behavior of the system when it reaches a steady state.

3.1 Steady-state Equations

We have the following equations using the birth and death process and relating the system's state to a steady state.

$$(\lambda_1 + \gamma)P_{n,4} = \lambda_1 P_{n-1,4} + \delta P_{n,1}; \quad n \geq 0 \tag{1}$$

$$(\lambda + \alpha)P_{n,0} = q\mu P_{n,1}; \quad n \geq 1 \tag{2}$$

$$(\lambda_0 + \mu + \nu + \delta)P_{n,1} = \lambda_0 P_{n-1,1} + \lambda P_{n,0} + \lambda P_{n,2} + \alpha P_{n+1,0} + (\alpha + \theta)P_{n+1,2} + \xi P_{n,3}; \quad n \geq 1 \tag{3}$$

$$(\lambda_0 + \nu + \delta)P_{0,1} = \alpha P_{1,0} + (\alpha + \theta)P_{1,2} + \xi P_{0,3} + \gamma P_{0,4}; \tag{4}$$

$$(\lambda + \alpha + \theta)P_{n,2} = p\mu\ P_{n,1}; \quad n \geq 1 \tag{5}$$

$$(\lambda_2 + \xi)P_{n,3} = \lambda_2 P_{n-1,3} + \nu P_{n,1}; \quad n \geq 0 \tag{6}$$

where, $P_{-1,j} = 0, \quad j = 1, 3, 4$. By analyzing and understanding this stationary distribution, valuable insights into the long-term behavior and characteristics of the queueing system can be obtained within the framework of the QBD process. Let $\Pi_j(z), j = 0, 1, 2, 3, 4$ be the partial generating functions which

are given as follows

$$\Pi_0(z)=\sum_{n=1}^{\infty}z^nP_{n,0};\quad \Pi_1(z)=\sum_{n=0}^{\infty}z^nP_{n,1};\quad \Pi_2(z)=\sum_{n=1}^{\infty}z^nP_{n,2}$$
$$\Pi_3(z)=\sum_{n=0}^{\infty}z^nP_{n,3};\quad \Pi_4(z)=\sum_{n=0}^{\infty}z^nP_{n,4},\quad |\ z\ |\leq 1$$

3.2 System Performance Measure

Theorem 3.1 *The mean orbit sizes when the server is in system states such as busy, idle, in search period, under repair, and on vacation for the Markovian retrial queue with multiple vacations, an unreliable server, customer balking, and an orbital search mechanism are respectively given by*

$$N_1 = CP_{0,1}$$
$$N_0 = \frac{q\mu}{\lambda+\alpha}N_1$$
$$N_2 = \frac{p\mu}{\lambda+\alpha+\theta}N_1$$
$$N_3 = \frac{\lambda_2\nu BP_{0,1}+\nu\xi N_1}{\xi^2}$$
$$N_4 = \frac{\lambda_1\delta BP_{0,1}+\delta\gamma N_1}{\gamma^2}$$

The mean number of customers in the orbit is $N = N_0 + N_1 + N_2 + N_3 + N_4$.

where,

$$C=\frac{\left(\frac{\alpha q\mu}{\lambda+\alpha}+\frac{(\alpha+\theta)p\mu}{\lambda+\alpha+\theta}\right)\left(\lambda_0+\frac{\lambda_2\nu}{\xi}(1+\frac{\lambda_2}{\xi})+\frac{\lambda_1\delta}{\gamma}(1+\frac{\lambda_1}{\gamma})\right)}{\left(\lambda_0-\frac{\alpha q\mu}{\lambda+\alpha}-\frac{(\alpha+\theta)p\mu}{\lambda+\alpha+\theta}+\frac{\lambda_2\nu}{\xi}+\frac{\lambda_1\delta}{\gamma}\right)^2}$$

$$P_{0,1}=\frac{(\lambda+\alpha)(\lambda+\alpha+\theta)\xi\gamma}{q\mu(B-1)(\lambda+\alpha+\theta)\xi\gamma+B(\lambda+\alpha)(\lambda+\alpha+\theta)\xi\gamma+p\mu(\lambda+\alpha)\xi\gamma(B-1)+\nu B(\lambda+\alpha)}$$

4 Cost Analysis

The total cost function $TC(\mu,\theta)$ is given by

$$TC(\mu,\theta)=C_hN+C_vP_v+C_iP_i+C_bP_b+C_sP_s+C_rP_r+C_wW+C_m\mu+C_\theta\theta \tag{7}$$

The costing attributable to different aspects of the system are as follows:
C_h : Cost for sustaining per customer in the retrial space during unit time.
C_v : Cost/unit time of the server while in vacation period.
C_i : The cost per unit time when the server is sitting idle in the system.
C_b : Cost for the server in per unit time in the normal busy mode.
C_s : Cost of the server in the orbital search state per unit of time.
C_r : The cost spent per customer per unit time when the server is in breakdown state.
C_w : The cost agreed upon per unit time spent by the customer waiting for service.
C_m : Cost/unit time of rendering service by the server with rate μ while in busy state.
C_θ : Cost/unit time of the server while searching for customers in the orbit with rate θ.

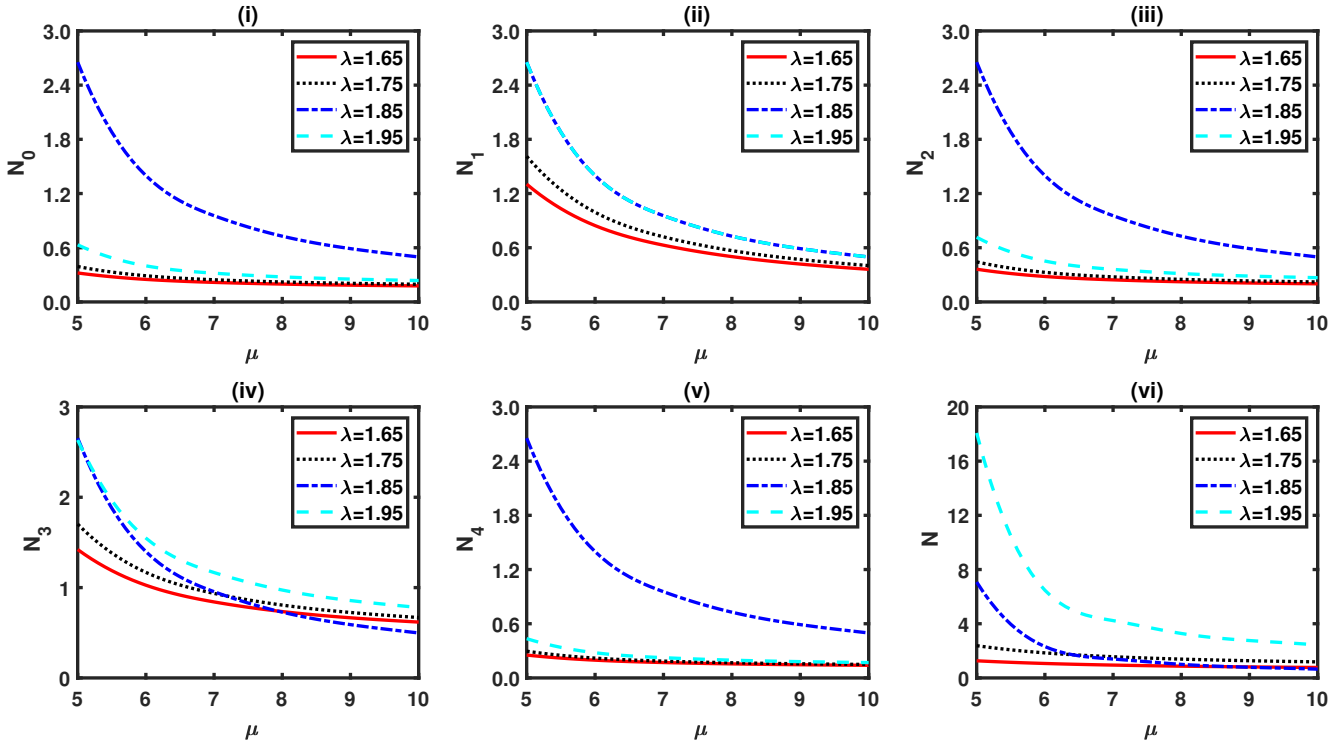

Figure 1: Line graphs of the mean orbit sizes and the service rate of the server (μ) for different arrival rates.

5 Numerical Results

Figure 1(i-vi) illustrates the variations observed in the graphs depicting the mean orbit sizes concerning different states of the server, considering varying service rates and arrival rates. The analysis presented in Figure 1 provides valuable insights into the relationship between service rate, arrival rate, and the resulting mean orbit sizes. The findings depicted in Figure 1 indicate that an improvement in the service rate leads to a reduction in the mean orbit size.

Figure 2 displays the plots illustrating the total cost function with respect to the decision parameters μ and θ. In particular, Figure 2(i, ii) provides evidence of the convex nature of the TC function, revealing the presence of a minimum value for certain combinations of the pair (μ, θ).

6 Conclusion

This study examines the utilization of the orbital search technique in addressing the retrial queue problem, incorporating server breakdown challenge and multiple vacation opportunities. The model described in this study offers enhanced realism and value as it considers all of these occurrences. We emphasize the use of the probability generating functions approach to analytically determine the probabilities of the server's state. This allows us to infer the server's state and proportion accurately and evaluate the crucial factors that influence its changes. Additionally, we explore various system features and construct the total cost function using these probabilities. To further enhance the evaluation of system performance, numerical tests are conducted across different factors.

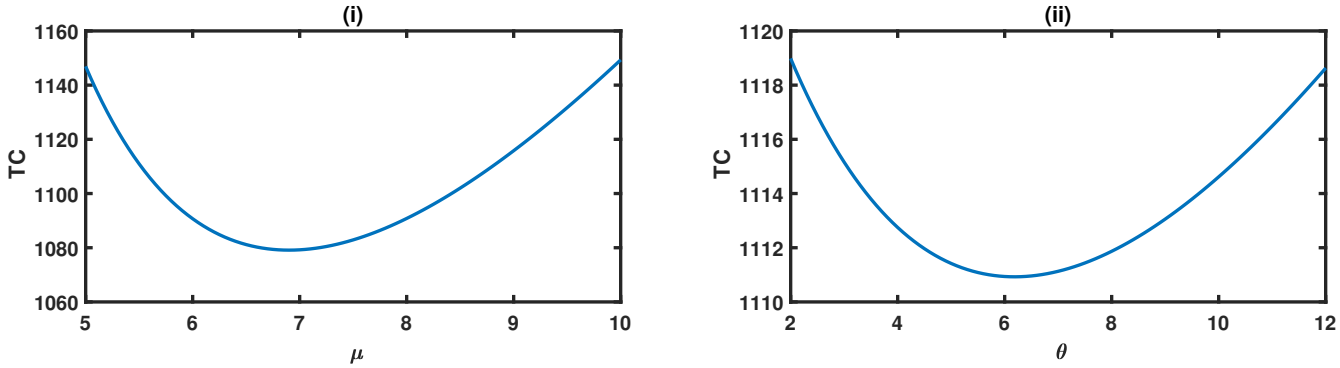

Figure 2: Plot of total cost (TC) wrt system's decision parameters (i) μ, (ii) θ.

References

[1] J. R. Artalejo and A. Gómez-Corral, *Retrial Queueing Systems: A Computational Approach*. Springer-Verlag Berlin Heidelberg, 2008.

[2] J. Kim and B. Kim, "A survey of retrial queueing systems," *Annals of operations research*, vol. 247, pp. 3–36, 2016.

[3] M. D'Arienzo, A. N. Dudin, S. A. Dudin, and R. Manzo, "Analysis of a retrial queue with group service of impatient customers," *Journal of Ambient Intelligence and Humanized Computing*, vol. 11, pp. 2591–2599, 2020.

[4] T.-H. Liu, F.-M. Chang, J.-C. Ke, and S.-H. Sheu, "Optimization of retrial queue with unreliable servers subject to imperfect coverage and reboot delay," *Quality Technology & Quantitative Management*, vol. 19, no. 4, pp. 428–453, 2022.

[5] D. Fiems, "Retrial queues with constant retrial times," *Queueing Systems*, vol. 103, no. 3, pp. 347–365, 2023.

[6] B. K. Kumar and J. Raja, "On multiserver feedback retrial queues with balking and control retrial rate," *Annals of Operations Research*, vol. 141, pp. 211–232, 2006.

[7] P. Wüchner, J. Sztrik, and H. de Meer, "Finite-source m/m/s retrial queue with search for balking and impatient customers from the orbit," *Computer Networks*, vol. 53, no. 8, pp. 1264–1273, 2009.

[8] J.-C. Ke, T.-H. Liu, S. Su, and Z.-G. Zhang, "On retrial queue with customer balking and feedback subject to server breakdowns," *Communications in Statistics-Theory and Methods*, vol. 51, no. 17, pp. 6049–6063, 2022.

[9] A. Krishnamoorthy, T. Deepak, and V. Joshua, "An m— g— 1 retrial queue with nonpersistent customers and orbital search," *Stochastic Analysis and Applications*, vol. 23, no. 5, pp. 975–997, 2005.

[10] S. Gao and J. Wang, "Performance and reliability analysis of an m/g/1-g retrial queue with orbital search and non-persistent customers," *European Journal of Operational Research*, vol. 236, no. 2, pp. 561–572, 2014.

[11] N. Sangeetha and K. U. Chandrika, "Mx/g/1 retrial g-queue with multistage and multi-optional services, feedback, randomized j vacation and orbital search," in *AIP Conference Proceedings*, vol. 2516, p. 100003, AIP Publishing LLC, 2022.

[12] I. Dimitriou, "A mixed priority retrial queue with negative arrivals, unreliable server and multiple vacations," *Applied Mathematical Modelling*, vol. 37, no. 3, pp. 1295–1309, 2013.

[13] Z. Wang, L. Liu, and Y. Q. Zhao, "Equilibrium customer and socially optimal balking strategies in a constant retrial queue with multiple vacations and n-policy," *Journal of Combinatorial Optimization*, pp. 1–39, 2022.

[14] L. Lakaour, D. Aissani, K. Adel-Aissanou, K. Barkaoui, and S. Ziani, "An unreliable single server retrial queue with collisions and transmission errors," *Communications in Statistics-Theory and Methods*, vol. 51, no. 4, pp. 1085–1109, 2022.

[15] F.-M. Chang, T.-H. Liu, and J.-C. Ke, "On an unreliable-server retrial queue with customer feedback and impatience," *Applied Mathematical Modelling*, vol. 55, pp. 171–182, 2018.

Economical Order Inventory Policies for Perishable Items with Permissible Delay in Payment under Credit Policy and Effect of Advertisement, Time, and Price-Discount

Vijender Yadav[*1], **Ankur Saurav**[2], **and Chandra Shekhar**[3]

[1,2,3]Department of Mathematics, Birla Institute of Technology and Science Pilani, Pilani Campus, Pilani, Rajasthan, 333 031 (India).

[1]vijenderyadav9497@gmail.com; [2]ankuranuraag2013@gmail.com; [3]chandrashekhar@pilani.bits-pilani.ac.in

Keywords:
Time-dependent power demand pattern;
Price-discount and Advertisement-dependent demand;
Permissible delay in payment;
Deterioration;
Interest on credit.

Paper type:
Research Article

Abstract

The strategic utilization of permissible delay in payment and credit period by suppliers presents a valuable opportunity to mitigate holding costs for retailers. This research delves into an inventory model aimed at minimizing the total cost for perishable items through the implementation of trade credit financing. However, several factors, including time, demand index, advertisements, selling price, and discounts, collectively influence the demand for these items, which are thoroughly examined in this study. In the highly competitive marketing economy, the primary objective is to determine optimal ordering policies and pricing strategies. This study analyzes real-life challenges within the inventory system, such as deterioration, partial backlogging, and lost sales. To validate the proposed model, a series of numerical examples are presented, compared, and solved using the meta-heuristic algorithm QPSO. Additionally, the convexity of each non-linear objective problem is visually analyzed. Furthermore, a sensitivity analysis of the objective functions is conducted with respect to key parameters, affirming the efficacy of the proposed approach.

1 Introduction

Logistics and supply chain systems are fundamental to industrial development and have a significant impact on national competitiveness. A key focus in current logistics systems is the utilization of permissible delay in payment. Suppliers offer a period of time, known as permissible delay in payment, referred as Trade Credit, for customers to settle their accounts, thereby attracting more customers. After this period, an interest is charged on unsold items. In the current competitive market, this serves as an attractive alternative to price discounts, benefiting retailers. Numerous researchers have examined the effect of permissible delay in payment in the literature. Sarkar et al. (2015) investigated a perishable inventory model under permissible delay in payment. Singh and Rathore (2015) studied a mathematical model considering the effects of inflation and trade credit. Other researchers, such as Shukla et al. (2017), Das et al. (2021), Astanti et al. (2022), Roy and Mashud (2022), have also focused on this concept. Duary et al. (2022) derived an economic order quantity (EOQ) model for capacity constraints, considering the effect of deterioration and the condition of advance and delay in payment policy.

Deterioration is a critical aspect in every inventory system, particularly for products like fruits, vegetables, and dairy products that deteriorate over time. The first decaying inventory model was examined by Ghare and Schrader (1963). Sicilia et al. (2014) analyzed a deterministic inventory system with power pattern time-dependent demand for perishable products. Other researchers, such as Sarkar et al. (2015), Viji and Karthikeyan (2018), Duary et al. (2022), have incorporated the concept of deterioration in their models. Mondal et al. (2022) considered an inventory model for deteriorating items with preservation technology investments under trapezoidal type demand. Ouaret (2022) constructed a stochastic optimum production control problem for a single machine multi-product manufacturing system with perishable products in the presence of random disturbances. Fan and Ou (2023) proposed a dynamic lot sizing approach with bounded inventory for a perishable product.

When analyzing deteriorating inventory, the demand rate plays a crucial role. Suppliers have the option to employ advertising, financial incentives, or a combination of both to stimulate sales. However, various variables, including time, the demand index, advertisements, selling price, and discounts, influence the demand. San-Jose et al. (2018) developed an instantaneous replenishment policy for backlogged shortage with price and time-dependent demand. San-Jose et al. (2021) extended this by considering demand as a function of advertisement as well. Aarya et al. (2022) introduced an inventory model with selling price and time-dependent demand rate for perishable items under a finite time horizon. San-Jos'e et al. (2022) examined an inventory system with time-dependent power demand pattern and partial backlog. Khan et al. (2023) studied demand related to price, freshness, and advertisements under certain conditions. The present paper is remarkable in studying the impact of demand patterns characterized by power functions over time, linear relationships for price discounts and advertisements, as well as deterioration and shortage under trade credit.

Based on the literature review and identifying research gaps in the area of inventory management, we developed a trade-credit-based EOQ model. The primary objective of our proposed study is to analyze real-life problems within the inventory system, including deterioration, partial backlogging, and lost sales. Additionally, we assess the benefits of permissible delay in payment, credit period, discount facilities, and interest on credit in the proposed model. Throughout our study, we consider demand patterns characterized by power functions over time, linear relationships for price and discounts, and exponential relationships for the frequency of advertisements.

2 Notations and Assumptions

In this section, we introduce the notations and assumptions used in formulating the proposed economic order quantity (EOQ) inventory model for perishable items.

- The demand for items follows a power demand pattern with respect to time t and a linear relationship with price p, discount d, and advertisement A. Therefore, the demand can be represented as:

*Corresponding author

$$D(t,p,A) = \frac{1}{n}A^{\gamma}a - bp + cd\left(\frac{t}{T}\right)^{\frac{(1-n)}{n}}$$

where $a > 0$, $b > 0$, $c > 0$, and $n > 0$ are the demand index parameters, and γ represents the elasticity of advertisement.

- The lead time is assumed to be constant.
- The product is considered to deteriorate at a constant rate θ.
- Partially backlogged shortages are allowed and denoted by B, where $B = \eta; 0 \leq \eta \leq 1$ (constant) , η is backlogging parameter.
- The ordering cost K, unit purchase cost C_0, unit holding cost C_1, unit shortage cost C_2, and unit lost sale cost C_3 are constant.
- Throughout the inventory cycle, the retailer earns interest on the revenue generated and pays interest on the remaining payable amount.
- The interest earning rate on revenue is denoted by I_e, while the interest paying rate on the remaining payable amount is denoted by I_p.
- Suppliers allow a retailer to delay payment by offering a credit period M that is less than the inventory cycle time T. The retailer is responsible for paying the interest charges on the items in stock at a rate of I_p.

3 Mathematical Model

The proposed model considers a supply chain partnership between a supplier and a retailer. In this section, we analyze the costs associated with different inventory phases, taking into account the trade-credit policy. At the beginning of each inventory cycle, denoted as $t = 0$, the maximum inventory level is assumed to be S. The inventory level gradually depletes mainly due to demand and partially due to deterioration during the time interval $[0, T_0]$. At time $t = T_0$, the inventory is completely depleted, leading to partially backlogged shortages during the time interval $[T_0, T]$. The maximum allowed shortage at time $t = T$ is represented by B. Under the credit policy, the supplier offers a credit period M that is shorter than the inventory cycle time T, i.e., $M \leq T$. The rate of change in inventory level at any time t during the inventory cycle length $[0, T]$ is governed by the following differential equations:

$$\frac{dI_1(t)}{dt} + \theta I_1(t) = -D, \qquad 0 \leq t \leq T_0 \tag{1}$$

$$\frac{dI_2(t)}{dt} = -\eta D, \qquad T_0 \leq t \leq T \tag{2}$$

By solving the differential equations (1) and (2) with the initial conditions $I_1(0) = S$ and $I_2(T_0) = 0$, the total quantity of items ordered in one inventory cycle is given by:

$$Q = A^{\gamma}T\{a - bp + cd\}\left[\eta + \left(1 - \eta + \frac{\theta T}{1+n}\right)\left(\frac{T_0}{T}\right)^{1+\frac{1}{n}}\right] \tag{3}$$

To analyze the costs associated with the inventory system and the trade-credit policy, we define the total cost per unit time (TCU). Under the suggested inventory relationship, all ordering, purchasing, holding, shortage, lost sale, and interest charges are borne by the retailer. The retailer's total cost per inventory cycle, calculated as the ratio of total cost (TC) and the inventory cycle time (T), represents the TCU. The total cost (TC) is given by:

TC = Ordering Cost(OC) + Purchasing Costs(PC) + Holding Cost(HC) + Shortage Cost(SC) + Lost Sale Cost(LSC) + Interest Payable Cost(IP) - Interest Earning Cost(IE).

where,

$$OC = K$$

$$PC = C_0Q$$

$$HC = C_1A^{\gamma}TT_0\{a - bp + cd\}\left(\frac{1}{1+n} + \frac{\theta T_0}{4n+2} - \frac{\theta^2T_0^2}{(6n+2)}\right)\left(\frac{T_0}{T}\right)^{\frac{1}{n}}$$

$$SC = \frac{1}{n+1}C_2\eta A^{\gamma}T\{a - bp + cd\}\left[nT - \{(n+1)T - T_0\}\left(\frac{T_0}{T}\right)^{\frac{1}{n}}\right]$$

$$LSC = C_3(1-\eta)A^{\gamma}T\{a - bp + cd\}\left[1 - \left(\frac{T_0}{T}\right)^{\frac{1}{n}}\right]$$

Since credit period is smaller than cycle time, thus retailer can use the sales revenue to earn interest at rate I_e and pay interest I_p to the supplier beyond the fixed credit period. Thus,

$$IP = \frac{1}{n+1}C_0A^{\gamma}TI_p\{a - bp + cd\}\left[nT - \left((n+1)T - M\right)\left(\frac{M}{T}\right)^{\frac{1}{n}}\right]$$

$$IE = \frac{n}{n+1}pA^{\gamma}T^2I_e\{a - bp + cd\}$$

Therefore,total cost per unit of time (TCU) is given by

$$TCU = \frac{TC}{T} \tag{4}$$

$$\therefore TCU = \frac{1}{T}\left[K + C_0A^{\gamma}T\{a - bp + cd\}\left[\eta + \left(1 - \eta + \frac{\theta T}{1+n}\right)\left(\frac{T_0}{T}\right)^{1+\frac{1}{n}}\right] + C_1A^{\gamma}TT_0\{a - bp + cd\}\left(\frac{1}{1+n} + \frac{\theta T_0}{4n+2} - \frac{\theta^2T_0^2}{(6n+2)}\right)\left(\frac{T_0}{T}\right)^{\frac{1}{n}}\right.$$
$$+ \frac{1}{n+1}C_2\eta A^{\gamma}T\{a - bp + cd\}\left[nT - \{(n+1)T - T_0\}\left(\frac{T_0}{T}\right)^{\frac{1}{n}}\right] + C_3(1-\eta)A^{\gamma}T\{a - bp + cd\}\left[1 - \left(\frac{T_0}{T}\right)^{\frac{1}{n}}\right] + \frac{1}{n+1}C_0A^{\gamma}TI_p\{a$$
$$\left. - bp + cd\}\left[nT - \left((n+1)T - M\right)\left(\frac{M}{T}\right)^{\frac{1}{n}}\right] - \frac{n}{n+1}pA^{\gamma}T^2I_e\{a - bp + cd\}\right] \tag{5}$$

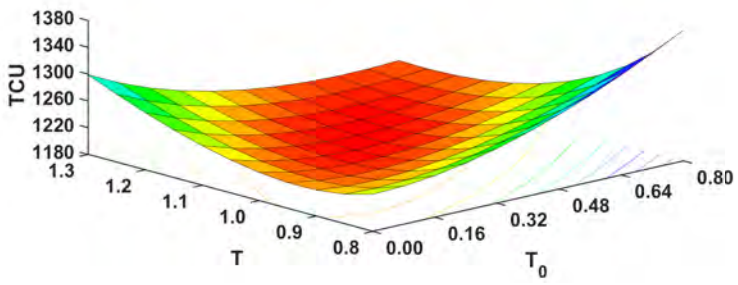

Figure 1: Surface graph of TCU w.r.t T_0 and T

The optimum total cost per unit of time is the objective of this study, and our goal is to minimize TCU, *i.e.* $TCU(T_0^*, T^*) = \min TCU$ subject to $T_0 < T$. Since, our objective function TCU in Eq. 5 is too complex to employ the classical theory of derivatives for optimization. Therefore, we use the quantum-behaved particle swarm optimization (QPSO) meta-heuristic optimisation technique to calculate the optimal total cost $TCU(T_0^*, T^*)$.

4 Quantum-behaved particle swarm optimization (QPSO)

Quantum-behaved particle swarm optimization (QPSO) is an optimization algorithm that combines principles from quantum mechanics and Particle Swarm Optimization (PSO) to solve optimization problems. The motivation behind incorporating quantum probability principles into the algorithm was to introduce a more directed and oriented search process, replacing the purely random search. QPSO is particularly suitable for nonlinear and non-differentiable optimization problems, offering a straightforward and simple-to-use approach with fewer parameters and a high capacity to handle challenging optimization tasks. In QPSO, the probability of a particle being located at a particular position, denoted as x_i, is determined by the probability density function $|\Psi(x,t)|^2$. This function depends on the potential field experienced by the particle during the optimization process. The particles in QPSO move iteratively according to specific equations, allowing them to explore the search space and converge towards optimal solutions. QPSO's utilization of quantum probability principles enhances its effectiveness in finding optimal solutions for various optimization problems.

$$C_{T_2} = \begin{cases} X(t+1) = p + \beta |X_{best} - X(t)| ln(\frac{1}{u}) & \text{if, } k \geq 0.5 \\ X(t+1) = p - \beta |X_{best} - X(t)| ln(\frac{1}{u}) & \text{if, } k < 0.5 \end{cases} \tag{6}$$

Mean best (X_{best}) of the population is defined as the mean of the best positions of all particles and the parameter β is called contraction-expansion coefficient.

5 Numerical Results

In this section, we provide a numerical example to illustrate the behavior of proposed model. We consider an inventory system with specific parameter values given in their respective units: $a = 250$, $b = 8$, $p = 25$, $c = 5$, $d = 7$, $A = 30$, $\gamma = 0.1$, $K = 100$, $C_0 = 8$, $C_1 = 2.5$, $C_2 = 9.5$, $C_3 = 3$, $\theta = 0.17$, $\eta = 0.6$, $n = 2$, $M = 0.06$, $I_p = 0.19$, and $I_e = 0.05$. By substituting these values into Eq. (5), we calculate the numerical value of the total cost per unit time (TCU). Figure 1 depicts a surface graph illustrating the convexity of TCU with respect to the decision variables T_0 and T. The graph visually demonstrates the relationship between the values of T_0, T, and TCU. To obtain the optimal value of TCU, we employ the QPSO algorithm. Figure 2 displays the contour plot of the total cost function TCU for the variables T_0 and T, presenting the feasible solution space. We configure the QPSO algorithm with a population size of 30, 30 iterations, and 16 runs for implementation. The iteration results are presented in Figures 2 - 3. Figure 2 shows convergence of solution points in feasible region iteratively and also validate the usefulness of QPSO algorithm. Figure 3 specifically illustrates the convergence of the QPSO algorithm across multiple runs.

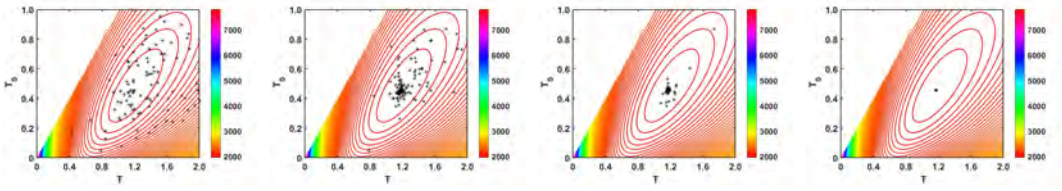

(a) Iteration=1 (b) Iteration=12 (c) Iteration=18 (d) Iteration=27

Figure 2: Several generations of QPSO algorithm on the contour of $TCU(T_0, T)$

After employing QPSO algorithm, the optimal values for T_0^* and T^* are determined as 0.4550 and 1.1704, respectively. Correspondingly, the optimum order quantity Q^* is calculated as 197.5487 units, and the associated total cost per unit time TCU^* amounts to Rs. 1206.8750. These results indicate the optimal configuration of the inventory system and the associated cost implications based on the given parameter values.

By varying the values of the parameters, we can conduct a sensitivity analysis, which provides valuable insights into the dependence of optimal solutions on cost and other relevant parameters. This analysis allows us to gain a comprehensive understanding of the researched model and its behavior under different scenarios. Sensitivity analysis aids in exploring the robustness and flexibility of the proposed model, enabling us to assess the impact of parameter changes on the optimal solution. Through this process, we can identify critical factors that significantly influence the performance and cost implications of the inventory system. Sensitivity analysis serves as a valuable tool in decision-making processes, as it helps stakeholders evaluate different scenarios and make informed choices based on a deeper understanding of the model's dynamics and performance across a range of parameter values.

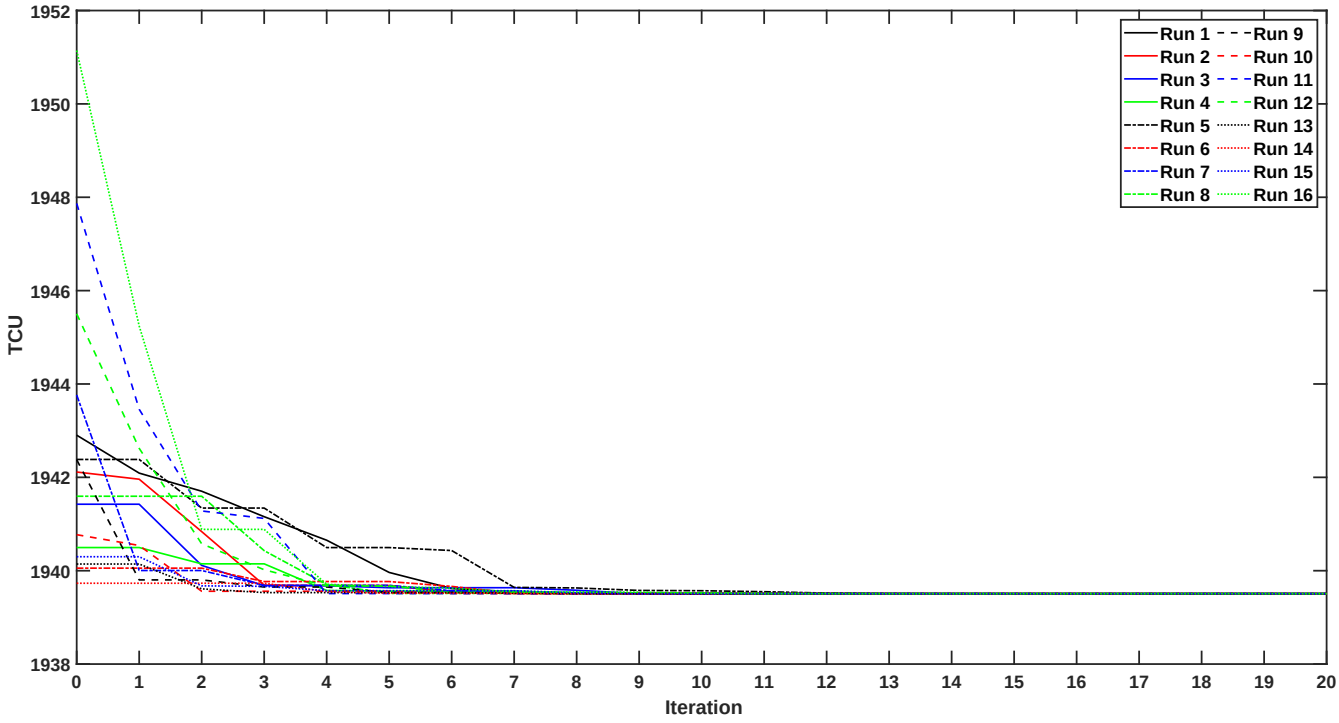

Figure 3: Run graph of several iterations of QPSO

6 Conclusions

In the present article, we develop an *EOQ* model for perishable items with permissible delay in payments under credit policy. Effect of time dependent power demand pattern, Advertisement and price-discount is also considered with partially backlogged shortages. In addition, the conditions of the existence and uniqueness of the optimal solutions to the model have been discussed in detail under all possible situations. Mathematical model is provided for finding optimal solution. In addition, the results of the present study suggest that optimal replenishment policies may help retailers to establish the optimal total cost. The proposed model is applicable in the market in which demand is varying with time, price and advertisement (like fruits, vegetables, etc.). Therefore, it is essential for practitioners to own a realistic inventory model that really captures and simulates their business environment. The Proposed model can be further extended by considering other factors of inventory control like time dependent deterioration rate, inflation, controllable lead time etc.

7 References

1. Aarya, D.D., Rajoria, Y.K., Gupta, N., Raghav, Y.S., Rathee, R., Boadh, R., and Kumar, A. (2022): Selling price, time dependent demand and variable holding cost inventory model with two storage facilities, Materials Today: Proceedings, Vol. 56, No. 1, pp. 245-251.
2. Astanti, R.D., Daryanto, Y., and Dewa, P.K. (2022): Low-carbon supply chain model under a vendor-managed inventory partnership and carbon cap-and-trade policy, Journal of Open Innovation: Technology, Market and Complexity, Vol. 8, No. 30.
3. Das, S., Khan, M.A.A., Mahmoud, E.E., Abdel-Aty, A.H., Abualnaja, K.M., and Shaikh, A.A. (2021): A production inventory model with partial trade credit policy and reliability, Alexandria Engineering Journal, Vol. 60, No. 1, pp. 1325-1338.
4. Duary, A., Das, S., Arif, M.G., Abualnaja, K.M., Khan, M.A.A., Zakarya, M., and Shaikh, A.A. (2022): Advance and delay in payments with the price-discount inventory model for deteriorating items under capacity constraint and partially backlogged shortages, Alexandria Engineering Journal, Vol. 61, pp. 1735-1745.
5. Fan, J. and Ou, J. (2023): On dynamic lot sizing with bounded inventory for a perishable product, Omega, Vol. 119, ID. 102895.
6. Ghare, P.M. and Schrader, G.H. (1963): A model for exponentially decaying inventory system, Journal of Industrial Engineering, Vol. 14, No 5, pp. 238-243.
7. Khan, M.A.A., Shaikh, A.A., Khan, A.R., and Alrasheedi, A.F. (2023): Advertising and pricing strategies of an inventory model with product freshness-related demand and expiration date-related deterioration, Alexandria Engineering Journal, Vol. 73, pp. 353-375.
8. Mondal, R., Shaikh, A.A., Bhunia, A.K., Hezam, I.M., and Chakrabortty, R.K. (2022): Impact of trapezoidal demand and deteriorating preventing technology in an inventory model in interval uncertainty under backlogging situation, Mathematics, Vol. 10, No. 78.
9. Ouaret, S. (2022): Production control problem with semi-Markov jump under stochastic demands and deteriorating inventories, Applied Mathematical Modelling, Vol. 107, pp. 85-102.
10. Roy, D. and Mashud A.H.M. (2022): Optimizing profit in a controlled environment: Assessing the synergy between preservation technology and cap-and-trade policy, Journal of King Saud University - Science, Vol. 34, ID. 101899.
11. San-José, L.A., Sicilia, J., and Pablo, D.A.L. (2018): An inventory system with demand dependent on both time and price assuming backlogged shortages, European Journal of Operational Research, Vol. 270, No. 3, pp. 889-897.

12. San-José, L.A., Sicilia, J., and Jalbar, B.A. (2021): Optimal policy for an inventory system with demand dependent on price, time and frequency of advertisement, Computers & Operations Research, Vol. 128, ID. 105169.
13. San-José, L.A., Sicilia, J., Pando, V., and Alcaide-López-de-Pablo, D. (2022): An inventory system with time-dependent demand and partial backordering under return on inventory investment maximization, Computers & Operations Research, Vol. 145, ID. 105861.
14. Sarkar, B., Saren, S., and Cárdenas-Barrón, L.E. (2015): An inventory model with trade-credit policy and variable deterioration for fixed lifetime products, Annals of Operations Research, Vol. 229, pp.677-702.
15. Shukla, H.S., Tripathi, R.P., and Siddiqui, A. (2017): EOQ model with time induced demand, trade credits and price discount on shortages: a periodic review, Global Journal of Pure and Applied Mathematics, Vol. 13, No. 8, pp. 3961-3977.
16. Singh, S.R. and Rathore, H. (2015): Optimal payment policy with preservation technology investment and shortages under trade credit, Indian Journal of Science and Technology, Vol. 8, pp. 203-212.
17. Viji, G. and Karthikeyan, K. (2018): An economic production quantity model for three levels of production with Weibull distribution deterioration and shortage, Ain Shams Engineering Journal, Vol. 9, pp. 1481-1487.
18. Sicilia, J., De-la-Rosa, M.G., Acosta, J.F., and López-de-Pablo, D.A. (2014): An inventory model for deteriorating items with shortages and time-varying demand, International Journal of Production Economics, Vol. 155, pp. 155-162.

Penalised Markowitz Portfolio Model with Augmented Lagrangian

Kornelia N. David, Sunday A. Reju, and Serge N. Neossi

Mathematics, Statistics and Actuarial Science, Namibia University of Science and Technology, Windhoek, Namibia
Author for correspondence: Sunday A. Reju, Email: sreju@nust.na.

Abstract

This article formulates and solve the Markowitz Portfolio model using the Augmented Lagrangian optimisation method. Our portfolio consists of a set of financial assets from different financial markets including the local Namibian market. Historical market prices of these assets are used to formulate the Markowitz Portfolio model. The research investigates how the Augmented Lagrangian method together with the use of penalty parameters improves solutions to portfolio optimisation models in terms of asset allocation, minimising risk and maximising returns, which are all major aspects of portfolio optimisation.

Keywords: Portfolio Optimisation, Markowitz Portfolio Model, Augmented Lagrangian, Penalty Parameters, Investment

Introduction

Portfolio optimisation is a formal mathematical approach to making investment decisions across a collection of financial instruments or assets. The classical approach to portfolio optimisation is known as modern portfolio theory (MPT), and it involves categorising the investment universe based on risk (standard deviation) and return, and then choosing the collection of investments that achieve a desired risk versus return trade off (Lee and Lee 2010). By optimising certain criteria of the portfolio, an investor advances his chances of earning interest on his investments and avoids loss of funds which arises from risks exposure. These risks include market risks, or risks associated with the company where the funds are placed. The output of the optimisation process is a distribution of weights of these instruments in the portfolio (Beasley 2013).

The Markowitz portfolio model

The Markowitz portfolio optimisation model is formulated as a minimisation problem, that minimises the portfolio return variance subject to a minimum expected value of return (Ho, Sun, and Xin 2015).

$$\left.\begin{aligned} \text{Minimise } \sigma_p{}^2 &= \sum_{i=1}^{n}\sum_{i=1}^{n} x_i x_j \sigma_{ij} \\ \text{subject to } \sum_{i=1}^{n} x_i E(r_i) - \mu &= 0 \\ \sum_{i=1}^{n} x_i &= 1 \end{aligned}\right\} \qquad (1)$$

where

σ_p^2 = variance of a portfolio (p)
x_i= share of wealth invested in the ith asset
x_j = share of wealth invested in the jth asset
σ_{ij} = Covariance between asset i and j
$E(r_i) = \mu_i$= expected return of asset i
μ= the desired weighted return of the portfolio

The efficient frontier

The efficient frontier is a set of optimal portfolios that have the highest expected return for a given level of risk or the lowest risk for a given level of expected return and These are the portfolios that investors are most interested in holding (Zivot 2013). The efficient frontier is presented graphically in figure 1 below.

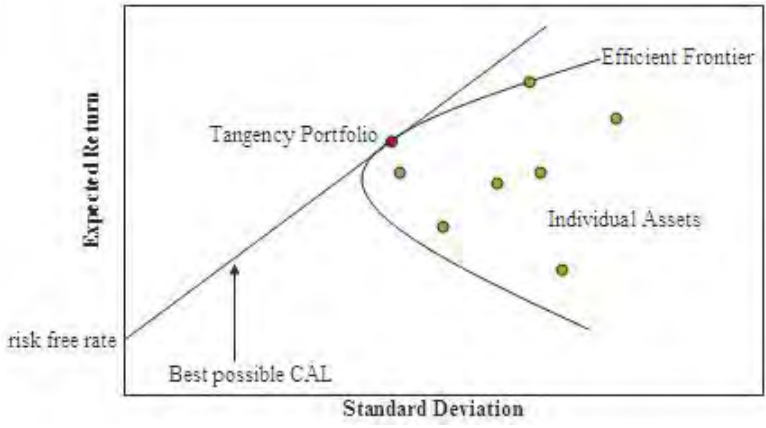

Figure 1. Efficient frontier

The Augmented lagrangian

The augmented lagrangian is applicable to non-linear programming problems of the form:

$$\left.\begin{array}{r} \text{Minimise } f(x) \\ \text{subject to } h(x) = 0 \\ g(x)0 \\ x \in \Omega \end{array}\right\} \tag{2}$$

where h:$R^n \longrightarrow R^m, g : R^n \longrightarrow R^p, f : R^n \longrightarrow R$ are smooth and $\Omega \subset R^n$ is an n-dimensional box i.e. $\Omega = \{x \in R^n \mid lxu\}$.

The Augmented Lagrangian of equation (2) is formulated as:

$$L_\rho(x, \lambda) = f(x) + \lambda^T h(x) + \frac{\rho}{2}\|h(x)\|^2 \tag{3}$$

The gradient

The first derivative of equation (3) is:

$$\Delta L_\rho(x, \lambda) = \Delta f(x) + \lambda^T \Delta h(x) + \frac{2\rho}{2} h(x)h'(x) \tag{4}$$

Let $\lambda^T = \lambda$ and $h'(x) = \Delta hx$, then

$$\Delta L_\rho(x, \lambda) = \Delta f(x) + \lambda \Delta h(x) + \rho h(x).\Delta h(x)$$

Therefore the gradient of the Augmented Lagrangian of equation (3) is:

$$\Delta_x L_\rho(x, \lambda) = \Delta f(x) + \Delta h(x)\,(\lambda + \rho h(x)) \tag{5}$$

The hessian

By taking the second derivative of equation (5), the hessian of the Augmented Lagrangian function is:

$$\Delta_{xx} L_\rho(x, \lambda) = \Delta_x \left[\Delta f(x) + \lambda \Delta h(x) + \rho h(x).\Delta h(x)\right] \tag{6}$$

$$= \Delta^2 f(x) + \lambda \Delta^2 h(x) + \Delta_x \left[\rho h(x).\Delta h(x)\right] \tag{7}$$

The derivative of the last term of equation (7) is found by using the product rule, hence, let $u = \rho h(x)$ and $v = \Delta h(x)$. The product rule formula is, $u'v + v'u$.
Therefore, equation (7) becomes:

$$\begin{aligned} \Delta_{xx} L_\rho(x, \lambda) &= \Delta^2 f(x) + \lambda \Delta^2 h(x) + \rho \Delta^2 h(x).h(x) + \rho \Delta h(x).h(x)' \\ &= \Delta^2 f(x) + \Delta^2 h(x)\left[\lambda + \rho h(x)\right] + \rho \Delta h(x).\Delta h(x) \\ &= \Delta^2 f(x) + \Delta^2 h(x)\left[\lambda + \rho h(x)\right] + \rho \Delta^2 h(x) \end{aligned} \tag{8}$$

Equation (8) is the general equation for computing the hessian of the Augmented Lagrangian function.

The second order sufficiency conditions

Let $x^* \in R^n$ and $\lambda^* \in R^m$ satisfy the following conditions

$$\Delta_x L_\rho(x^*, \lambda^*) = 0 \tag{9}$$

$$\gamma' \Delta^2_{xx} L^\rho(x^*, \lambda^*)\gamma 0, \forall \gamma \neq 0 \tag{10}$$

$$\text{with } \Delta h(x^*)'\gamma = 0$$

Then x^* is a strict local minimum. If ρ is larger than a threshold, then x^* also satisfies these conditions for the Augmented Lagrangian $L_\rho(., \lambda^*)$ and hence is a strict local minimum of the Augmented Lagrangian $L_\rho(., \lambda^*)$ corresponding to λ^* (Aarti, n.d.).

Theorem: 1 *Let x^* be a local solution of equation (2) at which the Karush-Kunh-Tucker optimality conditions are satisfied (i.e. the gradients $\Delta c_i(x_*), i \subset \epsilon$, are linearly independent vectors), and the second sufficient conditions specified in equation (9) and (10) are satisfied for ($\lambda = \lambda^*$). Then, there is a threshold penalty value $\bar{\mu}$ such that for all $\mu \geq \bar{\mu}$, x^* is a strict local minimiser of $L(x, \lambda^*; \rho)$*

The Lagraginan of the Markowitz portfolio model

The augmented lagrangian of the Markowitz portfolio model in equation (2) using equation (3) is:

$$\begin{aligned} L_\rho(x_1, x_2, \ldots, x_n, \lambda_1, \lambda_2, \rho) = &\sum_{i=1}^{n}\sum_{j=1}^{n} x_i x_j \sigma_{ij} + \lambda_1 \left(\sum_{i=1}^{n} x_i E(r_i) - \mu\right) \\ &+ \lambda_2 \left(\sum_{i=1}^{n} x_i - 1\right) + \frac{\rho}{2}\left|0\left(\sum_{i=1}^{n} x_i E(r_i) - \mu\right)\right| \\ &+ \frac{\rho}{2}\left|0\left(\sum_{i=1}^{n} x_i - 1\right)\right|0^2 \end{aligned} \tag{11}$$

Where λ_1, λ_2 are lagrange multipliers and ρ is the penalty parameter.

while the hessian which is obtained using equation (8) is given by:

$$\Delta_{xx}L_{\rho}(x,\lambda) = \sum_{i=1}^{n}\sum_{j=1}^{n}\Delta^2(x_i x_j \sigma_{ij}) + \sum_{i=1}^{n}\Delta^2(x_i E(r_i)-\mu)\left[\lambda_1 + \rho\sum_{i=1}^{n}(x_i E(r_i)-\mu)\right] + \sum_{i=1}^{n}\Delta^2(x_i-1)\left[\lambda_2 + \rho\sum_{i=1}^{n}(x_i-1)\right] + \rho\Delta^2\left(\sum_{i=1}^{n}x_i E(r_i)-\mu\right) + \rho\Delta^2\left(\sum_{i=1}^{n}x_i - 1\right) \quad (12)$$

The analysis of the Markowitz portfolio model

The data used in the analyses of the model is the monthly historical prices for a three year period ranging from January 2016 to January 2020. The data was extracted from the global investing website (https://www.investing.com/), an investment website which keeps track of all worldwide investment records. Table 1 below summarises assets from selected markets.

Table 1. List of assets

	Asset Region	Asset sticker	Assets description
x_1	United States	MSFT	Microsoft Corporation
x_2	United States	JPM	JPMorgan Chase Co
x_3	United States	US5Y Note	United State 5-Year
x_4	Euro zone	BARC	Barclays PLC
x_5	Euro zone	ALVG	Alliaz SE VNA O.N.
x_6	Euro zone	EURO BUND	EURO BUND
x_7	South Africa	OMUJ	Old Mutual Johannesburg
x_8	South Africa	ABSPp	Absa Bank Ltd
x_9	Namibia	NBS	Namibia Breweries
x_{10}	Namibia	NAM3Y BOND	Namibia 3-Year bond

Assets' returns

By using monthly historical prices of assets in table 1, we compute monthly returns of each of these assets using the following formula as discussed under chapter two.

$$R_{it} = ln\left(\frac{p_{it+1}}{p_{it}}\right) \quad (13)$$

where R_{it} is the index return i in period t, and p_{it} is the index price i in period t.

Results of this computation are monthly returns of assets under the portfolio which are presented graphically as follows:

Figure 2. United States market assets monthly returns

Figure 3. Eurozone market assets monthly returns

Figure 4. South Africa market assets monthly returns

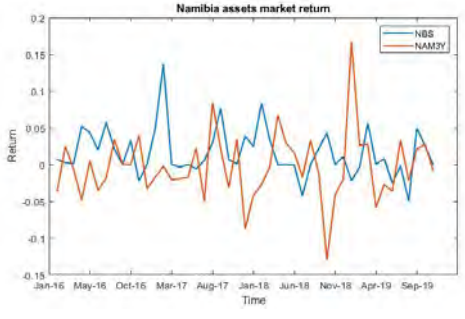

Figure 5. Namibia market assets monthly returns

Numerical formulation of the model

The objective of the model in equation (1) is to minimise portfolio risk measured by the variances among all assets of our portfolio. This is easily measured by the covariance matrix (*COV*) of all assets in the portfolio. The covariance matrix for returns of all assets of the portfolio was computed using excel data analysis tools and the results are presented in the table below.

$$COV = \begin{bmatrix} 0.00241 & 0.00127 & -0.00010 & 0.00053 & 0.00128 & -0.00012 & 0.00092 & 0.00011 & -0.00033 & 0.00018 \\ 0.00127 & 0.00349 & -0.00030 & 0.00297 & 0.00222 & -0.00032 & 0.00144 & -0.00020 & 0.00002 & 0.00036 \\ -0.00010 & -0.00030 & 0.00006 & -0.00042 & -0.00026 & 0.00007 & -0.00017 & 0.00005 & -0.00003 & -0.00003 \\ 0.00053 & 0.00297 & -0.00042 & 0.00667 & 0.00263 & -0.00052 & 0.00093 & -0.00028 & 0.00068 & 0.00042 \\ 0.00128 & 0.00222 & -0.00026 & 0.00263 & 0.00284 & -0.00046 & 0.00118 & -0.00036 & -0.00002 & 0.00042 \\ -0.00012 & -0.00032 & 0.00007 & -0.00052 & -0.00046 & 0.00024 & -0.00024 & 0.00007 & -0.00007 & 0.00001 \\ 0.00092 & 0.00144 & -0.00017 & 0.00093 & 0.00118 & -0.00024 & 0.00248 & -0.00026 & 0.00008 & -0.00007 \\ 0.00011 & -0.00020 & 0.00005 & -0.00028 & -0.00036 & 0.00007 & -0.00026 & 0.00055 & -0.00001 & -0.00011 \\ -0.00033 & 0.00002 & -0.00003 & 0.00068 & -0.00002 & -0.00007 & 0.00008 & -0.00001 & 0.00109 & -0.00023 \\ 0.00018 & 0.00036 & -0.00003 & 0.00042 & 0.00042 & 0.00001 & -0.00007 & -0.00011 & -0.00023 & 0.00212 \end{bmatrix}$$

Figure 6. covariance matrix

By making use of equation (1), the variance-covariance matrix in figure (6) and average returns of all the assets in the portfolio , the study's Markowitz portfolio model is formulated as follows:

$$\begin{aligned} \text{Minimise } \sigma_p{}^2 = {} & 0.00241x_1^2 + 0.00349x_2^2 + \cdots + 0.00212x_{10}^2 \\ & +2(0.00127x_1x_2 - 0.00010x_1x_3 \cdots + 0.00018x_1x_{10}) \\ & +2(-0.00030x_2x_3 + 0.00297x_2x_4 + \cdots + 0.00036x_2x_{10}) \\ & +2(-0.00042x_3x_4 - 0.00026x_3x_5 \cdots - 0.00003x_3x_{10}) \\ & +2(0.00263x_4x_5 - 0.00052x_4x_6 + \cdots + 0.00042x_4x_{10}) \\ & +2(-0.00046x_5x_6 + 0.00118x_5x_7 \cdots + 0.00042x_5x_{10} \\ & +2(-0.00024x_6x_7 + 0.00024x_6x_8 \cdots + 0.00001x_6x_{10}) \\ & +2(-0.00026x_7x_8 + 0.00008x_7x_9 \cdots - 0.00007x_7x_{10}) \\ & +2(-0.00001x_8x_9 - 0.00011x_8x_{10} - 0.00023x_9x_{10}) \end{aligned} \tag{14}$$

$$\text{s.to } 0.02064x_1 + 0.01386x_2 + \cdots - 0.00302x_{10} - \mu = 0 \tag{15}$$

$$x_1 + x_2 + \cdots + x_9 + x_{10} - 1 = 0 \tag{16}$$

The algorithm used in the study was developed by (Kaardal 2016) This algorithm solves the local minima of optimisation problems similar to equation (2). The algorithm uses the Augmented Lagrangian to find a feasible local minimum of the objective function which satisfies the first order of Karush-Kunh-Tucker sufficient conditions. The first order minimisation techniques are employed in the algorithm and therefore computation of the hessian of the problem is not required. In the algorithm, the Lagrangian is minimised using the projected gradient descent with intermediate updates of the Lagrange multiplier and the penalty parameter (Kaardal 2016).

The required parameters of the Markowitz portfolio model for the algorithm are the gradient of the model's objective function imported as a matrix and the gradients of the model's constraints imported as an array whose respective columns represent the gradient of each constraint.

Solutions to the Markowitz Portfolio Model

Variables of the Markowitz portfolio model discussed in the above section are input in the source code for the Augmented Lagrangian. The model problem is defined in its own m-file where all the parameters of the model are stored. The investor chooses the expected desired rate of returns to be achieved from the portfolio which is usually bounded between the lowest and the highest individual assets' average returns.

Other required inputs of the algorithm are the penalty value, the factor by which the penalty is increased after every violation of the constraints (*gma* = 2), the initial Lagrange multipliers ($\lambda_1 = \lambda_2 = 0$) and initial weights assigned to all assets ($x_1 = x_2 = \cdots = x_{10} = 0.1$). The penalty parameter is considered to be bounded, however, choosing a penalty value which falls within the boundary of the optimal values and the penalty factor is troublesome. There is no systematic way of choosing this value in the literature, hence the trial method was used to select the penalty value and the penalty factor that make the problem converge to optimal solutions.

Different penalty values were selected to test the convergence of the algorithm for the Markowitz portfolio model. It was observed that the smaller the penalty, the slower (numbers of iterations i.e. IT) it takes for the problem to converge, however, the solution converges to the exact objective function value for different penalty values.

The table below summarises a portion of the results obtained by the Augmented Lagrangian algorithm with the penalty value $\rho = 0.0005$ and *gma* = 2.

From the table above, portfolio 15 gives the global minimum variance to our model ($\sigma_p^2 = 0.000023$), with an expected return of 0.0007 and proportions of each asset as indicated in the table. This is shown as follows

The efficient frontier of the model

The efficient frontier is a set of portfolios that have the highest expected returns for a given level of risk or the lowest risk for a given level of expected return (Investopedia, n.d.). On the graph of efficient frontier which is a parabola opening up to the right, there are no portfolios above the efficient frontier, while portfolios that are inside the frontier are considered to be inefficient (Zivot 2013). The results of the Markowitz portfolio model from the previous section are used to build the efficient frontier graph below, where MV represents the minimum variance portfolio and AL represents the Augmented Lagrangian solution. The Generalized Reduced Gradient (GRG) optimisation method was used to solve for the same model and the results are plotted against results of the Augmented Lagrangian to test its efficiency.

P	μ	σ^2	x_1	x_2	x_3	x_4	x_5	x_6	x_7	x_8	x_9	x_{10}	λ_1	λ_2	IT
1	-0.0021	0.000036	-6.4%	-3.2%	63.4%	5.4%	7.2%	19.1%	8.2%	9.0%	-4.8%	2.2%	-0.0094	0.0001	18
2	-0.0019	0.000035	-6.0%	-2.9%	63.2%	4.9%	7.2%	19.1%	7.9%	8.8%	-4.2%	2.2%	-0.0088	0.0001	18
3	-0.0017	0.000033	-5.7%	-2.7%	62.9%	4.7%	7.1%	19.0%	7.6%	8.6%	-3.7%	2.1%	-0.0082	0.0001	18
4	-0.0015	0.000032	-5.4%	-2.5%	62.6%	4.5%	7.1%	19.0%	7.3%	8.4%	-3.2%	2.1%	-0.0077	0.0001	18
5	-0.0013	0.000031	-5.0%	-2.2%	62.3%	4.3%	7.1%	18.9%	7.0%	8.2%	-2.6%	2.0%	-0.0071	0.0001	18
6	-0.0011	0.000030	-4.6%	-1.9%	61.9%	4.0%	7.0%	19.4%	6.6%	7.9%	-1.5%	2.1%	-0.0062	0.0001	17
7	-0.0009	0.000028	-4.3%	-1.6%	62.2%	3.9%	6.9%	18.5%	6.3%	7.6%	-1.4%	1.8%	-0.0056	0.0001	18
8	-0.0007	0.000027	-3.9%	-1.4%	62.0%	3.7%	6.8%	18.4%	6.1%	7.4%	-0.9%	1.8%	-0.0051	0.0001	18
9	-0.0005	0.000026	-3.6%	-1.2%	61.7%	3.5%	6.8%	18.4%	5.8%	7.2%	-0.4%	1.7%	-0.0045	0.0001	18
10	-0.0003	0.000026	-3.3%	-0.9%	61.4%	3.4%	6.8%	18.3%	5.5%	7.0%	0.2%	1.7%	-0.0040	0.0001	18
11	-0.0001	0.000025	-3.0%	-0.7%	61.2%	3.2%	6.7%	18.3%	5.3%	6.8%	0.7%	1.6%	-0.0035	0.0001	18
12	0.0001	0.000025	-2.6%	-0.4%	60.6%	2.9%	6.7%	18.7%	4.9%	6.7%	1.5%	1.6%	-0.0025	0.0001	17
13	0.0003	0.000024	-2.3%	-0.2%	60.6%	2.8%	6.6%	18.2%	4.7%	6.4%	1.8%	1.5%	-0.0024	0.0001	18
14	0.0005	0.000024	-2.0%	0.0%	60.4%	2.6%	6.6%	18.1%	4.4%	6.2%	2.3%	1.4%	-0.0019	0.0001	18
15	**0.0007**	**0.000023**	**-1.6%**	**0.3%**	**60.5%**	**2.4%**	**6.5%**	**17.8%**	**4.1%**	**5.9%**	**2.9%**	**1.4%**	**-0.0012**	**0.0001**	**18**
16	0.0009	0.000024	-1.3%	0.5%	58.7%	2.2%	6.6%	18.7%	3.8%	5.9%	3.6%	1.3%	-0.0005	0.0001	16
17	0.0011	0.000024	-1.1%	0.6%	57.3%	2.0%	6.8%	19.5%	3.7%	6.0%	4.1%	1.3%	-0.0001	0.0001	15
...	...	...	...	...	...	...	...	...	...	...	...	...	...	...	...
...	...	...	...	...	...	...	...	...	...	...	...	...	...	...	...
...	...	...	...	...	...	...	...	...	...	...	...	...	...	...	...
100	0.0177	0.000360	25.4%	20.1%	36.1%	-13.1%	2.5%	14.2%	-19.4%	-11.7%	48.7%	-2.9%	0.0672	-0.0002	23
101	0.0179	0.000368	25.8%	20.4%	35.8%	-13.2%	2.4%	14.1%	-19.6%	-11.9%	49.3%	-2.9%	0.0680	-0.0001	23
102	0.0181	0.000378	25.9%	20.4%	35.3%	-13.3%	2.2%	14.3%	-19.6%	-12.3%	49.7%	-2.6%	0.0425	-0.0001	25
103	0.0183	0.000386	26.3%	20.6%	34.8%	-13.5%	2.0%	14.4%	-19.7%	-12.7%	50.4%	-2.5%	0.0427	0.0000	27
104	0.0185	0.000394	26.6%	21.0%	34.9%	-13.7%	2.2%	14.0%	-20.3%	-12.7%	50.9%	-2.9%	0.0709	-0.0001	24
105	0.0187	0.000403	27.0%	21.2%	34.6%	-13.9%	2.1%	14.0%	-20.6%	-12.9%	51.4%	-2.9%	0.0715	-0.0001	24
106	0.0189	0.000411	27.3%	21.5%	34.3%	-14.1%	2.1%	14.0%	-20.8%	-13.1%	52.0%	-3.0%	0.0718	-0.0001	24
107	0.0191	0.000420	27.6%	21.7%	34.1%	-14.3%	2.0%	13.9%	-21.2%	-13.3%	52.5%	-3.0%	0.0733	-0.0001	24
108	0.0193	0.000430	27.8%	21.9%	33.7%	-14.4%	1.9%	13.9%	-21.2%	-13.6%	53.0%	-2.9%	0.0455	0.0001	25
109	0.0195	0.000438	28.2%	22.2%	33.6%	-14.7%	1.9%	13.8%	-21.7%	-13.7%	53.5%	-3.1%	0.0739	-0.0001	24
110	0.0197	0.000447	28.6%	22.4%	33.2%	-14.8%	1.9%	13.7%	-21.9%	-14.0%	54.1%	-3.1%	0.0755	-0.0001	24
111	0.0199	0.000456	28.9%	22.6%	33.0%	-15.0%	1.8%	13.6%	-22.3%	-14.2%	54.7%	-3.2%	0.0763	-0.0001	24
...	...	...	...	...	...	...	...	...	...	...	...	...	...	...	...
∞	...														

Figure 7. Markowitz portfolio model Augmented Lagrangian Solution

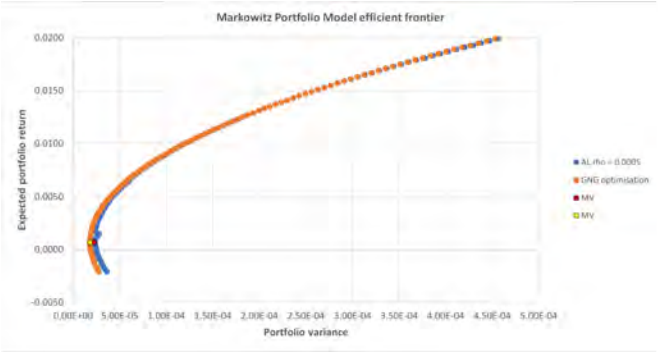

Figure 8. Markowitz Efficient frontier

The tangent (optimal) portfolio of the Markowitz portfolio model

Given the set of portfolios on the efficient frontier in figure **??**, which portfolio will an investor choose? From this set of efficient portfolios, investors will choose the portfolio that accords with their risk preferences. Very risk averse investors will opt for portfolios that have low risk and these are portfolios very close to the global minimum variance portfolio. In contrast, very risk tolerant investors will ignore risk and seek portfolios which offers high expected returns (Zivot 2013).

To get an optimal portfolio, an investor can choose to combine risky assets with a risk free asset in a portfolio, by making use of the Sharpe ratio. This is achieved by maximising the Sharpe ratio given the portfolio's expected return, portfolio's expected variances and the risk free rate. The Augmented Lagrangian algorithm is also used to solve for the maximum Sharpe ratio.

The efficient frontier in this case results in a straight line in the mean-variance space with a y-intercept being the risk free rate i.e. r_f, and the slope of the line being the maximum of the Sharpe ratios. The optimal portfolio is represented by the point where this line is tangent to the initial efficient frontier.

By using the same concept as that of the Markowitz portfolio model, the Sharpe ratio maximisation problem is formulated as follows:

$$\left.\begin{aligned} &\text{Maximise } SR_p = \frac{\mu_p - r_f}{\sigma_p} \\ &\text{subject to } \sum_{i=1}^{10} x_i \mu_i = \mu_p \\ &\sum_{i=1}^{n}\sum_{i=1}^{n} x_i x_j \sigma_{ij} = \sigma_p^2 \\ &\sum_{i=1}^{n} x_i = 1 \end{aligned}\right\} \tag{17}$$

By using the general Sharpe ratio formula in equation (17) and the same data set used in the Markowitz portfolio model, our Sharpe ratio is formulated. Due to difficulties in determining the optimal penalty value for the Sharpe ratio maximisation, the model was solved using the Generalised Reduced Gradient (GRG) non-linear optimisation method instead of the Augmented Lagrangian and the results obtained appears in the table below. The risk free rate is fixed to $r_f = 0.005$ a random choice that was made, while μ_p and σ_p^2 values are known from the table in Figure 7.

p	μ_p	σ^2	SR	x_1	x_2	x_3	x_4	x_5	x_6	x_7	x_8	x_9	x_{10}
1	-0.0021	0.000036	-1.18159	-7.60%	1.81%	96.90%	3.26%	5.09%	3.55%	2.60%	-0.07%	-5.82%	0.28%
2	-0.0019	0.000036	-1.14831	-7.15%	1.80%	96.85%	2.78%	4.78%	3.62%	2.37%	-0.07%	-5.20%	0.28%
3	-0.0017	0.000033	-1.16426	-6.71%	1.85%	95.36%	2.80%	5.02%	3.79%	2.41%	-0.07%	-4.74%	0.28%
4	-0.0015	0.000032	-1.15291	-6.50%	1.88%	94.06%	2.60%	5.17%	4.23%	2.35%	-0.07%	-4.00%	0.28%
5	-0.0013	0.000031	-1.14004	-5.94%	1.90%	93.19%	2.36%	5.12%	4.52%	2.26%	-0.07%	-3.62%	0.28%
6	-0.0011	0.000030	-1.11432	-5.47%	1.90%	91.94%	2.04%	5.06%	5.31%	2.19%	-0.07%	-3.18%	0.28%
7	-0.0009	0.000028	-1.1117	-4.95%	1.94%	90.02%	1.92%	5.33%	6.19%	2.21%	-0.07%	-2.88%	0.29%
8	-0.0007	0.000027	-1.09206	-4.10%	1.94%	89.32%	1.76%	5.14%	6.40%	2.10%	-0.07%	-2.76%	0.29%
9	-0.0005	0.000026	-1.07127	-3.45%	2.02%	88.07%	1.63%	4.96%	7.00%	2.04%	-0.07%	-2.48%	0.29%
10	-0.0003	0.000026	-1.04742	-2.82%	2.14%	87.00%	1.50%	4.85%	7.40%	1.94%	-0.07%	-2.22%	0.28%
11	-0.0001	0.000025	-1.02101	-2.54%	2.29%	83.29%	1.41%	5.28%	10.06%	1.94%	-0.07%	-1.95%	0.29%
12	0.0001	0.000025	-0.98524	-2.24%	2.45%	79.72%	1.34%	5.84%	12.61%	1.84%	-0.07%	-1.77%	0.29%
13	0.0003	0.000024	-0.96048	-2.27%	2.84%	76.00%	1.53%	7.24%	13.83%	2.04%	-0.07%	-1.43%	0.29%
14	0.0005	0.000024	-0.92647	-1.44%	3.05%	75.60%	1.51%	6.88%	13.42%	2.01%	-0.07%	-1.26%	0.29%
15	0.0007	0.000023	-0.89314	-1.00%	4.02%	75.70%	1.42%	5.30%	13.33%	1.87%	-0.07%	-0.85%	0.28%
16	0.0009	0.000024	-0.84174	-0.80%	5.21%	77.72%	1.36%	5.57%	9.76%	1.71%	-0.07%	-0.67%	0.28%
17	0.0011	0.000024	-0.79705	-0.53%	6.81%	79.36%	1.02%	3.29%	8.97%	1.24%	-0.07%	-0.36%	0.26%
...	...	...	...	...	...	...	...	...	...	...	...	...	...
...	...	...	...	...	...	...	...	...	...	...	...	...	...
40	0.0057	0.000050	0.099146	7.81%	6.77%	60.77%	-1.67%	1.27%	8.23%	-0.26%	0.05%	16.71%	0.25%
41	0.0059	0.000052	0.124587	7.34%	6.95%	57.45%	-2.51%	2.48%	11.05%	-0.36%	0.05%	17.28%	0.26%
42	0.0061	0.000055	0.14887	7.34%	6.53%	55.75%	-2.47%	3.23%	11.49%	-0.65%	0.05%	18.47%	0.26%
43	0.0063	0.000057	0.17198	7.65%	6.97%	55.13%	-2.85%	2.97%	11.98%	-0.95%	0.05%	18.80%	0.26%
44	0.0065	0.000060	0.194018	8.20%	6.48%	55.01%	-2.91%	3.03%	11.61%	-1.37%	0.05%	19.65%	0.26%
45	0.0067	0.000062	0.215991	7.73%	8.35%	53.91%	-3.06%	3.14%	12.46%	-2.37%	0.05%	19.54%	0.25%
46	0.0069	0.000065	0.236145	8.38%	7.91%	53.30%	-3.22%	3.12%	12.50%	-2.51%	0.05%	20.23%	0.25%
47	0.0071	0.000068	0.255328	9.26%	7.65%	53.00%	-3.43%	3.12%	12.53%	-2.87%	0.05%	20.44%	0.25%
48	0.0073	0.000071	0.273647	9.50%	7.88%	52.26%	-3.49%	3.15%	12.56%	-3.22%	0.05%	21.06%	0.25%
49	0.0075	0.000074	0.291129	10.12%	7.93%	52.17%	-3.86%	3.15%	12.77%	-3.86%	0.05%	21.22%	0.25%
50	0.0077	0.000077	0.307812	9.79%	8.28%	51.05%	-3.73%	3.20%	12.74%	-4.13%	0.05%	22.51%	0.25%
51	0.0079	0.000080	0.323735	10.54%	8.47%	50.58%	-3.95%	3.22%	12.91%	-4.52%	0.05%	22.46%	0.25%
52	0.0081	0.000084	0.338979	10.61%	8.67%	50.20%	-4.19%	3.24%	13.08%	-5.12%	0.05%	23.21%	0.25%
53	0.0083	0.000087	0.353529	10.93%	9.16%	49.63%	-4.35%	3.31%	13.19%	-5.61%	0.05%	23.44%	0.25%
54	**0.0085**	**0.000091**	**0.36745**	**10.74%**	**9.22%**	**47.23%**	**-4.09%**	**4.23%**	**15.09%**	**-6.12%**	**-0.07%**	**24.09%**	**0.28%**

Figure 9. Solutions to portfolios of risky assets combined with a risk free asset

From portfolio 55 (i.e. p = 55), feasibility for the Sharpe ratio does not exist, hence the maximum Sharpe ratio when a risk free rate r_f = 0.005 is combined with risky assets occurs under portfolio 54, where the Sharpe ratio value is 0.36745. This implies that the ideal portfolio that investors can choose on the efficient frontier would be portfolio 54 which has an expected portfolio return (μ_p) of 0.0085 and an expected portfolio variance (σ_p^2) of 0.000091. The proportions of all assets in this portfolio are indicated in figure 12 above. The risk free rate and the optimal (tangent) portfolio (TP) are plotted on the efficient frontier graph as seen in Figure 10.

Figure 10. Markowitz Efficient frontier with a tangent portfolio

If we draw a line connecting the R_f and the TP (tangent portfolio) the resultant line will be tangent to the efficient frontier curve which indicates that this portfolio is considered to be the ideal optimal portfolio when a risk free rate r_f of 0.005 is combined with the risky assets.

Conclusion

In conclusion, ours results show how the Augmented Lagrangian method improves solutions to portfolio optimisation models in terms of assets diversification. A set of portfolios were achieved where the risk was observed to be minimal while maintaining a fair distribution of assets within the portfolio. Our study was able to verify an assumption by Harry Markowitz on investors' behavior, that they are only willing to accept a higher amount of risk if they are compensated by higher expected returns.

References

Aarti, Singh. n.d. Augmented lagrangian and the method of multipliers.

Azizah, E, E Rusyaman, and S Supian. 2017. Optimization of investment portfolio weight of stocks affected by market index. In *Iop conference series: materials science and engineering,* 166:012008. 1. IOP Publishing.

Bayraktar, Ertugrul, and Ayse Humeyra Bilge. 2012. Determination the parameters of markowitz portfolio optimization model. *arXiv preprint arXiv:1210.5859.*

Beasley, JE. 2013. Portfolio optimisation: models and solution approaches. In *Theory driven by influential applications,* 201–221. Informs.

Birgin, Ernesto G, and José Mario Martınez. 2012. Augmented lagrangian method with nonmonotone penalty parameters for constrained optimization. *Computational Optimization and Applications* 51 (3): 941–965.

Chen, Wei-Peng, Huimin Chung, Keng-Yu Ho, and Tsui-Ling Hsu. 2010. Portfolio optimization models and mean–variance spanning tests. In *Handbook of quantitative finance and risk management,* 165–184. Springer.

Gitman, Lawrence J, Roger Juchau, and Jack Flanagan. 2015. *Principles of managerial finance.* Pearson Higher Education AU.

Ho, Michael, Zheng Sun, and Jack Xin. 2015. Weighted elastic net penalized mean-variance portfolio design and computation. *SIAM Journal on Financial Mathematics* 6 (1): 1220–1244.

Investopedia. n.d. Efficient frontier. https://www.investopedia.com/terms/e/efficientfrontier.asp.

Kaardal, Joel T. 2016. Augmented lagrangian method for equality, inequality, and bounded optimization (matlab, octave). github. https://github.com/jkaardal.

Lee, Cheng-Few, and John Lee. 2010. *Handbook of quantitative finance and risk management.* Springer Science & Business Media. https://doi.org/10.1007/978-0-387-77117-5.

Mangram, Myles E. 2013. A simplified perspective of the markowitz portfolio theory. *Global journal of business research* 7 (1): 59–70.

Rocha, Ana Maria AC, and Edite MGP Fernandes. 2011. Numerical study of augmented lagrangian algorithms for constrained global optimization. *Optimization* 60 (10-11): 1359–1378.

Treynor, Jack L, and Fischer Black. 1973. How to use security analysis to improve portfolio selection. *The journal of business* 46 (1): 66–86.

Zivot, Eric. 2013. Introduction to portfolio theory. *University of Washington,* https://faculty.washington.edu/ezivot/econ424/.

Numerical investigation on MAP/PH/1 Inventory Retrial Queueing System With Constant Retrial Rate, Single Vacation, Breakdown and Repair

G. Ayyappan[1] and S. Meena*[2]

[1]Department of Mathematics, Puducherry Technological University, Puducherry, India.
[2]Department of Mathematics, Puducherry Technological University, Puducherry, India.

Abstract

This study investigates a retrial queueing inventory system with the constant retrial rate, single vacation, breakdown and repair. We have assumed that the customers arrive according to Markovian arrival process and the server to provide the phase type services to the customers. The inventory is replenished according to an (s, S) policy and the replenishing time is assumed to follow the exponential distribution. If either inventory level zero or no customers in the orbit or both, then the server goes for a vacation. At any time the server may breakdown, the server immediately go for a repair process and the customer joins the infinite size of orbit. The vacation time and repair time follows the phase type distribution. The stability condition, the steady state probability vector analysis and few system performance measures are given.

Keywords: Queueing-inventory; Markovian Arrival Process; Phase-type distribution; (s, S)-type policy; Retrial; Server Vacation; Breakdown; Repair; Matrix-analytic method.

1 Model Description

Consider a single server retrial inventory queueing model. The customers arrival according to the Markovian Arrival Process(MAP) is specified by two m x m matrices (D_0, D_1), $D = D_0 + D_1$, which is an irreducible infinitesimal generator. The matrix D_0 means no arrival at the system, the matrix D_1 means arrival at the system. The arrival rate λ is given by $\lambda = \pi D_1 e$. The system is performed on an FCFS basis. With the notation (α, T) of order n, the length of the server's service is thought to be a PH-distribution, where $T^0 + Te = 0$ so that $T^0 = -Te$. The average service rate μ is given by $\mu = [\alpha(-T)^{-1}e]^{-1}$. Each customer want a single inventory unit. The inventory is replenished according to an (s, S) policy and the replenishing time τ is assumed to follow the exponential distribution. If either inventory level zero or no customers in the orbit or both, then the server goes for a vacation. The vacation time follows PH-distribution with parameter (γ, V) of order n_1. At any time the server may breakdown, the server immediately go for a repair process and the customer joins the infinite size of orbit. The breakdown rate σ follows exponential distribution.

*Corresponding Author. Email: meena.s@pec.edu.

The repair time follows PH distribution with parameter (β, S) of order n_2. The average vacation rate η and repair rate ζ follows exponential distribution.

2 The QBD process of Matrix Generation

We have described our model's notation for the basis of generating the QBD process in this section as follows

- $\otimes$-A Kronecker product represents the product of any two different order matrices, can refer to the works in Steeb and Hardy, 2011
- $\oplus$-The sum of any two distinct orders of matrices is represented by the Kronecker sum.
- I_k-It represents an identity matrix of order k.
- $e_i{}'(m)$-It represents an m-dimensional row vector with 1 in the i^{th} position and 0 elsewhere.
- $e_i(m)$-It represents an m-dimensional column vector with 1 in the i^{th} position and 0 elsewhere.
- e-Each entry in a column vector of appropriate dimension is 1.
- λ stands for the customer arrival rate, which is defined by $\lambda = \pi D_1 e_m$.
- μ_1 stands for the customer's service rate, which is defined by $\mu = [\alpha(-T)^{-1}e_n]^{-1}$
- η stands for the vacation rate of the server, which is defined by $\eta = [\gamma(-V)^{-1}e_{n_1}]^{-1}$
- ζ stands for the repair rate of the server, which is defined by $\zeta = [\psi(-P)^{-1}e_{n_2}]^{-1}$
- Let N(t) be the number of customers in the orbit at epoch t
- Let I(t) be the inventory level at epoch t
- Let V(t) be the server status at epoch t

$$V(t) = \begin{cases} 0, \text{ if the server is on vacation,} \\ 1, \text{ if the server is in idle,} \\ 2, \text{ if the server is busy,} \\ 3 \text{ if the server is in repair process} \end{cases}$$

- $J_1(t)$ represents the vacation process as framed by phases.
- $J_2(t)$ represents the repair process as framed by phases.
- S(t) represents the service process as framed by phases.

- M(t) represents the arrival process as framed by phases.

Let { N(t), V(t), I(t) $J_1(t)$, $J_2(t)$, S(t), M(t) : $t \geq 0$} denote the Continuous Time Markov Chain (CTMC) with state level independent Quasi-Birth and Death process, the state space of which is as follows,

$$\Omega = l(0) \cup l(q),$$

where

$$\begin{aligned} l(0) =& \{(0,0,a,j_1,k) : 0 \leq a \leq S, 1 \leq j_1 \leq n_1, 1 \leq k \leq m\} \\ & \cup \{(0,1,a,k) : 0 \leq a \leq S, 1 \leq k \leq m\} \\ & \cup \{(0,2,a,j,k) : 1 \leq a \leq S, 1 \leq j \leq n, 1 \leq k \leq m\} \end{aligned}$$

for $q \geq 1$,

$$\begin{aligned} l(q) =& \{(q,0,a,j_1,k) : 0 \leq a \leq S, 1 \leq j_1 \leq n_1, 1 \leq k \leq m\} \\ & \cup \{(q,1,a,k) : 0 \leq a \leq S, 1 \leq k \leq m\} \\ & \cup \{(q,2,a,j,k) : 1 \leq a \leq S, 1 \leq j \leq n, 1 \leq k \leq m\} \\ & \cup \{(q,3,a,j_2,k) : 1 \leq a \leq S, 1 \leq j_2 \leq n_2, 1 \leq k \leq m\} \end{aligned}$$

The infinitesimal matrix generation of the QBD process is given by

$$Q = \begin{bmatrix} B_{00} & B_{01} & 0 & 0 & 0 & 0 & \dots \\ B_{10} & A_1 & A_0 & 0 & 0 & 0 & \dots \\ 0 & A_2 & A_1 & A_0 & 0 & 0 & \dots \\ 0 & 0 & A_2 & A_1 & A_0 & 0 & \dots \\ \vdots & \vdots & \vdots & \ddots & \ddots & \ddots & \vdots \\ \vdots & \vdots & \vdots & \vdots & \ddots & \ddots & \ddots \end{bmatrix}$$

3 Invariant Analysis

We analyze our model under some conditions that the system is stable.

3.1 Condition Analysis for Stableness

Let us define the matrix A such that $A = A_0 + A_1 + A_2$. It clearly shows that the arrangement of the square matrix A of order is $((S+1)n_1m + (S+1)m + Snm + Sn_2m)$ and this matrix is irreducible infinitesimal generator matrix.

Let φ indicate the steady-state probability vector of A satisfying $\varphi A = 0$ and $\varphi e = 1$. The stability condition $\varphi A_0 e < \varphi A_2 e$ is obtained after some algebraic manipulation, which turns out to

be

$$\sum_{a=0}^{S}\varphi_{0a}(e_{n_1}\otimes D_1e_m)+\varphi_{10}(D_1e_m)+\sum_{a=1}^{S}\varphi_{2a}(e_n\otimes(D_1e_m+\sigma e_m))$$
$$+\sum_{a=1}^{S}(e_{n_2}\otimes D_1e_m) \quad < \quad \sum_{a=1}^{S}\varphi_{1a}(\psi e_m)$$

3.2 Analysis of Steady-State Probability Vector

Consider the steady-state probability vector x of Q and it is divided into $x=(x_0,x_1,x_2,\dots)$. x_0 has a dimension of $(S+1)n_1m+(S+1)m+Snm$ while $x_1,\ x_2,\dots$ have a dimension of $(S+1)n_1m+(S+1)m+Snm+Sn_2m$. Then x satisfied the condition $xQ=0$ and $xe=1$.

Furthermore, if the system is stable with the vector x, the following equation provides the remaining sub vectors except for the boundary states.

$$x_q=x_1R^{q-1},\ q\geq 2$$

where the rate matrix R indicates the minimal non-negative solution of the matrix quadratic equation as $R^2A_2+RA_1+A_0=0$, as referred to by Neuts, 1984 and satisfies the relation $RA_2e=A_0e$.

The sub vectors of x_0 and x_1 were calculated by solving the subsequent equations.

$$x_0B_{00}+x_1B_{10}=0$$
$$x_0B_{01}+x_1(A_1+RA_2)=0$$

The normalizing condition is subject to

$$x_0e_{(S+1)n_1m+(S+1)m+Snm}+x_1(I-R)^{-1}e_{(S+1)n_1m+(S+1)m+Snm+Sn_2m}=1$$

As a result, the rate matrix R could be mathematically calculated using crucial procedures in the Latouche algorithm for logarithmic reduction of R Latouche and Ramaswami, 1999.

4 System Performance Measures

- Expected number of customers in the orbit

$$E_{orbit}=\sum_{q=1}^{\infty}px_pe$$

- Expected inventory level

$$E_{inv}=\sum_{q=0}^{\infty}\sum_{a=1}^{S}\sum_{j_1=1}^{n_1}\sum_{k=1}^{m}ax_{q0aj_1k}+\sum_{q=0}^{\infty}\sum_{a=1}^{S}\sum_{k=1}^{m}ax_{q1ak}$$
$$+\sum_{q=0}^{\infty}\sum_{a=1}^{S}\sum_{j=1}^{n}\sum_{k=1}^{m}ax_{q2ajk}+\sum_{q=1}^{\infty}\sum_{a=1}^{S}\sum_{j_2=1}^{n_2}\sum_{k=1}^{m}ax_{q3aj_2k}$$

- Expected Reorder rate

$$E_R = \sum_{j=1}^{n}\sum_{k=1}^{m} x_{02(s+1)jk}(T^0\gamma \otimes I_m)e + \sum_{q=1}^{\infty}\sum_{j=1}^{n}\sum_{k=1}^{m} x_{q2(s+1)jk}(T^0 \otimes I_m)e$$

References

Latouche, G. and Ramaswami, V. (1999). *Introduction of Matrix Analytic Methods in Stochastic Modeling*. Society for Industrial and Applied Mathematics, Philadelphia.

Neuts (1984). Matrix-analytic methods in queuing theory. *European Journal of Operational Research*, 15:2–12.

Steeb, W. and Hardy, Y. (2011). *Matrix Calculus and Kronecker Product: A Practical Approach to Linear and Multilinear Algebra*. World Scientific Publishing, Singapore.

SMALL AREA ESTIMATION OF HOUSEHOLD CONSUMPTION EXPENDITURE IN KHOMAS REGION, NAMIBIA, USING THE FAY-HERRIOT EBLUP MODEL

Selma N. Shifotoka*[1], Dibaba B. Gemechu[1], Dismas Ntirampeba[1], and Rakesh Kumar[1,2]

[1]Department of Mathematics, Statistics and Actuarial Science, Namibia University of Science and Technology
[2]School of Mathematics, Shri Mata Vaishno Devi University, Katra, India

Abstract

In the absence of censuses and administrative records, sample surveys are widely used to provide statistical estimates of many variables of interest. However, sample survey designs usually focus on achieving a particular degree of precision for estimates at a higher level of aggregation than that of sub-populations within the target population. Therefore, sample sizes for such sub-populations are typically small and non-representative. Small Area Estimation (SAE) techniques were developed to produce reliable estimates for sub-populations for which survey samples are either too small or just zero. This study applied a model-based SAE approach to estimate small area estimates of correlated response variables for constituencies in Khomas region, using the 2015/16 Namibia Household Income and Expenditure data, borrowing strength from auxiliary data that was obtained from the Namibia 2011 Population and Housing Census, as well as the 2017 National Atlas. Specifically, the study estimated food and non-food consumption expenditure, using a univariate and a bivariate Fay Herriot (FH) model. Based on the results of the EBLUP-FH estimation, the distribution of food and non-food expenditure varied across the constituencies in Khomas region. The variation in the model-based estimates was found to be lower than the direct estimates, for both response variables, and even lower for the estimates resulting from the bivariate Fay-Herriot model.

Keywords: Small Area Estimation; Fay-Herriot models; Household Consumption Expenditure.

1 Introduction

Sample survey designs usually focus on achieving a particular degree of precision for estimates at a higher level of aggregation than that of subgroups within the target population, and as such sample sizes for such subgroup are typically small and non-representative (Mukhopadhyay and McDowell, 2011). The lack of subgroup-specific data for small areas creates a considerable challenge in statistical estimation from sample surveys, and has led to the development of Small Area Estimation

*Corresponding Author. Email: selmamegameno@gmail.com.

(SAE) techniques (Rao and Molina, 2015).

SAE is the application of statistical methods and techniques for producing sufficient population estimates for small domains/areas (Ngaruye et al., 2017). In SAE applications, small areas or small domains are defined as sub-populations for which specific survey samples are not enough to produce direct estimates with reliable precision (Rao, 2003). This paper applied model-based SAE techniques to provide small area estimates of food and non-food consumption expenditure estimates for constituencies in Khomas region, Namibia.

1.1 Approaches to Small Area Estimation (SAE)

In general, statistical estimates are computed by either direct or indirect methods (Rao, 2003; Bucyibaruta, 2014). While direct estimates are only based on sample information, indirect estimation are based on data from additional sources.

1.1.1 Direct estimation

This approach considers only the sample information from the particular domain of interest for estimation (Rao, 2003; Rao and Molina, 2015). Suppose there are D small areas of interest. Let U_d denote the finite population of area d, where $d = 1, \ldots, D$. Additionally, let N_d and n_d denote the number of population units and sample units respectively, in area d. Let w_{id} denote the sampling weight for the sampled unit i in the domain d ($i = 1, \ldots, n_d$). If the units have unequal sampling selection probabilities within the domain, then the Horvitz-Thompson estimator of the population mean for the domain can be defined as:

$$\bar{y}_{wd} = \frac{\sum_{i=1}^{n_d} w_{id} y_{id}}{\sum_{i=1}^{n_d} w_{id}}, \tag{1}$$

where $\bar{y}_{wd}$ denotes the response variable for the i^{th} unit in the d^{th} domain.
As noted earlier, the sample sizes for sub-populations that make up survey samples are typically small and non-representative at the subgroup level. As a result, direct estimates at the subgroup level tend to be inaccurate with very large standard errors, and therefore lead to inadequate levels of statistical precision (Rao, 2003). Moreover, direct estimates from random samples do not account for variation between small areas, and can be extremely biased if the assumption of homogeneity within small areas is violated (Ngaruye et al., 2017). Based on these challenges, indirect estimation is more preferred over direct estimation.

1.1.2 Indirect estimation

This approach uses not only sample information, but "borrows strength" from other data sources through statistical models, in order to increase the precision of domain specific estimates (Rao and Molina, 2015). Auxiliary data helps in explaining the variation in the response variable(s) even better, by accounting for variations between units and between areas (Liu, 2009). Since the precision of indirect estimates does not depend on the sub-population sample sizes, they are relatively

more precise for sub-populations with small samples and can have smaller variances than direct estimates, on condition that the model used fits the subgroup data (Bucyibaruta, 2014). As noted by Czajka et al., 2014, two widely applied indirect models are the unit level and area level models.

(i) Unit level model
If auxiliary information is available at both domain and sampling unit level, then the basic unit level model, popularly known as the Battesse-Harter-Fuller model is considered. To generally describe this model, assume U be a population consisting of N units and D small areas of interest. Then, U can be partitioned into sub-populations U_d of size N_d, where $N = \sum_{d=1}^{D} N_d$, $d = 1, \ldots, D$. Let the sample size of the survey be n, and the sample size in each domain be n_d, such that $n = \sum_{d=1}^{D} n_d$. The standard unit-level model is defined as:

$$y_{di} = \mathbf{x}_{di}^T \boldsymbol{\beta} + u_d + \epsilon_{di}, \tag{2}$$

where y_{di} is the response variable of interest for the i^{th} unit in domain d, $i = 1, \ldots, n_d$, $\mathbf{x}_{di}^T$ is the vector of p unit level auxiliary information for the for the i^{th} unit in domain d, $\boldsymbol{\beta}$ is a p x 1 vector of unknown, fixed regression coefficients, u_d are the random effects, and ϵ_{di} represents the random sampling error. u_d and ϵ_{di} are assumed to be independent, and distributed as $N(0, \sigma_u^2)$ and $N(0, \sigma_\epsilon^2)$, respectively.

(ii) Area level model

If auxiliary information is available only at small area level, then the basic area level model, popularly known as the Fay Herriot model, is considered. Generally, an area level model is made up of two components; the sampling model that captures the direct survey estimates and sampling error, as well as the linking model that relates the true population value to a set of area-specific auxiliary variables with unknown random area effects (Liu (2009)). The basic area level model is described in greater detail in the Methodology section.

2 Methodology

2.1 Data

The main data source from which annual household consumption expenditure on food and non-food data for Khomas region were obtained is the 2015/16 Namibia Household Income and Expenditure Survey (NHIES). The Khomas region has 10 constituencies in total and all of them were included in the NHIES sample design, by a total of 1084 households. The survey also provided sampling weights and sample sizes for each constituency. After direct estimation of the weighted mean household consumption expenditure per constituency, the resulting weighted means for food and non-food were used as response variables for the Fay Herriot models. The auxiliary variables at constituency level were obtained from the 2011 Namibia Population and Housing Census (PHC), as well as from the Namibia Statistics Agency's 2017 national Atlas. The auxiliary variables (X_1, X_2, X_3 and X_4) used for the univariate and bivariate models were selected based on backward selection. These are Number of households that own a car, number of employed head of households, average household

size and number of schools in the constituency.

2.2 Model descriptions

The study applied the area level model to relate the response variable to area-specific auxiliary variables. Generally, assume that the auxiliary data is only available at area level, for each domain d, let this data be denoted by $\boldsymbol{x_d} = (x_{1d}, x_{2d}, \ldots, x_{pd})^T$. Then y_d is assumed to be linearly related to x_d through the following linking model:

$$y_d = \mathbf{x}_d^T \boldsymbol{\beta} + u_d, \tag{3}$$

where y_d is the response variable of interest for domain d, $d = 1, \ldots, D$, $\mathbf{x}_d^T$ is the vector of p domain level auxiliary information for each domain d, $\boldsymbol{\beta}$ is a p x 1 vector of unknown, fixed regression coefficients, and u_d are the random effects, with mean 0 and variance ν_{ud}. Assume that $\hat{y_d}$ is an unbiased direct estimator for y_d, where y_d contains the sampling error denoted as ϵ_d. Then, the sampling model is defined as:

$$\hat{y_d} = y_d + \epsilon_d, \tag{4}$$

where ϵ_d are sampling errors of the direct estimators, with mean 0 and variance $\nu_{\epsilon d}$.
Combining equations (3) and (4) yields the basic area-level model, commonly referred to as the Fay-Herriot Model (FH), which is defined as:

$$\hat{y_d} = \mathbf{x}_d^T \boldsymbol{\beta} + u_d + \epsilon_d, \tag{5}$$

where $d = 1, \ldots, D$, $\epsilon_d \sim N(0, \nu_{\epsilon d})$ and $u_d \sim N(0, \nu_{ud})$. However, when two variables of interest are correlated, we consider the bivariate model, which is a special case of the multivariate Fay-Herriot model discussed by Benavent and Morales (2016).

Let U be a finite population partitioned into D domains. For each domain d (where $d = 1, \ldots, D$), let $\boldsymbol{\theta_d} = (\theta_{d1}, \theta_{d2})'$ be the vector of the two response variables of interest. Additionally, let $\boldsymbol{y_d} = (y_{d1}, y_{d2})'$ be a vector of direct estimators of $\boldsymbol{\theta}_d$. Firstly, assume that $\boldsymbol{\theta}_d$ is related to the area-specific auxiliary variables $\boldsymbol{X_d} = diag(\boldsymbol{x_{d1}}, \boldsymbol{x_{d2}})$ with p explanatory variables $\boldsymbol{x_{dj}} = (x_{dj1}, \ldots, x_{djp})$, for $j = 1, 2$ through the linear model:

$$\boldsymbol{\theta_d} = \boldsymbol{X_d}\boldsymbol{\beta} + u_d, \tag{6}$$

where $\boldsymbol{\beta}$ is a vector of regression coefficients and u_d is distributed as $N(0, \nu_u)$.
Secondly, the direct estimator $\boldsymbol{y_d}$ follows a sampling model, given by:

$$\boldsymbol{y_d} = \theta_d + \epsilon_d, \tag{7}$$

where $d = 1, \ldots, D$ and ϵ_d are assumed to follow the distribution $N(0, \nu_\epsilon)$, where ν_ϵ is a 2×2 covariance matrix of sampling errors. The combination of models (6) and (7) yields the bivariate Fay-Herriot model as:

$$\boldsymbol{y_d} = \boldsymbol{X}_d\boldsymbol{\beta} + u_d + \epsilon_d, \tag{8}$$

where $d = 1, \ldots, D$, ϵ_d and u_d are assumed to be independent of each other, and are distributed as $N(0, \nu_{\epsilon d})$ and $N(0, \nu_{ud})$, respectively. $\boldsymbol{y_d} = (y_{d1}, y_{d2})'$ is an Emperical Best Linear Unbiased

Prediction estimator (EBLUP) for $\boldsymbol{\theta_d} = (\theta_{d1}, \theta_{d2})'$, based on the assumption that the variance component of the direct estimators are known and they are normally distributed.

This study applied the Fay-Herriot model as follows. The study considered the Khomas regional population U of size N, that can be partitioned in D small areas (constituencies) denoted by μ_d and each with a population size N_d, where $d = 1, \cdots, D$. The study aimed to estimate the average consumption expenditure for each constituency. Let θ_i , $i = 1, \cdots, N$ be the consumption expenditure for the i^{th} household. The average weighted consumption expenditure for a constituency d is defined as the average of $\theta_i = \mu_d = \frac{\sum_{i=1}^{n_d} w_{id}\theta_{id}}{\sum_{i=1}^{n_d} w_{id}}$. The Fay Herriot model is a mixed model that also includes random effects μ_d, where $\mu_d \sim N(0, \sigma_\mu^2)$.

Model (5) was therefore contextualized to be the univariate Fay Herriot model used in this study as:

$$\hat{\mu_d} = \mathbf{x}_d'\boldsymbol{\beta} + \mu_d + \epsilon_d, d = 1, ..., D. \tag{9}$$

where $\hat{\mu}_d$ is the direct estimator of the weighted mean expenditure, $\mathbf{x}_d'$ denotes the small area-specific auxiliary variables, $\boldsymbol{\beta}$ denotes the fixed regression coefficients, μ_d are the parameters of interest (average consumption expenditure on both food and non-food) for a given constituency d and ϵ_d denotes the sampling error.
The Fay Herriot model was further extended to a bivariate case where food and non food expenditure, respectively denoted by μ_{1d} and μ_{2d} were separately modelled for each constituency d. Assuming that $\hat{\mu_d} = (\hat{\mu_{d1}}, \hat{\mu_{d2}})$' is a direct estimator of μ_d, Model (8) was therefore contextualized to be the Bivariate Fay Herriot model used in this study as:

$$\hat{\mu_d} = \mathbf{x}_d'\boldsymbol{\beta}_d + \mu_d + \epsilon_d, \tag{10}$$

3 Results and discussions

This section compares the direct estimation method to the univariate and bivariate modelling methods, and concludes with a graphical presentation of constituency food and non-food household consumption expenditure estimates. Table 1 presents the regression parameters resulting from the Fay-Herriot models. The standard errors of the regression parameters of the bivariate model are lower than those observed from the univariate model, which indicates the that the bivariate model was the better fit.

Figure 1 presents the direct and the FH EBLUPs expenditure estimates for average expenditures. The results indicate that although the distribution is consistent across the three methods of estimation, the direct estimation method yields larger estimates than those resulting from the FH models, and yielded more outliers in the estimation of average food expenditure.

Figure 2 presents a comparisons of Coefficients of Variation (CVs) for the direct estimates and the FH EBLUPs expenditure estimates. Overall, the direct estimation method yielded larger CVs, which indicates a relatively greater level of dispersion around the mean, compared to the indirect

Table 1: Regression parameters of the Fay Herriot models

Univariate Fay Herriot model				Bivariate Fay Herriot model			
Variable	β	Std. error	p.value (α=0.05)	Variable	β	Std. error	p.value (α=0.05)
	Food expenditure				Food expenditure		
(Intercept)	-181660.00	88765.00	**0.0407**	(Intercept)	-165620.00	81875.00	**0.0431**
Car owning HHs	86841.00	25663.00	**0.0007**	Car owning HHs	85540.00	24692.00	**0.0005**
Number of employed heads of HHs	235060.00	109330.00	**0.0316**	Number of employed heads of HHs	218680.00	101920.00	**0.0319**
HH size	18455.00	8073.50	**0.0223**	HH size	16882.00	7522.60	**0.0248**
Number of schools	-2235.00	720.31	**0.0019**	Number of schools	-2120.40	693.44	**0.0022**
	Non-food expenditure				Non-food expenditure		
(Intercept)	-223420.00	526100.00	0.6711	(Intercept)	-209710.00	479700.00	0.6620
Car owning HHs	837680.00	193480.00	**0.0000**	Car owning HHs	816070.00	181830.00	**0.0000**
Number of employed heads of HHs	90415.00	600640.00	0.8803	Number of employed heads of HHs	82122.00	548880.00	0.8811
HH size	42984.00	48804.00	0.3785	HH size	40752.00	44633.00	0.3612
Number of schools	-8775.00	4246.00	**0.0388**	Number of schools	-8278.90	3983.30	**0.0377**

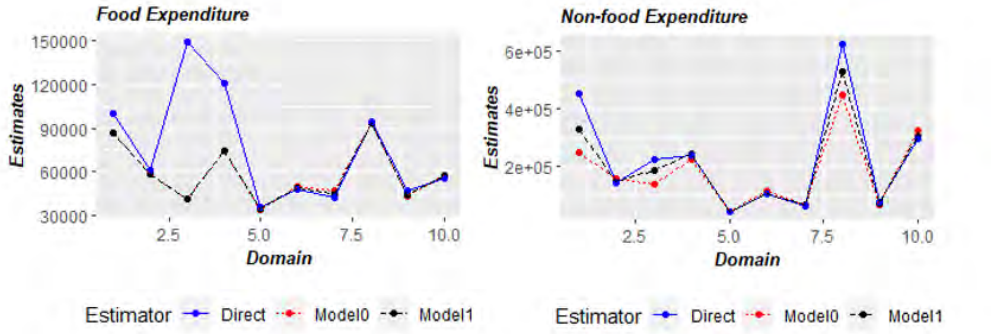

Figure 1: Comparisons of expenditure estimates

estimation methods. The univariate and bivariate models are therefore considered to be more preferable in estimating expenditure.

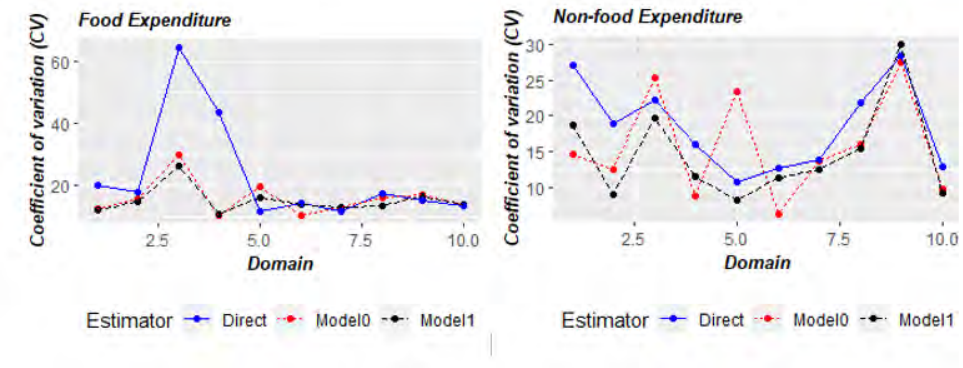

Figure 2: Comparisons of CVs of expenditure estimates

Figure 3 presents a comparison of Root Mean Square Errors (RMSE) of the estimates. Although the RMSEs for the two models follow a similar pattern, the bivariate model yielded lower RMSEs.

It can be concluded that the bivariate model produces a smaller level of variation.

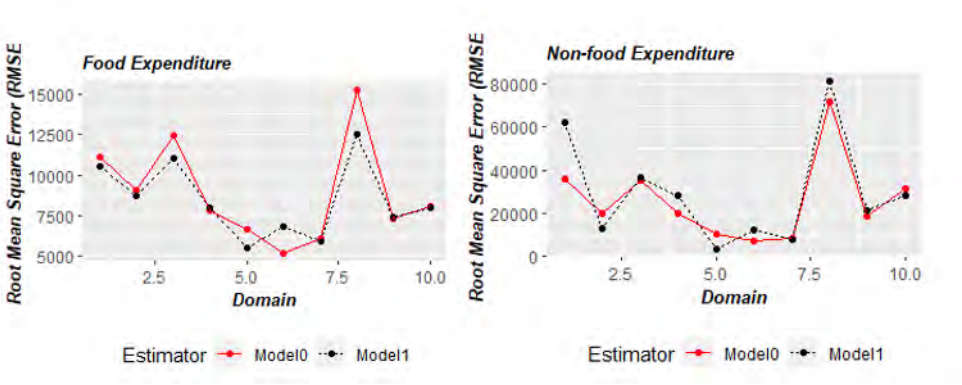

Figure 3: Comparisons of RMSEs of expenditure estimates

Figure 4 presents the estimated average expenditure from the best performing model, namely the Bivariate FH model. The results indicate a variation in average food and non-food expenditure across constituencies, with Windhoek East, Khomasdal, John Pandeni and Katutura East constituencies recording the highest expenditures. In general, the results obtained in this study were in coherent with Benavent and Morales (2016) and Permatasari and Ubaidillah (2021) who studied MFH models for small area estimation of dichotomous response variables, poverty.

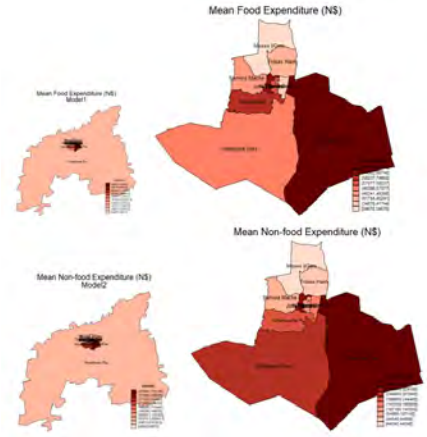

Figure 4: Bivariate FH model expenditure estimates

4 Conclusions

The study has demonstrated that the FH modelling approach does not only produce more efficient estimates than the direct estimates, but the estimation improves further when the correlation in

response variables is considered. For future work, this estimation could be further improved by considering more auxiliary data and accounting for spatial correlation, to quantify relations among neighbouring households on small area estimates of correlated response variables.

References

Benavent, R. and Morales, D. (2016). Multivariate fay–herriot models for small area estimation. *Computational Statistics & Data Analysis*, 94:372–390.

Bucyibaruta, G. (2014). *Statistical Models for Small Area Estimation*. PhD thesis, Centro de Investigación en Matemáticas.

Czajka, J. L., Sukasih, A., Maccarone, A., et al. (2014). Small area estimation: New developments and directions for hhs data. Technical report, Mathematica Policy Research.

Liu, B. (2009). *Hierarchical Bayes estimation and empirical best prediction of small-area proportions*. University of Maryland, College Park.

Mukhopadhyay, P. K. and McDowell, A. (2011). Small area estimation for survey data analysis using sas software. In *SAS Global Forum*, volume 2011, page 96.

Ngaruye, I., Nzabanita, J., Rosen, D. v., and Singull, M. (2017). Small area estimation under a multivariate linear model for repeated measures data. *Communications in Statistics-Theory and Methods*, 46(21):10835–10850.

Permatasari, N. and Ubaidillah, A. (2021). msae: An R Package of Multivariate Fay-Herriot Models for Small Area Estimation. *The R Journal*, 13(2):111–122.

Rao, J. N. (2003). *Small Area Estimation*. John Wiley & Sons.

Rao, J. N. and Molina, I. (2015). *Small area estimation*. John Wiley & Sons.

LATENT GROWTH MIXED MODEL OF THE PROGRESSION OF HIV USING CD4 COUNTS: A CASE STUDY OF NAMIBIA

Authors:

Samuel Ndungula[1]
Namibia University of Science and Technology

Victor Katoma[2]
Namibia University of science and Technology

EXTENDED ABSTRACT

Introduction

The application of Latent Growth Models and Latent Growth Mixed Models to longitudinal data such as CD4 count data is an important extension of traditional methods of measuring clinical change. Traditional approaches such as ANOVA and Multiple Regression analysis only mean changes and treat differences in individuals as error variance. However, error variances often contain valuable information which Latent class models use to predict change more accurately and can be used on CD4 count change in individuals and individual classification on antiretroviral treatment.

The focus of this research was to analyse the patterns of change of CD4 counts when the patient is initiated on ART, as well as to investigate different patterns of growth caused by population heterogeneity. This study further sought to analyse how different predictors affect the initial CD4 counts of patients and how they influence the change in the counts overtime.

Literature has found that lower CD4+ cell counts are associated with disease progression, and ART can increase CD4+ cell counts. Several covariates, including age, education, income, and treatment duration, can influence CD4+ cell count progression. Interpretation of the effects of these covariates is essential in assessing treatment efficacy and predicting viral failure.

Various statistical models, such as linear mixed models and Poisson-Gamma-Normal models, have been used to analyze CD4+ cell count progression. These models have identified significant predictors of CD4+ cell count changes, including baseline CD4+ counts, age, gender, BMI, and treatment period. The use of these models helps to understand how patients respond to treatment over time. In conclusion, this article emphasizes the importance of ART in HIV treatment and monitoring CD4+ cell counts to assess disease progression. Adherence to treatment and Interpretation the factors that influence CD4+ cell count progression is crucial for the success of HIV treatment programs.

Methodology

This longitudinal study employed a Latent Growth Mixed Model to account for the existence of unobserved influences on CD4 count change through unobserved population heterogeneity. The study sample was clinical data extracted from 466 HIV+ patients, registered at a state hospital in Windhoek Namibia. Each of these patients had four measurements from 2011-2019. The results showed that there existed unobserved population heterogeneity with a conditional 4-class mixed model having the best fit. The demographic variables (age, sex, weight and region) were used as the predictors in the Latent Growth Model, and exploratory data analysis was conducted using R, while the Latent growth Models were conducted using Mplus software.

Results

The study revealed that most patients (34.3%) started their ART at stage 3 with CD4 counts between 200 and 350 cells/mm^3, while smaller percentages began treatment at stages 1, 2, and 4. It further revealed that female patients were more (68.2%) compared to males (31.8%). The average CD4 counts showed an increasing trend over time, with the lowest count at treatment initiation and the highest recorded at time 3. The average CD4 count at

treatment initiation was 318.57 ± 206.246 cells/mm³, with the highest recorded at 1290 cells/mm³ and the lowest at 4 cells/mm³. The baseline characteristics were as follows: The average baseline age of patients was 33.82±7.97 years (range: 16-69 years), and the average baseline weight was 52.02 ± 12.68 kg (range: 21 to 115 kg). The WHO baseline stages were as follows: Most patients (34.3%) were in stage III, followed by stage IV (31.5%) and stage I (16.7%). Stage I patients consistently showed higher CD4 levels compared to those in earlier stages. CD4 count variability was highest in stage III patients and lowest in stage II patients. Male patients had an average baseline CD4 count of 266.7, while female patients had 342.82. Female patients began ART with higher CD4 counts than male patients, and this difference increased over time.

In terms of individual profile analysis, there was significant variations, with some showing steep progress while others remained flat. The female patients had greater variations, but the difference were minimal, while male patients displays more erratic growth patterns.

The Comparative Fit Index (CFI) was discovered to be 0.943, and the Tucker-Lewis Index (TLI) had a value of 0.931, indicating a decent fit for the model. Moreover, the Root Mean Square Error of Approximation (RMSEA) stood at 0.289, which falls within an acceptable range. These findings collectively suggest that the Unconditional Latent Growth Model is a suitable selection for examining the changes in CD4 counts among HIV patients over time.

Conditional Latent Growth Model was used to analysis CD4 change in HIV patients during four time points. The model showed good fit, with significant results for chi-square test and fit indices (CFI = 0.947, TLI = 0.918, RMSEA = 0.038). Initial CD4 counts had variation, and negative correlation was observed between intercepts and slopes, indicating patients starting with high CD4 counts were more likely to experience decline over time. Age had negative impact on baseline CD4, while gender had positive impact. However, neither age nor gender

significantly affected CD4 change rate. R-squared values showed reliable predictions of CD4 growth, with second time point being least reliable.

A Conditional Latent Growth Model was applied to analyze CD4 changes in HIV patients across four time points. The model demonstrated good fit with significant chi-square results ($\chi 2$) and favourable fit indices (CFI = 0.941, TLI = 0.852, RMSEA = 0.06). Baseline CD4 values exhibit variability, and a negative correlation was observed between intercepts and slopes, indicating patients with higher initial CD4 counts were more likely to experience a decline over time. Covariates such as "Region," "Weight," and "Age" had significant effects on the baseline CD4, while "Gender" had a positive impact on the initial CD4 count. However, none of the covariates significantly influenced the rate of CD4 change over time.

Latent Profile Analysis was used to examine heterogeneity in CD4 longitudinal data of HIV patients, and the results of the Lo-Mendel-Rubin Adjusted LRT test and the Voung-Lo-Mendell-Rubin test indicated a significant difference ($p < 0.0001$) between the models, suggesting the presence of latent classes (5 classes to be specific).

A latent growth mixture model 1 was tested to investigate CD4 changes in HIV patients over four time points using Mplus 8.8. The model showed good fit with a log-likelihood h0 value of -12192.958, aBIC of 24439.384, BIC of 24496.512, and AIC of 24421.916. The final class proportions were as follows: latent class 1 (18.30%), latent class 2 (2.10%), latent class 3 (1.40%), and latent class 4 (78.2%). Latent class 3 demonstrated the highest growth tendency, while latent class 2 had a decreasing tendency, latent class 1 had the least change, and latent class 4 had consistently low CD4 counts but showed an increasing growth tendency. Lastly, a latent growth mixture model 2 was used to analyze CD4 changes in HIV patients over four time points, considering age and gender as covariates. The model demonstrated a good fit, indicated by the log-likelihood h0 value of -12178.888, AIC of 24401.776, BIC of 24492.948,

and ABIC of 24423.125. The findings indicated that age had a negative effect on the baseline CD4 count, while gender had a positive effect on the initial CD4 count. However, neither age nor gender significantly influenced the rate of CD4 change over time. There were no notable variations in CD4 values across different time points and no significant relationship between the baseline CD4 count and the growth over time.

Discussion

The research explored HIV infection progression in patients on ART, by focusing on CD4 count data. They saw that CD4 counts rose over time, aligning with earlier findings. Female patients had a higher average CD4 count than males. The research hypothesized existence of population heterogeneity and different growth trajectories, and covariates like Age, Gender, Weight, and Region could predict latent growth curve. The hypotheses were tested using models, confirming population heterogeneity and identifying age and gender as significant predictors of initial CD4 count, but not of growth over time. The study revealed four latent classes, each with different CD4 count averages and growth rates. The study suggested patients with high initial CD4 counts tend to experience small CD4 count decline after starting ART, while patients with low initial CD4 counts show larger growth rates over time. Introducing covariates reduced variability of growth factors.

Conclusion

The study revealed that CD4 count changes among HIV patients ART. This mostly points to heterogeneity in the population due to class. Using covariates like gender and age on CD4 counts reveals that these concomitant factors paly a significant role in HIV progression. High starting CD4 counts minor drop while low starting counts see much up counts over time. It is recommended, each person starting CD4 counts be considered while taking covariates such as gender and age into consideration to obtain best results. Further research should also focus on sample size effects as the difference between male and female sizes was relatively large.

References

Aavani, P., & Allen, L. J. S. (2019). The role of CD4 T cells in immune system activation and viral reproduction in a simple model for HIV infection. Applied Mathematical Modelling, 75, 210–222. https://doi.org/10.1016/J.APM.2019.05.028 Abera, B., Walle, F., Tewabe, T., Alem, A., & Yessin, M. (2010). ART-naive HIV patients at Feleg-Hiwot Referral Hospital Northwest, Ethiopia. Ethiopian Journal of Health Development, 24(1), 3–8. https://doi.org/10.4314/ejhd.v24i1.62939 Andualem, B. D., & Ayele, B. T. (2020). Progression of HIV Disease Among Patients on ART in Ethiopia: Application of Longitudinal Count Models. 7(February), 1–9. https://doi.org/10.3389/fpubh.2019.00415 Anglemyer, A., Rutherford, G. W., Horvath, T., Baggaley, R. C., Egger, M., & Siegfried, N. (2013). Antiretroviral therapy for prevention of HIV transmission in HIV-discordant couples. Cochrane Database of Systematic Reviews, 2013(4). https://doi.org/10.1002/14651858.CD009153.pub3 Aunola, K., Leskinen, E., Lerkkanen, M.-K., & Nurmi, J.-E. (2004). Developmental Dynamics of Math Performance From Preschool to Grade 2. Journal of Educational Psychology, 96(4), 699–713. https://doi.org/10.1037/0022-0663.96.4.699 Barclay, T. R., Hinkin, C. H., Castellon, S. A., Mason, K. I., Reinhard, M. J., Marion, S. D., Levine, A. J., & Durvasula, R. S. (2007). Age-associated predictors of medication adherence in HIV-positive adults: Health beliefs, self-efficacy, and neurocognitive status. Health Psychology, 26(1), 40–49. https://doi.org/10.1037/0278-6133.26.1.40

Digital technologies, Fourth Industrial Revolution and mathematics education nexus in emerging economies: A systematic analysis.

Dr. Ruth Eegunjobi[1]* Dr. Shihaleni Ndjaba[2] Rosalia Mwalundilange[3]

*r.eegunjobi@ium.edu.na

Abstract

The Fourth Industrial Revolution (4IR) can potentially transform mathematics education in emerging economies to a higher developmental level by increasing personalised learning and improving students' computational thinking across multiple aspects of mathematics. 4IR will, predictably, alter traditional teaching and learning methods in emerging economies. This disruptive technology will alter logical reasoning, critical thinking, and the analysis and solution of real-world problems. The Preferred Reporting Items for Systematic Literature Review and Meta-Analysis (PRISMA) of secondary data sources, primarily peer-reviewed reputable journal articles, served as the foundation for this article. The goal is to reach conclusions and identify research gaps. The findings show that the main challenge for academic institutions in emerging economies is finding dynamic ways to integrate 4IR technologies into mathematics instruction. Future researchers should use mixed methods or experimental research designs to investigate the 4IR and teaching and learning nexus in emerging economies. The current scientific study adds to theory, practice, and future research directions.

Keywords: Fourth Industrial Revolution (4IR); emerging economies; new digital technologies; Mathematics Education.

1. Introduction

In emerging economies, raising understanding of digital technology in mathematics education and learning can help them cope with the disruptive complexity of the Fourth Industrial Revolution (4IR). Due to 4IR, emerging economy teaching and learning dynamics have grown more visible over the last two decades (Costan et al., 2021). Thus, mathematics education will use more digital technology. Augmented reality (AR) will replace most math teaching aids in emerging economies Bulut and Ferri (2023), which is much better than traditional methods and lets students interact with three-dimensional models in the real world, especially in geometry and other complex concepts. Digital technologies will close the schooling gap. Laufer et al. (2021), improve teacher effectiveness Qureshi et al. (2021), promote self-directed learning Maphalala (2021), and increase access to educational resources will affect mathematics education output and quality.

Previous research has studied how mobile technology affects Ghanaian mathematical education (Twum and Ayite, 2020; Chakoma and Makonye, 2020), the impact of digital education interventions in low-income countries, and the transformative potential of digital technologies in mathematics education. On the other hand, the current novel research study aims to analyze the relationship between digital technologies and the evolution of teaching and learning in emerging economies, evaluate the use of 4IR in mathematics education in emerging economies, and explore digital technologies and their links to 4IR for future mathematics education improvement. Theories from Preferred Reporting Items for Systematic Literature Review and Meta-Analysis helped researchers address study objectives and fill literature gaps.

2. Methodology

To achieve the study's objectives, a systematic review of secondary data sources, primarily peer-reviewed journal articles, was conducted using the Preferred Reporting Items for Systematic Review and Meta-Analyses (PRISMA). This method uses a strict set of guidelines in conducting systematic literature reviews and has been used by researchers because of its replicability, ability to draw conclusions and identify gaps in the existing literature. (Denyer and Tranfield, 2009). Compared to other methodologies, PRISMA advances scientific knowledge by investigating research questions. The procedure entailed a systematic and thorough search of databases for existing literature on digital technologies, 4IR, and mathematics education in emerging economies. First, a database was searched for peer-reviewed articles, reports, proceedings, and perspectives.

Secondly, newspapers and some online sources were excluded to ensure the results' validity and reliability. Keywords related to 4IR, digital technologies, and mathematics education were included to improve search results. Thirdly, search items with no full-text non-related content were excluded to meet the exclusion and inclusion criteria, while articles with partial or close relationships were included. During the evaluation process, compatibility was performed to determine how suitable the selected articles were. Fourth, the research objectives were aligned to ensure a concise approach to the entire process. Finally, data extraction and population were carried out following the content analysis procedure (Nyagadza et al., 2020). The population procedure was done by comparing, integrating, and summarising themes found during the systematic review process.

2.1 Articles consulted

Scopus and Web of Science were the primary databases used because they are the world's largest abstract and citation databases of peer-reviewed literature. Other inclusion criteria included (i) articles from 2016, as the 4IR became an increasingly popular subject following the Hanover Fair in 2011. (ii) English-language articles; and (iii) articles published in journals and books.

2.2 Collection of articles

The literature has not comprehensively explored the nexus between mathematics education, 4IR and digital technologies in emerging economies. The process included the keywords "Digital technologies, 4IR, mathematics and emerging economies. The results were further filtered based on year of publication, language, and document type (i.e., article). A total of 24 articles were identified and appropriate from the search process for this study.

3. Results

This section presents PRISMA findings on the relationship between digital technologies, the Fourth Industrial Revolution, and mathematics education in emerging economies.

3.1 Digital Technologies, Teaching and Learning in Emerging Economies

Digital technologies have emerged due to 4IR dynamic, disruptive technologies. 4IR is now a buzzword and gaining traction across different sectors of the economy. Accordingly, 4IR, perceived as a fusion of many technologies and perceived to blur the boundaries between the physical, digital, and biological spheres, is now attracting increasing attention from policymakers, business practitioners, and academics. Digital technologies have shifted the educational system's

paradigm from being a knowledge provider to a co-creator of information, a mentor, and an accessor (Abid et al., 2022). Furthermore, facilitating access to educational resources and promoting interactive and engaging learning experiences can help students in emerging economies realise their full potential. Personalised learning, collaboration and communication, and remote learning opportunities have all contributed to the expansion of mathematics education. While developed countries use digital technologies effectively, most emerging economies do not and are still catching up. Digital technologies are frequently associated with developing customisable and tailored education, meeting specific needs by assisting each student in studying at their own pace. However, there is a need in many developing economies to improve curricula and invest in digital technologies (Oke and Fernandes, 2020).

3.2 4IR in Mathematics Teaching and Learning in Emerging Economies

4IR involves creating new systems that blend physical and digital technology for a more connected population of active users (Tripathi and Gupta, 2021). Integrating 4IR developing technology will create new academic prospects for emerging economies. It will close the educational gap and prepare students for digital and tech-driven employment. Most 4IR research focuses on high school mathematics teachers' readiness and disposition to adopt 4IR technologies, the use of mathematics education to promote social justice and sustainability in the 4IR era, 4IR's sufficiency as a disruptive educational trend to promote sustainable open education, and technology-based teaching methods for embedding sustainable mathematics higher education. Thus, 4IR will enhance mathematics education, promote computational thinking, and give students hands-on experience. The transformation of South African mathematics education supports this claim. Other developing economies in underdeveloped countries are still struggling. Emerging economies struggle to use 4IR for teaching and learning due to insufficient infrastructure, a lack of continuous professional development, and a mathematics curriculum that does not accommodate 4IR changes (Ukobizaba, 2022).

3.3 Digital Technologies, 4IR, and Human Capital

Digital technology, 4IR, and mathematics education can reduce educational inequities in emerging nations by offering equal access to learning (Naidoo and Reddy, 2023). Remote and underserved children can access educational resources and experienced educators online via digital technologies. This can help level the playing field and provide quality mathematical instruction to

pupils without good schools or teachers. Giving developing country teachers tools and resources to better their teaching would help them much more. Online platforms and educational software include lesson plans, teaching tools, and interactive activities to improve math learning. Teachers can use technology to design interactive lessons, track student progress, and provide timely feedback.

4. Conclusion

This section explores consequences, study limits, future research, and emerging economy policy recommendations. UNESCO emphasizes the relevance of digital literacy and mobile technology in developing education and equipping people with the skills to engage fully in digital society. Digital technology can help emerging nations prepare for the digital economy by boosting innovation, sustainable development, and inclusive growth. By 2030, artificial intelligence, virtual reality, and advanced data analysis will be more integrated into mathematics education. Technical issues, access issues, and a poor internet connection would result. Student disadvantage and low-quality or erroneous content cause confusion and misconceptions. Equitable access to technology, specialized teacher training, curriculum design that promotes 21st-century skills, and robust privacy and quality rules are needed to address these concerns. These potential drawbacks must be addressed to ensure digital technology in mathematics education serves all learners and fosters equal and relevant educational experiences. The study is confined to the literature studied, which may impair generalizability. Future studies may examine individual countries or cross-cultural economic comparisons. Theories on underlying subjects may be included in future investigations. Researchers should employ mixed techniques or experimental approaches to study the 4IR and teaching and learning nexus in emerging economies.
Developing economies should consider the following for policy proposals to profit from the fast-changing academic scene. Some suggestions:

(a) Increase digital infrastructure access in remote locations to bridge the digital divide.
(b) Invest in teacher training. This might be done by investing more in teacher digital literacy and technology integration training.
(c) Adapt teaching methods and curriculum to meet the demands of the 4IR through review and updating.

References

Ayanwale, M. A., Ndlovu, M., & Oladele, J. I. (2022). Mathematics Education and the Fourth Industrial Revolution: Are the High School Mathematics Teachers Ready?. In *Mathematics Education in Africa: The Fourth Industrial Revolution* (pp. 77-96). Cham: Springer International Publishing.

Bulut, M., & Ferri, R. B. (2023). A systematic literature review on augmented reality in mathematics education. *European Journal of Science and Mathematics Education*, *11*(3), 556-572.

Chaka, C. (2022, April). Is Education 4.0 a sufficient innovative, and disruptive educational trend to promote sustainable open education for higher education institutions? A review of literature trends. In *Frontiers in Education* (Vol. 7, p. 824976).

Denyer, D., & Tranfield, D. (2009). Producing a systematic literature review. In D. A. Buchanan & A. Bryman (Eds.), The sage handbook of organisational research methods (pp. 671–689). Sage Publications.

Laufer, M., Leiser, A., Deacon, B., Perrin de Brichambaut, P., Fecher, B., Kobsda, C., & Hesse, F. (2021). Digital higher education: a divider or bridge builder? Leadership perspectives on edtech in a COVID-19 reality. *International Journal of Educational Technology in Higher Education*, *18*, 1-17.

Liu, E., Li, Y., Cai, S., & Li, X. (2019). The effect of augmented reality in solid geometry class on students' learning performance and attitudes. In *Smart Industry & Smart Education: Proceedings of the 15th International Conference on Remote Engineering and Virtual Instrumentation 15* (pp. 549-558). Springer International Publishing.

Maphalala, M. C., Mkhasibe, R. G., & Mncube, D. W. (2021). Online Learning as a Catalyst for Self-Directed Learning in Universities during the COVID-19 Pandemic. *Research in Social Sciences and Technology*, *6*(2), 233-248.

Naidoo, J., & Reddy, S. (2023). Embedding Sustainable Mathematics Higher Education in the Fourth Industrial Revolution Era Post-COVID-19: Exploring Technology-Based Teaching Methods. *Sustainability*, *15*(12), 9692.

Nyagadza, B., Kadembo, E. M., & Makasi, A. (2020a). Exploring internal stakeholders' emotional attachment & corporate brand perceptions through corporate storytelling for branding. Cogent Business & Management, 7(1), 1–22.

Oke, A., & Fernandes, F. A. P. (2020). Innovations in teaching and learning: Exploring the perceptions of the education sector on the 4th industrial revolution (4IR). *Journal of Open Innovation: Technology, Market, and Complexity*, *6*(2), 31.

Qureshi, M. I., Khan, N., Raza, H., Imran, A., & Ismail, F. (2021). Digital Technologies in Education 4.0. Does it Enhance the Effectiveness of Learning?.

Tripathi, S., & Gupta, M. (2021). A holistic model for global industry 4.0 readiness assessment. Benchmarking: An International Journal, 1463–5771.

Twum, R., & Ayite, D. M. K. (2020). The use of mobile technology to enhance learning among University of Cape Coast health science education students. *International Journal of Innovative Science and Research Technology*, *5*(5), 1667-1673.

Ukobizaba, F., Nsabayezu, E., & Uworwabayeho, A. (2022). Is Africa Ready for the Fourth Industrial Revolution?. In *Mathematics Education in Africa: The Fourth Industrial Revolution* (pp. 1-18). Cham: Springer International Publishing.

Optimizing Costs for the Multi-unit Machine Repair Problem with Primary and Secondary Repairer in the $M/M/R+1$ Configuration

Mahendra Devanda, Suman Kaswan, and Chandra Shekhar*
Department of Mathematics, Birla Institute of Technology and Science Pilani, Pilani Campus, Pilani, Rajasthan, 333 031 (India).
mahendradevandamaths@gmail.com; sumanchaudharymh@gmail.com; chandrashekhar@pilani.bits-pilani.ac.in

Abstract

correct with scientific terminology, research word, good English, systematic writing, plagiarism free content (do not change the LaTex formatting) for "" This research paper investigates a complex machine repair problem involving multiple operating units and the use of warm spares, alongside a skilled repairer allocation strategy. The problem entails immediate attention by an available repairer whenever a unit fails. The system comprises R primary repairers and a single secondary repairer, where the former handle basic maintenance and low-skilled repairs, while the latter focuses on critical repair or final tasks. To address this problem, a mathematical model is formulated, and the recursive method is employed to solve it. Probability distributions for different states are determined to derive performance indices. Additionally, a cost model is developed to minimize the predicted cost function per unit of time by optimizing decision parameters. Teaching-learning-based optimization, a metaheuristic approach, is implemented to achieve this optimization and identify the optimal decision parameters for a cost-effective service system. *Keywords.* Warm standby, Primary repairers, Secondary repairer, Teaching-learning based optimization, Cost analysis.

1 Introduction

Machines play a pivotal role in driving industry and facilitating economic growth within the rapidly evolving and automated landscape. However, failures and glitches pose significant obstacles, negatively impacting industrial productivity, efficiency, and profitability. Consequently, the development of machine repair models has emerged as a paramount area of focus for research and innovation. Machine repair problems have become a primary concern for the industry, as they directly influence the ability of companies to operate seamlessly, minimize disruptions, and maintain competitiveness in a dynamic marketplace. Skilled repair experts are instrumental in addressing various concerns, including productivity, safety, cost efficiency, technological advancements, and sustainability, enabling businesses across diverse sectors to effectively sustain the optimal functioning of their machines.

In the context of Industry 4.0, machine repair problems assume critical importance due to their profound impact on various operational aspects, including downtime, efficiency, productivity, predictive maintenance, data-driven decision-making, quality, customer satisfaction, and knowledge dissemination. To fully harness the advantages offered by Industry 4.0 and achieve optimal functioning of interconnected systems in the industrial sector, it becomes imperative to address maintenance problems in an efficient and proactive manner.

The advent of Industry 4.0, characterized by the integration of cyber-physical systems, the Internet of Things (IoT), and data analytics, has significantly heightened the demand for intelligent and efficient repair solutions. Real-time monitoring, sensor technology, and advanced analytics have revolutionized traditional machine repair models, shifting them from reactive approaches to proactive and predictive methodologies. These advanced models have the potential to minimize downtime, optimize maintenance schedules, and enhance overall efficiency. Moreover, the utilization of Artificial Intelligence (AI) and Machine Learning (ML) systems enables the analysis of vast volumes of data, unveiling valuable insights, and enabling accurate forecasting of machine problems, thereby transforming the landscape of machine maintenance.

Several researchers have made noteworthy contributions to the field of machine repair modeling. Wang [1] developed a profit model for $M/M/R$ machine repair problems. Wang et al. [2] explored the sensitivity analysis of $M/M/R$ machine repair problems, incorporating factors such as balking, reneging, and switching failure employing direct search and steepest descent methods and identify optimal decision variables. Jain et al. [3] delved into the investigation of a Markovian model that incorporates switching failure of warm standby in machine repair problems. Shekhar et al. [4] introduced a single server Markovian queueing model with feedback, incorporating the second kind of modified Bessel function. Shekhar et al. [5] analyzed the reliability characteristics of a Markovian warm-spare nodes provisioning computing network, considering factors such as common cause failure, switching failure, and vacation interruption. Furthermore, Devanda et al. [6] developed a fuzzified imperfect repair model to address redundant machine repair problems, utilizing nonlinear parametric program techniques.

In the realm of machine repair, Takacs [7] proposed a Markovian machine repair problem involving multiple machines serviced by a single repairman. Delia and Rafael [8] investigated a maintenance model encompassing failures and inspection, which followed Markovian arrival processes and incorporated two repair modes. Maheshwari et al. [9] tackled the challenge of multi-repairmen machine repair problems, considering the presence of various types of warm standby units. Jain et al. [10] examined a machine repair problem involving mixed spares under an N-policy and incorporating two types of repair facilities. The researchers derived performance measures and cost functions using recursive method techniques. Shekhar et al. [11] focused on redundant machine repair problems, specifically studying the optimal (N, F) policy. Jain and Meena [12] developed a comprehensive multi-unit

*Corresponding author

Markovian machining system, which included two unreliable heterogeneous repairmen and mixed types of spare. Recently, Gao and Wang [13] conducted a sensitivity analysis of a redundant system featuring random inspection and multiple repairmen under repair pressure.

By continuously advancing the field of machine repair modeling and incorporating cutting-edge technologies, researchers can contribute to the realization of efficient and proactive maintenance strategies. These strategies will not only ensure the optimum functioning of interconnected systems but also unlock the full potential of Industry 4.0, thereby promoting sustained industry growth and economic prosperity.

2 Model Discription

This study addresses a Markovian model comprising M operating units, R primary repairers, and one secondary repairman. For the well-functioning of the system, atleast m units are required. Hence, maximum $L = M - m + 1$ failures are allowed. The model is defined based on the following assumptions and notations:

- The inter-failure time between consecutive operating units is modeled by an exponential distribution with a mean of $\frac{1}{\lambda}$. There is no failed units in the initial state ($t = 0$), but after the time t, let's there are n failed units in the system, and the state-depended failure rate is calculated as:
$$\lambda_n = (L - n)\lambda \; ; \quad n = 0, 1, 2, \ldots, L-1, L$$
- Upon failure, an operating unit is immediately sent to the repair facility, without any time loss. The repair facility consists of two phases: the initial phase and the final phase. Each failed operating unit undergoes both phases.
- During the initial phase, the primary repairers are responsible for repairing the operating unit, while the secondary repairman takes over during the final phase.
- The failed operating unit cannot directly interact with the secondary repairman. Instead, it is initially assigned to a primary repairer, who works on the unit. Once the primary repair is completed, the unit needs to be inspected and approved by the secondary repairman.
- To complete the repair process, the primary repairer transitions to the final phase, documenting the faults identified and the work performed during the initial phase.
- If the secondary repairman is occupied with other primary repairers in the final phase, they wait in a queue according to a first-come, first-served policy.
- Subsequently, based on the work division policy, the secondary repairman and the primary repairer collaborate to handle the remaining tasks that require the involvement of the secondary repairman. Finally, the secondary repairman approves the repaired unit for reintegration into the main operating units.
- The repair times for both the primary repairer and the secondary repairman are exponentially distributed with rates denoted as μ_i and α, respectively, where
$$\mu_i = \begin{cases} (i-j)\mu \; ; & 0 \le i \le R \;\&\; 0 \le j \le i \\ (R-j)\mu \; ; & R \le i \le L \;\&\; 0 \le j \le R \end{cases}$$
and
$$\alpha = \Gamma + \frac{b}{(\Gamma - \mu)}$$

The system state is represented by pairs $Z = \{(I, F)\}$ where I denotes the number of failed units in the initial phase, and F denotes the number of primary repairers in the final phase. The joint probability distribution is denoted by $P_{i,j}$ and defined by $P_{i,j} = P\{I = i, J = j\}; i = 0, 1, 2, \ldots, L-1, L \;\&\; j = 0, 1, 2$.

$$\mathbf{Q} = \begin{bmatrix} \mathbf{X}_0 & \mathbf{Z}_0 & \mathbf{0} & \mathbf{0} & \mathbf{0} & \mathbf{0} & \cdots & \mathbf{0} & \mathbf{0} & \mathbf{0} & \mathbf{0} \\ \mathbf{Y}_0 & \mathbf{X}_1 & \mathbf{Z}_1 & \mathbf{0} & \mathbf{0} & \mathbf{0} & \cdots & \mathbf{0} & \mathbf{0} & \mathbf{0} & \mathbf{0} \\ \mathbf{0} & \mathbf{Y}_1 & \mathbf{X}_2 & \mathbf{Z}_2 & \mathbf{0} & \mathbf{0} & \cdots & \mathbf{0} & \mathbf{0} & \mathbf{0} & \mathbf{0} \\ \mathbf{0} & \mathbf{0} & \mathbf{Y}_2 & \mathbf{X}_3 & \mathbf{Z}_2 & \mathbf{0} & \cdots & \mathbf{0} & \mathbf{0} & \mathbf{0} & \mathbf{0} \\ \mathbf{0} & \mathbf{0} & \mathbf{0} & \mathbf{Y}_3 & \mathbf{X}_4 & \mathbf{Z}_2 & \cdots & \mathbf{0} & \mathbf{0} & \mathbf{0} & \mathbf{0} \\ \vdots & \vdots & \vdots & \ddots & \ddots & \ddots & \ddots & \vdots & \vdots & \vdots & \vdots \\ \mathbf{0} & \mathbf{0} & \mathbf{0} & \mathbf{0} & \mathbf{0} & \mathbf{0} & \mathbf{0} & \mathbf{Y}_{L-3} & \mathbf{X}_{L-2} & \mathbf{Z}_2 & \mathbf{0} \\ \mathbf{0} & \mathbf{0} & \mathbf{0} & \mathbf{0} & \mathbf{0} & \mathbf{0} & \mathbf{0} & \mathbf{0} & \mathbf{Y}_{L-2} & \mathbf{X}_{L-1} & \mathbf{Z}_2 \\ \mathbf{0} & \mathbf{0} & \mathbf{0} & \mathbf{0} & \mathbf{0} & \mathbf{0} & \mathbf{0} & \mathbf{0} & \mathbf{0} & \mathbf{Y}_{L-1} & \mathbf{X}_L \end{bmatrix}_{L+1 \times L+1}$$

The tri-diagonal block matrix $\mathbf{Q}$ is derived from the corresponding transition rate matrix of the Markovian chain. The block entries of the above tri-diagonal matrix are defined below. Let $\mathbf{P}_0 = \; P_{0,0}$, $\mathbf{P}_1 = (P_{1,0}, P_{1,1})$, and $\mathbf{P}_i = (P_{i,0}, P_{i,1}, P_{i,2})$ be the 3-dimensional probability vector for i^{th} row where $2 \le i \le L$. Let $\mathbf{P}_i = [\mathbf{P}_0, \mathbf{P}_1, \mathbf{P}_2, \ldots, \mathbf{P}_{L-1}, \mathbf{P}_L]$ be corresponding steady-state probability vector of matrix $\mathbf{Q}$.

$$\mathbf{X}_0 = \big[-\lambda_0\big]_{1\times 1}; \quad \mathbf{X}_1 = \begin{bmatrix} -(\lambda_1 + \mu) & 0 \\ \mu & -(\lambda_1 + \alpha) \end{bmatrix}_{2\times 2}; \quad \mathbf{X}_i = \begin{bmatrix} -(\lambda_i + 2\mu) & 0 & 0 \\ 2\mu & -(\lambda_i + \mu + \alpha) & 0 \\ 0 & \mu & -(\lambda_2 + \alpha) \end{bmatrix}_{3\times 3}; \quad 2 \le i \le L-1$$

$$\mathbf{X}_L = \begin{bmatrix} -2\mu & 0 & 0 \\ 0 & -(\mu+\alpha) & 0 \\ 0 & \mu & -\alpha \end{bmatrix}_{3\times3} ; \quad \mathbf{Y}_0 = \begin{bmatrix} \lambda_0 \\ 0 \end{bmatrix}_{2\times1} ; \quad \mathbf{Y}_1 = \begin{bmatrix} \lambda_1 & 0 \\ 0 & \lambda_1 \\ 0 & 0 \end{bmatrix}_{3\times2} ; \quad \mathbf{Y}_i = \begin{bmatrix} \lambda_i & 0 & 0 \\ 0 & \lambda_i & 0 \\ 0 & 0 & \lambda_i \end{bmatrix}_{3\times3} ; \quad 2 \le i \le L-1$$

$$\mathbf{Z}_0 = \begin{bmatrix} 0 & \alpha \end{bmatrix}_{1\times2} \quad \mathbf{Z}_1 = \begin{bmatrix} 0 & \alpha & 0 \\ 0 & 0 & \alpha \end{bmatrix}_{2\times3} \quad \mathbf{Z}_2 = \begin{bmatrix} 0 & 0 & 0 & 0 \\ 0 & 0 & \alpha & 0 \\ 0 & 0 & 0 & \alpha \end{bmatrix}_{3\times4}$$

3 Cost Function

We have formulated a comprehensive total cost function per unit time for the $M/M/R+1/(M,m)$ machine repair model featuring two types of repairers in terms of performance charachteristic. The key performance characteristics are computed as

The proportion of the secondary server's time that is spent in an idle time

$$I_T = \sum_{i=0}^{L} P_{i,0}$$

Mean number of failed units in the system

$$L_S = \sum_{i=0}^{1} iP_i e_{i+1} + \sum_{i=2}^{L} iP_i e_2$$

Mean number of primary repairer in the C-mode

$$L_J = \sum_{i=0}^{1} P_i a_i + \sum_{i=2}^{L} P_i a_2$$

Mean number of failed operating units in the system

$$E_F = \sum_{i=0}^{L-1} (M-i)\lambda_i P_i + m\lambda_d P_L$$

The cost function plays a pivotal role in the machine repair model, facilitating performance evaluation, optimization, resource allocation, and fault diagnosis. Our ultimate objective is to determine the optimal number of primary repairers and repair rate for the system. By doing so, we aim to minimize the overall cost incurred by the system and maximize its profitability. The expected total cost function (TC) is derived as follows:

$$TC = C_1 \times (1 - I_T) + C_2 \times L_S + C_3 \times L_J + C_4 \times E_F \times (1 - Qmu) + C_5 \times R + C_6 \times \mu$$

In the derived total cost function, we assign specific costs to different components, which are denoted as follows:

C_1 represents the cost per unit time associated with the proportion of the secondary server's time spent in utilization.
C_2 denotes the cost per unit time for each failed machine present in the system.
C_3 signifies the cost per unit time for the expected number of primary repairers in the F-phase.
C_4 represents the cost per unit time when the primary repairers are busy in the F-phase.
C_5 corresponds to the cost per unit time for a single primary repairer.
C_6 indicates the cost per unit time associated with the service.

4 Numerical Analysis

Numerical analysis serves as a crucial tool in computational research, providing a mathematical framework to analyze, interpret, and validate research findings. For the studied MRP model, we conduct numerical experiments for different parameters, and the results are presented in Figure 1 and Table 1. To conduct the analysis, we fixed the values of default parameters, including $M = 30$, $m = 2$, $R = 7$, $\lambda = 1.2$, $\lambda_d = 1.5$, $\Gamma = 3$, $b = 100$, $\omega = 1.3$, $\delta = 1$, $C_1 = 20$, $C_2 = 25$, $C_3 = 80$, $C_4 = 12$, $C_5 = 25$, and $C_6 = 25$. We then examined the impact of varying parameters, such as M, m, μ, λ, λ_d, and Γ, on the system's performance measures.

Fig. 1 illustrates the convergence of solution points to optimal positions over multiple iterations. It considers various randomly established solutions and demonstrates the convergence of the optimal total cost (TC) across these iterations. This convergence validates the effectiveness of Teaching-Learning Based Optimization for achieving optimal analysis. Table 1 presents the numerical results and reveals that as the number of active units increases in our system, both the optimal total cost and the service rate of primary repairers improve.

This finding aligns with our model and provides further validation. These results provide valuable insights for enhancing the performance and cost-effectiveness of machining systems. By analyzing the impact of failure types and making informed maintenance and standby provisioning decisions, system operators can optimize system performance and resource allocation.

5 Conclusion

This article presents an optimal cost analysis for the multi-unit machine repair problem in a configuration with primary and secondary repairers, following the $M/M/R+1/L$ model. The proposed model incorporates practical characteristics of machining

systems, such as the average number of active units, two types of repairers (Primary and Secondary), and the work-division policy. A Markovian approach is used to analyze the multi-unit machining system with different repair rates for the two types of repairers. The steady-state probabilities are determined using the matrix analytical method, which considers queue characteristics and enables performance analysis. A cost function is defined to capture relevant factors in the repair process, and the goal is to minimize the total cost by optimizing the decision variables. To achieve this optimization, a teaching-learning-based optimization technique is employed. This swarm intelligence approach simulates a teaching-learning-based classroom environment to enhance the search for the optimal solution. By applying this technique, the article provides insights into efficient resource allocation and system configuration for effective machine repair.

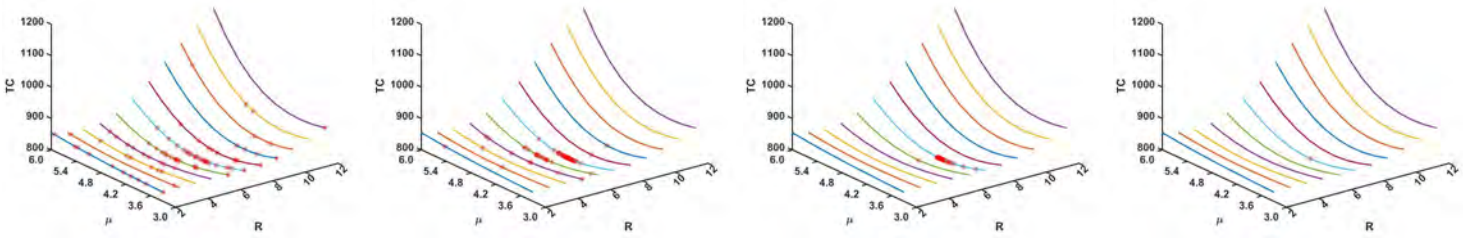

Iteration=1 Iteration=8 Iteration=15 Iteration=22

Figure 1: Convergence of iteration of Teaching-Learning based Optimization for $M = 30; m = 2; R = 7; \lambda = 1.2; \lambda_d = 1.5, \Gamma = 3; b = 100; \omega = 1.3; \delta = 1; C_1 = 20; C_2 = 25; C_3 = 80; C_4 = 12; C_5 = 25; C_6 = 25$

Table 1: Optimal expected total cost $TC(R^*, \mu^*)$ for the various parameter: $M = 30; m = 2; R = 7; \lambda = 1.2; \lambda_d = 1.5, \Gamma = 3; b = 100; \omega = 1.3; \delta = 1$

$M, m, \mu, \lambda, \lambda_d, \gamma$	R^*	μ^*	**TC**(R^*, μ^*)	**Mean Fitness**	**Worst Fitness**	**Time elapsed**
30, 2, 5, 1.2, 1.5, 3	6	4.4402861	806.9684546	1.0000002343	1.0000003789	126.2484480
40, 2, 5, 1.2, 1.5, 3	6	4.0500049	1055.5657970	1.0000006351	1.0000008973	175.9011704
50, 2, 5, 1.2, 1.5, 3	6	5.8179903	1305.5646167	1.0000001269	1.0000009255	169.2569432
30, 1, 5, 1.2, 1.5, 3	6	3.4585316	806.9684586	1.0000002311	1.0000006601	94.6634258
30, 2, 5, 1.2, 1.5, 3	6	4.4402861	806.9684546	1.0000001198	1.0000001008	93.5966877
30, 3, 5, 1.2, 1.5, 3	6	5.0518807	806.9683796	1.0000009012	1.0000007231	93.0493842
30, 2, 5, 1.2, 1.5, 3	6	4.4402861	806.9684546	1.0000009314	1.0000008454	289.6055630
30, 2, 6, 1.2, 1.5, 3	4	4.0776960	836.6521440	1.0000008149	1.0000000804	109.8451741
30, 2, 7, 1.2, 1.5, 3	3	4.4985248	868.5784713	1.0000001049	1.0000005760	253.8028803
30, 2, 5, 0.7, 1.5, 3	6	4.1821980	806.9668251	1.0000008116	1.0000001244	118.2474656
30, 2, 5, 1.2, 1.5, 3	6	4.4402861	806.9684546	1.0000001378	1.0000009127	116.7965025
30, 2, 5, 1.7, 1.5, 3	6	5.3048583	806.9700842	1.0000009611	1.0000006426	129.7795921
30, 2, 5, 1.2, 1.0, 3	6	3.4919127	637.7032411	1.0000002853	1.0000008845	108.2200725
30, 2, 5, 1.2, 1.5, 3	6	4.4402861	806.9684546	1.0000003399	1.0000008697	94.0410792
30, 2, 5, 1.2, 2.0, 3	2	4.5689590	878.3855629	1.0000002339	1.0000009164	96.4768404
30, 2, 5, 1.2, 1.5, 2	4	4.4882852	832.4700136	1.0000006311	1.0000002004	93.8064037
30, 2, 5, 1.2, 1.5, 3	6	4.4402861	806.9684546	1.0000007971	1.0000007562	95.1903519
30, 2, 5, 1.2, 1.5, 4	6	3.3938262	791.8671621	1.0000001222	1.0000007894	92.2753809

References

[1] K. H. Wang, "Profit analysis of the $m/m/r$ machine repair problem with spares and server breakdowns," *Journal of the Operational Research Society*, vol. 45, no. 5, pp. 539–548, 1994.

[2] K. H. Wang, J. B. Ke, and J. C. Ke, "Profit analysis of the m/m/r machine repair problem with balking, reneging, and standby switching failures," *Computers & operations research*, vol. 34, no. 3, pp. 835–847, 2007.

[3] M. Jain, C. Shekhar, and S. Shukla, "Markov model for switching failure of warm spares in machine repair system," *Journal of Reliability and Statistical Studies*, vol. 7, no. 1, pp. 57–68, 2014.

[4] C. Shekhar, A. Kumar, and S. Varshney, "Modified bessel series solution of the single server queueing model with feedback," *International Journal of Computing Science and Mathematics*, vol. 10, no. 3, pp. 313–326, 2019.

[5] C. Shekhar, N. Kumar, A. Gupta, A. Kumar, and S. Varshney, "Warm-spare provisioning computing network with switching failure, common cause failure, vacation interruption, and synchronized reneging," *Reliability Engineering & System Safety*, vol. 199, p. 106910, 2020.

[6] M. Devanda, C. Shekhar, and S. Kaswan, "Fuzzified imperfect repair redundant machine repair problems," *International Journal of System Assurance Engineering and Management*, pp. 1–20, 2023.

COST-BENEFIT ANALYSIS OF A THREE NON-IDENTICAL UNIT STANDBY SYSTEM WITH WEIBULL FAILURE AND REPAIR LAWS

LAXMI RAGHUVANSHI, RAKESH GUPTA and PRADEEP CHAUDHARY

Department of Statistics, Ch. Charan Singh University, Meerut-250004

Email ID: laxya.raghav@gmail.com, smprgccsu@gmail.com and pc25jan@gmail.com

ABSTRACT

The paper deals with the reliability and cost-benefit analysis of a three non-identical units namely-super priority(sp), priority (p) and ordinary (o) cold standby system model. A single repairman is always available with the system to repair a failed unit. The priorities in respect of operation and repair are being given to sp-unit over p, o-units and to p-unit over o-unit. All failure and repair time distributions of the units are assumed to follow weibull with different parameters. Several measures of system effectiveness are obtained by using regenerative point technique.

Keywords: Reliability, MTSF, availability, regenerative-point, pre-emptive repeat priority.

INTRODUCTION

The incorporation of redundancies is a very practical and widely applicable technique in the present compatative scenario for increasing the effectiveness of highly sophisticated systems. A large number of researchers have analysed two and more identical/non-identical units standby redundant system models by using the different techniques. Gupta and Tyagi (2016) analysed a two non-identical unit standby system model assuming that one of the unit namely priority (p) unit gets preference in both operation and repair over the other ordinary (o) unit. After the failure of p-unit, the o-unit in standby mode may require some maintenance action with probability $\bar{\theta}(=1-\theta)$ before starting its operation. The failure and repair times of each unit as well as maintenance action time of stand by unit are taken independent random variables of discreet nature having geometric distributions. Gupta and Vinodiya (2018) presented the reliability analysis of a cold standby system composed of two non-identical units-unit 1 and unit 2. Unit-1 gets the priority in operation over unit 2. So, unit-1 is never used as cold standby. Two types of failures are considered only in unit-1 and so its repair is also of two

types. All the failure time distributions are taken exponential and repair times are assumed to follow general distributions.

Gupta and Sharma (2018) analysed a system model of two non-identical units- priority (p) and ordinary (o). The repair of o-unit is performed by regular repairman who is always available with the system whereas to repair the p-unit a skilled repairman is needed who takes some significant time to reach the system from outside. Kour et al. (2019) carried out the analyses of a two non-identical unit cold standby system model assuming that the priority unit it goes for rest after operating for a random time period. A switching device is used to shift the failed unit to repair mode which may be perfect or imperfect at the time of need.

Saini et al. (2021) developed a stochastic model of a two non-identical units. One unit is treated as original and other as duplicate. Initially original unit is operative and duplicate is kept under cold standby. The model is analysed by incorporating the concepts of preventive maintenance, maximum operation time and priority in repair to original unit over the duplicate one. A single repair facility is considered to repair each type of unit. Failure and repair times of the units are assumed to follow general distributions.

Patawa et al. (2022) studied the stochastic behavior of a two dissimilar units cold standby repairable system with waiting time facility. The time to failure of each unit is assumed to follow exponential distribution whereas the repair time distributions of units are taken to be one parametric Lindley. The m.l.e. and Bayes estimates are obtained of various measures of system effectiveness.

More recently Raghuvanshi et al. (2021) analysed a model of two non-identical units cold standby system. A helping unit is also considered to protect the failure of priority unit. Failure time distributions of all the units are taken exponential whereas repair time distributions are taken general. Gupta et al. (2020) analysed a three unit cold and warm standby system model assuming that warm standby unit becomes operative instantaneously upon the failure of an operative unit whereas cold standby unit needs activation to become operative or to be warm standby. Distributions of time to failure, time to repair and activation time are taken as independent random variables of discrete nature having geometric distributions.

The purpose of the present paper is to analyse a three non-identical unit cold standby system model by considering Weibull distributions for both failure and repair times with common shape parameters and different scale parameters. Gupta et al. (2013) in fact analysed a two dissimilar unit cold standby system model with Weibull failure and repair time

distributions. They have assumed that one unit gets priority in operation as well as in repair over the other unit.

In the model under study we have obtained the following measures of system effectiveness useful to system designers and operation managers by using regenerative point technique-

i. Steady state transition probabilities and mean sojourn times.
ii. Reliability of the system and mean time to system failure (MTSF).
iii. Point-wise and steady-state availability of the system.
iv. Expected up (operative) time of the system during time interval (0, t).
v. Expected busy period of the repairman in time interval (0, t).
vi. Net expected profit earned by the system in time interval (0, t) and in steady-state.

The curves for MTSF and Profit function have also been sketched in respect of various parameter and important conclusions are drawn.

ASSUMPTIONS AND SYSTEM DESCRIPTION

The system consists of three non-identical units: unit-1, unit-2 and unit-3 and these are named as super priority (sp) unit, priority (p) unit and ordinary (o) unit respectively. Each unit has two modes- normal (N) and total failure (F). For the successful operation of the system the operation of only one unit is needed. Initially the sp-unit is operative and the other two are kept in cold standby. A single repairman is always available to repair a failed unit. The switching device to put the standby unit into operation is always perfect and instantaneous. The preference in operation and repair is being given to the sp-unit over p and o-units. However, the preference in operation and repair is also given to p-unit over the o-unit. Each repaired unit works as good as new. The failure and repair time distributions of each unit are taken to be independent having the Weibull density with common shape parameter and different scale parameters as follows-

$$f_i(t) = \alpha_i p t^{p-1} \exp\left(-\alpha_i t^p\right) \text{ and}$$

$$g_i(t) = \beta_i p t^{p-1} \exp\left(-\beta_i t^p\right)$$

Where $t \geq 0;\ \alpha_i, \beta_i, p > 0$ and $i = 1,2,3$ respectively for unit $1, 2$ and 3.

α_i / β_i i=1,2,3 are the scale parameter of failure/repair time distribution for i-th unit and p is the common shape parameter of failure and repair time distributions of each of units-1,2 and 3, $F_i(\bullet) / G_i(\bullet)$ is the C.d.f. of failure/repair time of i-th unit.

Symbols for the states of the system:

$N_o^i\,(i=1,2,3)$: unit-i is in normal mode and operative.

N_s^2 / N_s^3 : unit-2 / unit-3 is in normal mode and kept into cold standby.

$F_r^i\,(i=1,2,3)$: unit-i is in failure mode and under repair.

F_w^2 / F_w^3 : unit-2 / unit-3 is in failure mode and waiting for repair.

Using these symbols, the possible states of the system along with the transition time c.d.fs. are shown in the transition diagram (Fig.1). In this figure we observe that the states $S_0, S_1, S_2, S_3, S_5, S_6$ and S_7 are up states and state S_4 is the failed state.

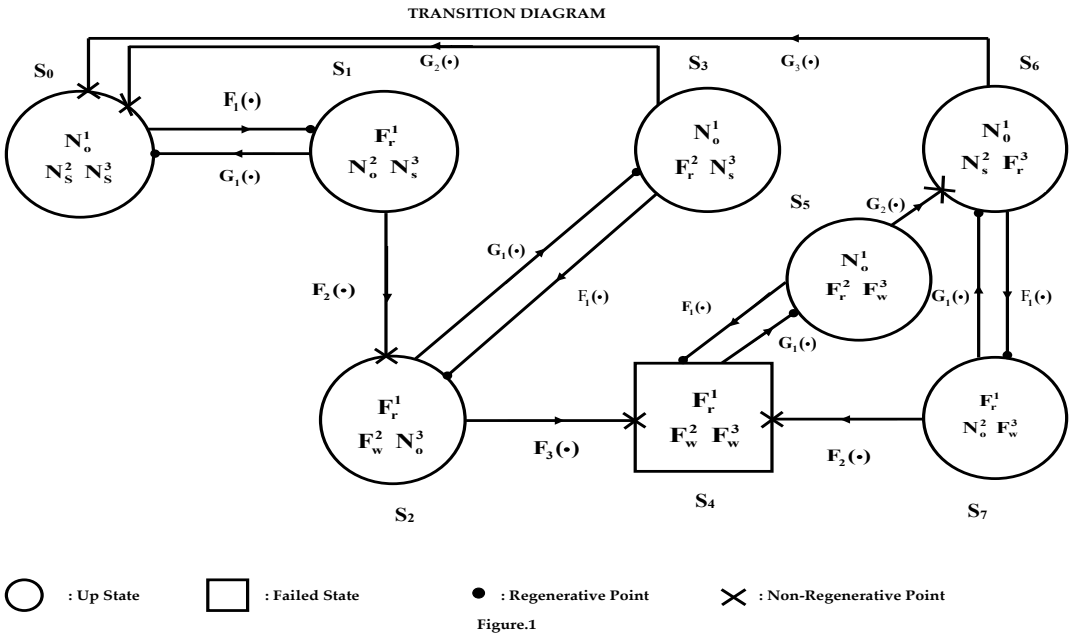

Figure.1

REFERENCES

[1] Gupta P. and P. Vinodiya (2018), 'Analysis of reliability of a two non-identical units cold standby repairable system has two types of failure'. *Int. J. of Computer Sciences and Engineering*, Vol. 6(11), pp. 907.

[2] Gupta R. and A. Tyagi (2016), 'Cost-benefit analysis of a two priority unit standby system with maintenance and geometric distributions of random variable'. *IAPQR Transactions*, Vol. 41(2), pp. 75-88.

[3] Gupta R. and N. Sharma (2018), 'A two-unit standby system with skilled and regular repairman to repair priority and ordinary units'. *J. of Rajasthan Academy of Physical Sciences*, Vol. 17(3& 4), pp. 111-126.

[4] Gupta S., P. Chaudhary and Vaishali (2020), 'A three unit warm and cold standby system model of discrete parametric Markov Chain'. *J. of Reliability Theory and Applications*, Vol. 15(4), pp. 117.

[5] Kour D., J. P. Singh and N. Sharma (2019), 'Effectiveness analysis of a two non-identical unit standby system with switching device and proviso of rest'. *Int. J. of Mathematical, Engineering and Management Sciences*, Vol. 4(6), pp. 1496-1507.

[6] Patawa R., P. S. Pundir, A. K. Singh and A. Singh (2022), 'Some inference on reliability measures of two non-identical units cold standby system waiting for repair'. *Int. J. of System Accurance Engineering and Management*, Vol. 13, pp. 172-188.

[7] Raghuvanshi L., R. Gupta and P. Chaudhary (2021), 'A two non-identical unit standby system with helping unit of the priority unit'. *Int. J. Of Agricultural and Statistical Sciences*, Vol. 17(2), pp. 873-881.

[8] Saini M., K. Devi and A. Kumar (2021), 'Stochastic modeling of a non-identical redundant system with priority in repair activities'. *J. of Thailand Statistician*, Vol. 19(1), pp. 154-161.

Wavelet Application to Geomagnetic Disturbances Modelling and Monitoring in Power Networks

Ilenikemanya D. Ndadi[1] **& Sunday A. Reju**[2]

[1]Department of Mathematics, Statistics and Actuarial Sciences, Namibia University of Science and Technology, Windhoek, Namibia
indadi@nust.na

[2]Department of Mathematics, Statistics and Actuarial Sciences, Namibia University of Science and Technology, Windhoek, Namibia
sreju@nust.na

ABSTRACT

Wavelets are powerful tools in signal processing and data compression. The wavelet transforms constitute excellent alternatives to Fourier transforms in many situations and they are ideal when signals are not periodic as in GIC signals. This paper specifically employs the Haar wavelet transform to investigate the optimal GIC energy in selected NAMPOWER substations' GIC data during two GMD events in 2013 and 2015. The results reveal some significant events during specific times of the day to suggest appropriate network disturbance mitigation strategies for the selected stations.

Keywords: *Geomagnetic disturbances, Geomagnetically induced currents; Wavelets; Haar wavelets; Optimal control*

INTRODUCTION

Geomagnetic disturbances (GMDs) are perturbations in the earth's geomagnetic field, which are results of the interactions between magnetic fields and the earth's conductivity (Lee, 1997).

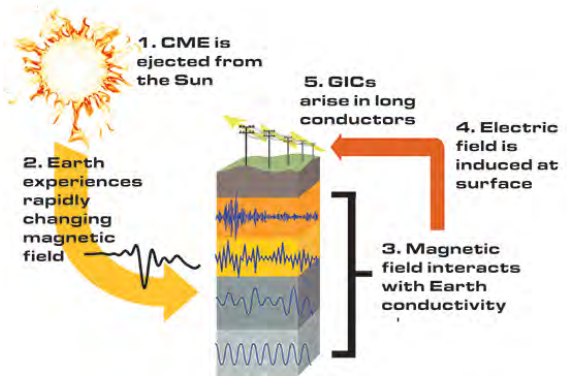

Figure 1: GMD storm interaction with Earth and Transmission lines (Koen and Gaunt, 2002)

Geomagnetic disturbances can have a severe effect on man made equipment. Figure 2 below shows an example.

Figure 2: Examples of some worn out man made equipment.

Modelling and Calculation of Geomagnetic Induced Currents

According to Pirjola (2002), we have two parts for carrying out the GIC modelling:

- Determination of the horizontal geoelectric field at the Earth's surface ("geophysical part").
- Computation of GIC in the network produced by the geoelectric field ("engineering part").

The computational part of GIC is given by:

$$I_{gic} = a\mathbf{E_x} + b\mathbf{E_y}, \tag{1}$$

where I_{gic} represents the GIC flowing through the substation, a and b are the substation parameters corresponding to the eastward electric field of 1 V/km and the GIC corresponding to the northward electric field of 1 V/km, respectively. $\mathbf{E_x}$ represents the electric field in the northward direction and $\mathbf{E_y}$ represents the electric field in the eastern direction.

The solution of the geophysical part is based on the following Maxwell's equations:

$$\nabla \cdot \mathbf{D} = \rho v \tag{2}$$

$$\nabla \cdot \mathbf{B} = 0 \tag{3}$$

$$\nabla \times \mathbf{E} = -\frac{\partial \mathbf{B}}{\partial t} \tag{4}$$

$$\nabla \times \mathbf{H} = \sigma \mathbf{E} + \frac{\partial \mathbf{D}}{\partial t} \tag{5}$$

Haar Wavelet Transform

The Haar transform decomposes a discrete signal into two subsignals of half its length.

The two subsignals are:

1. Running average (trends/approximation).

$$a_m = \frac{f_{2m-1} + f_{2m}}{\sqrt{2}} \tag{6}$$

2. Running difference (fluctuations/details).

$$d_m = \frac{f_{2m-1} - f_{2m}}{\sqrt{2}} \tag{7}$$

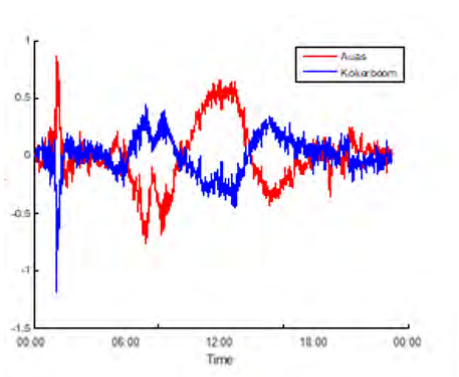

(a) Auas-Kokerboom GIC wavelet signals (July 2013)

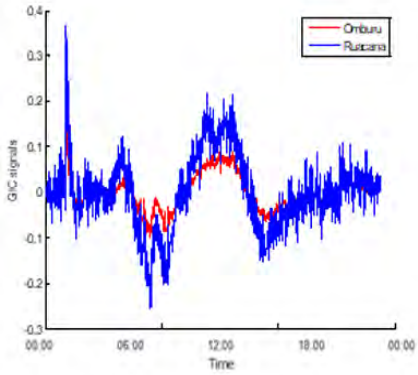

(b) Omburu-Ruacana GIC wavelet signals (July 2013)

Figure 3: Superposed GIC Haar wavelet signal profiles for the 24 July 2013

Optimal control model for GMD

The optimal control model for minimising the energy of signals is given by:

$$\begin{aligned} Minimise\ G &= \int_{t_0}^{t_f} \Big(\sum_{k=-\infty}^{\infty} \Big| \int_{-\infty}^{\infty} (a\mathbf{E}_x + b\mathbf{E}_y)\phi_k(t)dt \Big|^2 \\ &+ \sum_{k=-\infty}^{\infty} \sum_{j=0}^{\infty} \Big| \int_{-\infty}^{\infty} (a\mathbf{E}_x + b\mathbf{E}_y)\psi_{j,k}(t)dt \Big|^2 + u^2 \Big) dt \end{aligned} \tag{8}$$

subject to

$$\left.\begin{aligned} \frac{\partial^2 \mathbf{E_x}}{\partial t^2} + \frac{\partial^2 \mathbf{E_y}}{\partial t^2} = \frac{1}{\mu_0 \varepsilon_0} \Big[\frac{\partial^2 \mathbf{E_x}}{\partial x^2} + \frac{\partial^2 \mathbf{E_y}}{\partial y^2} - u(t) \Big] \\ \mathbf{E}_x(0) = \mathbf{E}_y(0) = \mathbf{E'}_x(0) = \mathbf{E'}_y(0) = \mathbf{E}_0 \end{aligned}\right\} \tag{9}$$

where $\phi_k(t)$ and $\psi_{j,k}(t)$ are the scaling(trends) and wavelet(fluctuations) functions, respectively, and u is the control.

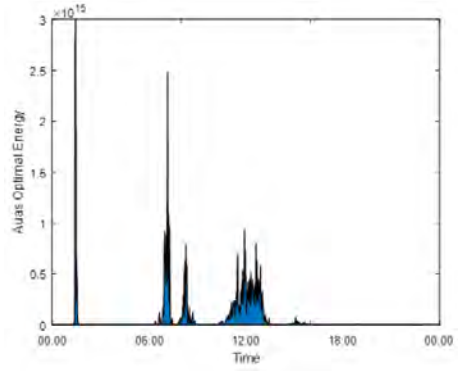

(a) 24 July 2013

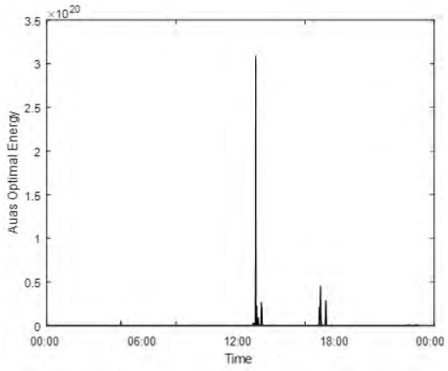

(b) 17 March 2015

Figure 4: Auas Optimal GIC Energy

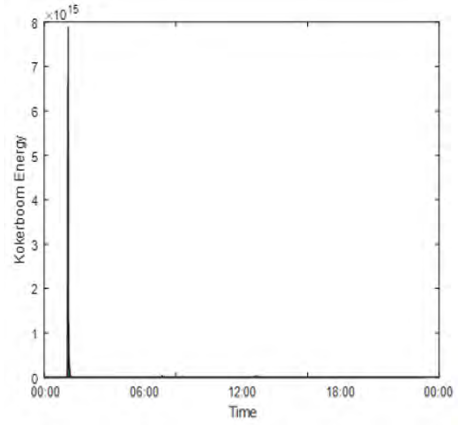

(a) 24 July 2013

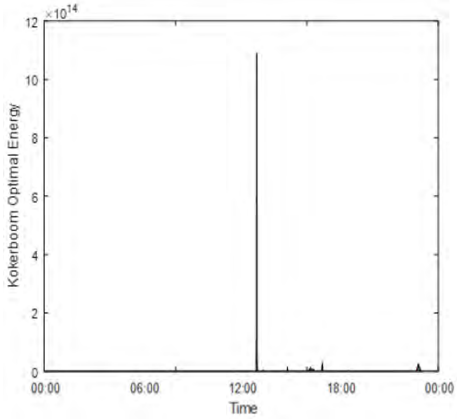

(b) 17 March 2015

Figure 5: Kokerboom Optimal GIC Energy

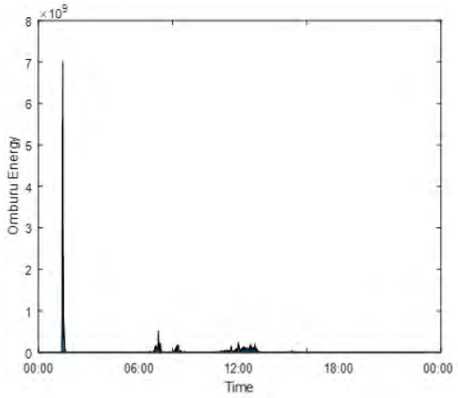

(a) 24 July 2013

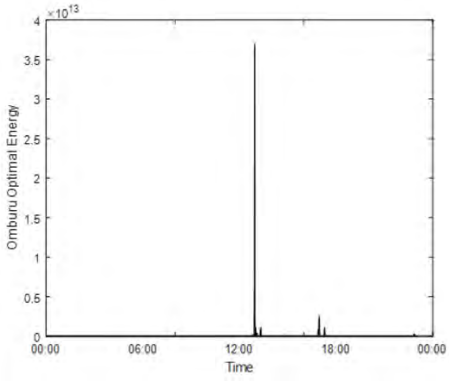

(b) 17 March 2015

Figure 6: Omburu Optimal GIC Energy

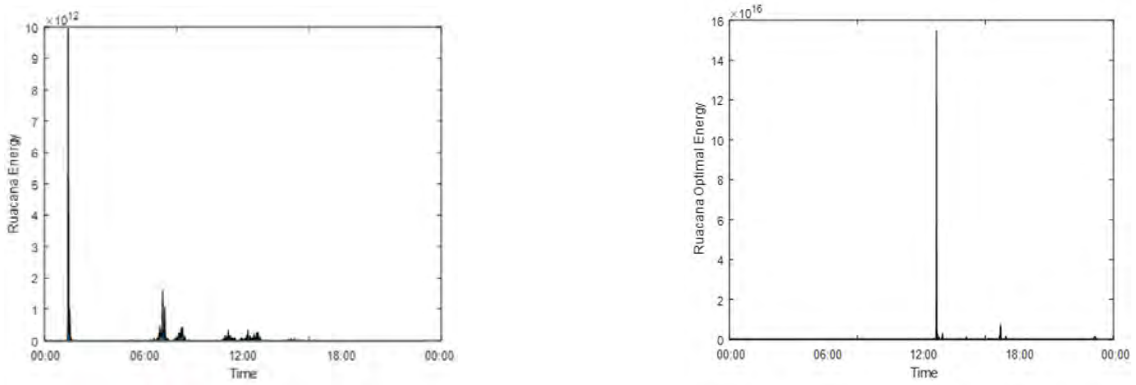

(a) 24 July 2013 (b) 17 March 2015

Figure 7: Ruacana Optimal GIC Energy

Conclusions

- From the optimal solutions for the stations, period of the day that requires special GIC monitoring appears to be during the morning hours and especially around the mid-day for the two solar events studied,
- Among the four stations, Omburu had the minimum GIC in 2013, followed by Ruacana.
- For the Auas-Kokerboom power line, Auas maximum GIC was less than that of Kokerboon (the latter experiencing the maximum GIC among all the four stations in 2013, occurring around the mid-night).
- In 2015, however, Omburu had the minimum GIC, followed by Kokerboom.
- For the Auas-Kokerboom power line, Kokerboom maximum GIC was less than that of Auas (the former experiencing the maximum GIC among all four stations in 2015, occurring around the mid-day).

References

Koen, J. and Gaunt, T. (2002). *Geomagnetically induced currents in the Southern African electricity transmission network*. PhD thesis, Citeseer.

Lee (1997). Solar flare occurrence rate and probability in terms of the sunspot classification supplemented with sunspot area and its changes. *Solar Physics*, 281(2):639–650.

Pirjola, R. (2002). Review on the calculation of surface electric and magnetic fields and of geomagnetically induced currents in ground-based technological systems. *Surveys in geophysics*, 23(1):71–90.

Optimal Inventory Policies for Pricing, Promotional efforts, and Preservation for Deteriorating Items with Price-Dependent Stochastic Demand

Mamta Keswani* and Dr.U.K.Khedlekhar†
Department of Mathematics and Statistics
Dr. H.S. Gour Central University, Sagar
M.P. - 470003, India

Abstract

In the present study, we design an inventory model for deteriorating items with partial backlogging wherein demand is stochastic in nature and a bivariate function of price and time. We incorporated promotional efforts in the model to promote business activities in declining market demand. We formulated a mathematical model with the objective to maximize expected profit by determining the optimal selling price and the optimal replenishment schedule. Some useful theoretical results are established to deduce the optimality of decision variables. To illustrate the proposed model two numerical examples have been solved. Further, a numerical example has been extended to perform a sensitivity analysis of the model and discuss specific managerial insights for inventory managers.

Keywords: Deterioration; Preservation; Promotional Efforts; Stochastic Demand.

1. Literature Review

∗ Numerous researchers have developed models for joint pricing, promotion, and inventory control, including Zhang (2008), He *et al.* (2009), De and Sana (2013), and Dash (2014). Maihami and Karimi (2014) devised an inventory model for determining the optimal pricing policy for non-instantaneous deteriorating items with

*E-mail: mamtakeswani01@gmail.com
†E-mail: sudhanshu_tomar@yahoo.com

promotional efforts, considering price-sensitive demand, which is stochastic, and shortages were assumed to be partially backlogged.

* Commonly, uncertainty in demand is considered probabilistic or stochastic demand. Stochastic demand is defined as $D(p, \varepsilon) = d(p) + \varepsilon$ in the additive case and $D(p, \varepsilon) = d(p).\varepsilon$ in the multiplicative case, where $d(p)$ is a deterministic decreasing or increasing function that captures the relationship between demand and price, and ε is a random variable (Soni and Chauhan 2018). For example, Dada (2007) developed the stochastic demand in the newsvendor model to account for many unrealistic assumptions.

2. Research Gap and Objectives

* After reviewing the literature of inventory management, we get results which shows demand is deterministic, but in realistic situations the demand is not certain.

* And the other major concern is that every research assumed that the life expectancy of all items is same which emerges the concept of deterioration, we study the nature of deteriorating items with Stochastic Demand.

* To the best of our knowledge, we have not found any academic research that considered demand is uncertain.

* The study jointly analyses the effect of deterioration in the life cycle of different items and optimal preservation investments.

* Further, we investigate no one could jointly find the optimality of these factors, such as stochastic demand, deterioration, preservation technology, and promotional efforts.

Research Objectives

The objectives of the current work are: In the research work offered, the researcher will develop mathematical models in the following areas:

* Stochastic demand,

* Deterioration,

* Preservation Technology,

* Marketing Efforts,

* Production Problem,

* Shortages with a Suitable Backlog Rate Effect,

* Green Investment (to reduce greenhouse gas emissions).

This study will find the facts and opinions on the inventory management process and principles. It will also give brief information about the inventory management and business goals of the retail units. Our main objectives are to find the following points:

* To make systems more efficient and reliable,
* To design modern systems to attain optimum usage,
* To determine the best pricing methods for perishable products that optimises the total profit,
* Find out the optimal sales price of a product when it depends on the time,
* To provide suggestions to improve the inventory optimization discussion with suitable parameters,
* To develop an analysis of the model with deterioration, stochastic demand, and supply will be treated as price-dependent variables.

Assumption of the Model

The proposed mathematical model of inventory replenishment problem is developed under the following assumptions and notations.

- The order size is finite, but the replenishment rate is limitless.
- The basic demand function is $(D(p)+\varepsilon)$, where $D(p)$ is a declining and deterministic function of the selling price, p, and e is a non-negative and continuous random variable,$E(\varepsilon) = \mu$.
- The expense of promotional efforts $PC = K(\rho-1)^2[\int_0^1 (D(p)+\varepsilon)dt]^\alpha$, where $K > 0$ and α is a constant, is an increasing function of promotional effort and basic demand. As the promotional effort increases, so will market demand and the cost of the promotional effort.
- The demand function is influenced by promotional effort ξ and can be expressed by mark-up over the promotional effort,i.e., $\rho(D(p) + \varepsilon)$
- The item deteriorates at a $\theta(t)$ rate of deterioration, where $0 < \theta(t) < 1$ Furthermore, deteriorating units are not repaired or replaced during the replenishment cycle.
- The proportion of reduced deterioration rate, $m(\xi)$ is a continuous, concave, and increasing function of capital investment.
- There is no need to be concerned about shortages. The inventory model starts with scarcity and finishes with a stockpile of nothing. During a stock-out situation, a portion of demand is back-ordered, and the rest is partially backlogged.

Variables in Decision-Making and parameters

t_1 : The point of replenishment; the length of the shortage period is [0,t_1].

t_2 : The amount of time it takes for inventory to reach zero.

p : The price per unit for which a product is being sold.

ξ : The cost of preservation technique per unit.

A : The cost of ordering per order.

C : The cost of purchasing per unit.

C_h : The cost of retaining a unit for a given period of time.

C_b : The cost of a backorder per unit of time.

C_1 : The per-unit cost of lost sales.

ε : Non-negative and continuous random variable with $E(\varepsilon)=\mu$.

ρ : The public relations effort, $\rho \geq 1$.

w : The maximum amount of money can be put into preservation technology.

Q : The ordering quantity per cycle.

$I_n(t)$: Negative inventory level at time t, where $0 \leq t \leq t_1$

$I_p(t)$: Positive inventory level at time t, where $t_1 \leq t \leq t_1 + t_2$

$m(\xi)$: Reduced deterioration rate as a percentage $0 \leq m(\xi) \leq 1$

Π_A : The optimal total profit per unit time for the inventory system.

3. Mathematical Modelling and Analysis

- The inventory model, which starts with a shortage, is the subject of this investigation. Partially backlogged shortages begin to build up during $[0, t_1]$.
- At the first replenishment point t_1, the backlogged demand is fulfilled, and the rest of the lot size adjusts demand until time t_2. A figure depicts the depletion of the inventory.

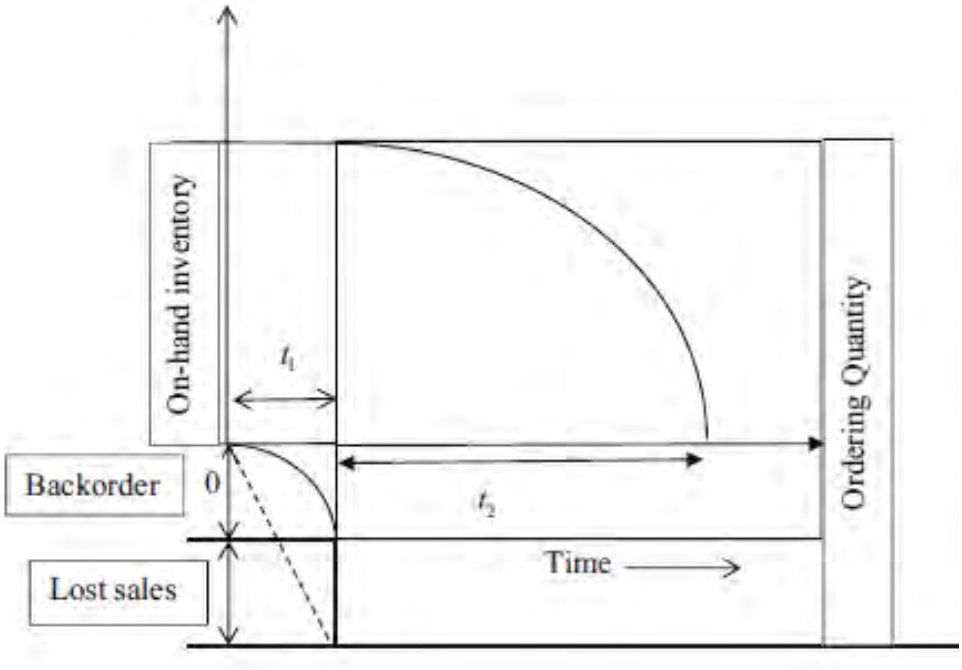

Figure 1: Graphical representation of inventory system.

- During the time span $[t_1, t_2]$, the combined impacts of demand and deterioration. Preservation technology helps to reduce deterioration. As mentioned previously, this process is repeated.

Analysis of phase type queueing system with startup times and single vacation

[1]G. Ayyappan, [2]K. Thilagavathy
[1]Department of Mathematics, Puducherry Technological University, Puducherry, India.
[2]Department of Mathematics, Hindustan Institute of Technology and Science, Chennai, India
Email: [1]ayyappanpec@hotmail.com, [2]thilagakarthik95@gmail.com

Corresponding author: K. Thilagavathy
Corresponding author ORCID iD: 0000-0002-2583-8219

Abstract

In this paper, we examine a single server queueing model in which customers arrive based on the Markovian Arrival Process (MAP) and their corresponding service process is based on phase-type (PH) distribution. When the service completion epoch, the server goes on vacation. Then, after completion of vacation who return to the system and will do the startup process for offering service whether the customer is present in the system or not. If any customer is available in the system will get service immediately otherwise the service will be idle until the customer arrives at the system. The model is solved in steady-state using Matrix-Analytic Method (MAM). We have established the stability condition for the model. Some important performance measures of the system have been presented. Further, the busy period analysis of the model is discussed.

Keywords: MAP, PH-Distribution, Startup time, phase-type vacation, Matrix analytic method.

AMS Subject Classification (2010): 60K25, 68M20, 90B22.

1 The Model Description

In this model, we consider a server queueing model in which customer's arrival follows the Markovian arrival process with representation (D_0, D_1) of order m in which the matrix D_0 denotes there is no customer arrive to the system and the matrix D_1 denotes customer arrives to the system. The service for the arriving customers follows phase-type distribution with representation (α, T) of order n. When the service completion epoch to the customers, the server will go on vacation which follows phase-type distribution with representation (β, S) of order l. Return from vacation, the server will do the startup process before initiate the service process which will definitely do whether the customer present in the system or not. If customers available in the system when startup process completion epoch, immediately the waiting customers will receive service or else if there is no customers present in the system, the server will remain idle in the system up to the customer's arrive to the system. The startup times follows an exponential distribution with parameter γ.

2 Notations for Generator Matrix

In this section, we describe the notations of the model for the sake of generating the quasi-birth-and-death process as follows:.

- $N(t)$ indicates the number of customers in the system.
- $S(t)$ indicates the status of the server, where

$$V(t) = \begin{cases} 0, & \text{if the server is avail on vacation under phase-type} \\ 1, & \text{if the server is doing the startup process} \\ 2, & \text{if the server is being an idle state} \\ 3, & \text{if the server offering service under phase-type} \end{cases}$$

- $V(t)$ indicates the server's vacation considered under phase-type.
- $J(t)$ indicates the service process considered under phase-type.
- $M(t)$ indicates the arrival process considered under Markovian arrival process.
- Let $\{(N(t), S(t), V(t), J(t), M(t)) : t \geq 0\}$ is the continuous time Markov chain with the quasi-birth-and-death process such that the corresponding state-space is as follows:

$$\Omega = l(0) \cup l(p)$$

where
$l(0) = \{(0,0,r_1,s) : 0 \leq r_1 \leq l;\ 1 \leq s \leq m\} \cup \{(0,q,s) : q = 1,2;\ 1 \leq s \leq m\}$

for $p \geq 1$,

$l(p) = \{(p,0,r_1,s) : 1 \leq r_1 \leq n;\ 1 \leq s \leq m\} \cup \{(p,1,s) : 1 \leq s \leq m\}$
$\cup \{(p,3,r_2,s) : 1 \leq r_2 \leq n;\ 1 \leq s \leq m\}$

3 The Matrix Generation

The infinitesimal generator matrix of the QBD process is provided by,

$$Q = \begin{bmatrix} B_{00} & B_{01} & \mathbf{0} & \mathbf{0} & \mathbf{0} & \mathbf{0} & \cdots & \cdots \\ B_{10} & A_1 & A_0 & \mathbf{0} & \mathbf{0} & \mathbf{0} & \cdots & \cdots \\ \mathbf{0} & A_2 & A_1 & A_0 & \mathbf{0} & \mathbf{0} & \cdots & \cdots \\ \mathbf{0} & \mathbf{0} & A_2 & A_1 & A_0 & \mathbf{0} & \cdots & \cdots \\ \vdots & \vdots & \vdots & \ddots & \ddots & \ddots & & \vdots \\ \vdots & \vdots & \vdots & & \ddots & \ddots & \ddots & \vdots \end{bmatrix}$$

The block matrices of the above mentioned Q are described as follows:

$$B_{00} = \begin{bmatrix} S \oplus D_0 & S^0 \otimes I_m & \mathbf{0} \\ \mathbf{0} & D_0 - \gamma I_m & \gamma I_m \\ \mathbf{0} & \mathbf{0} & D_0 \end{bmatrix}, \quad B_{01} = \begin{bmatrix} I_l \otimes D_1 & \mathbf{0} & \mathbf{0} \\ \mathbf{0} & D_1 & \mathbf{0} \\ \mathbf{0} & \mathbf{0} & \alpha \otimes D_1 \end{bmatrix},$$

$$B_{10} = \begin{bmatrix} \mathbf{0} & \mathbf{0} & \mathbf{0} \\ \mathbf{0} & \mathbf{0} & \mathbf{0} \\ T^0 \otimes \beta & \mathbf{0} & \mathbf{0} \end{bmatrix}, \quad A_1 = \begin{bmatrix} S \oplus D_0 & S^0 \otimes I_m & \mathbf{0} \\ \mathbf{0} & D_0 - \gamma I_m & \alpha \otimes \gamma I_m \\ \mathbf{0} & \mathbf{0} & T \oplus D_0 \end{bmatrix},$$

$$A_2 = \begin{bmatrix} \mathbf{0} & \mathbf{0} & \mathbf{0} \\ \mathbf{0} & \mathbf{0} & \mathbf{0} \\ \mathbf{0} & \mathbf{0} & T^0\alpha \otimes I_m \end{bmatrix}, \quad A_0 = \begin{bmatrix} I_l \otimes D_1 & \mathbf{0} & \mathbf{0} \\ \mathbf{0} & D_1 & \mathbf{0} \\ \mathbf{0} & \mathbf{0} & I_n \otimes D_1 \end{bmatrix}.$$

4 Condition for Stableness

We examine our model under certain conditions to ensure whether the system is stable.

4.1 Stability Condition

Let us consider the variable A is defined as $A = A_0 + A_1 + A_2$. It shows that the order of the square matrix A of order is $(lm + m + nm)$ and it is an irreducible infinitesimal generator matrix. Let $\boldsymbol{\zeta}$ denote the steady-state probability vector of the matrix A must satisfying the conditions $\boldsymbol{\zeta}A = 0$ and $\boldsymbol{\zeta}e = 1$. Then the vector $\boldsymbol{\zeta}$ is subdivided by $\boldsymbol{\zeta} = (\zeta_0,\ \zeta_1,\ \zeta_2)$, where ζ_0 is of dimension $lm + 2m$, $\zeta_1,\ \zeta_2,\ \zeta_3$,... are of dimension $lm + m + nm$. The Markov process has the quasi-birth-and-death structure. The stability of the model must satisfy the condition $\boldsymbol{\zeta}A_0e < \boldsymbol{\zeta}A_2e$, which is both the necessary and sufficient condition of quasi-birth-and-death process. Thus, the vector $\boldsymbol{\zeta}$ is acquired by evaluating the following expressions.

$\zeta_0[S \oplus D] = 0.$
$\zeta_0[S^0 \otimes I_m] + \zeta_1[D - \gamma I_m] = 0.$
$\zeta_1[\alpha \otimes \gamma I_m] + \zeta_2[(T + T^0\alpha) \oplus D] = 0.$
subject to normalizing condition

$\zeta_0 e_{lm} + \zeta_1 e_m + \zeta_2 e_{nm} = 1.$

After some algebraic computation, the stability condition of the model $\boldsymbol{\zeta}A_0\mathrm{e} < \boldsymbol{\zeta}A_2\mathrm{e}$ which is turns to be

$$\{\zeta_0[e_l \otimes D_1 e_m] + \zeta_1[D_1 e_m] + \zeta_2[e_n \otimes D_1 e_m]\} < \{\zeta_2[T^0 \otimes_m]\}$$

4.2 Steady-state Probability Vector Analysis

Let the variable $\mathbf{x}$ denote the steady-state probability vector of the quasi-birth-and-death matrix Q and it is subdivided as $\mathbf{x} = (\mathbf{x}_0,\ \mathbf{x}_1,\ \mathbf{x}_2,...)$. Note that

$\mathbf{x}_0$ is of dimension $(lm + 2m)$, $\mathbf{x}_1, \mathbf{x}_2, \mathbf{x}_3, ...$ are of dimension $(lm + m + nm)$. Then, the vector $\mathbf{x}$ satisfies the condition $\mathbf{x}Q = 0$ and $\mathbf{x}e = 1$.

Nonetheless, the stability condition is satisfied and the sub-vectors of $\mathbf{x}$ exclude for $\mathbf{x}_0$ and $\mathbf{x}_1$ corresponds to the different level states are given by the following equations,

$$\mathbf{x}_j = \mathbf{x}_1 \ R^{j-1}, \ \ j \geqslant 2.$$

where the rate matrix R indicates the minimal non-negative solution of the matrix quadratic equation as $R^2A_2 + RA_1 + A_0 = 0$. Thus the queueing system is stable and the rate matrix R of order $(lm + m + nm)$ which is obtained from the quadratic equation and also satisfy the condition $RA_2e = A_0e$.

The sub-vectors of $\mathbf{x}_0$ and $\mathbf{x}_1$ are obtained by solving the following equations:

$$\mathbf{x}_0B_{00} + \mathbf{x}_1B_{10} = 0,$$
$$\mathbf{x}_0B_{01} + \mathbf{x}_1(A_1 + RA_2) = 0.$$

The normalizing condition is subjected to

$$\mathbf{x}_0e + \mathbf{x}_1(I - R)^{-1}e = 1.$$

Therefore, the R matrix can be obtained mathematically using the required steps involving in the iteration method.

5 Busy Period Analysis

- The time interval between the customer's arrival to an null system and the after first epoch, the system becomes once again empty is referred to as a busy period. As a result, it signifies the beginning of the transition from level 1 to level 0. After visiting at least one other level, the busy cycle characterises the first time they return to level 0.

- We begin with a brief overview of the fundamental period before moving on to the busy period. It would be the first passage time from the level j to level $j-1, j \geqslant 2$ when the quasi-birth-and-death process is taken into account.

- Individually, the instances $j = 0, 1$ corresponds to the boundary states must be discussed. It's worth noting that $(lm + m + nm)$ states correspond to each and every level j, $j \geqslant 1$. When the states are arranged in lexicographic order, the state (j, k) of level j denotes the k^{th} state of level j.

- In this case, let $G_{kk'}(u, \mathrm{x})$ represent the conditional probability that the quasi-birth-and-death process visits the level $j-1$ in order to make changes to u transitions to the left and moreover enters the state (j, k'), with the constraint that it starts up in the state (j, k) at epoch $t = 0$.

To begin, let us define the notion of the joint transform

$$\text{“}\widetilde{G}_{kk'}(z,s) = \sum_{u=1}^{\infty} z^u \int_0^{\infty} e^{-s\mathrm{x}} dG_{kk'}(u,\mathrm{x}) \quad ;\mid z \mid \leq 1, Re(s) \geq 0\text{”}$$

and the matrix is indicated as $\widetilde{G}(z,s) = \widetilde{G}_{kk'}(z,s)$ then the above-mentioned matrix $\widetilde{G}(z,s)$ which fulfils the equation

$$\text{“}\widetilde{G}(z,s) = z(sI - A_1)^{-1}A_2 + (sI - A_1)^{-1}A_0\widetilde{G}^2(z,s)\text{”}.$$

✠ The matrix of $G = G_{kk'} = \widetilde{G}(1,0)$ could be taken for the first passage time, except for the boundary states. Suppose, we already know the matrix R then one could find the matrix G utilising the following result

$$G = -(A_1 + RA_2)^{-1}A_2$$

Otherwise, one can utilise the notion of logarithmic reduction algorithm to determine the values of the G matrix.

References

[1] Ayyappan G, Karpagam S (2018) An $M^{[X]}/G(a,b)/1$ Queueing System with Breakdown and Repair, Stand-By Server, Multiple Vacation and Control Policy on Request for Re-Service. Mathematics 6:1-18. DOI: 10.3390/math6060101

[2] Rakesh Kumar, Bhupender Kumar Som (2015): A Finite Capacity Single Server Queuing System with Reverse Reneging, *American Journal of Operational Research*, Vol. 5, No. 5, pp. 125-128.

[3] Rakesh Kumar, Sapana Sharma (2019): Transient analysis of an M/M/c queuing system with retention of reneging customers, *International Journal of Operational Research*, Vol. 36, No. 1, pp. 78-91.

[4] Yang,T., Templeton, J.G.C. (1987): A Survey on Retrial Queues, *Queueing Systems*, Vol. 2, pp. 201-233.

[5] Yang, D-Y., Wu, C-H. (2019): Performance analysis and optimization of a retrial queue with working vacations and starting failures, *Mathematical and Computer Modelling of Dynamical Systems*, pp. 1-19.

[6] Neuts MF (1994) Matrix-Geometric solutions in Stochastic Models - An Algorithmic Approach. 2nd ed., Dover Publications Inc., New york.

[7] Senthamarai Kannan K, Jabarali A (2014) Parameter Estimation of Single Server Queue with Working Vacations, Research & Reviews: Journal of Statistics, Special Issue on Recent Statistical Methodologies and Applications. 2:94-98

A BAYESIAN STUDY OF A TWO NON-IDENTICAL UNIT COLD STANDBY SYSTEM WITH PREPARATION FOR REPAIR AND CORRELATED FAILURE AND REPAIR TIMES

Vashali Saxena, Rakesh Gupta*, Prof. Bhupendra Singh
[1] Departmet of Statistics,
Chaudhary Charan Singh University, Meerut-250004, India
Vaishalistat412@gmail.com; *smprgccsu@gmail.com; bhupendra.rana@gmail.com

Abstract

The system comprises of two non- identical unit (unit-1 and unit-2). Unit-1 gets priority in operation over the unit-2 so system initially starts functioning the operation of unit-1 and unit-2 is kept as cold standby. Each unit has two possible modes- Normal (N) and total failure (F). Upon failure of a unit it is sent for preparation before starting its repair. A single repairman is always available with the system for the preparation of a failed unit for repair and to perform the repair. Unit-1 gets priority for preparation and for repair of a failed unit over the unit-2. The preparation time follows exponential distribution with different parameters for both the units. The failure and repair times of each unit are correlated random variables having their Joint distribution as Bivariate exponential with different parameters for unit-1 and unit-2. Each repaired unit work as good as new. The maximum likelihood approach and Markov chain Monte Carlo techniques, respectively, are used to estimate the unknown parameters that are utilised to assess the measure of system effectiveness, such as the MTSF and Profit function of the composite system. Gamma priors have been utilised in the Bayesian approach to produce Bayes estimates of unknown parameters under squared error loss functions. The Fisher informational matrix and Bayesian approach are used to derive the interval estimates of the baseline reliability function

Keywords: Mean sojourn time, MTSF, availability, expected busy period of repairman, net expected profit, Bayesian estimation, highest posterior density intervals, Maximum likelihood estimation.

Introduction

The goal of this study is to create a methodology for reliability-based design optimization for series systems and a fresh approach for cutting costs associated with computation. Engineers encounter new difficulties in the highly competitive market of today because of the complexity of new technology applications and design. The likelihood that a system or product will carry out its intended function for the predetermined amount of time can be referred to as reliability.

Numerous researchers have thoroughly investigated the stochastic behaviour of two non-identical unit system models in previous scholarly works. Several authors including Chaudhary (2018) & Gupta (2018) have explored the system model, which comprises two non-identical units arranged in a distinct configuration while considering different assumptions. The above authors have assumed that a totally failed unit immediately enters into repair facility for its maintenance. In real situations, it has been observed so many times that a failed unit needs some preparation time before starting in repair.

So using the concept of preparation time, authors including Gupta (2013) & Gupta (2019) analysed that the stochastic behaviour of a two-identical/ non-identical unit cold standby system model assuming that a totally failed unit needs some preparation work before going into repair and after completion of preparation, the unit is sent for repair. The failure and repair times of the units are treated as uncorrelated random variables in all of the aforementioned system models. Yet, it has been found that in many real-world scenarios, the system is present when there is some form of link between

the failure and repair times of the system's units. By applying the concept of correlation, researchers, as referenced in Tyagi (2015) & Chaudhary (2022) have examined the analysis of a system model comprising two non-identical or identical units, where there exists a correlation between the failure and repair times of the units.

To integrate prior knowledge into the analysis and explore the behaviour of repairable systems under different assumptions, several researchers have utilized the Bayesian technique in their studies. In the realm of reliability theory, various authors, such as those mentioned in references Gupta (2018), Patawa (2022) & Yadavalli (2022a, 2022b) have analyzed redundant system models consisting of two units. They have examined Bayesian concepts such as asymptotic confidence limits for the steady state availability of a two-unit parallel system, patience time, and waiting facility.

So far no work has been done regarding the concept of Bayesian study in the system of correlated failure and repairs. Using various priors for the parameters, a two non-identical component system with associated failure and repairs is evaluated from a Bayesian perspective in this study. It is expected that previous knowledge about the model's parameters exists and can be computationally converted into suitable prior distributions based on prior experience with dependability data of a similar nature.

This study adds some more important results to the study of two non-identical unit with correlated failure and repair times repairable system model under classical and Bayesian estimation technique. The objective of this research is to investigate and compare the classical and Bayesian approaches for modeling and analyzing the reliability of such systems. The joint distributions of failure and repair times of each unit are taken to be bivariate exponential with p.d.f. of the type-

$$f(x,y) = \alpha\beta(1-r)\, e^{-(\alpha x+\beta y)} I_0\left(2\sqrt{\alpha\beta r x y}\right); \alpha,\beta,x,y>0; \quad 0 \le r < 1$$

where,

$$I_0(z) = \sum_{k=0}^{\infty} \frac{\left({}^{z}/_{2}\right)^{2k}}{(k!)^2}$$

is the modified Bessel function of type-I and order zero.

Using these state probabilities, explicit formulations for the following reliability and performance measurement have been constructed:

1. The probabilities of the system being in various state at an epoch t.
2. Reliability and MTSF
3. Point wise and steady state availabilities
4. Expected uptime of the system and expected busy period of repairman during (0,t)
5. Net expected profit gain by the system during (0, t) and in steady state
6. Estimation of Parameters, MTSF and Profit Function by Classical estimation and Bayesian estimation.

Assumption:

1. The system comprises of two non- identical unit (unit-1 and unit-2). Unit-1 gets priority in operation over the unit-2 so system initially starts functioning the operation of unit-1 and unit-2 is kept as cold standby.
2. Each unit has two possible modes- Normal (N) and total failure (F).
3. Upon failure of a unit it's sent for preparation before starting its repair.
4. A single repairman is always available with the system for the preparation of a failed unit for repair and to perform the repair.
5. Unit-1 gets priority for preparation and for repair of a failed unit over the unit-2.
6. The preparation time follows exponential distribution with different parameters for both the units.

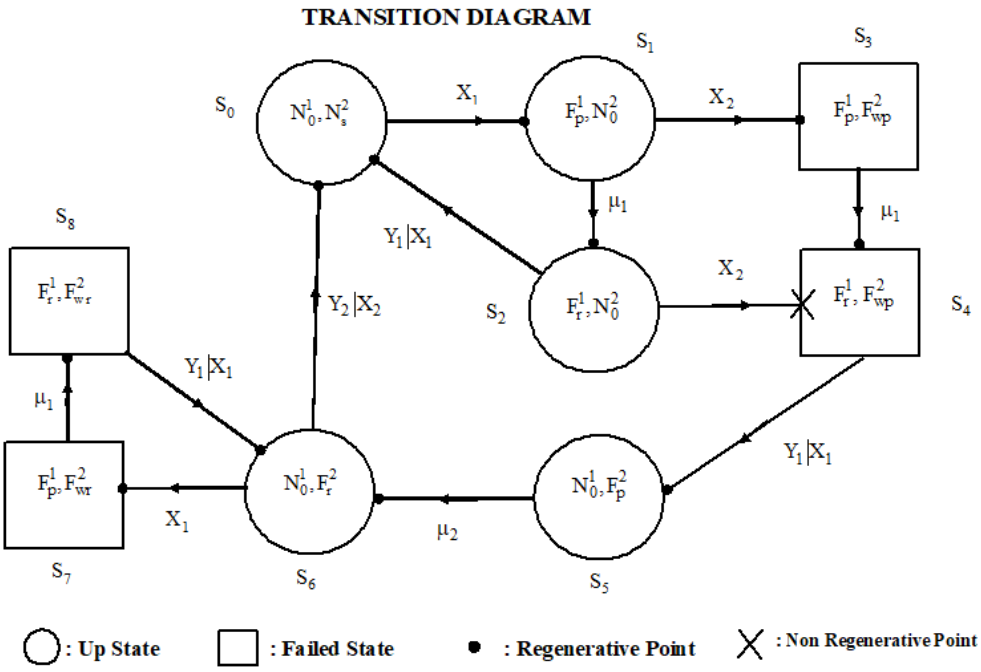

7. The failure and repair times of each unit are correlated random variables having their Joint distribution as Bivariate exponential with different parameters for unit-1 and unit-2.

8. Each repaired unit work as good as new.

Considering the above symbols in view of assumptions stated in section 2, the possible states of the system are shown in the transition diagram represented by Fig. 1. It is to be note that the epoch of transition into the state S_2 from S_5 is non-regenerative, whereas all the other entrance epochs into the states of the systems are regenerative.

To conduct a comparative evaluation of the two approaches, we undertake a two-unit cold standby system comprising non-identical components. We employ both the classical and Bayesian approaches to estimate the system's MTSF and Profit function. The Bayesian framework facilitates more precise estimations by integrating supplementary information and accommodating diverse failure characteristics. The case study provides evidence of the superior performance of the Bayesian approach and underscores its practical significance in real-world reliability engineering applications. Additionally, the capability to update beliefs based on observed data enhances the predictive capacity of the Bayesian approach. Using the above assumption our goal is to find out Reliability, MTSF , availability, Busy period of repairman, and also find a classical and Bayesian approach for the case of that the parameters of MTSF and Profit function of the repairable system are unknown and have to be estimated from appropriate prior distribution. The MTSF and Profit function are also studied through graph in respect of parameter failure rate α_1 with different value on X axis, repair rate β_1 and correlation value r_2.

References

[1] Chaudhary, P., & Masih, S. (2018). A Two Identical Unit Parallel Systm With Two Phase Repair And Waiting Time of Repirman For Phase-I Repair. International Journal of Agricultural & Statistical Sciences, 14(2).

[2] Chaudhary, P., Masih, S., & Gupta, R. (2022). A Two Non-Identical Unit Parallel System with Repair and Post Repair Policies of a Failed Unit and Correlated Lifetimes. Reliability: Theory & Applications, 17(3 (69)), 40-51.

[3] Gupta, P., & Vinodiya, P. (2018). Analysis of reliability of a two non-identical units cold standby repairable system has two types of failure. International Journal of Computer Sciences and Engineering, 6(11), 907-913.

[4] Gupta, R., Chaudhary, A., Jaiswal, S., & Singh, B. (2018). Classical And Bayesian Analysis of A Two Identical Unit Standby System With Fault Detection, Minor And Major Repairs Under Geometric Distributions. International Journal of Agricultural & Statistical Sciences, 14(2).

[5] Gupta, R., & Bhardwaj, P. (2013). A two-unit standby system with two operative modes of the units and preparation time for repair. Journal of reliability and Statistical Studies, 87-100.

[6] Patawa, R., Pundir, P. S., Sigh, A. K., & Singh, A. (2022). Some inferences on reliability measures of two-non-identical units cold standby system waiting for repair. International Journal of System Assurance Engineering and Management, 1-17.

[7] Yadavalli, V. S. S., Botha, M., & Bekker, A. (2002). Asymptotic confidence limits for the steady state availability of a two-unit parallel system with'preparation time'for the repair facility. Asia-Pacific Journal of Operational Research, 19(2), 249.

[7] L. Takács, "On a stochastic process concerning some waiting time problems," *Theory of Probability & Its Applications*, vol. 2, no. 1, pp. 90–103, 1957.
[8] M. C. Delia and P. O. Rafael, "A maintenance model with failures and inspection following markovian arrival processes and two repair modes," *European Journal of Operational Research*, vol. 186, no. 2, pp. 694–707, 2008.
[9] S. Maheshwari, P. Sharma, and M. Jain, "Machine repair problem with k-type warm spares, multiple vacations for repairmen and reneging," *International Journal of Engineering and Technology*, vol. 2, no. 4, pp. 252–258, 2010.
[10] M. Jain, C. Shekhar, and S. Shukla, "A time-shared machine repair problem with mixed spares under n-policy," *Journal of Industrial Engineering International*, vol. 12, pp. 145–157, 2016.
[11] C. Shekhar, M. Jain, A. A. Raina, and J. Iqbal, "Optimal (n, f) policy for queue-dependent and time-sharing machining redundant system," *International Journal of Quality & Reliability Management*, 2017.
[12] M. Jain and R. K. Meena, "Vacation model for markov machine repair problem with two heterogeneous unreliable servers and threshold recovery," *Journal of Industrial Engineering International*, vol. 14, pp. 143–152, 2018.
[13] S. Gao, Z. Wang, *et al.*, "Sensitivity analysis for a redundant system with random inspection and repairmen under repair pressure," *Scientific Programming*, vol. 2023, 2023.

Optimal Analysis of a Sustainable Inventory Model for a Controllable Carbon Emission with Two Warehouse System and Hybrid Cash-Advance Payment

Ankur Saurav[*1], Vijender Yadav[2], and Chandra Shekhar[3]

[1,2,3]Department of Mathematics, Birla Institute of Technology and Science Pilani, Pilani Campus, Pilani, Rajasthan, 333 031 (India).
[1]ankuranuraag2013@gmail.com; [2]vijenderyadav9497@gmail.com; [3]chandrashekhar@pilani.bits-pilani.ac.in

Keywords:
Sustainable economic order quantity;
Hybrid cash-advance payment;
Two warehouse system;
Green technology;
Carbon emission.

Paper type:
Research Article

Abstract

Mitigating carbon emissions while pursuing economic goals is a primary concern for organizations in today global economy. Recent researches highlight the efficacy of investing in green technology to reduce carbon emissions associated with distinguished inventory activities. However, to ensure uninterrupted supply during periods of high demand and avoiding stock-out situations, organizations may adopt a warehouse-on-rent inventory system. Additionally, retailers have found an efficient cash flow in the form of an effective hybrid cash-advance payment policy with discounts, which stimulate demand also. Aim of the paper is to determine cycle time and ordered quantity in order to minimize total cost. To validate the Sustainable Economic Order Quantity $SEOQ$ model, several numerical examples are examined using the nature-inspired optimization technique: Teaching-Learning-Based Optimization $TLBO$. Finally, sensitivity analysis provides managerial implications by demonstrating the significant influence of key parameters on the optimal total cost in the proposed model.

1 Introduction

In terms of industrial growth and global competitiveness, uninterrupted, eco-efficient, and cost-efficient supply chain management is a vital and intriguing issues for every organization. The primary goal of analysis is optimal lot sizing and minimizing the total cost. From various inventory phases, the present world faces the major determinants of global warming due to carbon emission. In the literature on effective sustainable inventory management, several researchers focused on studying how various inventory systems responded to reduce carbon emissions associated with various economic and operational activities. Hovelaque and Bironneau (2015) conceptualized inventory model with emission and price dependent demand. Mishra et al. (2020) formulated an SEPQ model with controllable carbon emissions by investing in green technology via carbon cap & tax policies. Shi et al. (2020) and Sarkar et al.(2021) studied a carbon taxation policy for carbon emissions during various inventory phases. Mashud et al.(2021) examined the green and preservation technology investment to minimize carbon emissions and product deterioration. Lu et al. (2022) presented a global supply chain-based production-inventory model for perishable items under various carbon emission policy.

Also, to ensure incessant supply at high demand, organizations may adopt an on-rent multi-warehouse inventory system. In general, a retailer owns a limited-capacity warehouse, defined own warehouse OW. Stocks exceeding the OW capacity must be stored in a rented warehouse RW at additional rent cost, transportation cost, maintenance cost, etc that can be balanced with extra revenue and increased satisfactory demand supply. Many authors have studied two-warehouse inventory problem (Sett et al.(2012), Agrawal et al.(2013), Xu et al.(2017), Alamri and Syntetos(2018), Manna et al.(2021)). Rahman et al.(2022) formulated a two-warehouse inventory model for a perishable items under preservation technology.

Demand is an important factor in every inventory system. Normally, it is not constant and may fluctuate due to selling price, quality, time, advertisement, stock availability, etc. Sett et al. (2012) presented two-warehouse system with increasing demand function. San-Jose et al. (2018) developed an inventory model whose demand is a bivariate function of price and time. Later, San-Jose et al. (2021) studied an inventory problem associated with price, advertisement, and time dependent demand. Aarya et al. (2022) investigated the impact of selling price and time-dependent demand on two warehouse inventory system. The present study considers the price sensitive demand, as well as it is influenced with advertising frequency and timing. Additionally, retailers promotes an eco-efficient cash-flow in the form of an effective hybrid cash-advance payment with discounts, which entices more customers and boosts demand. In this facility, retailer provides partial payment of the purchase price before receiving the product by borrowing loan. Shi et al.(2020), Duary et al.(2022), and Alshanbari et al.(2022) formulated an inventory model for perishable items under advance payment arrangement with trade credit and mixed-cash, respectively.

Based on a comprehensive literature survey, we have identified research gaps in the field of inventory management and formulated the $SEOQ$ model. Our model focuses on perishable items stored in both owned and rented warehouses, considering varied cash-flow arrangements and policies. To promote sustainability, we have incorporated elements such as green technology, preservation technology, carbon cap and tax regulations. Additionally, we take into account factors such as advance payment options, credit policies, discount facilities, and loan provisions in our analysis. The demand for the perishable items is influenced by time, price, and advertisement, which are crucial factors in our inventory model. We determine the economic lot size through optimal analysis, aiming to minimize costs and improve overall performance.

2 Notations and Assumptions

In this section, the governing notations and assumptions have been provided to formulate the mathematical model of the studied sustainable inventory model with varied opportunities, challenges, and policies.

- Demand for the perishable items is function of advertisement (A), elasticity (γ), selling price (p), and time (t). It is mathematically expressed as

$$D(A,p,t) = A^{\gamma}(a - bp + ct), \text{ where } a, b, c, \gamma \geq 0.$$

*Corresponding author

- The time horizon of the inventory system is assumed to be infinite and lead time is constant.
- The item deteriorate with constant rate θ in both OW and RW warehouses.
- Shortages are allowed with partially backlogged due to lost sales, and is algebraically conceptualized as

$$B(t) = \delta, \text{ where } 0 \leq \delta \leq 1 \text{ is backlogging parameter.}$$

- The capacity of owned warehouse (OW) is F units. Since the holding cost of rented warehouse (RW) (C_{R1}) is higher compared to that of OW (C_{O1}), the customer's demand is fulfilled from RW first.
- The ordering cost K, unit purchase cost C_0, unit holding cost C_{R1} and C_{O1} for RW and OW respectively, unit shortage cost C_2, and advertisement cost C_3 are constant.
- Retailer pre-pay a portion $\beta(0 < \beta < 1)$ of the total purchase cost in advance at time $t = M$ and the remaining amount would be paid at the time of delivery. Moreover, retailer borrows money with interest rate of I_e. The supplier offers a discount d on total purchase cost at the time of delivery.
- The investment G in green technology is for long run and have positive impact on carbon regulation as it reduces the carbon emission by factor $\xi(1 - e^{-mG})$.
- If sum of carbon emission during ordering (k_1), holding (k_2 & k_3 for OW and RW respectively), and purchasing (k_4) exceeds the carbon cap Z, the tax is imposed with rate λ rupees per kilogram.

3 Mathematical Model

In this section, we describe the dynamic of inventory level (I) in one order cycle time T and derive the associated costs, cost incurred due to carbon emissions, and total cost for the proposed model. In time interval $[0, T_1]$, inventory of OW decreases due to deterioration while inventory of RW reduces due to combine effect of demand as well as deterioration. In time interval $[T_1, T_2]$, the demand of customer is satisfied by OW. So, corresponding inventory reduces due to both demand and deterioration. At time T_2, shortage starts and maximum allowed shortage is B. If $I_{R1}(t)$ represent the instantaneous inventory level of RW in time interval $[0, T_1]$; and if $I_1(t)$, $I_2(t)$, and $I_3(t)$ represent the inventory level of OW in time interval $[0, T_1]$, $[T_1, T_2]$, and $[T_2, T]$ respectively; then the rate of change in inventory at time t in $[0, T]$ is governed by the following differential equations

$$\frac{dI_{R1}(t)}{dt} + \theta I_{R1}(t) = -D, \qquad 0 \leq t \leq T_1 \tag{1}$$

$$\frac{dI_1(t)}{dt} + \theta I_1(t) = 0, \qquad 0 \leq t \leq T_1 \tag{2}$$

$$\frac{dI_2(t)}{dt} + \theta I_2(t) = -D, \qquad T_1 \leq t \leq T_2 \tag{3}$$

$$\frac{dI_3(t)}{dt} = -\delta D, \qquad T_2 \leq t \leq T \tag{4}$$

Using the initial conditions $I_{R1}(0) = S - F$, $I_{R1}(T_1) = 0$, $I_1(0) = F$, $I_2(T_2) = I_3(T_2) = 0$, and $I_3(T) = -B$ and solving the differential equations (1, 2, 3, and 4), the total quantity of items ordered in one ordered cycle is given by:

$$Q = A^{\gamma}\left[\frac{1}{\theta^2}\left(\{c - (a - bp)\theta\} - \{c - (a - bp + cT_2)\theta\}e^{\theta T_2}\right) + \frac{\delta}{2}\left(T\{2a - 2bp + cT\} - T_2\{2a - 2bp + cT_2\}\right)\right] \tag{5}$$

Each of the costs associated with ordering, purchasing, loan, holding, shortage, green technology, and emissions are shifted to the retailer under proposed inventory relationship. In light of this, the retailer's total cost per order cycle T, denoted byTCU, is ratio of total cost (TC) and order cycle T, where, the total cost (TC) is given by;

$$TC = \text{Ordering Cost}(OC) + \text{Purchasing Costs}(PC) + \text{Loan Cost}(LC) + \text{Holding Cost}(HC) + \text{Shortage Cost}(SC) + \text{Advertisement Cost}(AC) + \text{Carbon Emission Cost(Ordering, Holding \& Purchasing)}(CEC)$$

where, $OC = K$

$PC = C_0(1 - d)Q$

$LC = C_0 I_e M \beta Q$

$HC = \frac{1}{\theta^2}A^{\gamma}C_{R1}\left[T_1\{c - (a - bp + \frac{cT_1}{2})\theta\} + \frac{1}{\theta}(1 - e^{\theta T_1})\{c - (a - bp + cT_1)\theta\}\right] + \frac{1}{\theta^3}A^{\gamma}C_{O1}\left[(e^{\theta T_1} - 1)[\{c - (a - bp + cT_1)\theta\} - \{c - (a - bp + cT_2)\theta\}e^{\theta(T_2 - T_1)}] + \theta[\{c - \theta(a - bp)\}(T_2 - T_1) - \frac{1}{2}c\theta(T_2^2 - T_1^2)] + (1 - e^{\theta(T_2 - T_1)})\{c - (a - bp + cT_2)\theta\}\right]$

$SC = \frac{1}{2}C_2\delta A^{\gamma}\left[\{(a - bp)(T^2 - T_2^2) + \frac{c}{3}(T^3 - T_2^3)\} - T_2(T - T_2)(2a - 2bp + cT_2)\right]$

$AC = C_3 A$

$CEC = \lambda\left(-ZT + (1 - \xi(1 - e^{-mG}))\left(k_1 + \frac{1}{\theta^2}A^{\gamma}k_2\left[T_1\{c - (a - bp + \frac{cT_1}{2})\theta\} + \frac{1}{\theta}(1 - e^{\theta T_1})\{c - (a - bp + cT_1)\theta\}\right] + \frac{1}{\theta^3}A^{\gamma}k_3\left[(e^{\theta T_1} - 1)[\{c - (a - bp + cT_1)\theta\} - \{c - (a - bp + cT_2)\theta\}e^{\theta(T_2 - T_1)}] + \theta[\{c - \theta(a - bp)\}(T_2 - T_1) - \frac{1}{2}c\theta(T_2^2 - T_1^2)] + (1 - e^{\theta(T_2 - T_1)})\{c - (a - bp + cT_2)\theta\}\right] + k_4 Q\right)\right)$

Therefore, total cost per unit of time (TCU) is given by

$$TCU = \frac{TC}{T} \tag{6}$$

$$\therefore TCU = \frac{1}{T}\Bigg[K + C_0A^{\gamma}(1 + I_eM\beta - d)\Bigg[\frac{1}{\theta^2}\Big(\{c-(a-bp)\theta\} - \{c-(a-bp+cT_2)\theta\}e^{\theta T_2}\Big) + \frac{\delta}{2}\Big(T\{2a-2bp+cT\} - T_2\{2a-2bp+cT_2\}\Big)\Bigg] + \frac{1}{\theta^2}A^{\gamma}\Big(C_{R1} + \lambda k_2\Big(1-\xi(1-e^{-mG})\Big)\Big)\Bigg\{T_1\Big\{c-\Big(a-bp+\frac{cT_1}{2}\Big)\theta\Big\} + \frac{1}{\theta}(1-e^{\theta T_1})\Big\{c-(a-bp+cT_1)\theta\Big\}\Bigg\} + \frac{1}{\theta^3}A^{\gamma}\Big(C_{O1} + \lambda k_3\Big(1-\xi(1-e^{-mG})\Big)\Big)\Bigg\{(e^{\theta T_1}-1)\Big[\Big\{c-(a-bp+cT_1)\theta\Big\} - \Big\{c-(a-bp+cT_2)\theta\Big\}e^{\theta(T_2-T_1)}\Big] + \theta\Big[(T_2-T_1)\Big\{c-\theta(a-bp)\Big\} - \frac{1}{2}c\theta(T_2^2 - T_1^2)\Big] + (1-e^{\theta(T_2-T_1)})\{c-(a-bp+cT_2)\theta\}\Bigg\} + \frac{1}{2}C_2\delta A^{\gamma}\Big[\Big\{(a-bp)(T^2-T_2^2) + \frac{c}{3}(T^3-T_2^3)\Big\} - T_2(T-T_2)(2a-2bp+cT_2)\Big] + C_3A + \lambda\Big(-ZT + \Big(1-\xi(1-e^{-mG})\Big)\Big[k_1 + k_4\Big(A^{\gamma}\Big[\frac{1}{\theta^2}\Big(\{c-(a-bp)\theta\} - \{c-(a-bp+cT_2)\theta\}e^{\theta T_2}\Big) + \frac{\delta}{2}\Big(T\{2a-2bp+cT\} - T_2\{2a-2bp+cT_2\}\Big)\Big]\Big)\Big]\Big)\Bigg] \tag{7}$$

The objective is to minimize total cost per unit time of the retailer. So, the optimization problem is framed as

$$TCU(T_2^*, T^*) = \min TCU \quad \text{subject to} \quad T_2^* \le T^* \tag{8}$$

Since, the objective function TCU in Eq. (7) under constraint is too complex to solve via first-order derivatives. Therefore, to determine the optimal total cost $TCU(T_2^*, T^*)$, we opt the meta-heuristic optimization technique, teaching-learning-based optimization (TLBO).

4 Teaching-Learning-Based Optimization (TLBO)

TLBO is a population-based meta-heuristic optimization technique which imitates the classroom environment to optimize a given objective function. In TLBO, a student learn from both the teacher and learner phases. Therefore, TLBO algorithm has two phases.

Teacher Phase: (Students learn from the teacher and gain knowledge)
In the teacher phase, a new solution is generated with the help of the teacher (minimum fitness value). Let X_{mean} be the mean of the population. The TLBO algorithm suggests the following equation for generation of new solution:

$$X_{new} = X_{old} + r(X_{best} - T_f X_{mean}) \tag{9}$$

where T_f is the teaching factor and is either 1 or 2. If X_{new} is better than X_{old}. Then replace X_{old} with X_{new}.

Learner Phase: (Students learn from one another)
In the learner phase, randomly chosen a student from class, say, $X_{partner}$. Other students interact and exchange their knowledge. The following equation helps to generate the new solution for this phase:

$$X_{new} = X + r(X - X_{partner}), \tag{10}$$

where r is a random number between 0 and 1. Also, the partner student $X_{partner}$ has higher fitness than X.

5 Numerical Results

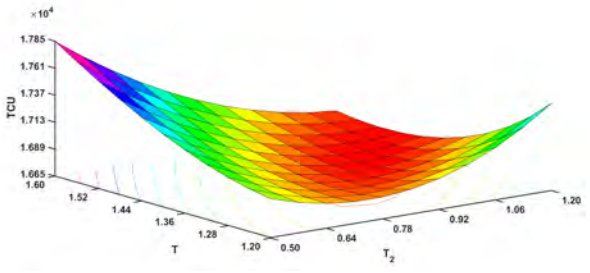

Figure 1: Surface graph of TCU w.r. to T_2 and T

The paper presents numerical results to validate the proposed inventory model. For numerical and graphical justification, we consider $a = 250, b = 0.5, c = 5, p = 300, A = 50, \gamma = 0.1, K = 1000, C_0 = 80, I_e = 0.08, M = 0.2, d = 0.11, \beta = 0.6, \theta = 0.15, \delta = 0.35, C_{R1} = 15, C_{O2} = 7, C_2 = 140, c_3 = 70, T_1 = 0.5, Z = 2000, \lambda = 0.3, \xi = 0.45, G = 150, m = 0.8, k_1 = 120, k_2 = 8, k_3 = 5, k_4 = 35$. Using the hypothetical values of all parameters and associated costs, we determine the numeric value of TCU from Eq. (7). The convexity of our objective function TCU for decision variables T_2 and T can be seen from surface graph shown in Fig 1.

To obtain the optimal value of our objective function, we opt teaching-learning-based optimization (TLBO) algorithm inspired by classroom learning environment. The feasible solution space is depicted as the contour of the total cost function TCU for T_2 and T in Fig. 2. For the implementation of TLBO, we consider 100 population size, 30 iteration and 16 runs. The iteration results are depicted in Fig. 2 - 3. Fig. 3 represents the convergence of the TLBO for multiple runs. After several iterations, the optimal values of $T_2^* = 1.1001$ and $T^* = 1.4161$. Also, the optimum order quantity Q^* is 226.38 units, and the optimal total cost per unit time $TCU(T_2^*, T^*)$ is Rs. 16905.2824 at $T_2^* = 1.1001$ and $T^* = 1.4161$ and corresponding economic lot size is $Q^* = 226.38$.

For elaborate study, we can perform a sensitivity analysis by changing values of major parameters. From sensitivity analysis, we can obtain in-depth insights for studied model.

6 Conclusions

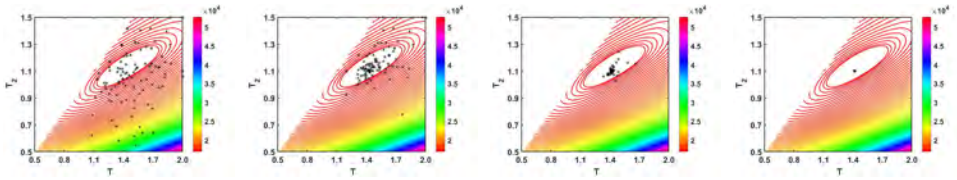

(a) Iteration=1 (b) Iteration=12 (c) Iteration=18 (d) Iteration=27

Figure 2: Several generations of TLBO algorithm on the contour of $TCU(T_2, T)$

We have done comprehensive study on a two warehouse sustainable inventory model and deals with non-instantaneous deteriorating items, hybrid cash-advance payment provision, and discount option. We consider demand of the item to be price sensitive and affected linearly by time and advertisement. To address the natural hazardous of carbon emission, consideration of green technology makes more realistic in the modeling of inventory control. The primary objective of our study is to optimize the total cost per unit time. We have presented numerical illustration of the studied model. Our research focuses on the applicability of this model to various perishable goods such as vegetables, fruits, grains, and seasonal products. The studied model can be extended with potential avenues like time dependent deterioration rate, rebate on deteriorating phase products, return policies, etc.

7 References

1. Aarya, D.D., Rajoria, Y.K., Gupta, N., Raghav, Y.S., Rathee, R., Boadh, R., and Kumar, A. (2022): Selling price, time dependent demand and variable holding cost inventory model with two storage facilities, Materials Today: Proceedings, Vol. 56, No. 1, pp. 245-251.
2. Agrawal, S., Banerjee, S., and Papachristos, S. (2013): Inventory model with deteriorating items, ramp-type demand and partially backlogged shortages for a two warehouse system, Applied Mathematical Modelling, Vol. 37, pp. 8912-8929.
3. Alamri, A.A. and Syntetos, A.A. (2018): Beyond LIFO and FIFO: exploring an allocation-in-fraction-out (AIFO) policy in a two-warehouse inventory model, International Journal of Production Economics, Vol. 206, pp. 33-45.
4. Alshanbari, H.M., El-Bagoury, A.A.H., Khan, M.A., Mondal, S., Shaikh, A.A., and Rashid, A. (2022): Economic order quantity model with Weibull distributed deterioration under a mixed cash and prepayment scheme, Computational Intelligence and Neuroscience, Vol. 2021, ID. 9588685.
5. Duary, A., Das, S., Arif, M.G., Abualnaja, K.M., Khan, M.A.A., Zakarya, M., and Shaikh, A.A. (2022): Advance and delay in payments with the price-discount inventory model for deteriorating items under capacity constraint and partially backlogged shortages, Alexandria Engineering Journal, Vol. 61, pp. 1735-1745.
6. Hovelaque, V. and Bironneau, L. (2015): The carbon-constrained EOQ model with carbon emission dependent demand, International Journal of Production Economics, Vol. 164, pp. 285-291.
7. Lu, C.J., Gu, M., Lee, T.S., and Yang, C.T. (2022): Impact of carbon emission policy combinations on the optimal production-inventory decisions for deteriorating items, Expert Systems with Applications, Vol. 201, ID. 117234.
8. Manna, A.K., Akhtar, M., Shaikh, A.A., and Bhunia, A.K. (2021): Optimization of a deteriorated two-warehouse inventory problem with all-unit discount and shortages via tournament differential evolution, Applied Soft Computing, Vol. 107, ID. 107388.
9. Mashud, A.H.M., Roy, D., Daryanto, Y., Chakrabortty, R.K., and Tseng, M.L. (2021): Sustainable inventory model with controllable carbon emissions, deterioration and advance payments, Journal of Cleaner Production, Vol. 296, ID. 126608.
10. Mishra, U., Wu, J.Z., and Sarkar, B. (2020): A sustainable production-inventory model for a controllable carbon emissions rate under shortages, Journal of Cleaner Production, Vol. 256, ID. 120268.
11. Rahman, M.S., Duary, A., Shaikh, A.A., and Bhunia, A.K. (2022): An application of real coded Self-organizing Migrating Genetic Algorithm on a two-warehouse inventory problem with Type-2 interval valued inventory costs via mean bounds optimization technique, Applied Soft Computing, Vol. 124, ID. 109085.
12. San-José, L.A., Sicilia, J., and Pablo, D.A.L. (2018): An inventory system with demand dependent on both time and price assuming backlogged shortages, European Journal of Operational Research, Vol. 270, No. 3, pp. 889-897.
13. San-Jose, L.A., Sicilia, J., and Jalbar, B.A. (2021): Optimal policy for an inventory system with demand dependent on price, time and frequency of advertisement, Computers & Operations Research, Vol. 128, ID. 105169.
14. Sarkar, B., Sarkar, M., Ganguly, B., Eduardo, L., and Cárdenas-Barrón (2021): Combined effects of carbon emission and production quality improvement for fixed lifetime products in a sustainable supply chain management, International Journal of Production Economics, Vol. 231, ID. 107867.
15. Sett, B.K., Sarkar, B., and Goswami, A. (2012): A two-warehouse inventory model with increasing demand and time varying deterioration, Scientia Iranica, Vol. 19, No. 6, pp. 1969-1977.
16. Shi, Y., Zhang, Z., Chen, S.C., Cárdenas-Barrón, L.E., and Skouri, K. (2020): Optimal replenishment decisions for perishable products under cash, advance, and credit payments considering carbon tax regulations. International Journal of Production Economics, Vol. 223, ID. 107514.
17. Xu, X., Bai, Q., and Chenc, M. (2017): A comparison of different dispatching policies in two-warehouse inventory systems for deteriorating items over a finite time horizon, Applied Mathematical Modelling, Vol. 41, pp. 359-374.
18. Yu, C., Qu, Z., Archibald, T.W., and Luan, Z. (2020): An inventory model of a deteriorating product considering carbon emissions, Computers & Industrial Engineering, Vol. 148, ID. 106694.

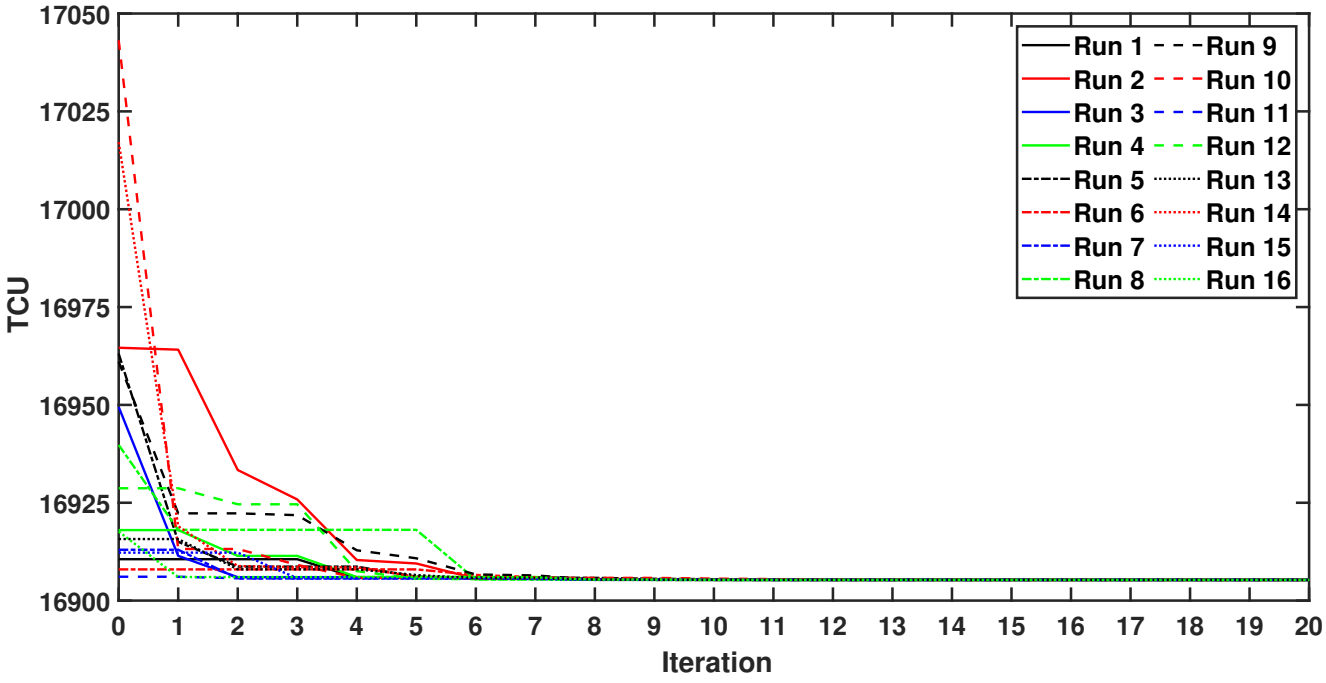

Figure 3: Run graph of several iterations of TLBO

An $M/M/2$ Heterogeneous Servers Queueing System with Differentiated Vacations Subject to Servers Breakdown

V Karthick[1] and V Suvitha *[2]

[1,2]Department of Mathematics, Faculty of Engineering and Technology, SRM Institute of Science and Technology Kattankulathur

Abstract

This research work analyses a heterogeneous two servers queueing system with differentiated vacations and servers breakdown. The steady state probability vector of the number of customers in the system was evaluated as a Quasi-birth and death (QBD) process, and the stationary condition was obtained using the matrix geometric method. Some system performance measures are obtained. The effects of parameters on the performance measures are shown through table.

Keywords: Differentiated vacations; Heterogenous servers;Matrix geometric method; Quasi birth death process; Server breakdown.

1 Introduction

In the service facility center, it is often observed that the server becomes unavailable for a certain period of its job duration and during that period, also called the vacation period, either it takes rest or performs some supplementary jobs. Queueing model, along with the server's vacation is known as vacation queuing model, and is proposed by [1]. Recently [2],[3] are aslo studied about the vacation queueing models.

There are some types of queueing vacations, including differentiated vacation. Initially [4] proposed the queueing model with differentiated queueing vacations. Many researchers including [5],[6] are analysed about differentiated vacation queueing systems. Recent decades have seen an increasing interest in queueing systems with server breakdowns. In earlier many reserchers including [7],[8],[9] are analysed about the single server queueing system with server breakdown. In this work we are concentrating on two server queueing system with differentiated vacations.

2 Model description

Here we are consider an $M/M/2$ heterogeneous servers queueing system with differentiated vacations subject to servers breakdown. The assumptions of the model are described as following:

*Corresponding Author. Email: suvithav@srmist.edu.in

1. Arrival of customers follows a Poisson process with rate λ. Arriving customers form a single waiting line based on the order of their arrivals. The total number of potential customers and the system capacity are assumed to be infinite.

2. The two servers provide heterogenous exponential service to customers on a First-Come First-Service (FCFS) basis with service rates μ_j,where $j = 1, 2$.

3. Type I vacation is taken after the servers has exhaustively served all the customers in the system, where the number of customers served is at least one. If the servers returns from a vacation to find an empty queue, a new random vacation of type II initiates. On returning from either type I or II vacation, if there are some customers in the system, the server immediately start servicing customers until the system is empty again.

4. The type-I (type-II) vacation periods of the servers follows exponential distribution with vacation rates $\theta_j(\ \gamma_j)$ where $j = 1, 2$.

5. In addition servers may get breakdown in any one server alone busy states, follows exponential distribution with rates α_1 and α_2 .

6. Also the repair to servers starts immediately, repair follows exponential distribution with rates β_1 and β_2.

3 Steady-state Analysis

3.1 Stationary Condition

To obtain the stationary condition we first define the matrix $A = A_0 + A_1 + A_2$. It is readily known that A is an irreducible generator of a Markov process.
Let $\pi = (\pi_0, \pi_1, \pi_2, \pi_3, \pi_4, \pi_5)$ be a stationary probability vector of this Markov process. Then, π satisfies the linear equations: πA=0, πe=1
Following Neuts[10], the system is stable if and only if $\pi A_0 e < \pi A_2 e$.
That is the system is stable if and only if $\rho < 1$ where

$$\rho = \frac{\lambda}{(\mu_1 + \mu_2)}$$

3.2 Matrix geometric Solution

Let $H(t)$ and $I(t)$ be the stationary random variables for the number of customers in the system and the status of servers. We denote the stationary probability by
$P_{n,i} = \lim_{t\to\infty} P(L(t) = n, I(t) = i)$, $(n, i) \in \Omega$. Under the stationary condition $\rho < 1$, the stationary probability vector P of the generator Q exists. This stationary probability vector P is partitioned as $P = (p_0, p_1, p_2, ...)$, where $p_0 = (p_{00}, p_{04})$, $p_1 = (p_{10}, p_{11}, p_{12}, p_{14}, p_{15})$ $p_i = (p_{i0}, p_{i1}, p_{i2}, p_{i3}, p_{i4}, p_{i5})$ for $i \geq 2$. Based on the matrix-geometric solution method in Netus[10], the stationary probability vector P is given by

$$p_0 B_{00} + p_1 B_{10} = 0 \tag{1}$$

$$p_0 B_{01} + p_1 B_{11} + p_2 B_{21} = 0 \tag{2}$$

$$p_1B_{12} + p_2B_{22} + p_3B_{32} = 0 \tag{3}$$

$$p_2B_{23} + p_3A_1 + p_4A_2 = 0 \tag{4}$$

$$p_iA_0 + p_{i+1}A_1 + p_{i+2}A_2 = 0 \text{ for } i \geq 3 \tag{5}$$

$$p_i = p_3R^{(i-3)} \text{ for } i \geq 4 \tag{6}$$

where R is the rate matrix is the minimal non-negative solution of the matrix quadratic equation (see Neuts (1981)). Substituting the (6) in (4) we have

$$p_1B_{12} + p_2(A_1 + RA_2) = 0 \tag{7}$$

and the normalizing condition is

$$p_0e_1 + p_1e_2 + p_2(I - R)^{-1}e_3 = 1 \tag{8}$$

where e_1,e_2,e_3 are column vectors with all the elements equal to one with appropriate order. The matrix R is the minimal non-negative solution of the matrix quadratic equation as follows:

$$R^2A_2 + RA_1 + A_0 = 0 \tag{9}$$

The matrix R is called rate matrix with a spectral radius of less than one. We can calculate the rate matrix R approximately by using the iterative method.

Theorem 3.1 *The boundary probability vectors are given by*
$p_0 = -p_2B_{21}D^{-1}B_{10}B_{00}^{-1}$
$p_1 = p_2B_{21}D^{-1}$
and p_2 is determined by the following equations:

$$\begin{cases} p_2(B_{21}D^{-1}B_{12} + A_1 + RA_2) = 0 \\ p_2[-B_{21}D^{-1}B_{10}B_{00}^{-1}e_1 + B_{21}D^{-1}e_2 + (I - R)^{-1}e_3] = 1 \end{cases} \tag{10}$$

4 Numerical Analysis

In this section, we have presented some numerical illustrations in order to validate our analytical results by table. For table 1 we are taking the parameters as follows: μ_1=16, μ_2=14, α_1=9, α_2=8, β_1=12, β_2=10, θ_1=5, θ_2=4, γ_1=7, γ_2=6. Table 1 show the effect of λ on mean number of customers in the system for different states. From that table we observe that if the arrival rate is, increasing then the mean number of customers in 4 states (server 1 alone busy state($E(L_{1b})$), server 2 alone busy state($E(L_{2b})$), both servers busy state($E(L_b)$) and breakdown state($E(L_{br})$)) are increasing and decreasing in vacation states (type-I(($E(L_{1t})$)) and type-II($E(L_{2t})$)).

λ	$E(L_{1b})$	$E(L_{2b})$	$E(L_b)$	$E(L_{1t})$	$E(L_{2t})$	$E(L_{br})$
12	0.34446	0.29724	0.87445	0.14323	0.12360	0.31214
13	0.36215	0.31064	1.05762	0.13641	0.11592	0.33090
14	0.37767	0.32221	1.26173	0.12889	0.10818	0.34767
15	0.39092	0.33189	1.48727	0.12092	0.10047	0.36232
16	0.40186	0.33967	1.73479	0.11271	0.09289	0.37477

Table 1: Effect of λ on mean number of customers for different states

5 Conclusion

In this work we have analysed a two-server heterogenous Markovian queueing system with differentiated vacations and servers breakdown. We have provided the stationary condition and boundary probability vectors for our model. Also we have give some numerical resutls through tables and also graphed the influence of the λ on steady state probabilities.

References

Y. Levy and U. Yechiali, Utilization of idle time in an $M/G/1$ queueing system, Management Science,22(2), pp.202–211 (1975)

G. Sapkota and R. P. Ghimire, Mathematical Analysis of M/M/C Vacation Queueing Model with a Waiting Server and Impatient Customers,Journal of Mathematics and Statistics, 18(1), pp.36-48 (2022).

R. Tian R, Z. G. Zhang and S. Su, On Markovian queues with single working vacation and bernoulli interruptions, Probability in the Engineering and Informational Sciences 36(3), pp.616 - 643 (2022).

O. C. Ibe and O. A. Isijola, M/M/1 Multiple Vacation Queueing Systems with Differentiated Vacations, Modelling and Simulation in Engineering,(2014)

M. I. G. Suranga Sampath, K. Khalidass and L. Jicheng, Transient Analysis of an M/M/1 Queueing System Subjected to Multiple Differentiated Vacations, Impatient Customers and a Waiting Server with Application IEEE 802.16e Power Saving Mechanism, Indian Journal of pure and applied mathematics,51, pp.297-320 (2020).

M. I. G. Suranga Sampath and L. Jicheng, Impact of Customers Impatience on an M/M/1 Queueing System Subject to Differentiated Vacations with a Waiting Server, Quality Technology and Quantitative Management, 17(2), pp. 125-148, (2018).

M. Seenivasan and R. Abinaya, Markovian Queueing Model with Single Working Vacation and Server Breakdown, Journal of Computational Analysis and Applications, 30(2), pp.409–421 (2022).

S. R. Chakravarthy, R. Kulshrestha, A queueing model with server breakdowns, repairs, vacations, and backup server, Operations Research Perspectives 7, pp.100131 (2020).

R. R. Das, V. N. Devi, A. Rathore and K.Chandand, Analysis of Markovian queueing system with server failures, N-policy and second optional service, International Journal of Nonlinear Analysis and Applications, 13(1), pp.3073-308 (2022).

M. F. Neuts, Matrix-geometric solutions in stochastic models: an algorithmic approach, Courier Corporation 1994.

Proceedings of the

1st International Conference on Mathematical and Statistical Sciences (ICMSS-1)

Published by

NAMIBIA UNIVERSITY OF SCIENCE AND TECHNOLOGY

ISBN:978-99916-55-80-2

Department of Mathematics, Statistics and Actuarial Science
Faculty of Health, Natural Resources and Applied Sciences
Namibia University of Science and Technology
Private Bag 13388, Windhoek, NAMIBIA
W:https://icmss.nust.na/
E: lnewaka@nust.na; icmss.nust@gmail.com
T: +264 61 207 2913